CHAPTER 2
TABLE OF CONTENTS

FIGURES

TABLES

THIS PAGE LEFT BLANK INTENTIONALLY

2. STRUCTURAL EVALUATION

This chapter presents structural design criteria, weights, mechanical properties of materials, and general package standards. It demonstrates that the GA-4 cask design is capable of meeting all normal conditions of transport and all hypothetical accident conditions. This chapter also documents the results of the analyses that were performed to provide assurance that the designs satisfy all requirements for licensing.

The structural evaluation of the cask was performed using both analytical and model testing. Three-dimensional (3-D) finite element (FE) analysis was used to determine the cask and component stresses for each normal (Section 2.6) and accident (Section 2.7) loading condition, including each impact orientation. Stresses are tabulated for a set of predetermined points. If the location of the highest stress is different from the predetermined points, the results at the point of highest stress are also presented.

The force-deflection characteristics of the impact limiters (Section 2.10.3.3) are based on test data and are computed using GA's ILMOD computer code (Section 2.10.1.4) which computes the footprint and crush force for any crush orientation and depth. ILMOD is used to compute the maximum and minimum force-versus-deflection curves, taking into account variations in manufacturing and material tolerances, temperature effects, and strain rate effects. The output from ILMOD was verified by comparison to 1/4-scale model crush tests.

The g-levels for the 3-D-FE cask and other component analyses and the impact limiter crush depths and loads were computed using the GACAP computer code (Section 2.10.1.1), a dynamic numerical-integration impact analysis program similar to the NRC's SCANS program. A quasi-static analysis was performed in which the cask was modeled as a rigid body. GACAP was not used to compute the cask stresses.

A series of half-scale model tests (Section 2.10.13), consisting of three 30-ft (9-m) drops onto an essentially unyielding surface and four 40-in. (1-m) drops onto a mild steel punch, were performed to support the analytical structural evaluation of the cask. The GA-4 model successfully passed all tests.

2.1 Structural Design

The GA-4 cask is designed to meet the loading and environmental conditions defined in Title 10 of the *Code of Federal Regulations*, Part 71 (10 CFR Part 71 [Ref. 2.1-1]). The general approach taken for the structural evaluation of the GA-4 shipping cask is based on analysis techniques that utilize current state-of-the-art methods to verify the safety of the design. All features of the design were verified. The analysis uses a quasistatic approach to calculate stresses.

2.1.1 Discussion

The GA-4 cask consists of

1. A Type XM-19 stainless steel cask body with a bolted closure.
2. Depleted uranium (DU) used as a gamma shield along the sides of the cask.
3. Neutron shielding around the sides of the cask.
4. A Type XM-19 stainless steel fuel cavity liner with a fuel support structure welded to it.
5. Four lifting and tiedown trunnions and two redundant lifting sockets.
6. Two identical aluminum honeycomb energy-absorbing impact limiters, located over the ends of the cask.

The containment boundary retains the radioactive contents. The containment boundary consists of the cask body (cask body wall, flange and bottom plate), cask closure, gas sample port, drain valve, and primary O-ring seals.

Chapter 1 gives a more detailed description of the packaging.

2.1.2 Design Criteria

This section defines the stress allowables and load combinations used to design the GA-4 cask. These design criteria meet the following safety requirements taken from 10 CFR Part 71.51:

1. For normal conditions of transport, there shall be no loss or dispersal of radioactive contents, as demonstrated to a sensitivity of 10^{-6} A_2/h; no significant increase in external radiation levels; and no substantial reduction in the effectiveness of the packaging.
2. For hypothetical accident conditions, there shall be no escape of radioactive material exceeding a total amount A_2 in one week, and no external radiation dose rate exceeding 1 R/h at 1 m from the external surface of the package.

2.1.2.1 Load Combinations. Tables 2.1-1 and 2.1-2 show the load combinations for which the cask is evaluated for normal conditions of transport and hypothetical accident conditions, respectively. These load combinations envelop the loading combinations specified by 10 CFR Part 71 and Nuclear Regulatory Commission (NRC) Regulatory Guide 7.8 (Ref. 2.1-2). Each condition is applied separately, except for the following hypothetical accident conditions, which are applied sequentially to determine the maximum cumulative damage: a 9-m (30-ft) drop,

TABLE 2.1-1
SUMMARY OF LOAD COMBINATIONS FOR NORMAL CONDITIONS OF TRANSPORT

			Applicable Initial Condition							
			Ambient Temperature		Insolation		Decay Heat		Internal Pressure	
Loading Condition	Analysis Section	Load Case	100°F	−20°F	Max.	0	Max.	0	Max.	Min.
Hot environment: 100°F ambient temperature	2.6.1.3	1[(a)]			X		X		X	
Cold environment: −40°F ambient temperature	2.6.2	2				X		X		X
Minimum external pressure: 3.5 psia	2.6.3	3	X		X		X		X	
Maximum external pressure: 20 psia	2.6.4[(b)]	4		X		X		X		X
Vibration and shock normally incident to the mode of transport	2.6.5	5	X		X		X		X	
	2.6.5	6		X		X		X		X
Water spray	2.6.6	7								
Free drop: 1-ft drop	2.6.7	8	X		X		X		X	
	2.6.7	9		X		X		X		X

(a)This case produces the maximum temperatures.
(b)The hot condition without internal pressure was analyzed to conservatively envelop load case 4.

TABLE 2.1-2
SUMMARY OF LOAD COMBINATIONS FOR HYPOTHETICAL ACCIDENT CONDITIONS

			Applicable Initial Condition							
			Ambient Temperature		Insolation		Decay Heat		Internal Pressure	
Accident Condition	Analysis Section	Load Case	100°F	−20°F	Max.	0	Max.	0	Max.	Min.
Free drop: 30 ft	2.7.1	1	X		X		X		X	
	2.7.1	2		X		X		X		X
Puncture: drop onto bar	2.7.2	3	X		X		X		X	
	(a)	4		X		X		X		X
Thermal: fire accident	2.7.3	5	X			X	X		X	
Immersion	2.7.5	6	X		X		X			

[a] The cold condition produces higher design margins than the hot conditions primarily because of the higher allowable and therefore is not reported.

followed by a 1-m (40-in.) drop onto a mild steel punch, followed by exposure to a 30-min 800°C (1475°F) environment. In addition, as specified in 10 CFR Part 71.61, the containment system shall not collapse, buckle or allow inleakage of water when subjected to 290 psi external water pressure.

2.1.2.2 Stress Allowables. This section describes the stress allowables used in the design of the cask components and discusses the built-in factors of safety inherent in them.

2.1.2.2.1 Containment Boundary. Table 2.1-3 presents the containment boundary stress criteria. As recommended by NRC Regulatory Guide 7.6 (Ref. 2.1-3) these elastic analysis stress allowables are compatible with Article NB-3000 and Appendix F of the American Society of Mechanical Engineers *Boiler and Pressure Vessel Code* (ASME Code)(Ref. 2.1-4), Section III, Div. 1, "Rules for Construction of Nuclear Power Plant Components." These allowables prevent ductile rupture of metallic components of the containment boundary, which consist of the cask body side wall, closure, bottom plate, closure bolts, gas sample port, and drain valve. The analysis uses the material property data corresponding to the design stress values (S_m), yield strengths (S_y), and ultimate strengths (S_u) given in Appendix I of the ASME Code. Table 2.3-1 summarizes these material properties. Table 2.1-4 summarizes allowable stresses as a function of temperature.

2.1.2.2.2 Noncontainment Components. Tests or analysis shall show that the noncontainment components—neutron shield, DU gamma shield, fuel cavity liner, fuel support structure (FSS), honeycomb impact limiters, impact limiter support structure (ILSS) and honeycomb impact limiter attachment bolts—withstand the normal conditions of transport without substantial reduction of the effectiveness of the component. Tests or analysis shall show that the noncontainment components withstand the hypothetical accident conditions without jeopardizing the safety of the cask, as defined in 10 CFR Part 71 and summarized at the beginning of Section 2.1.2. The function of each component is considered in determining its acceptance criteria for continued effectiveness.

The stress criteria listed in Table 2.1-5 apply to the fuel cavity liner, fuel support structure, neutron shield structure, ILSS and impact limiter attachment bolts. Table 2.1-4 summarizes the stress allowables as a function of temperature.

The following criteria for the other individual components shall ensure that their effectiveness is not reduced.

1. The DU shall be assumed to carry no bending or tensile loads, but it may transfer compressive loads during normal and accident conditions and may provide backing for the containment wall during the puncture event.

2. The [Prop. Info.] neutron shield shall remain in place and the neutron shield structure shall not leak during normal conditions.

TABLE 2.1-3
CONTAINMENT BOUNDARY STRESS CRITERIA

Stress Category	Normal Conditions	Accident Conditions
Components other than bolts		
Primary[g] membrane stress intensity[a]	S_m	Lesser of 2.4 S_m and 0.7 S_u
Primary membrane + bending stress intensity[b][g]	1.5 S_m	Lesser of 3.6 S_m and S_u
Range of primary + secondary stress intensity[c]	3.0 S_m	Not applicable
Bearing stress	S_y[d]	S_y for seal surfaces S_u elsewhere
Pure primary shear stress	0.6 S_m[e]	0.42 S_u
Bolts		
Membrane stress	2.0 S_m	Lesser of S_y and 0.7 S_u
Membrane + bending stress[f]	3.0 S_m	S_y
Pure primary shear stress	0.6 S_m	0.42 S_u

[a]Definition according to NRC Regulatory Guide 7.6, Paragraph B.4 and ASME Code, NB-3221.1. Example: average stress across cask body at middle of cask wall and at the rounded corners.

[b]Definition according to NRC Regulatory Guide 7.6, Paragraph B.3, B.4 and ASME Code, NB-3221.3. Example: The bending component of primary stress shall be the stress proportional to the distance from the centroid of the section.

[c]Definition according to NRC Regulatory Guide 7.6, Paragraph C.4.

[d]From ASME Code, NB-3227.1.

[e]From ASME Code, NB-3227.2.

[f]Not considering stress concentrations.

[g]Primary stresses include all bending stresses in shells that are not shells of revolution, and interference stresses due to differential thermal expansion.

TABLE 2.1-4
ALLOWABLE STRESSES (ksi)

Stress Category	Normal Conditions				Accident Conditions				
	70°F	200°F	300°F	400°F	70°F	200°F	300°F	400°F	600°F
Components other than bolts (Type XM-19 stainless steel)									
Primary membrane stress intensity	33.3	33.2	31.4	30.2	70	69.7	66.0	63.5	61.5
Primary membrane + bending stress intensity	50	49.8	47.1	45.3	100	99.5	94.3	90.7	87.8
Range of primary + secondary stress intensity	100	99.6	94.2	90.6	N/A	N/A	N/A	N/A	N/A
Bearing stress (general)	55	47	43.4	40.8	100	99.5	94.3	90.7	87.8
Bearing stress (seal surface)	55	47	43.4	40.8	55	47	43.4	40.8	37.3
Primary shear stress	20	19.9	18.8	18.1	42	41.8	39.6	38.1	36.9
Bolts (SB-637, Alloy NO7718)									
Membrane stress	100	96	93.8	92.2	129.5	123.2	121.1	119	--
Membrane + bending stress	150	144	140.7	138.3	150	144	140.7	138.3	135.6
Primary shear stress	30	28.8	28.1	27.7	77.7	73.9	72.7	71.4	--

TABLE 2.1-5
STRESS CRITERIA FOR FSS, FUEL CAVITY LINER, NEUTRON SHIELD STRUCTURE, ILSS, AND IMPACT LIMITER ATTACHMENT BOLTS

Stress Category	Normal Conditions	Accident Conditions
Components other than bolts		
Primary membrane stress intensity[a]	S_m	Lesser of 2.4 S_m and 0.7 S_u
Primary membrane + bending stress intensity[a]	1.5 S_m	Lesser of 3.6 S_m and S_u
Range of primary + secondary stress intensity	3.0 S_m	Not applicable
Bearing stress	S_y	S_u
Pure primary shear stress	0.6 S_m	0.42 S_u
Bolts		
Membrane stress	Greater of 2.0 S_m and S_y	Greater of S_y and 0.7 S_u
Membrane + bending stress	Greater of 3.0 S_m and S_y	S_u
Pure primary shear stress	0.6 S_m	Greater of 0.6 S_y and 0.42 S_u

[a]Primary stresses include all bending stresses and interference stresses due to differential thermal expansion in the cavity liner.

3. The impact limiters are allowed to exceed yield under all conditions. They shall not bottom out during impact loading, and no rigid component of the cask (e.g., trunnion) shall strike the unyielding surface during the drop events.

4. The trunnions shall be designed not to yield during the 2g vertical, 10g longitudinal and 5g transverse shock loading defined in 10 CFR Part 71.45(b)(1). The trunnions shall be designed to fail before the cask wall under excessive load.

2.1.2.2.3 Design Margins. The design margins (D.M.) presented in this report are defined as

D.M. = (allowable stress/actual stress intensity) –1.

These design margins are in addition to margins of safety built into the allowable stresses.

2.1.2.3 Brittle Fracture. The choice of austenitic stainless steel and nonferrous nickel-base alloy steel for the containment boundary components (such as the cask body, closure, penetrations, and closure bolts) and noncontainment components (such as the fuel cavity liner, fuel support structure, and impact limiter attachment bolts) precludes failure by brittle fracture, since these alloys remain ductile at temperatures below the minimum design temperature.

The DU is not used as a structural member. It is encased in stainless steel inerted with helium, which prevents oxidation and other adverse chemical reactions.

2.1.2.4 Fatigue. Subparagraph NB-3222.4 of the ASME Code, Section III, and NRC Regulatory Guide 7.6 requirements shall govern fatigue stress evaluation. Figures. 2.1-1 and 2.1-2 and Tables 2.1-6 and 2.1-7, abstracted from the ASME Code, present the fatigue design allowables for stainless steel. Figure 2.1-3 and Table 2.1-8, abstracted from the ASME Code, present the fatigue design allowables for high-strength bolts. The cask is designed for an assumed 50-year life and 25 fuel shipments (round-trips) per year.

1. High-alloy Bolts. Fatigue is evaluated according to NB-3232.3 of the ASME Code, including the appropriate number of torquing and untorquing cycles. The number of cycles shall be based on 50 one-way trips per year. The bolts can be replaced if necessary.

2. Containment Boundary, Lifting and Tiedown Trunnions, Redundant Lifting Sockets, Fuel Cavity Liner, and Fuel Support Structure. The designer shall evaluate fatigue for (1) the appropriate number of cycles of extreme normal condition temperature, pressure, lifting, and dead load (50 x 50 = 2,500 cycles); (2) vibration loading based on the peak trailer-bed vibration accelerations in draft ANSI Standard N14.23 (Ref. 2.1-5), where the criterion requires that the cask be designed for continuous operation at a response equal to 75 percent of the peak trailer-bed vibration accelerations.

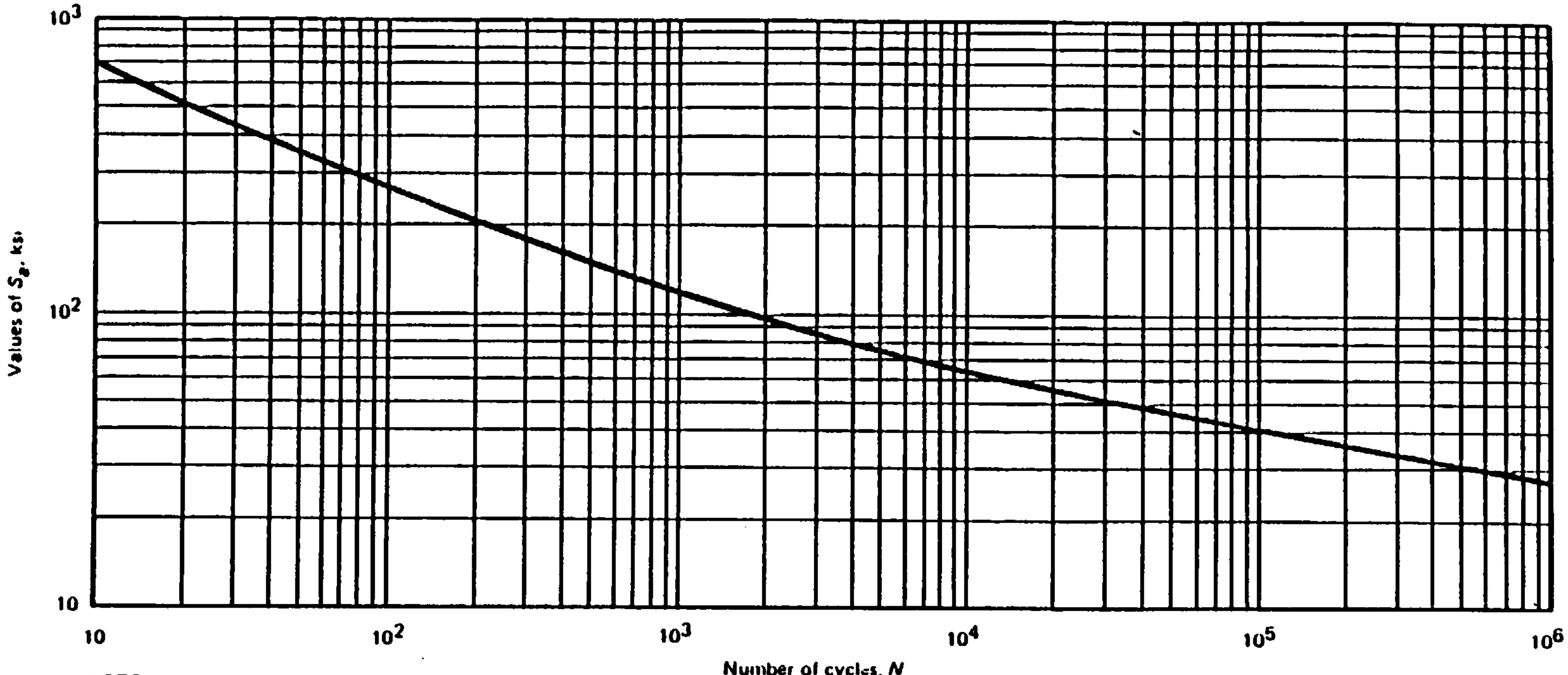

NOTE:
E = 28.3 X 10^6 psi

FIG. I-9.2.1 DESIGN FATIGUE CURVE FOR AUSTENITIC STEELS, NICKEL-CHROMIUM-IRON ALLOY, NICKEL-IRON-CHROMIUM ALLOY, AND NICKEL-COPPER ALLOY FOR S_a > 28.2 ksi, FOR TEMPERATURES NOT EXCEEDING 800°F
(For $S_a \leq$ 28.2 ksi, use Fig. I-9.2.2.)
Table I-9.1 Contains Tabulated Values and a Formula for Accurate Interpolation of This Curve

Fig. 2.1-1. Stainless steel design fatigue curve (S_a > 28.2 ksi), abstracted from the ASME Code

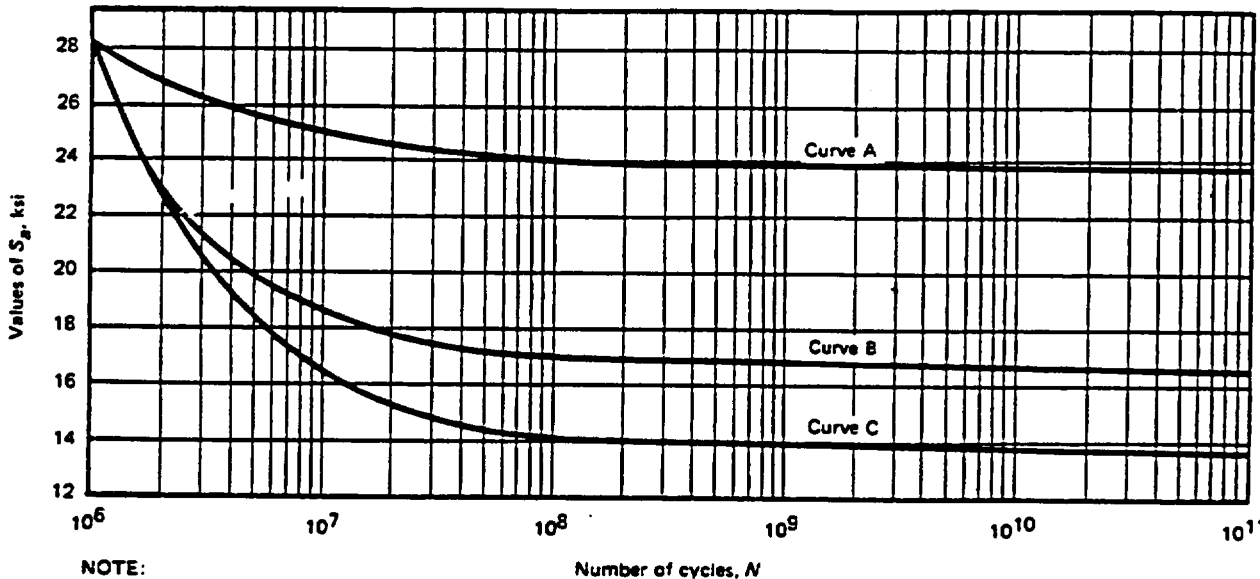

NOTE:
$E = 28.3 \times 10^6$ psi

Criteria for the Use of the Curves in This Figure
[Notes (1)–(5)]

Curve	Elastic Analysis of Material Other Than Welds and Adjacent Base Metal	Elastic Analysis of Welds and Adjacent Base Metal
A	$(P_L + P_b + Q)_{Range} \le 27.2$ ksi	...
B	$(P_L + P_b + Q)_{Range} > 27.2$ ksi and S_a is corrected for applied mean stress	$(P_L + P_b + Q)_{Range} \le 27.2$ ksi
C	$(P_L + P_b + Q)_{Range} > 27.2$ ksi	$(P_L + P_b + Q)_{Range} > 27.2$ ksi

NOTES:
(1) Range applies to the individual quantities P_L, P_b, and Q and applies to the set of cycles under consideration.
(2) Thermal bending stresses resulting from axial and radial gradients are excluded from Q.
(3) Curve A is also to be used with inelastic analysis with $S_a = \frac{1}{2} \Delta \epsilon_t E$, where $\Delta \epsilon_t$ is the total effective strain range.
(4) The maximum effect of retained mean stress is included in Curve C.
(5) The adjacent base metal is defined as three wall thicknesses from the center line of the weld.

FIG. I-9.2.2 DESIGN FATIGUE CURVE FOR AUSTENITIC STEELS, NICKEL-CHROMIUM-IRON ALLOY, NICKEL-IRON-CHROMIUM ALLOY, AND NICKEL-COPPER ALLOY FOR $S_a \le 28.2$ ksi, FOR TEMPERATURES NOT EXCEEDING 800°F
(For $S_a > 28.2$ ksi, use Fig. I-9.2.1.)
Table I-9.2.2 Contains Tabulated Values for Accurate Interpolation of This Curve

Fig. 2.1-2. Stainless steel design fatigue curve ($S_a \le 28.2$ ksi), abstracted from the ASME Code

TABLE 2.1-6
TABULATED FATIGUE ALLOWABLES, ABSTRACTED FROM THE ASME CODE

TABLE I-9.1
TABULATED VALUES OF S_a, ksi, FROM FIGS. I-9.0[1,2]

Figure	Curve	1E1	2E1	5E1	1E2	2E2	5E2	8.5E2 (Note (4))	1E3	2E3	5E3	1E4	1.2E4 (Note (4))	2E4	5E4	1E5	2E5	5E5	1E6
		Number of Cycles (Note (3))																	
I-9.1	UTS ≤ 80 ksi	580	410	275	205	155	105	. . .	83	64	48	38	. . .	31	23	20	16.5	13.5	12.5
I-9.2.1	. . .	708	512	345	261	201	148	. . .	119	97	76	64	. . .	55.5	46.3	40.8	35.9	31	28.3
I-9.4	MNS ≤ $2.7S_m$ (Note (5))	1150	760	450	320	225	143	. . .	100	71	45	34	. . .	27	22	19	17	15	13.5

NOTES:

(1) All notes on the referenced figures apply to these data.

(2) Interpolation between tabular values is permissible based upon data representation by straight lines on a log-log plot. Accordingly, for $S_i > S > S_j$

$$\frac{N}{N_i} = \left(\frac{N_j}{N_i}\right)^{\log(S_i/S)/\log(S_i/S_j)}$$

where S, S_i, and S_j are values of S_a; N, N_i, and N_j are corresponding numbers of cycles from design fatigue data.

Example: From the data given in the Table above, use the interpolation formula above to find the number of cycles N for $S_a = 53.5$ ksi when UTS ≤ 80 ksi in Fig. I-9.1:

$$\frac{N}{2000} = \left(\frac{5000}{2000}\right)^{\log(64/53.5)/\log(64/48)}$$

$N = 3540$ cycles

(3) The number of cycles indicated shall be read as follows: $IEJ = I \times 10^J$, e.g., $5E2 = 5 \times 10^2$ or 500.

(4) These data points are included to provide accurate representation of curves at branches or cusps.

(5) MNS is the Maximum Nominal Stress.

K-217 (6)
9-4-91

910469/A

TABLE 2.1-7
TABULATED STAINLESS STEEL FATIGUE ALLOWABLES (S_a ≤28.2 ksi), ABSTRACTED FROM THE ASME CODE

TABLE I-9.2.2
TABULATED VALUES OF S_a, ksi, FROM FIG. I-9.2.2[1,2]

Number of Cycles [Note (3)]	Curve A	Curve B	Curve C
1E6	28.2	28.2	28.2
2E6	26.9	22.8	22.8
5E6	25.7	19.8	18.4
1E7	25.1	18.5	16.4
2E7	24.7	17.7	15.2
5E7	24.3	17.2	14.3
1E8	24.1	17.0	14.1
1E9	23.9	16.8	13.9
1E10	23.8	16.6	13.7
1E11	23.7	16.5	13.6

NOTES:
(1) All notes on Fig. I-9.2.2 apply to these data.
(2) Interpolation between tabular values is permissible based upon data representation by straight lines on a log-log plot. See Table I-9.1, Note (2).
(3) The number of cycles indicated shall be read as follows:
IEJ = I × 10^J, e.g., 5E6 = 5 × 10^6 or 5,000,000

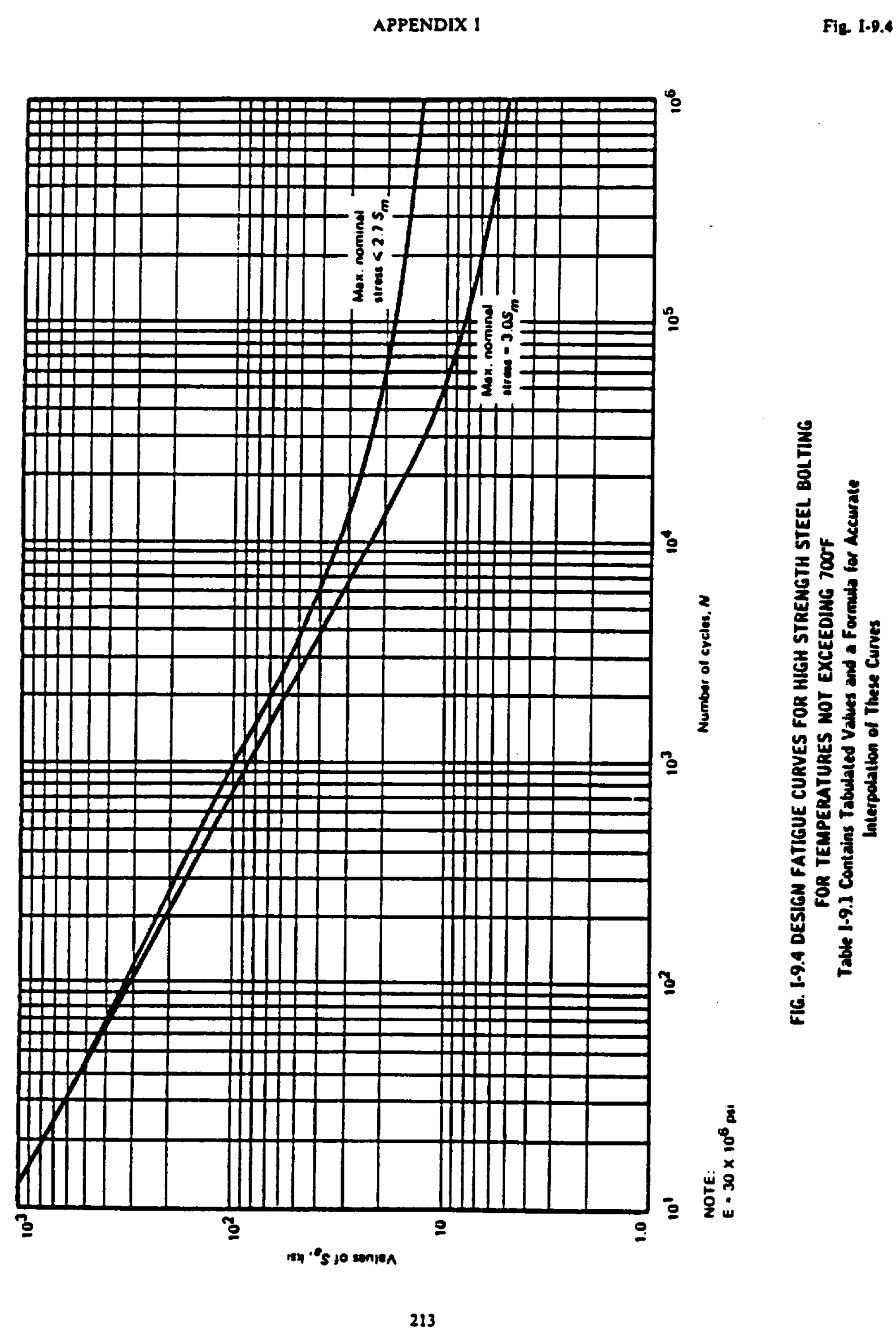

Fig. 2.1-3. High-strength steel bolting design fatigue curve, abstracted from the ASME Code

2.1.2.5 Ten-cycle Limit. Following NRC Regulatory Guide 7.6, C.7, the extreme total stress intensity range for containment boundary components between the initial state, the fabrication state, the normal operating conditions, and the hypothetical accident conditions shall be less than twice the value for S_a at 10 cycles, given by the appropriate design fatigue curves.

2.1.2.6 Buckling. These buckling criteria are based on the criteria of NUREG/CR-6322, "Buckling Analysis of Spent Fuel Basket," (Ref. 2.1-8).

The buckling resistance of the cask body, cavity liner and fuel support structure shall be evaluated and shown to meet the buckling criteria described herein. The buckling criteria in NUREG/CR-6322 were established for spent fuel baskets and are based on the criteria in ASME Section III, Subsection NF, Component Supports and Appendix F. The GA-4 cask body, cavity liner and FSS are essentially box beams that are evaluated by the methods presented in NUREG/CR-6322.

The analyses consider the effects of plasticity and material and geometric imperfections on the theoretical elastic buckling stress. As Figure 3 of NUREG/CR-6322 shows, the effect of initial imperfections on compressive elements other than cylinders is negligible and is therefore ignored. If the cask body and cavity liner/FSS structures are shown to be either compact or non-compact sections as shown in Ref. 2.1-6 [NF-3322.1d(1) and NF-3322.2(d)(2)] and NUREG/CR-6322, Section 6.23, then the individual compression elements (cask wall, cavity liner and FSS plate elements) are fully effective, do not need to be addressed separately and will not buckle.

References 2.1-9 and 2.1-10 state that for long rectangular plates like the walls of the cask body, cavity liner and FSS, normal or lateral loads actually increase the buckling strength due to longitudinal compression. Therefore, lateral loads on the wall will be accounted for by using the stress intensity at the location of maximum compression. Furthermore, the section properties of the cask body are the same about both axes, so that bending stress ratios about the x and y axes need not be considered separately.

The cask body buckling analysis shall not consider the stiffness of the neutron shield tank outer shell.

The neutron shield outer shell shall meet the buckling criteria given in Section III, Subsection NB, of the ASME B&PV Code for normal condition external pressure loads. Since the neutron shield shell is anchored to the cask body and since the overall stiffness of the cask body is much greater than the shell, overall buckling is precluded by the buckling resistance of the cask body.

2.1.2.6.1 Cask Body Buckling. The stability criteria defined in this section follow those for a Linear-Type Support as described in Section 6 of NUREG/CR-6322. Following is the analytical methodology for the cask body:

Step 1. Calculate the following properties of the cask body:

- I = moment of inertia,
- r = radius of gyration,
- ℓ = length of cask,
- k = effective length factor of cask,
- b = width of cask wall (width of cask wall to start of radius at corners per AISC, B5.1)
- t = thickness of cask wall,
- $k\ell/r$ = slenderness ratio of cask acting as a column,
- d = overall depth of cask cross section,
- L = laterally unsupported length of cask,
- M_1, M_2 = moments at ends of cask,
- S_y = cask yield stress at temperature.

Step 2. Check whether cask is a compact or non-compact section and calculate the width ratio as shown in NF-3322.1(d)(1), NF-3322.2(d)(2) and NUREG/CR-6322, Section 6.23. If the cask is shown to be a compact or non-compact section and the width-to-thickness ratio meets the criteria, then the individual compression elements (cask wall) are fully effective and will not buckle. Therefore, they do not need to be addressed separately.

(a) Compact section.

(1) Width-thickness ratio,

$b/t \le 190/\sqrt{S_y}$,

(2) Depth-thickness ratio,

$d/t \le (640/\sqrt{S_y})[1 - 3.74(f_a/S_y)]$ when $f_a/S_y \le 0.16$, or

$d/t \le 257/\sqrt{S_y}$ when $f_a/S_y > 0.16$, and

(3) Laterally unsupported length,

$L \le [1950 + 1200(M_1/M_2)](b/S_y)$, and

$d \le 6(b)$.

(b) Non-compact section width ratio.

$b/t \le 238\sqrt{S_y}$.

Step 3. Determine the axial compression allowables. For normal conditions, calculate the allowable axial compression using the following from NUREG/CR-6322, 6.21(2):

$F_a = S_y\,[0.47 - (k\ell/r)/444]$ if $k\ell/r \le 120$, or

$F_a = S_y\,[0.40 - (k\ell/r)/600]$ if $k\ell/r > 120$.

For accident conditions, calculate the allowable axial compression. The allowable stresses are taken from NUREG/CR-6322, section 6.31(b)(2) for heavy non-stress relieved, built up carbon steel sections using universal mill plate and then reduced by 12% to obtain allowable stresses for austenitic steel. The 12% reduction factor for stainless steel is equal to the ratio of the level A factors of safety for austenitic and carbon steels for Euler buckling stresses in the elastic range, which are 2.15 and 1.92, respectively, as given in NUREG/CR-6322, Section 6.32 and ASME Code, NF-3222.1(e)(1). The resulting allowable stresses are as follows:

$0 \le \lambda < 1$: $F_a = S_y\,[1 - (\lambda^2/4)]/[1.12(1.11 + 0.75\lambda + 0.83\lambda^2 - 0.81\lambda^3)]$, or

$1 \le \lambda \le \sqrt{2}$: $F_a = S_y\,[1 - (\lambda^2/4)]/(1.12 \times 1.88)$, or

$\lambda > \sqrt{2}$: $F_a = S_y/(1.12 \times 1.88 \times \lambda^2)$,

where

$$\lambda = \left[\sqrt{(S_y/E)}\right]\,[(k\ell/r)/\pi],$$

$$= \sqrt{(S_y/E)},$$

F_e = Euler buckling stress.

Step 4. Determine the maximum axial compressive stress in the cask body for normal and accident conditions and compare against the allowables defined in Step 3.

Step 5. Determine the bending allowables per NUREG/CR-6322. F_b is 0.66 S_y for normal conditions if the cask body is determined in Step 2a to be a compact section, and fS_y for accident conditions, where f is the shape factor. The shape factor is calculated using the following method:

$$f = \text{Shape Factor} = Ay_1/(I/c)$$

where

A = area of cask body cross section,

y_1 = distance to centroid of half cross sectional area of cask body,

c = distance from neutral axis to extreme fiber of cross section, and

I = moment of inertia of cask body cross section.

Step 6. Combined axial compression and bending. The cask body shall satisfy the following equations, which are taken from NUREG/CR-6322, Sections 6.22 and 6.32.

Normal conditions:

$f_a/F_a + C_m\,(f_b)/\{F_b\,[1 - (2.15f_a/F_e)]\} \le 1$, and

$f_a/(0.6S_y) + f_b/F_b \le 1$,

Accident conditions:

$f_a/F_a + C_m\,(f_b)/\{F_b\,[1 - (1.46f_a/F_e)]\} \le 1$, and

$f_a/(0.6S_y) + f_b/F_b \le 1$;

where

C_m = 0.85 for members with free end but joint translation permitted,

= $0.6 - 0.4(M_1/M_2)$ but not less than 0.4, where M_1/M_2 is the ratio of the small-to-larger moments on the fixed ends braced against translation and not subjected to transverse loading between supports.

F_a = allowable axial stress from the expressions given above in step 3,

F_e = Euler buckling stress,

F_b = bending allowable stress from step 5 above,

f_a = axial stress from step 4 above, and

f_b = Maximum bending stress. Either the maximum longitudinal bending stress due to longitudinal bending or the stress intensity at the location of maximum compression due to longitudinal bending and transverse bending, whichever is greater, shall be used. The stress intensity includes the effect of lateral loads on the wall.

2.1.2.6.2 Cask Body Buckling Due to 290 psi External Water Pressure Load. The 290 psi external water pressure condition required by 10 CFR Part 71.61 exerts an external pressure load on the cask body. Each containment boundary component shall be evaluated for combined axial compression and bending according to the criteria defined in 2.1.2.6.1, Steps 3 through 6. The allowables for accident conditions shall be used.

2.1.2.6.3 Cavity Liner and FSS Buckling. The stability criteria defined in this section follow those for a Linear-Type Support as described in Section 6 of NUREG/CR-6322. The analytical methodology for the cavity liner and FSS is as follows:

Step 1. Calculate the following properties of the cavity liner and FSS:

I = moment of inertia,

r = radius of gyration,

ℓ = length of liner and FSS,

k = effective length factor of cavity liner and FSS,

b = width of cavity liner and FSS wall elements,

t = thickness of cavity liner and FSS,

$k\ell/r$ = slenderness ratio of cavity liner and FSS acting as a column,

d = depth of cavity liner and FSS wall element,

L = laterally unsupported length of cavity liner and FSS,

M_1, M_2 = moments at ends of cavity liner and FSS, and

S_y = cavity liner and FSS yield stress at temperature.

Step 2. Check whether cavity liner and FSS structure is a compact or non-compact section and calculate the width ratio as shown in NF-3322.1(d)(1), NF-3322.2(d)(2) and NUREG/CR-6322, Section 6.23. If the cavity liner and FSS structure is shown to be a compact section and the width-to-thickness ratio meets the criteria, then the individual compression elements (cavity liner and FSS structure wall elements) are fully effective, will not buckle, and therefore do not need to be addressed separately, except that the lower cavity liner and FSS legs are evaluated for combined axial compression and bending during a side drop.

(a) Compact section.

(1) Width-thickness ratio,

$b/t \leq 190/\sqrt{S_y}$,

(2) Depth-thickness ratio,

$d/t \leq (640/\sqrt{S_y})[1 - 3.74(f_a/S_y)]$ when $f_a/S_y \leq 0.16$, or

$d/t \leq 257/\sqrt{S_y}$ when $f_a/S_y > 0.16$, and

(3) Laterally unsupported length,

$L \leq [1950 + 1200(M_1/M_2)](b/S_y)$, and

$d \leq 6(b)$.

(b) Non-compact section width ratio.

$b/t \leq 238\sqrt{S_y}$.

Step 3. Determine the axial compression allowables. For normal conditions, calculate the allowable axial compression using the following from NUREG/CR-6322, 6.21(2):

$F_a = S_y\,[0.47 - (k\ell/r)/444]$ if $k\ell/r \leq 120$, or

$F_a = S_y\,[0.40 - (k\ell/r)/600]$ if $k\ell/r > 120$.

For accident conditions, calculate the allowable axial compression. The allowable stresses are taken from NUREG/CR-6322, section 6.31(b)(2) for heavy non-stress relieved built up carbon steel sections using universal mill plate and then reduced by 12% to obtain allowable stresses for austenitic steel. The 12% reduction factor for stainless steel is equal to the ratio of the level A factors of safety for austenitic and carbon steels for Euler buckling stresses in the elastic range, which are 1.92 and 2.15 respectively, as given in NF-3222.1(e)(1). The resulting allowable stresses are as follows:

$0 \le \lambda < 1$: $F_a = S_y [1 - (\lambda^2/4)]/[1.12(1.11 + 0.75\lambda + 0.83\lambda^2 - 0.81\lambda^3)]$, or

$1 \le \lambda \le \sqrt{2}$: $F_a = S_y [1 - (\lambda^2/4)]/(1.12 \times 1.88)$, or

$\lambda > \sqrt{2}$: $F_a = S_y/(1.12 \times 1.88 \times \lambda^2)$,

where

$\lambda = \left[\sqrt{(S_y/E)}\right] [(k\ell/r)/\pi]$,

$= \sqrt{(S_y/E)}$,

F_e = Euler buckling stress.

Step 4. Determine the maximum axial compressive stress in the cavity liner and FSS structure for normal and accident conditions and compare against the allowables defined in Step 3.

Step 5. Determine the bending allowables per NUREG/CR-6322. F_b is 0.66 S_y for normal conditions if the cask body is determined in Step 2a to be a compact section, and fS_y for accident conditions, where f is the shape factor. The shape factor is calculated using the following method:

f = Shape Factor = $Ay_1/(I/c)$,

where

A = area of cavity liner and FSS structure cross section,

y_1 = distance to centroid of half cross sectional area of cavity liner and FSS structure,

c = distance to extreme fiber of cross section, and

I = moment of inertia of cavity liner and FSS cross section.

Step 6. Combined axial compression and bending. The stresses shall satisfy the following equations, which are taken from NUREG/CR-6322, sections 6.22 and 6.32.

Normal conditions:

$f_a/F_a + C_m (f_b)/\{F_b [1 - (2.15 f_a/F_e)]\} \le 1$, and

$f_a/(0.6S_y) + f_b/F_b \leq 1,$

Accident conditions:

$f_a/F_a + C_m (f_b)/\{F_b [1 - (1.46f_a/F_e)]\} \leq 1$, and

$f_a/(0.6S_y) + f_b/F_b \leq 1,$

where

C_m = 0.85 for members with free end but joint translation permitted,

= 0.6 – 0.4(M_1/M_2) but not less than 0.4, where M_1/M_2 is the ratio of the small-to-larger moments on the fixed ends braced against translation and not subjected to transverse loading between supports.

F_a = allowable axial stress from the expressions given above in step 3,

F_e = Euler buckling stress,

F_b = bending allowable stress from step 5 above,

f_a = axial stress from step 4 above, and

f_b = Maximum bending stress. Either the maximum longitudinal bending stress due to longitudinal bending or the stress intensity at the location of maximum compression due to longitudinal bending and transverse bending, whichever is greater, shall be used.

Step 7. Evaluate the lower legs of the cavity liner and FSS due to a 1-ft and 30-ft side drop as a beam column. The legs are loaded perpendicular to the cask axis from the inertial loading of the DU and contents and laterally from the same loading when the cask impacts in an angular orientation around its axis other than flat. The axial tension due to longitudinal bending of the cask is conservatively ignored. The stresses shall satisfy the following equations, which are taken from NUREG/CR-6322, sections 6.22 and 6.32.

Normal conditions:

$f_a/F_a + C_m (f_b)/\{F_b [1 - (2.15f_a/F_e)]\} \leq 1$, and

$f_a/(0.6S_y) + f_b/F_b \leq 1;$

Accident conditions:

$f_a/F_a + C_m (f_b)/\{F_b [1 - (1.46f_a/F_e)]\} \leq 1$, and

$f_a/(0.6S_y) + f_b/F_b \leq 1,$

where

C_m = 0.85 for members with free end but joint translation permitted,

= $0.6 - 0.4(M_1/M_2)$ but not less than 0.4, where M_1/M_2 is the ratio of the small-to-larger moments on the fixed ends braced against translation and not subjected to transverse loading between supports.

F_a = allowable axial stress from the expressions given above in step 3,

F_e = Euler buckling stress,

F_b = bending allowable stress from step 5 above,

f_a = axial stress from step 4 above, and

f_b = Maximum bending stress. The maximum lateral bending stress due to lateral bending.

2.1.2.6.4 Neutron Shield Outer Shell Assembly. The neutron shield outer shell is anchored to the cask body through the impact limiter support structure. Since the cask body is much stiffer than the outer shell, overall buckling is precluded by the buckling resistance of the cask body. However, the neutron shield shell shall be shown to not buckle due to the maximum normal condition external pressure that occurs when the cask is put into a fuel storage pool. The requirements of ASME Code, Section III, Subsection NB, NB-3133.3 and 3133.5 shall be used.

2.1.2.6.5 Impact Limiter Support Structure Ribs. The impact limiter support structure ribs are subjected to combined axial compression and bending loading when the cask is subjected to the normal condition 1-ft and accident condition 30-ft drops. The combined axial compression and bending criteria defined in Section 2.1.2.6.1 for the cask body shall be used.

2.2 Weight and Center of Gravity

The GA-4 cask has a maximum design weight of 55,000 lbs, which was used in all calculations. A nominal weight breakdown of its components is shown below. The center of gravity (CG) of the cask is 0.57 in. from its geometrical center toward the cask bottom end. As shown in the table, the maximum weight of the contents, including fuel, spacers and NFAH, is 6,648 lb.

TABLE 2.2-1
GA-4 CASK WEIGHT BREAKDOWN BY COMPONENT (LB)

Fuel support structure	751
Cavity liner	1,300
Gamma shield	24,535
Cask wall	6,661
Neutron shield [Proprietary Information]	3,026
Neutron shield structure	1,125
Closure	1,510
Bottom plate/flange	2,647
Impact limiter support structure	1,808
Impact limiters	3,925
Trunnions and lifting sockets	589
Total weight (empty)	47,877
Fuel spacers and NFAH (maximum)	6,648
Total weight (loaded)	54,525
Cask maximum weight per unit length at midspan (lb/in.)	265.2
Cask minimum weight per unit length at midspan (lb/in.)	225.7

THIS PAGE LEFT BLANK INTENTIONALLY

2.3 Mechanical Properties of Materials

The GA-4 cask is fabricated primarily of Type XM-19 austenitic stainless steel, high-strength bolts, aluminum honeycomb, depleted uranium (DU), [**Proprietary Information**] and boron carbide. For analysis, we used the material properties contained in Table 2-3-1 and the following:

1. DU gamma shield (Ref 2.3-1)

   a. 0.2% molybdenum alloy
   b. Density = 0.686 lb/in.^{3}
   c. Coefficient of thermal expansion
      4.5×10^{-6} in./in./°F (mean from room temperature to –20°F)
      6.1×10^{-6} in./in./°F (mean from room temperature to 200°F)
   d. Chemical composition:
      Fe = 150 ppm maximum
      C = 500 ppm maximum
      H = 10 ppm maximum
      Mo = 0.2 to 0.3% wt
      U-235 = less than 0.2%
   e. Minimum mechanical properties (not used; for reference only):
      Yield strength (0.2% offset) = 30 ksi minimum
      Ultimate tensile strength = 75 ksi minimum
      Charpy V-notch impact energy = 6 ft-lb minimum
   f. E = 30×10^6 psi

2. Honeycomb impact limiter

   a. Aluminum
   b.

Crush Strength	Density
1.40 ksi	(10.5 lb/ft^3)
0.73 ksi	(7.9 lb/ft^3)
0.22 ksi	(4.2 lb/ft^3)

   Crush strength varies by ± 12.5% over a temperature range of –20°F to 200°F. See Section 2.10.3.3 for strain rate effect on crush strength.

3. [**Prop. Info.**] neutron shield

[**Proprietary Information**]

[

Proprietary Information

]

4. <u>Criticality poison</u>

   a. Boron carbide (B_4C), B^{10} fraction enriched to 96% minimum
   b. Minimum density = 0.0879 lb/in.^{3} (0.96 of theoretical density)
   c. Coefficient of thermal expansion = 2.7×10^{-6} in./in.-°F (Ref. 2.3-3)

TABLE 2.3-1
MATERIAL PROPERTIES USED IN COMPONENT ANALYSIS

Material Specification	Temperature (°F)	Stress (ksi): Minimum Yield S_y	Stress (ksi): S_m	Stress (ksi): Engineering Ultimate S_u	Density (lb/in.^{3})	Modulus of Elasticity (10^6 psi)	Coefficient of Thermal Expansion (10^{-6} in./in.-°F): Instantaneous	Coefficient of Thermal Expansion (10^{-6} in./in.-°F): Mean from 70°F	Poisson's Ratio
Stainless Steel Type XM-19/FXM-19									
Reference		Table I-2.2[c]	Table I-1.2[c]	Table I-3.2[c]		Table I-6.0[c]	Table I-5.0[c]	Table I-5.0[c]	
Cask body, closure, fuel cavity liner, fuel support structure, port plugs, redundant lifting sockets, neutron shield outer skin, impact limiter, and trunnions SA-240 plate SA-182 forging	−100	--	--	--		29.1	--	8.06[i]	
	70	--	--	--	0.285	28.3	8.24	--	0.3
	100	55.0	33.3	100.0		--	8.35	8.30	
	200	47.0	33.2	99.5		27.6	8.67	8.48	
	300	43.4	31.4	94.3		27.0	8.95	8.65	
	400	40.8	30.2	90.7		26.5	9.21	8.79	
	500	38.8	29.7	89.1		25.8	9.44	8.92	
	600	37.3	29.2	87.8		25.3	9.64	9.03	
	700	36.3	28.8	86.5		24.8	9.82	9.15	
	800	35.3	28.2	84.8		24.1	9.97	9.25	
	900	34.6	--	82.5		--	--	--	
	1000	33.7	--	79.8		--	--	--	

TABLE 2.3-1 (Continued)
MATERIAL PROPERTIES USED IN COMPONENT ANALYSIS

Material Specification	Temperature (°F)	Stress (ksi) Minimum Yield S_y	S_m	Engineering Ultimate S_u	Density (lb/in.^{3})	Modulus of Elasticity (10^6 psi)	Coefficient of Thermal Expansion (10^{-6} in./in.-°F) Instantaneous	Mean from 70°F	Poisson's Ratio
Bolting Material Alloy NO7718									
Reference		(d)	Table I-1.3[a]	Table I-1.3[a]		Table I-6.0[a]	Table I-5.0[a]	Table I-5.0[a]	
Closure and impact limiter attachment bolts SB-637	-100	--	--	--		29.9	--	6.8[b]	
	70	150.0	50.0	185.0	0.296	29.0	7.05	--	0.3
	100	150.0	50.0	--		--	7.12	7.08	
	200	144.0	48.0	176.0[e]		28.3	7.39	7.22	
	300	140.7	46.9	173.0[e]		28.0	7.62	7.33	
	400	138.3	46.1	170.0[e]		27.6	7.84	7.45	
	500	136.8	45.6	169.0[e]		27.1	8.04	7.57	
	800	133.2	44.4	--		25.8	8.55	7.86	
	1000	129.3	43.1	--		24.7	--	8.07	

TABLE 2.3-1 (Continued)
MATERIAL PROPERTIES USED IN COMPONENT ANALYSIS

Material Specification	Temperature (°F)	Stress (ksi): Minimum Yield S_y	Stress (ksi): S_m	Stress (ksi): Engineering Ultimate S_u	Density (lb/in.^{3})	Modulus of Elasticity (10^6 psi)	Coefficient of Thermal Expansion (10^{-6} in./in.–°F): Instantaneous	Coefficient of Thermal Expansion (10^{-6} in./in.–°F): Mean from 70°F	Poisson's Ratio
Impact Limiter Material, Type XM-11									
Reference		(f)	(g)	(f)		(f)		(f)	
Impact limiter face sheets SA-412	70	50.0	--	90.0	.283	28.9	--	--	0.3
	200	39.8	26.6	81.4		27.8	--	9.3[h]	

[a]For temperatures above 800°F, properties were obtained from ASME Nuclear Components Code, Case N-47-23. Properties for temperatures 800°F and lower are from ASME Code, Section III, Division 1, Appendices.

[b]Obtained by extrapolation.

[c]Properties were taken from ASME Code, Section III, Division 1, Appendices.

[d]Yield stress of bolting material is 3 x S_m.

[e]S_u for bolting material at specified temperatures was obtained by scaling the curve in Ref. 2.3-2, p. 14, based on minimum ASME specified S_u at room temperature.

[f]Properties above 70°F taken from manufacturer's data and factored to obtain minimum.

[g]S_m equal to 2/3 S_y.

[h]The coefficient of thermal expansion for type XM-11 material is the mean from 80°F rather than the mean from 70°F.

[i]The value shown is for –40°F.

THIS PAGE LEFT BLANK INTENTIONALLY

2.4 General Standards for All Packages

The GA-4 shipping cask has been evaluated and found to comply with the general standards for all packages contained in 10 CFR Part 71.43. These standards address minimum package dimensions, positive closure, tamper-resistance of the package, chemical and galvanic reactions, valves and venting, resistance to normal conditions of transport, and maximum package surface temperatures. Compliance with these requirements and with the lifting and tiedown standards are discussed below.

2.4.1 Minimum Package Size

A complete package description is contained in Section 1.2. The major overall minimum outside dimensions of the GA-4 shipping cask are 39.75 in. dia. x 233.95 in. long. This exceeds the required minimum dimensions of 4.0 in. specified in 10 CFR Part 71.43.

2.4.2 Tamper-proof Feature

A wire tamper-indicating device is incorporated between the cask and each impact limiter. An intact seal will be positive evidence that the containment vessel has not been opened by unauthorized persons.

2.4.3 Positive Closure

10 CFR Part 71.43 specifies that the package be equipped with a positive closure that will prevent unintentional opening. The closure and penetrations on the GA-4 cask cannot be opened without unbolting and removing a 2,000-lb impact limiter and either the 12 1.00-in. closure bolts, the gas sample port and cap, or the drain valve and cover mentioned in Section 2.4.5.

2.4.4 Chemical and Galvanic Reactions

The packaging system has been evaluated for susceptibility to chemical or galvanic corrosion between individual components, between the contents and components, and between the environment and components.

The primary structural material for the packaging system is Type XM-19 stainless steel, which is corrosion-resistant in regard both to the cask contents and to the environment. None of the other cask components react with Type XM-19 stainless steel. Other components are the impact limiter and closure bolts, which are Alloy N07718; the gas sample port retainer and drain valve cover, which are 304 or XM-19 stainless steel; and the gas sample port and drain valve (and their quick-disconnects) and the drain port plug, all of which are 304 or 316 stainless steel. All of these metals have very similar potentials and will not corrode due to galvanic action.

Non-metallic components which may be exposed to the environment include the ethylene-propylene O-ring seals on the gas sample port, drain valve, drain port plug, and closure; the nitroxile wiper seal on the drain valve; a silicone lubricant coating the O-ring seals; an anti-seize compound applied to bolt threads; and an adhesive used to bind the quick-disconnect nipples to the gas sample port and drain valve.

The cask environment includes ambient air, water, helium, and boric acid from the fuel pool water. All of the materials discussed above are compatible with the environment and will not degrade or react. No paints are used anywhere on the cask. In particular, there are no zinc-coated surfaces which may liberate hydrogen gas from the boric acid in the fuel pool water.

The neutron shield [Proprietary Information] utilizing XM-19 or 300-series stainless steel. The steels will not degrade or corrode when exposed to the neutron shield.

Other packaging system components which are not constructed of Type XM-19 stainless steel are maintained in a moisture-free environment to inhibit galvanic or other corrosive reactions. The impact limiters, which are made of aluminum, are enclosed in an all-welded XM-11 stainless steel skin on the outside and an XM-19 stainless steel housing on the inside. The DU gamma shield is contained by the all-welded Type XM-19 cask body. Corrosion of the DU metal is prevented by backfilling the DU cavity with helium and welding a cover over the backfilling port. Operational temperatures of the DU for all conditions are typically 200°F or less and are well below 806°F, the lowest temperature cited in Ref. 2.4-1 at which a eutectic was observed to form. The tungsten shields protect the DU during the final closing welds of the shells, to prevent any eutectic from forming and to assure that the welds are sound. This shield configuration was developed and verified in the construction of the half-scale model.

All exposed external surfaces of the cask are corrosion resistant Type XM-19 stainless steel. This material has good resistance to intergranular corrosion since it is partially stabilized and has a maximum carbon content of only 0.06%. In addition, the FSS, the cavity liner, the cask body flange and cask body walls are not exposed to the external environment that could contain corrosive media (e.g., chlorides and sulfides).

2.4.5 Valves and Venting

The rules of 10 CFR Part 71.43 require that if the failure of a package valve or other device would allow radioactive contents to escape, the device must be protected against unauthorized operation and, except for a pressure relief device, must be provided with an enclosure to retain leakage. In addition, the package must not incorporate any feature intended to allow continuous venting.

The cavity gas sample port and drain valve are located in the thick closure plate and bottom plate. They are closed and covered with caps for shipment. They are protected from unauthorized operation because they are fully recessed and are covered by the 2000-lb impact limiters.

The gas sample port and drain valve are part of the containment system and are designed with sufficient structural integrity to withstand both normal and hypothetical accident conditions of transport. The design of the gas sample port, the drain valve, the closure seals, and the related passageways ensures that the total failure of any one O-ring seal will not result in the escape of internal cavity contents. Caps at the entrance to the gas sample port and drain valve prevent the plugs from inadvertently backing out.

2.4.6 Special Requirement for Irradiated Nuclear Fuel Shipments

This loading condition is a special requirement in 10 CFR Part 71.61 for packages used for irradiated nuclear fuel shipments. The cask is to be designed so that its undamaged containment system can withstand an external water pressure of 290 ksi without cask collapse, buckling, or inleakage of water.

2.4.6.1 Collapse Analysis. A three-dimensional (3-D) finite-element model representing the GA-4 cask was used to establish the stress state under the 290 psi external water pressure loading condition. This section presents the stresses for the containment boundary. A complete discussion of the analysis is presented in Section 2.10.2.

Tables 2.4-1 through 2.4-5 present a summary of the stress results for the flat model locations shown in Fig. 2.4-1. The results for the corner model are not presented because they were the same as those for the flat model. As shown in Tables 2.4-1 through 2.4-5, the stresses are much less than the allowables, providing a large design margin, where design margin (D.M.) is defined as

D.M. = (allowable stress/actual stress intensity) – 1

The allowable stresses are the same as for hypothetical accident conditions from Table 2.1-4. Therefore, the cask will not rupture or tear during a 290 psi external water pressure loading.

2.4.6.2 Buckling. The containment boundary has been shown to not buckle due to the 290 psi external pressure load. Section 2.10.7.2 contains a complete discussion of the analysis. The analysis uses the buckling criteria from Section 2.1.2.6.2.

The external water pressure exerts a membrane compression in the flat wall circumferential direction and bending due to the pressure on the flat wall. The minimum design margin against buckling for a combination of axial compression and bending is 2.06.

2.4.6.3 Inleakage of Water. The analyses in Sections 2.4.6.1 and 2.4.6.2 show that the stresses in the entire containment boundary are well below yield and that it has a large design margin against buckling. Therefore, there is no permanent deformation of the containment boundary that could affect the effectiveness of the primary seals and there will be no inleakage of water.

TABLE 2.4-1 CONTAINMENT WALL STRESSES (ksi), FLAT MODEL, EXTERNAL PRESSURE OF 290 psi (T = 200°F), SECTION A															
Stress Location		Node	Combined Stress Components						Principal Stresses			Stress Int.	Stress Type	Stress Limit	Design Margin
			Sx	Sy	Sz	Sxy	Syz	Sxz	S1	S2	S3				
1	Inside	1383	-0.85	-0.60	-6.61	-0.06	-1.59	0.24	-0.19	-0.86	-7.01	6.82	Pm+Pb	99.95	13.65
	Middle	1390	-1.89	-0.41	-1.85	-0.09	-0.88	-0.01	0.01	-1.89	-2.28	2.29	Pm	69.65	29.42
	Outside	1397	-3.13	-0.33	2.48	-0.09	-0.65	-0.29	2.64	-0.46	-3.15	5.78	Pm+Pb	99.95	16.28
2	Inside	1417	-2.92	-0.23	-2.05	0.62	-0.24	2.54	0.22	-0.28	-5.15	5.37	Pm+Pb	99.95	17.63
	Middle	1419	-1.24	-0.27	-0.63	0.27	-0.07	-0.21	-0.17	-0.62	-1.35	1.18	Pm	69.65	57.89
	Outside	1421	0.14	-0.33	0.59	0.08	0.22	-2.83	3.21	-0.32	-2.49	5.70	Pm+Pb	99.95	16.52
3	Inside	1466	-2.64	-2.64	-1.47	2.55	0.23	0.23	-0.02	-1.54	-5.18	5.17	Pm+Pb	99.95	18.34
	Middle	1465	-0.60	-0.60	-0.80	0.20	0.25	0.25	-0.20	-0.80	-1.00	0.81	Pm	69.65	85.47
	Outside	1464	0.92	0.92	-0.49	-1.49	0.24	0.24	2.41	-0.19	-0.86	3.27	Pm+Pb	99.95	29.53
4	Inside	9981	-0.23	-2.92	-2.05	0.62	2.54	-0.24	0.22	-0.28	-5.15	5.37	Pm+Pb	99.95	17.63
	Middle	9983	-0.27	-1.24	-0.63	0.27	-0.21	-0.07	-0.17	-0.62	-1.35	1.18	Pm	69.65	57.89
	Outside	9985	-0.33	0.14	0.59	0.08	-2.83	0.22	3.21	-0.32	-2.49	5.70	Pm+Pb	99.95	16.52
5	Inside	9947	-0.60	-0.85	-6.61	0.00	0.00	-1.59	-0.21	-0.85	-7.00	6.79	Pm+Pb	99.95	13.71
	Middle	9954	-0.41	-1.89	-1.85	0.00	0.00	-0.88	0.01	-1.89	-2.27	2.28	Pm	69.65	29.54
	Outside	9961	-0.33	-3.13	2.48	0.00	0.00	-0.65	2.62	-0.47	-3.13	5.75	Pm+Pb	99.95	16.38
6	Inside	27109	-0.23	-2.92	-2.05	-0.62	-2.54	-0.24	0.22	-0.28	-5.15	5.37	Pm+Pb	99.95	17.63
	Middle	27111	-0.27	-1.24	-0.63	-0.27	0.21	-0.07	-0.17	-0.62	-1.35	1.18	Pm	69.65	57.89
	Outside	27113	-0.33	0.14	0.59	-0.08	2.83	0.22	3.21	-0.32	-2.49	5.70	Pm+Pb	99.95	16.52
7	Inside	18594	-2.64	-2.64	-1.47	-2.55	-0.23	0.23	-0.02	-1.54	-5.18	5.17	Pm+Pb	99.95	18.34
	Middle	18593	-0.60	-0.60	-0.80	-0.20	-0.25	0.25	-0.20	-0.80	-1.00	0.81	Pm	69.65	85.47
	Outside	18592	0.92	0.92	-0.49	1.49	-0.24	0.24	2.41	-0.19	-0.86	3.27	Pm+Pb	99.95	29.53
8	Inside	18545	-2.92	-0.23	-2.05	-0.62	0.24	2.54	0.22	-0.28	-5.15	5.37	Pm+Pb	99.95	17.63
	Middle	18547	-1.24	-0.27	-0.63	-0.27	0.07	-0.21	-0.17	-0.62	-1.35	1.18	Pm	69.65	57.89
	Outside	18549	0.14	-0.33	0.59	-0.08	-0.22	-2.83	3.21	-0.32	-2.49	5.70	Pm+Pb	99.95	16.52
9	Inside	18511	-0.85	-0.60	-6.61	0.06	1.59	0.24	-0.19	-0.86	-7.01	6.82	Pm+Pb	99.95	13.65
	Middle	18518	-1.89	-0.41	-1.85	0.09	0.88	-0.01	0.01	-1.89	-2.28	2.29	Pm	69.65	29.42
	Outside	18525	-3.13	-0.33	2.48	0.09	0.65	-0.29	2.64	-0.46	-3.15	5.78	Pm+Pb	99.95	16.28

FPOUTER.TBL

TABLE 2.4-2 CONTAINMENT WALL STRESSES (ksi), FLAT MODEL, EXTERNAL PRESSURE OF 290 psi (T = 200°F), SECTION B

Stress Location		Node	Combined Stress Components						Principal Stresses			Stress Int.	Stress Type	Stress Limit	Design Margin
			Sx	Sy	Sz	Sxy	Syz	Sxz	S1	S2	S3				
1	Inside	2748	11.14	-0.05	5.08	0.08	-0.08	0.15	11.14	5.08	-0.05	11.19	Pm+Pb	99.95	7.93
	Middle	2755	-2.49	-0.26	-1.44	0.10	-0.11	-0.01	-0.24	-1.45	-2.49	2.25	Pm	69.65	29.96
	Outside	2762	-16.06	-0.50	-7.93	0.24	-0.01	-0.19	-0.50	-7.92	-16.06	15.57	Pm+Pb	99.95	5.42
2	Inside	2965	-8.88	-0.32	-2.71	1.83	0.12	1.40	0.12	-2.51	-9.53	9.64	Pm+Pb	99.95	9.36
	Middle	2967	-2.01	0.12	-1.09	1.29	0.22	-0.15	0.74	-1.07	-2.65	3.39	Pm	69.65	19.55
	Outside	2969	3.10	0.41	-0.09	0.59	-0.12	-1.46	3.77	0.32	-0.67	4.43	Pm+Pb	99.95	21.54
3	Inside	3053	-11.37	-11.37	-7.22	10.32	0.13	0.13	-1.05	-7.22	-21.68	20.64	Pm+Pb	99.95	3.84
	Middle	3052	-1.44	-1.44	-1.13	0.41	0.10	0.10	-0.92	-1.23	-1.85	0.93	Pm	69.65	74.10
	Outside	3051	5.70	5.70	3.28	-6.66	0.11	0.11	12.36	3.29	-0.97	13.33	Pm+Pb	99.95	6.50
4	Inside	11529	-0.32	-8.88	-2.71	1.83	1.40	0.12	0.12	-2.51	-9.53	9.64	Pm+Pb	99.95	9.36
	Middle	11531	0.12	-2.01	-1.09	1.29	-0.15	0.22	0.74	-1.07	-2.65	3.39	Pm	69.65	19.55
	Outside	11533	0.41	3.10	-0.09	0.59	-1.46	-0.12	3.77	0.32	-0.67	4.43	Pm+Pb	99.95	21.54
5	Inside	11312	-0.05	11.14	5.08	0.00	0.00	-0.08	11.14	5.08	-0.05	11.18	Pm+Pb	99.95	7.94
	Middle	11319	-0.26	-2.49	-1.44	0.00	0.00	-0.11	-0.25	-1.45	-2.49	2.24	Pm	69.65	30.08
	Outside	11326	-0.50	-16.06	-7.93	0.00	0.00	-0.01	-0.50	-7.93	-16.06	15.56	Pm+Pb	99.95	5.42
6	Inside	28657	-0.32	-8.88	-2.71	-1.83	-1.40	0.12	0.12	-2.51	-9.53	9.64	Pm+Pb	99.95	9.36
	Middle	28659	0.12	-2.01	-1.09	-1.29	0.15	0.22	0.74	-1.07	-2.65	3.39	Pm	69.65	19.55
	Outside	28661	0.41	3.10	-0.09	-0.59	1.46	-0.12	3.77	0.32	-0.67	4.43	Pm+Pb	99.95	21.54
7	Inside	20181	-11.37	-11.37	-7.22	-10.32	-0.13	0.13	-1.05	-7.22	-21.68	20.64	Pm+Pb	99.95	3.84
	Middle	20180	-1.44	-1.44	-1.13	-0.41	-0.10	0.10	-0.92	-1.23	-1.85	0.93	Pm	69.65	74.10
	Outside	20179	5.70	5.70	3.28	6.66	-0.11	0.11	12.36	3.29	-0.97	13.33	Pm+Pb	99.95	6.50
8	Inside	20093	-8.88	-0.32	-2.71	-1.83	-0.12	1.40	0.12	-2.51	-9.53	9.64	Pm+Pb	99.95	9.36
	Middle	20095	-2.01	0.12	-1.09	-1.29	-0.22	-0.15	0.74	-1.07	-2.65	3.39	Pm	69.65	19.55
	Outside	20097	3.10	0.41	-0.09	-0.59	0.12	-1.46	3.77	0.32	-0.67	4.43	Pm+Pb	99.95	21.54
9	Inside	19876	11.14	-0.05	5.08	-0.08	0.08	0.15	11.14	5.08	-0.05	11.19	Pm+Pb	99.95	7.93
	Middle	19883	-2.49	-0.26	-1.44	-0.10	0.11	-0.01	-0.24	-1.45	-2.49	2.25	Pm	69.65	29.96
	Outside	19890	-16.06	-0.50	-7.93	-0.24	0.01	-0.19	-0.50	-7.92	-16.06	15.57	Pm+Pb	99.95	5.42

FPOUTER.TBL

TABLE 2.4-3 CONTAINMENT WALL STRESSES (ksi), FLAT MODEL, EXTERNAL PRESSURE OF 290 psi (T = 200°F), SECTION C

Stress Location		Node	Combined Stress Components						Principal Stresses			Stress Int.	Stress Type	Stress Limit	Design Margin
			Sx	Sy	Sz	Sxy	Syz	Sxz	S1	S2	S3				
1	Inside	2937	12.99	-0.11	3.38	0.11	0.00	0.00	12.99	3.38	-0.11	13.10	Pm+Pb	99.95	6.63
	Middle	2944	-2.64	-0.15	-1.31	0.11	0.00	0.00	-0.14	-1.31	-2.65	2.51	Pm	69.65	26.79
	Outside	2951	-18.27	-0.18	-6.01	0.11	0.00	0.00	-0.18	-6.01	-18.27	18.09	Pm+Pb	99.95	4.53
2	Inside	3019	-10.84	-0.44	-3.86	2.16	0.00	-0.01	-0.01	-3.86	-11.27	11.25	Pm+Pb	99.95	7.88
	Middle	3021	-2.05	-0.44	-1.22	1.45	0.00	0.00	0.42	-1.22	-2.90	3.32	Pm	69.65	19.98
	Outside	3023	4.65	-0.51	0.77	0.90	0.00	0.00	4.80	0.77	-0.67	5.47	Pm+Pb	99.95	17.28
3	Inside	3188	-13.19	-13.19	-8.39	11.82	0.00	0.00	-1.37	-8.39	-25.01	23.64	Pm+Pb	99.95	3.23
	Middle	3187	-1.35	-1.35	-1.28	0.19	0.00	0.00	-1.16	-1.28	-1.54	0.38	Pm	69.65	181.71
	Outside	3186	6.97	6.97	3.71	-7.97	0.00	0.00	14.93	3.71	-1.00	15.93	Pm+Pb	99.95	5.27
4	Inside	11583	-0.44	-10.84	-3.86	2.16	-0.01	0.00	-0.01	-3.86	-11.27	11.25	Pm+Pb	99.95	7.88
	Middle	11585	-0.44	-2.05	-1.22	1.45	0.00	0.00	0.42	-1.22	-2.90	3.32	Pm	69.65	19.98
	Outside	11587	-0.51	4.65	0.77	0.90	0.00	0.00	4.80	0.77	-0.67	5.47	Pm+Pb	99.95	17.28
5	Inside	11501	-0.11	12.99	3.38	0.00	0.00	0.00	12.99	3.38	-0.11	13.10	Pm+Pb	99.95	6.63
	Middle	11508	-0.15	-2.64	-1.31	0.00	0.00	0.00	-0.14	-1.31	-2.64	2.50	Pm	69.65	26.90
	Outside	11515	-0.18	-18.27	-6.01	0.00	0.00	0.00	-0.18	-6.01	-18.27	18.09	Pm+Pb	99.95	4.53
6	Inside	28711	-0.44	-10.84	-3.86	-2.16	0.01	0.00	-0.01	-3.86	-11.27	11.25	Pm+Pb	99.95	7.88
	Middle	28713	-0.44	-2.05	-1.22	-1.45	0.00	0.00	0.42	-1.22	-2.90	3.32	Pm	69.65	19.98
	Outside	28715	-0.51	4.65	0.77	-0.90	0.00	0.00	4.80	0.77	-0.67	5.47	Pm+Pb	99.95	17.28
7	Inside	20316	-13.19	-13.19	-8.39	-11.82	0.00	0.00	-1.37	-8.39	-25.01	23.64	Pm+Pb	99.95	3.23
	Middle	20315	-1.35	-1.35	-1.28	-0.19	0.00	0.00	-1.16	-1.28	-1.54	0.38	Pm	69.65	181.71
	Outside	20314	6.97	6.97	3.71	7.97	0.00	0.00	14.93	3.71	-1.00	15.93	Pm+Pb	99.95	5.27
8	Inside	20147	-10.84	-0.44	-3.86	-2.16	0.00	-0.01	-0.01	-3.86	-11.27	11.25	Pm+Pb	99.95	7.88
	Middle	20149	-2.05	-0.44	-1.22	-1.45	0.00	0.00	0.42	-1.22	-2.90	3.32	Pm	69.65	19.98
	Outside	20151	4.65	-0.51	0.77	-0.90	0.00	0.00	4.80	0.77	-0.67	5.47	Pm+Pb	99.95	17.28
9	Inside	20065	12.99	-0.11	3.38	-0.11	0.00	0.00	12.99	3.38	-0.11	13.10	Pm+Pb	99.95	6.63
	Middle	20072	-2.64	-0.15	-1.31	-0.11	0.00	0.00	-0.14	-1.31	-2.65	2.51	Pm	69.65	26.79
	Outside	20079	-18.27	-0.18	-6.01	-0.11	0.00	0.00	-0.18	-6.01	-18.27	18.09	Pm+Pb	99.95	4.53

TABLE 2.4-4 CONTAINMENT WALL STRESSES (ksi), FLAT MODEL, EXTERNAL PRESSURE OF 290 psi (T = 200°F), SECTION D

Stress Location		Node	Combined Stress Components						Principal Stresses			Stress Int.	Stress Type	Stress Limit	Design Margin
			Sx	Sy	Sz	Sxy	Syz	Sxz	S1	S2	S3				
1	Inside	3399	12.98	-0.11	3.38	0.11	0.00	0.00	12.98	3.38	-0.11	13.09	Pm+Pb	99.95	6.63
	Middle	3406	-2.64	-0.15	-1.31	0.11	0.00	0.00	-0.14	-1.31	-2.65	2.51	Pm	69.65	26.79
	Outside	3413	-18.26	-0.18	-6.01	0.11	0.00	0.00	-0.18	-6.01	-18.26	18.08	Pm+Pb	99.95	4.53
2	Inside	3481	-10.83	-0.44	-3.86	2.15	0.00	0.00	-0.01	-3.86	-11.26	11.25	Pm+Pb	99.95	7.89
	Middle	3483	-2.05	-0.44	-1.22	1.45	0.00	0.00	0.42	-1.22	-2.90	3.32	Pm	69.65	19.98
	Outside	3485	4.64	-0.51	0.76	0.90	0.00	0.00	4.80	0.76	-0.67	5.46	Pm+Pb	99.95	17.30
3	Inside	3650	-13.18	-13.18	-8.38	11.82	0.00	0.00	-1.37	-8.38	-25.00	23.63	Pm+Pb	99.95	3.23
	Middle	3649	-1.35	-1.35	-1.29	0.19	0.00	0.00	-1.16	-1.29	-1.54	0.38	Pm	69.65	181.23
	Outside	3648	6.96	6.96	3.70	-7.96	0.00	0.00	14.92	3.70	-1.00	15.92	Pm+Pb	99.95	5.28
4	Inside	12045	-0.44	-10.83	-3.86	2.15	0.00	0.00	-0.01	-3.86	-11.26	11.25	Pm+Pb	99.95	7.89
	Middle	12047	-0.44	-2.05	-1.22	1.45	0.00	0.00	0.42	-1.22	-2.90	3.32	Pm	69.65	19.98
	Outside	12049	-0.51	4.64	0.76	0.90	0.00	0.00	4.80	0.76	-0.67	5.46	Pm+Pb	99.95	17.30
5	Inside	11963	-0.11	12.98	3.38	0.00	0.00	0.00	12.98	3.38	-0.11	13.09	Pm+Pb	99.95	6.64
	Middle	11970	-0.15	-2.64	-1.31	0.00	0.00	0.00	-0.15	-1.31	-2.64	2.50	Pm	69.65	26.90
	Outside	11977	-0.18	-18.26	-6.01	0.00	0.00	0.00	-0.18	-6.01	-18.26	18.08	Pm+Pb	99.95	4.53
6	Inside	29173	-0.44	-10.83	-3.86	-2.15	0.00	0.00	-0.01	-3.86	-11.26	11.25	Pm+Pb	99.95	7.89
	Middle	29175	-0.44	-2.05	-1.22	-1.45	0.00	0.00	0.42	-1.22	-2.90	3.32	Pm	69.65	19.98
	Outside	29177	-0.51	4.64	0.76	-0.90	0.00	0.00	4.80	0.76	-0.67	5.46	Pm+Pb	99.95	17.30
7	Inside	20778	-13.18	-13.18	-8.38	-11.82	0.00	0.00	-1.37	-8.38	-25.00	23.63	Pm+Pb	99.95	3.23
	Middle	20777	-1.35	-1.35	-1.29	-0.19	0.00	0.00	-1.16	-1.29	-1.54	0.38	Pm	69.65	181.23
	Outside	20776	6.96	6.96	3.70	7.96	0.00	0.00	14.92	3.70	-1.00	15.92	Pm+Pb	99.95	5.28
8	Inside	20609	-10.83	-0.44	-3.86	-2.15	0.00	0.00	-0.01	-3.86	-11.26	11.25	Pm+Pb	99.95	7.89
	Middle	20611	-2.05	-0.44	-1.22	-1.45	0.00	0.00	0.42	-1.22	-2.90	3.32	Pm	69.65	19.98
	Outside	20613	4.64	-0.51	0.76	-0.90	0.00	0.00	4.80	0.76	-0.67	5.46	Pm+Pb	99.95	17.30
9	Inside	20527	12.98	-0.11	3.38	-0.11	0.00	0.00	12.98	3.38	-0.11	13.09	Pm+Pb	99.95	6.63
	Middle	20534	-2.64	-0.15	-1.31	-0.11	0.00	0.00	-0.14	-1.31	-2.65	2.51	Pm	69.65	26.79
	Outside	20541	-18.26	-0.18	-6.01	-0.11	0.00	0.00	-0.18	-6.01	-18.26	18.08	Pm+Pb	99.95	4.53

FPOUTER.TBL

TABLE 2.4-5 CONTAINMENT WALL STRESSES (ksi), FLAT MODEL, EXTERNAL PRESSURE OF 290 psi (T = 200°F), SECTION E

Stress Location		Node	Combined Stress Components						Principal Stresses			Stress Int.	Stress Type	Stress Limit	Design Margin
			Sx	Sy	Sz	Sxy	Syz	Sxz	S1	S2	S3				
1	Inside	3861	12.98	-0.11	3.39	0.11	0.00	0.00	12.98	3.39	-0.11	13.09	Pm+Pb	99.95	6.64
	Middle	3868	-2.64	-0.15	-1.31	0.11	0.00	0.00	-0.14	-1.31	-2.65	2.51	Pm	69.65	26.79
	Outside	3875	-18.26	-0.18	-6.01	0.11	0.00	0.00	-0.18	-6.01	-18.26	18.08	Pm+Pb	99.95	4.53
2	Inside	3943	-10.83	-0.44	-3.86	2.15	0.00	0.00	-0.01	-3.86	-11.26	11.25	Pm+Pb	99.95	7.89
	Middle	3945	-2.05	-0.44	-1.22	1.45	0.00	0.00	0.42	-1.22	-2.90	3.32	Pm	69.65	19.98
	Outside	3947	4.64	-0.51	0.76	0.90	0.00	0.00	4.80	0.76	-0.67	5.46	Pm+Pb	99.95	17.30
3	Inside	4112	-13.18	-13.18	-8.38	11.82	0.00	0.00	-1.37	-8.38	-25.00	23.63	Pm+Pb	99.95	3.23
	Middle	4111	-1.35	-1.35	-1.29	0.19	0.00	0.00	-1.16	-1.29	-1.54	0.38	Pm	69.65	181.23
	Outside	4110	6.96	6.96	3.70	-7.96	0.00	0.00	14.92	3.70	-1.00	15.92	Pm+Pb	99.95	5.28
4	Inside	12507	-0.44	-10.83	-3.86	2.15	0.00	0.00	-0.01	-3.86	-11.26	11.25	Pm+Pb	99.95	7.89
	Middle	12509	-0.44	-2.05	-1.22	1.45	0.00	0.00	0.42	-1.22	-2.90	3.32	Pm	69.65	19.98
	Outside	12511	-0.51	4.64	0.76	0.90	0.00	0.00	4.80	0.76	-0.67	5.46	Pm+Pb	99.95	17.30
5	Inside	12425	-0.11	12.98	3.39	0.00	0.00	0.00	12.98	3.39	-0.11	13.09	Pm+Pb	99.95	6.64
	Middle	12432	-0.15	-2.64	-1.31	0.00	0.00	0.00	-0.15	-1.31	-2.64	2.50	Pm	69.65	26.90
	Outside	12439	-0.18	-18.26	-6.01	0.00	0.00	0.00	-0.18	-6.01	-18.26	18.08	Pm+Pb	99.95	4.53
6	Inside	29635	-0.44	-10.83	-3.86	-2.15	0.00	0.00	-0.01	-3.86	-11.26	11.25	Pm+Pb	99.95	7.89
	Middle	29637	-0.44	-2.05	-1.22	-1.45	0.00	0.00	0.42	-1.22	-2.90	3.32	Pm	69.65	19.98
	Outside	29639	-0.51	4.64	0.76	-0.90	0.00	0.00	4.80	0.76	-0.67	5.46	Pm+Pb	99.95	17.30
7	Inside	21240	-13.18	-13.18	-8.38	-11.82	0.00	0.00	-1.37	-8.38	-25.00	23.63	Pm+Pb	99.95	3.23
	Middle	21239	-1.35	-1.35	-1.29	-0.19	0.00	0.00	-1.16	-1.29	-1.54	0.38	Pm	69.65	181.23
	Outside	21238	6.96	6.96	3.70	7.96	0.00	0.00	14.92	3.70	-1.00	15.92	Pm+Pb	99.95	5.28
8	Inside	21071	-10.83	-0.44	-3.86	-2.15	0.00	0.00	-0.01	-3.86	-11.26	11.25	Pm+Pb	99.95	7.89
	Middle	21073	-2.05	-0.44	-1.22	-1.45	0.00	0.00	0.42	-1.22	-2.90	3.32	Pm	69.65	19.98
	Outside	21075	4.64	-0.51	0.76	-0.90	0.00	0.00	4.80	0.76	-0.67	5.46	Pm+Pb	99.95	17.30
9	Inside	20989	12.98	-0.11	3.39	-0.11	0.00	0.00	12.98	3.39	-0.11	13.09	Pm+Pb	99.95	6.64
	Middle	20996	-2.64	-0.15	-1.31	-0.11	0.00	0.00	-0.14	-1.31	-2.65	2.51	Pm	69.65	26.79
	Outside	21003	-18.26	-0.18	-6.01	-0.11	0.00	0.00	-0.18	-6.01	-18.26	18.08	Pm+Pb	99.95	4.53

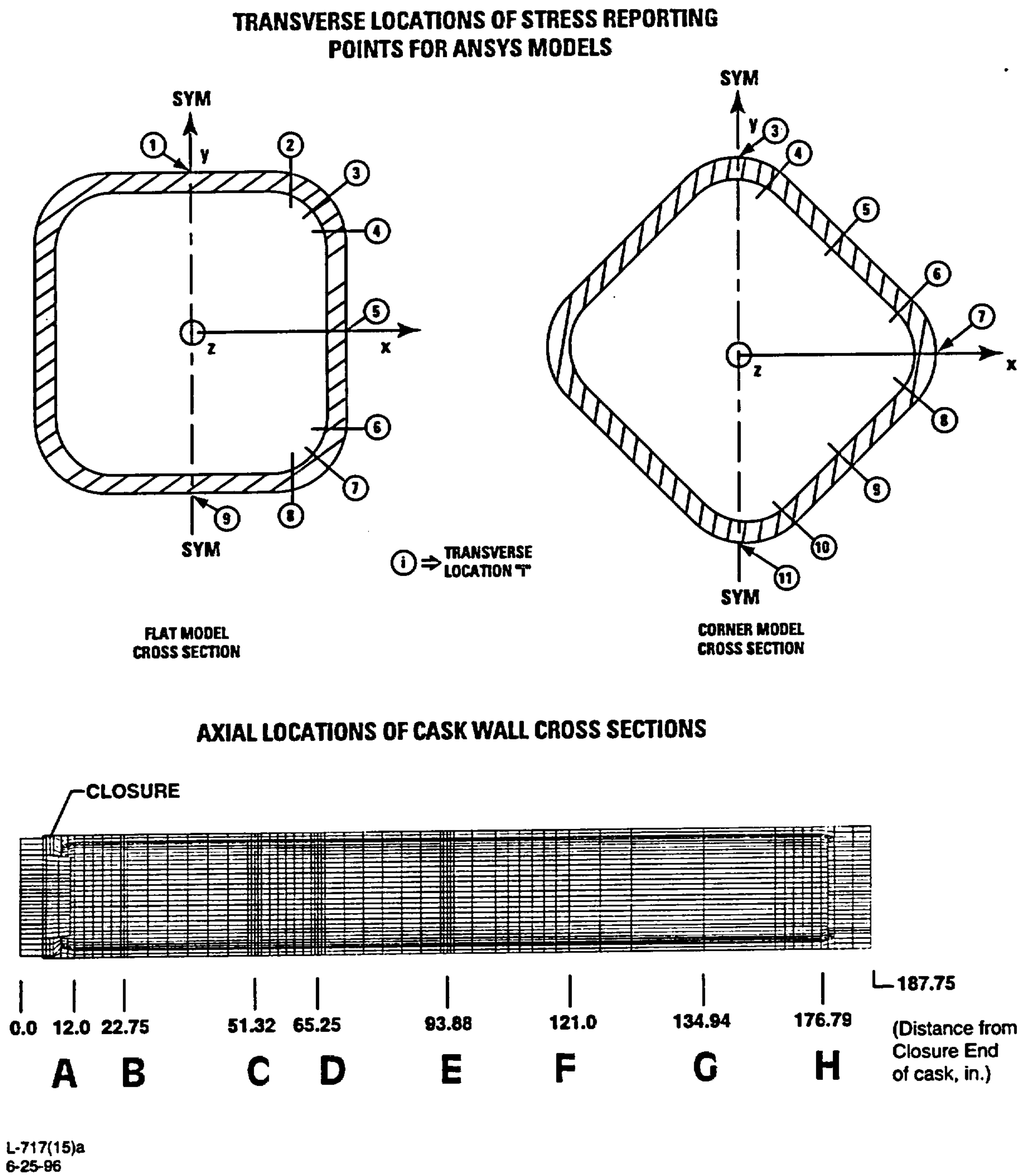

Fig. 2.4-1. Schematic of GA-4 cask wall showing symmetry planes

THIS PAGE LEFT BLANK INTENTIONALLY

2.5 Lifting and Tiedown Standards for All Packages

2.5.1 Lifting Trunnions

The structural evaluation of the trunnions, which follows, is for a longer trunnion of a previous design and is conservative since the bending moments analyzed are higher than in the current design and all other forces remain the same. Figures 2.5-1 through 2.5-3 show the configurations of the design analyzed and the present design. The present design is 1.03 in. shorter in length and has a reduced diameter for the lifting insert.

2.5.1.1 Trunnion Configuration. There are four lifting and tiedown trunnions on the cask. The trunnions are located on each side of the cask in the longitudinal plane of the cask's center of gravity (CG) and far enough from the CG to provide a stable condition while the cask is rotated between vertical and horizontal positions during lifting operations. They are attached to the cask corners in such a way that the cask hangs vertically through the CG on the crane. The front trunnions (the closure end) are used as the primary cask-lifting devices. The lifting device design loads have been doubled from a factor of safety of three (as specified in 10 CFR Part 71.45) or five (ANSI N14.6, Ref. 2.5-1) on the yield strength or ultimate, respectively, to a factor of safety of six and ten, respectively. Therefore, this trunnion pair is designed for critical load lifting of the fully loaded cask as described in ANSI N14.6.

The trunnions consist of cylinders having a 9.5-in. outside diameter (o.d.) at the outer (tiedown) end and an 11.5-in. o.d. at the connection to the cask (the inner end). An external 0.25-in.-thick sleeve is shrink-fitted on the 9.5-in. o.d. The outer end has an inside diameter (i.d.) of 6.0 in. (was 7.5 in.). Inside is a lifting insert as shown in Fig. 2.5-1. The ledge between the 10.0-in. sleeve and the 11.5-in. cylinder provides the bearing surface for the laterally applied tiedown loading (compression only). The ledge is 2.97 in. (was 4.00 in.) outboard of the cask's outer surface. The trunnions have two gussets oriented along the longitudinal axis (see Fig. 2.5-2) in addition to a weld buildup at the connection between the trunnion and the cask wall.

The 9.5-in. outer cylinder is offset 0.75 in. on the bottom trunnions, as shown in Fig. 2.5-3. This geometric offset provides load eccentricity to assure correct cask rotation onto the trailer.

2.5.1.2 Lifting Loads. The two lifting positions analyzed are the vertical and horizontal lift. The vertical cask lift utilizes the front two trunnions. All four trunnions are used to lift and move the cask horizontally.

The lifting loads on the front trunnions are computed in the following sections.

Allowable stresses for lifting. The trunnions shall be designed to a factor of safety of six on the yield strength or a factor of safety of ten on the ultimate strength.

Security-Related Information Figure Withheld Under 10 CFR 2.390.

a) Performed analysis using these dimensions

Security-Related Information Figure Withheld Under 10 CFR 2.390.

L-717(12)
8-23-96

b) New trunnion dimensions

Fig. 2.5-1. Front trunnion geometry, axial view

Security-Related Information Figure Withheld Under 10 CFR 2.390.

Fig. 2.5-2. Trunnion geometry, longitudinal view

Security-Related Information Figure Withheld Under 10 CFR 2.390.

Fig. 2.5-3. Rear (lower) trunnion geometry, axial view

For Type XM-19 (at 180°F):

S_y = 48,600 psi
S_u = 99,600 psi

The allowable stresses are

$$\frac{48,600}{6} = 8,100 \text{ psi} \quad \text{or} \quad \frac{99,600}{10} = 9,960 \text{ psi.}$$

This shows that the factor of safety of six against yield strength controls.

2.5.1.2.1 Vertical Lift. The lifting loads on the two front trunnions are computed as follows:

Assumptions:

1. Design weight = 55,000 lb – impact limiters,
= 55,000 lb – 3,900 = 51,100 lb,

2. Assuming a dynamic factor = 1.2, and

3. FS = 6.

Load per trunnion = (FS) (51,100)(1.2)/2
= 184,000 lb.

Using the moment arm representing the length from the support ledge to the applied force:

Forces at section A-A (Fig. 2.5-1),

$M_{A\text{-}A}$ = (3.25 – 1.12) (184,000),
= 392,000 in.-lb,

$F_{lateral}$ = 0,

F_{shear} = 184,000 lb.

2.5.1.2.2 Horizontal Lift. The lifting loads on the four trunnions in the horizontal lifting mode are developed as follows:

Assumptions:

1. Cask design weight = 55,000 lb (this load case includes the impact limiters),

2. Dynamic factor = 1.2, and

3. FS = 6 (conservative since horizontal lift is not considered a critical lift).

Load per trunnion:

Force per trunnion = (FS) (55,000)(1.2)/(4)
= 99,000 lb.

Using the moment arm representing the length from the support ledge to the applied force:

Forces at section A-A (Fig. 2.5-1)

M_{A-A} = (3.25 – 1.12)(99,000),
= 210,870 in.-lb,

$F_{lateral}$ = 0, and

F_{shear} = 99,000 lb.

The load direction in the four-trunnion horizontal lift position is ninety degrees away from the gussets support. This lift produces a heel/toe loading condition from the trunnion on the cask wall flat regions. The ANSYS model, described in Section 2.10.5.1 was used to develop the stresses in the cask under this loading. The highest stress point in the cask was, as mentioned, at the top/bottom position of the trunnion in the cask wall. The combined horizontal lift plus MNOP loading condition stresses are:

Top of trunnion, cask wall stress, P_m+P_b

	Stress (ksi)						
	S_x	S_y	S_z	S_{xy}	S_{yz}	S_{xy}	SI
Hor. lift	–19.01	–10.88	–14.65	14.0	.7	–1.34	
MNOP[(a)]	– .87	– .38	– .28	.69	0.0	0.0	
Total	–19.88	–11.26	–14.93	14.69	.7	–1.34	30.76

Bottom of trunnion, cask wall stress, P_m+P_b

	S_x	S_y	S_z	S_{xy}	S_{yz}	S_{xy}	SI
Hor. lift	19.01	10.88	14.65	14.0	.7	1.34	
MNOP[(a)]	– .87	– .38	– .28	– .69	0.0	0.0	
Total	18.14	10.5	14.37	13.31	.7	1.34	27.86

[(a)] The MNOP values were taken at Section C, stress points 6 and 8, outside, per Section 2.10.6, Table 2.10.6-20.

The minimum design margin in the cask wall, based on the yield strength at 180°F (S_y = 48.6 ksi) is (48.6/30.76) – 1 = + 0.58.

2.5.1.2.3 Results and Conclusions. The tiedown loads studied in Section 2.5.2 are larger than the lifting loads, and produce a higher stress state in the trunnion. The controlling design criterion for both loadings is limited to the yield strength. Therefore, the tiedown loading condition controls the design, and conclusions stated in the tiedown section are applicable to the lifting trunnions.

2.5.2 Tiedown Trunnions

The same trunnions described in the lifting trunnion section are used to support the cask and tie it down to the trailer during normal conditions of transport. The trunnions are welded to the cask and are considered a structural part of the package. They are designed to fail at loads which will not impair the ability of the package to meet other hypothetical accident conditions.

The tiedown system (Figs. 2.5-4 and 2.5-5) consists of four hinged pillow block assemblies (clamps), which are supported by lateral, vertical, and longitudinal braces welded to the trailer. These braces transmit the cask loads to the trailer's main I-beams. The two front pillow block assemblies have elongated openings to accommodate dimensional tolerances and cask longitudinal thermal expansion. Therefore, longitudinal loads are resisted by the bottom-end trunnions. Lateral gaps between the trunnion shoulder and the face of the pillow block assembly accommodate tolerances and lateral thermal expansion of the cask. The pillow block assemblies are each secured by a top-mounted captured bolt, which is designed to enhance remote handling.

The tiedown trunnions are designed not to yield during the 2g vertical, 10g longitudinal, and 5g transverse shock loading defined in 10 CFR Part 71.45b(1).

2.5.2.1 Tiedown Trunnion Loads. The trunnion tiedown loads due to the 2g vertical, 5g lateral, and 10g longitudinal shock loads are computed individually in Sections 2.5.2.1.1 through 2.5.2.1.3 and then combined in Section 2.5.2.1.4. The signs of the individual components are varied to ensure that the peak loads are evaluated. Each component is computed using the cask's 55,000-lb maximum design weight.

The cask tiedown system is designed as follows:

1. Longitudinal loads are taken by the two bottom-end trunnions. The closure-end tiedowns allow free play in the longitudinal direction, whereas the bottom-end tiedowns are snug (Fig. 2.5-5);

2. Lateral loads are taken in compression by two trunnions on the same side of the cask (Fig. 2.5-5); and

3. Vertical loads are taken by all four trunnions.

Figure 2.5-6 is a free-body diagram of the cask showing the tiedown loads, reactions, and the relationship between the trunnion reactions and cask center of gravity (CG). The CG of the cask is located 0.38 in. below the centerline through the trunnions and 0.57 in. aft of the midpoint between the trunnions (i.e., closer to the bottom trunnion).

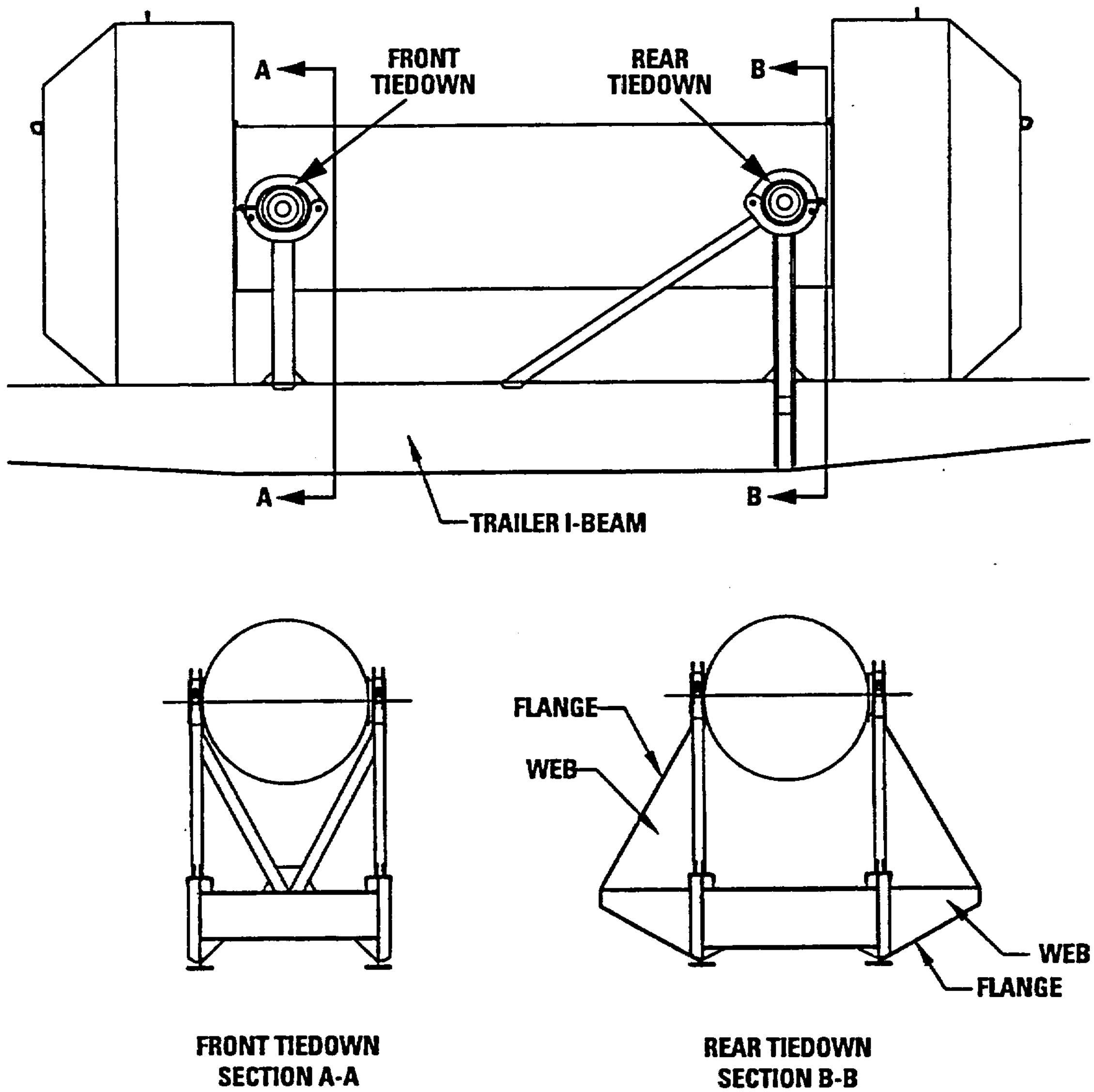

L-717(58)
7-18-96

Fig. 2.5-4. Trailer tiedown system

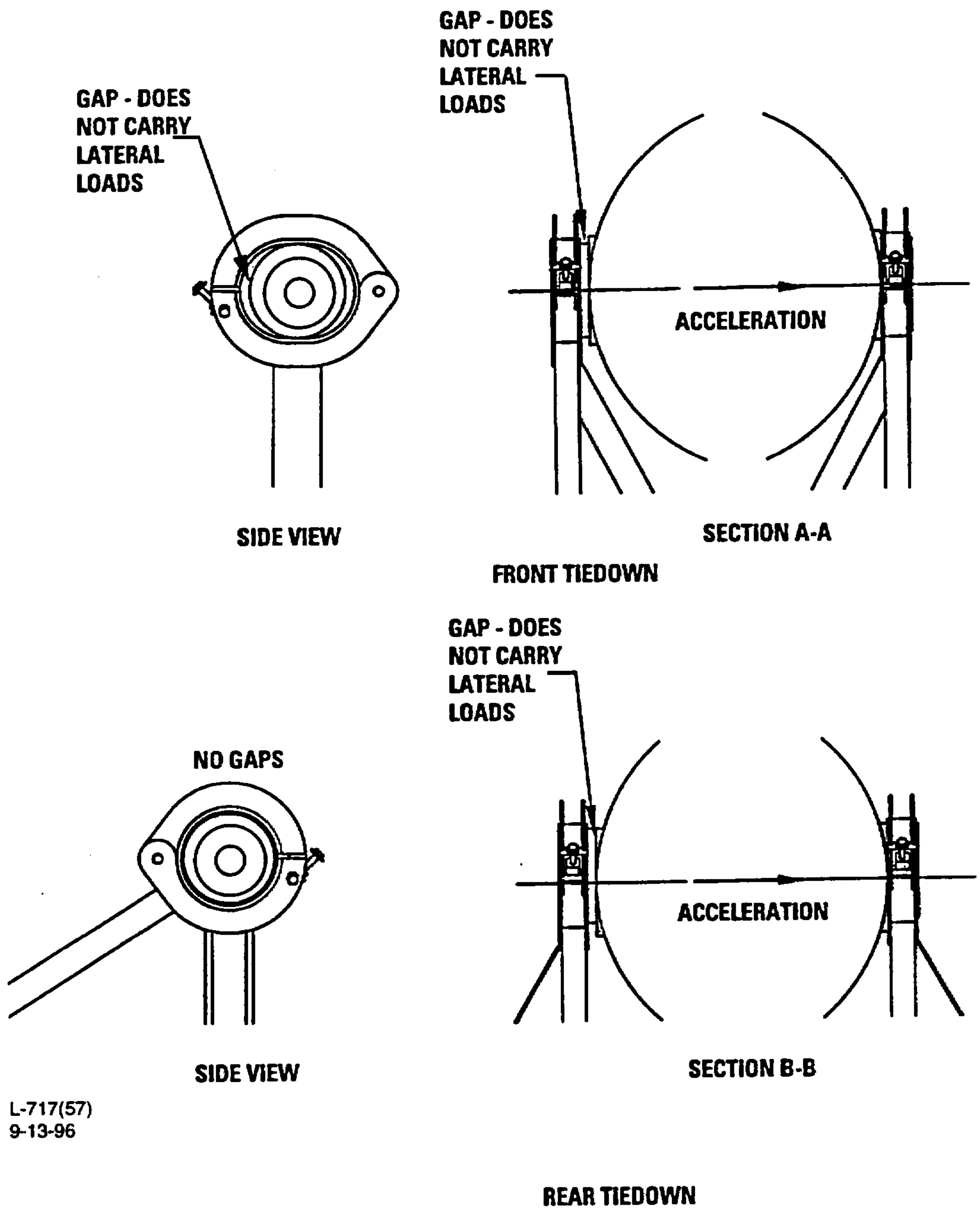

Fig. 2.5-5. Trailer tiedown system, pillow blocks

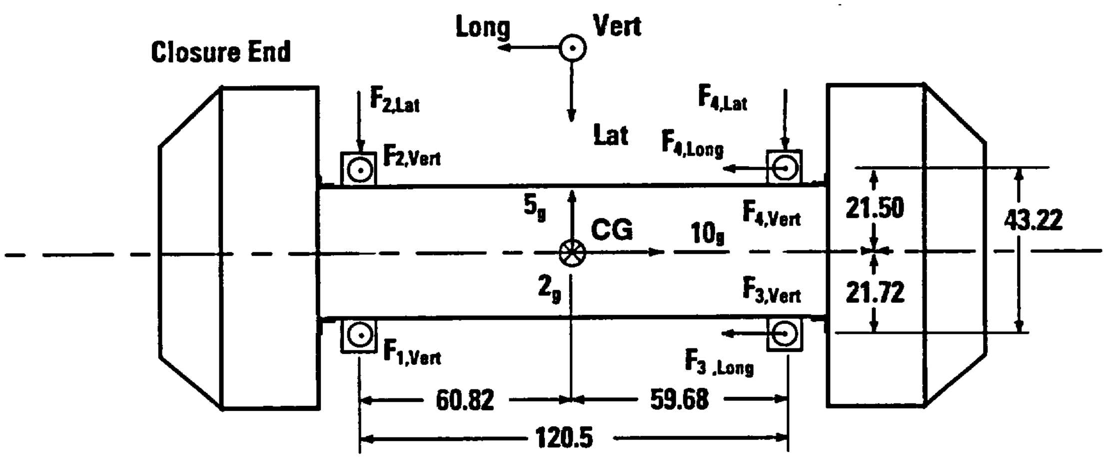

TOP VIEW

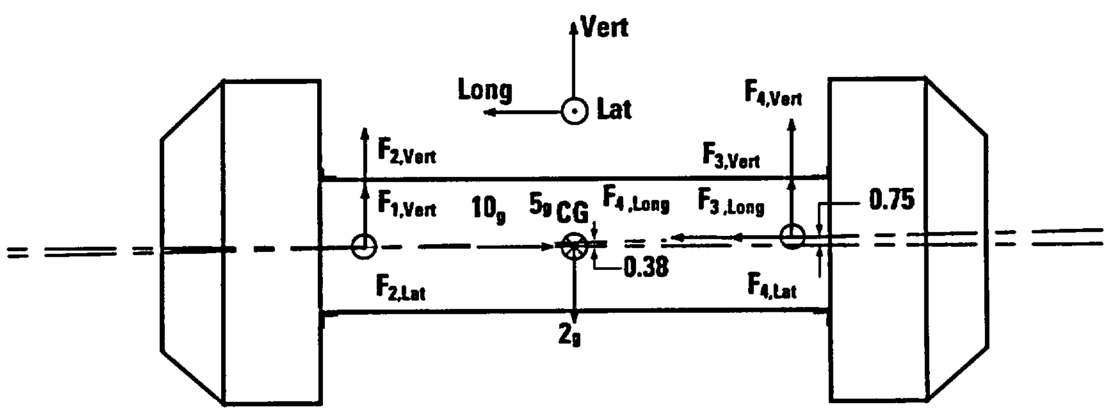

L-717(19)
6-17-96

SIDE VIEW

Fig. 2.5-6. Cask tiedown free-body diagram

In the lateral direction, the cask has 0.44 in. free play between the tiedowns. Consequently, when the cask is loaded in the lateral direction by enough to overcome friction, it slides over until it contacts the tiedown. At this point, the trunnion which is in contact with the tiedown is fully supported by the tiedown, while the trunnion on the other side is only partially in contact with the tiedown, as shown below.

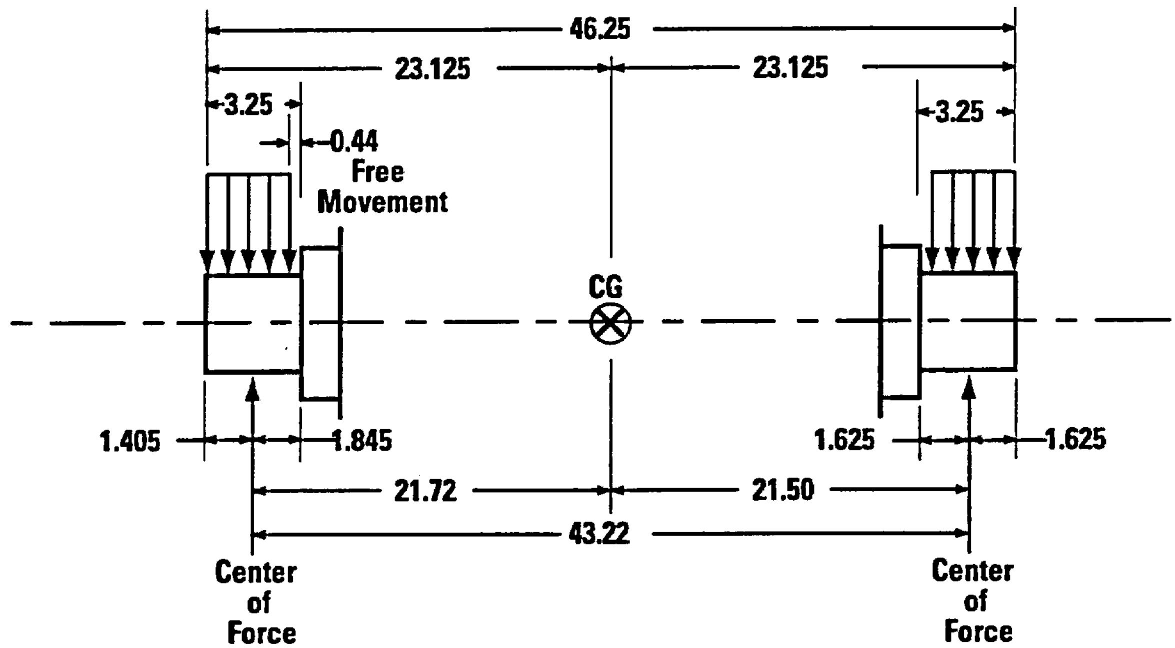

L-638(2)
8-23-96

The center of force on the side that reacts the lateral load (the trunnion on the right side in the sketch is at the center of the 3.25 in. length (1.625 in. from the end of the trunnion) since the trunnion is fully supported by the tiedown.

On the other side, the inner 0.44 in. is unsupported by the tiedown resulting in a center of force which is 1.405 in. [(3.25 – 0.44)/2] from the end of the trunnion and 1.845 in. from the base of the trunnion (Section A-A, Fig. 2.5-1).

Therefore, the center of force on one trunnion is 21.50 in. from the CG and the other is 21.72 in. from the CG.

2.5.2.1.1 Vertical Load (2g). The equations of static equilibrium for a vertical 2g load are

$$\Sigma F_{Vertical} = 0.0,$$

$$0.0 = F_{1,Vert} + F_{2,Vert} + F_{3,Vert} + F_{4,Vert} - W \times 2g, \qquad \text{(Eq. 1)}$$

$$\Sigma M_{Lateral\ Axis} = 0.0 \quad \text{(Lateral axis through CG)},$$

$\Sigma M_{Lateral\ Axis}$ = 0.0 (Lateral axis through CG),

$$0.0 = 60.82\ (F_{1,Vert} + F_{2,Vert}) - 59.68\ (F_{3,Vert} + F_{4,Vert}), \quad \text{(Eq. 2)}$$

$\Sigma M_{Longitudinal\ Axis}$ = 0.0 (Longitudinal axis through cask CG),

$$0.0 = (F_{1,Vert} + F_{3,Vert})\ 21.72 - (F_{2,Vert} + F_{4,Vert})\ 21.50, \quad \text{(Eq. 3)}$$

where

$F_{i,\ Vert}$ = Vertical load on trunnion i,

W = 55,000 lb = Maximum cask design weight.

From symmetry,

$$\frac{F_{1,Vert}}{F_{2,Vert}} = \frac{F_{3,Vert}}{F_{4,Vert}} = A \quad \text{(Eq. 4)}$$

Rewriting Eq. 4, we have,

$$F_{1,Vert} = A\ F_{2,Vert} \quad \text{(Eq. 5)}$$

$$F_{3,Vert} = A\ F_{4,Vert} \quad \text{(Eq. 6)}$$

Substituting Eqs. 5 and 6 into Eq. 2 gives:

$$0.0 = 60.82\ (1 + A)\ F_{2,Vert} - 59.68\ (1 + A)\ F_{4,Vert}, \text{ which gives}$$

$$F_{2,Vert} = \frac{59.68}{60.82} F_{4,Vert}, \text{ or}$$

$$= 0.9813\ F_{4,Vert}. \quad \text{(Eq. 7)}$$

From Eqs. 5 and 6 we also have

$$F_{1,Vert} = A\ (0.9813)\ F_{4,Vert}, \text{ and} \quad \text{(Eq. 8)}$$

$$F_{3,Vert} = A\ F_{4,Vert}. \quad \text{(Eq. 9)}$$

Using Eqs. 7, 8 and 9 in Eq. 3 gives

$$0.0 = (1.9813)\ A\ F_{4,Vert}\ (21.72) - (1.9813)\ F_{4,Vert}\ (21.50), \text{ or}$$

$$A = \frac{21.50}{21.72} = 0.9899. \quad \text{(Eq. 10)}$$

Substituting A into Eqs. 7 and 9,

$$F_{1,Vert} = 0.9714\ F_{4,Vert}, \quad \text{(Eq. 11)}$$

$$F_{3,Vert} = 0.9899\ F_{4,Vert}, \text{ and} \quad \text{(Eq. 12)}$$

Using Eqs. 1 and 7 gives

$$110{,}000 = (0.9714 + 0.9813 + 0.9899 + 1)\ F_{4,Vert}, \text{ or}$$

$$F_{4,Vert} = 27{,}900 \text{ lb.} \quad \text{(Eq. 13)}$$

Eqs. 7, 11, 12, and 13 are used to find

$$F_{1,Vert} = 27{,}102 \text{ lb,}$$

$$F_{2,Vert} = 27{,}379 \text{ lb,}$$

$$F_{3,Vert} = 27{,}619 \text{ lb, and}$$

$$F_{4,Vert} = 27{,}900 \text{ lb.}$$

2.5.2.1.2 Lateral Load (5g). Since the lateral reactions do not act along a line through the CG (see Fig. 2.5-6), vertical reactions also develop to counteract the resulting moment. The equations of static equilibrium for a 5g lateral load are

$$\Sigma F_{Vertical} = 0.0,$$

$$0.0 = F_{1,Vert} + F_{2,Vert} + F_{3,Vert} + F_{4,Vert}, \quad \text{(Eq. 1)}$$

$$\Sigma F_{Lateral} = 0.0,$$

$$0.0 = (F_{2,Lat} + F_{4,Lat}) - W \times 5g \quad \text{(Eq. 2)}$$

$$\Sigma M_{Vertical\ Axis} = 0.0 \quad \text{(Vertical axis through trunnion 4),}$$

$$0.0 = 120.5\ F_{2,Lat} - 59.68\ W\ (5g), \quad \text{(Eq. 3)}$$

$$\Sigma M_{Longitudinal\ Axis} = 0.0 \quad \text{(Longitudinal axis through trunnions 2 and 4),}$$

$$0.0 = 43.22\ (F_{1,Vert} + F_{3,Vert}) - 0.38\ W\ (5g), \quad \text{(Eq. 4)}$$

$$\Sigma M_{Lateral\ Axis} = 0.0 \quad \text{(Lateral axis through trunnions 3 and 4),}$$

$$0.0 = 120.5\ (F_{1,Vert} + F_{2,Vert}). \quad \text{(Eq. 5)}$$

From Eq. 3,

$F_{2,Lat}$ = 136,199 lb. (Eq. 6)

From Eqs. 2 and 6,

$F_{4,Lat}$ = 138,801 lb.

From Eq. 5,

$F_{1,Vert}$ = $-F_{2,Vert}$. (Eq. 7)

From Eqs. 1 and 4,

$F_{3,Vert}$ = $-F_{4,Vert}$. (Eq. 8)

From Eq. 4,

$F_{1,Vert} + F_{3,Vert}$ = 2,418 lb.

Assuming the load is shared between $F_{1,Vert}$ and $F_{3,Vert}$ in a manner analogous to a simply supported beam in equilibrium,

$$F_{1,Vert} = \frac{59.68}{120.5}(2{,}418) = 1{,}198 \text{ lb, and}$$

$$F_{3,Vert} = \frac{60.82}{120.5}(2{,}418) = 1{,}220 \text{ lb.}$$

From Eqs. 7 and 8,

$F_{2,Vert}$ = −1,198 lb, and

$F_{4,Vert}$ = −1,220 lb.

2.5.2.1.3 Longitudinal Load (10g). Again, the longitudinal reaction forces do not act through the CG, so vertical reactions develop. The equilibrium equations for 10g longitudinal load are

$\Sigma F_{Vertical}$ = 0.0,

0.0 = $F_{1,Vert} + F_{2,Vert} + F_{3,Vert} + F_{4,Vert}$, (Eq. 1)

$\Sigma F_{Longitudinal}$ = 0.0,

0.0 = $F_{3,Long} + F_{4,Long} - W \times 10g$, (Eq. 2)

$\Sigma M_{Vertical\ Axis}$ = 0.0, (Vertical axis through trunnion 4),

$$0.0 = 43.22\ F_{3,Long} - 21.50\ W\ (10g), \quad \text{(Eq. 3)}$$

$\Sigma M_{Longitudinal\ Axis}$ = 0.0 (Longitudinal axis through trunnions 2 and 4),

$$0.0 = 43.22\ (F_{1,Vert} + F_{3,Vert}), \quad \text{(Eq. 4)}$$

$\Sigma M_{Lateral\ Axis}$ = 0.0, (Lateral axis through trunnions 3 and 4),

$$0.0 = 120.5\ (F_{1,Vert} + F_{2,Vert}) - 0.38\ W\ (10g). \quad \text{(Eq. 5)}$$

From Eq. 3,

$$F_{3,Long} = 273{,}600\ \text{lb}, \quad \text{(Eq. 6)}$$

From Eqs. 2 and 6,

$$F_{4,Long} = 276{,}400\ \text{lb}.$$

From Eq. 5,

$$F_{1,Vert} + F_{2,Vert} = 1{,}734\ \text{lb}. \quad \text{(Eq. 7)}$$

Assuming the load is shared between $F_{1,Vert}$ and $F_{2,Vert}$ in a manner analogous to a simply supported beam,

$$F_{1,Vert} = \frac{21.50}{43.22}(1{,}734) = 863\ \text{lb}.$$

$$F_{2,Vert} = \frac{21.72}{43.22}(1{,}734) = 871\ \text{lb}.$$

From Eqs. 1 and 4,

$$F_{4,Vert} = -F_{2,Vert} = -871\ \text{lb}.$$

From Eq. 4,

$$F_{3,Vert} = -F_{1,Vert} = -863\ \text{lb}. \quad \text{(Eq. 8)}$$

2.5.2.1.4 Combined Loads. Table 2.5-1 summarizes the resultant trunnion loads due to the 2g vertical, 5g lateral, and 10g longitudinal shock loads. Since these shock loads are assumed to occur simultaneously and the sign (direction) of the load is arbitrary, they must be combined in manner that produces the largest loads.

TABLE 2.5-1
MAXIMUM TRUNNION LOADS (lb)

All Loads in Positive Direction

	F1		F2		F3			F4		
Load	Vert	Lat	Vert	Lat	Vert	Lat	Long	Vert	Lat	Long
2g Vertical	27,102		27,379		27,619			27,900		
5g Lateral	1,198		–1,198	136,199	1,220			–1,220	138,801	
10g Longitudinal	863		871		–863		273,600	–871		276,400
Combined	29,163		27,052	136,199	27,976		273,600	25,809	138,801	276,400

Negative Vertical Load

	F1		F2		F3			F4		
Load	Vert	Lat	Vert	Lat	Vert	Lat	Long	Vert	Lat	Long
–2g Vertical	–27,102		–27,379		–27,619			–27,900		
5g Lateral	1,198		–1,198	136,199	1,220			–1,220	138,801	
10g Longitudinal	863		871		–863		273,600	–871		276,400
Combined	–25,041		–27,706	136,199	–27,262		273,600	–29,991	138,801	276,400

Negative Longitudinal Load

	F1		F2		F3			F4		
Load	Vert	Lat	Vert	Lat	Vert	Lat	Long	Vert	Lat	Long
2g Vertical	27,102		27,379		27,619			27,900		
5g Lateral	1,198		–1,198	136,199	1,220			–1,220	138,801	
–10g Longitudinal	–863		–871		863		–273,600	871		–276,400
Combined	27,437		25,310	136,199	29,702		–273,600	27,552	138,801	–276,400

Table 2.5-1 presents three load combinations: (1) all signs positive, (2) the vertical load negative, and (3) the longitudinal load negative. The results show that the maximum trunnion loads occur at the rear trunnion that is carrying the lateral load when the vertical load is negative. Note that changing the direction of the lateral load causes the cask to move to the other side of the trailer, thus changing the lateral eccentricities and producing the mirror image of the case that is presented in Table 2.5-1 and shown in Fig. 2.5-6.

The maximum trunnion loads, rounded to the nearest 100 lb, are shown below. Since the sign convention is arbitrary, all loads are shown as positive.

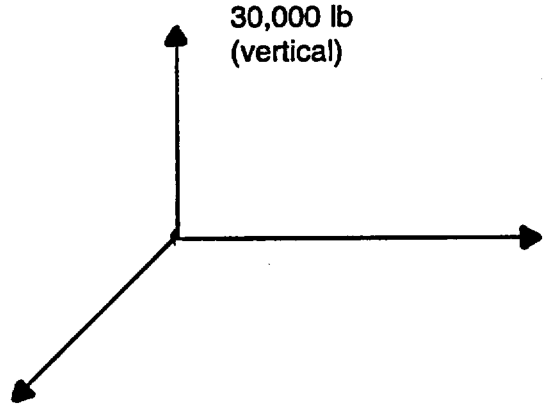

The resultant in the vertical/longitudinal plane is

$$F_{shear} = \sqrt{(276{,}400)^2 + (30{,}000)^2}\,,$$

$$= 278{,}000 \text{ lb longitudinal.}$$

The lateral load is applied on the outer cylinder of the trunnion 1.845 in. away from Section A-A in Fig. 2.5-1. Therefore, the forces at Section A-A are

$$M_{A\text{-}A} = (1.845)\,(278{,}000),$$

$$= 512{,}900 \text{ in.-lb},$$

$$F_{lateral} = 138{,}800 \text{ lb},$$

$$F_{shear} = 278{,}000 \text{ lb}.$$

2.5.2.2 Trunnion Analysis Results.

This section summarizes the results of the trunnion analyses. Section 2.10.5 discusses the analyses in detail.

2.5.2.2.1 ANSYS Analysis Results. The main objective of the ANSYS analysis is to determine the effect of the trunnion loading on (1) the cask wall, (2) at the intersection of the cask wall and trunnion, and (3) at the junction of the trunnion and gusset. We use two ANSYS models to accomplish this. The first model represents the trunnion configuration and surrounding cask wall. The second model uses a fine mesh to represent the junction of the trunnion and gusset, which is the most highly stressed area on the trunnion. Details are provided in Section 2.10.5.1.

Table 2.5-2 summarizes the ANSYS results for the points bearing the greatest stress from the tiedown loads. The locations of the critical points are shown in Fig. 2.5-7.

2.5.2.2.2 Outer Cylinder Trunnion Stress. Strength-of-material calculations are used to develop the stress state in the outer cylinder portion of the trunnion. Section 2.10.5.2 develops these stresses. The highest stress is 14.9 ksi, which is less than the yield stress at 180°F (S_y = 48.6 ksi). This yields a design margin of 2.26.

2.5.2.3 Conclusions. Two ANSYS models and strength-of-material calculations were used in this study to establish the stress state of the trunnion and the cask wall in the region of the trunnion attachment. The models use the 10g longitudinal, 5g transverse, and 2g vertical loads from 10 CFR Part 71.45b(1). This loading produced the highest combined trunnion loading condition, which was higher than the lifting loads. This loading condition, therefore, conservatively envelops the lifting loads for the trunnions. The resulting stresses, shown in Table 2.5-2 and Section 2.5.2.2.2, are well within the material yield strength. Table 2.5-2 also shows that the minimum design margins (D.M.) occur on the trunnion side (Point 2, D.M. = 0.13) and not on the cask wall (Point 5, D.M. = 0.53); therefore, if excessive force is put on the trunnions, this design ensures that the trunnions will fail before the cask wall.

2.5.3 Redundant Lift Sockets

2.5.3.1 Redundant Lift Socket Configuration. There are two redundant lift sockets in the cask that could be used for lifting of the cask in and around the pool area. These sockets and the upper lifting trunnions are used together if a redundant lift is desired.

The design loads have been doubled from a factor of safety of three (as specified in 10 CFR Part 71.45) or five (ANSI N14.6, Ref. 2.5-1) on yield strength or ultimate, respectively, to a factor of safety of six and ten, respectively. Therefore, this redundant lift socket pair is designed for critical load lifting of the fully loaded cask as described in ANSI N14.6.

The general arrangement of the redundant lift socket is shown in Fig. 2.5-8. The sockets are welded to the cask at a position 90° away from the existing trunnions at the end of the impact limiter support structure. The socket inserts are similar to the lifting trunnion inserts.

2.5.3.2 Lifting Loads. The two redundant lift sockets are used to lift and move the cask vertically only.

The allowable stresses for lifting are the same as those discussed in 2.5.1.2. This section shows that a factor of safety of six against yield strength controls.

TABLE 2.5-2
MAXIMUM STRESSES ON ANSYS TRUNNION ANALYSIS
CAUSED BY TIEDOWN LOADS

Location (Fig. 2.5-7)	Stress Intensity (ksi)	Allowable (ksi)	Design Margin
1	38.3	43.74[a]	+0.14
2	38.7	43.74[a]	+0.13
3	31.7	48.60	+0.53
4	34.0	43.74[a]	+0.29
5	31.8	48.60[b]	+0.53

[a]Based on yield at 180°F (48.6 ksi) and the weld quality factor of n = 0.9, as given in ASME Code Section III, Table NG-3352-1, for progressive PT weld examination.
[b]Based on yield at 180°F (48.6 ksi).

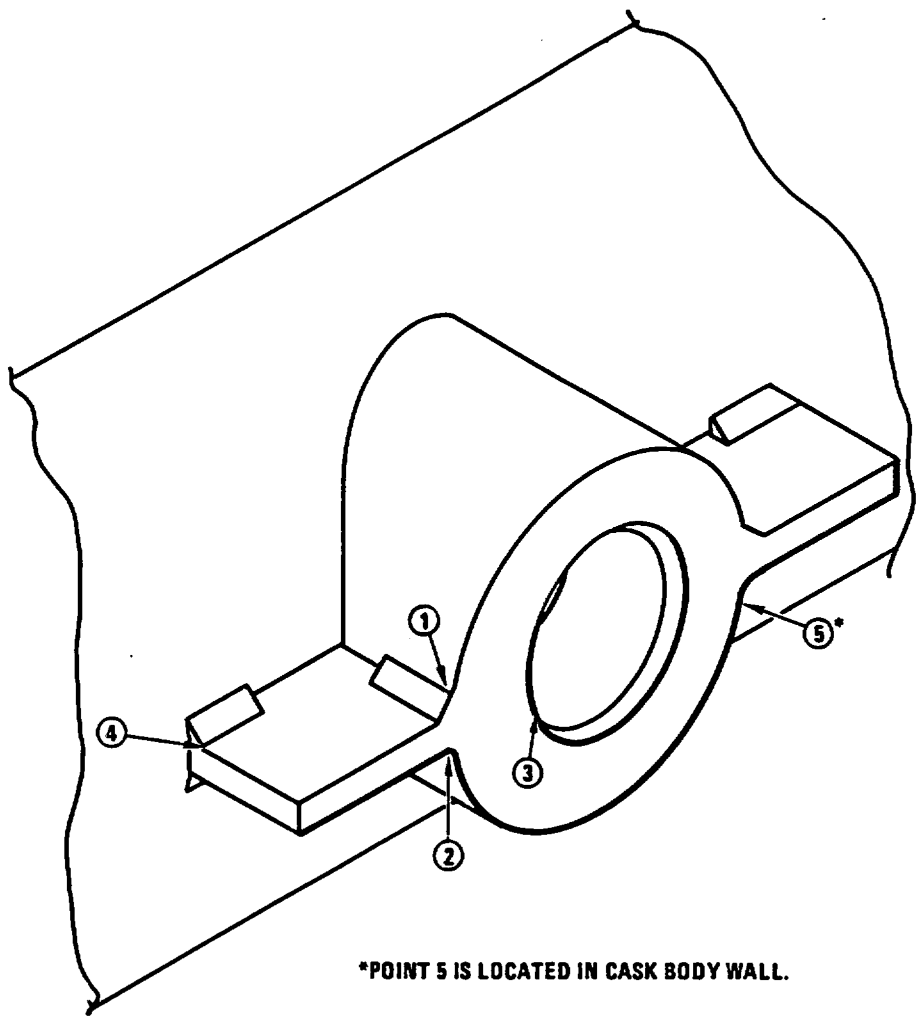

J-217(8)
9-5-91

Fig. 2.5-7. Maximum stress location points from ANSYS trunnion analysis

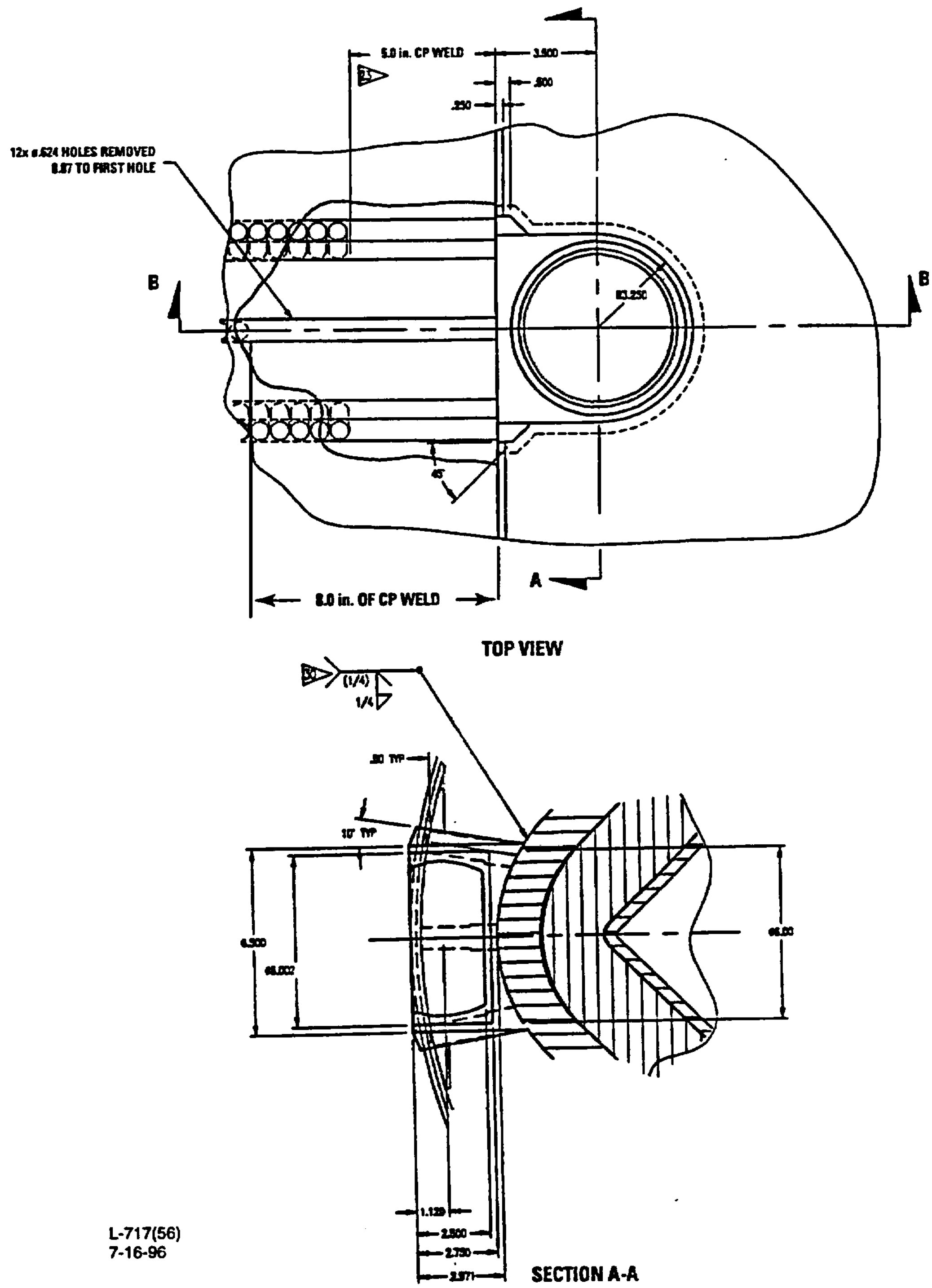

L-717(56)
7-16-96

Fig. 2.5-8. Redundant lift socket configuration

The loading condition imposed on the socket is the dead weight of the cask, as follows:

1. Design weight	55,000 lb—impact limiter, 55,000 – 3,925 = 51,100 lb,
2. Pool water in cask cavity	2,100 lb,
3. Dynamic factor	1.2,
4. FS	6,
Load per socket	=(FS) (53,200) (1.2)/2, = 191,520 lb.

2.5.3.3 Analysis. The three impact limiter support structure ribs attached to the sockets react the lifting load. There are no holes drilled at the ends of these ribs, as shown in Fig. 2.5-8. At these locations, the ribs are connected to the cask body with full penetration welds. There is a 1/4-in. groove and a 1/4-in. fillet weld around the outside of the socket. The following analysis conservatively ignores the resistance to the lifting loads by the remainder of the impact limiter support structure. The stress in the welds is as follows:

Center rib: For this analysis it is assumed that half the load is carried by the center rib and half by the outer ribs.

l = center rib full penetration weld length = 8 in.

t = rib thickness = 0.75 in.

P = load on center rib = 191,520/2 = 95,760 lb

τ = shear stress on center rib weld = 95,760/(.75 x 8) = 15,960 psi

The weld under the ribs is a full-penetration weld that is inspected with surface PT or MT, according to ASME Code, Section III, Subsection NG. The allowable stress for this weld is 0.65 x 55,000 psi = 35,750 psi. Therefore, the design has a margin of safety larger than six.

The bearing stress on the end of the center rib is

$$A_{rib} = (2.971 - .4 - 1)(.75) + (.88)(1.0) = 2.06 \text{ in.}^2,$$

$$\sigma_{bearing} = \frac{95,760}{2.06} = 46,485 \text{ psi.}$$

The allowable stress for this condition is the yield strength (55,000 psi). Therefore, the design has a margin of safety larger than six.

The welds on the two outer ribs and the weld around the sockets carry the remainder of the load. In the following calculations, the 1/4-in. fillet weld has been conservatively ignored.

Fig. 2.5-9 shows the calculations for the properties of the outer ribs and the socket welds. Using the values obtained, the maximum stresses are as follows:

P = load = 191,520/2 = 95,760 lb,

τ = shear stress = 95,760 lb/(11.7 in.^{2}) = 8,200 psi,

x = moment arm to lifting load = 1.85 in. (See Fig. 2.5-10),

M_t = total moment due to lifting load = 191,520 lb x 1.85 in. = 354,312 in.-lb,

$\sigma = M\, c_{max}/I$ = 354,312 x 6.94/145.35 = 16,917 psi,

$$\sigma_{max} = \frac{16,917}{2} + \sqrt{\left(\frac{16,917}{2}\right)^2 + (8,200)^2} = 20,240 \text{ psi.}$$

The weld under the ribs is a full-penetration weld that is inspected with surface PT or MT according to ASME Code, Section III, Subsection NG. The single-groove weld under the sockets is similarly inspected. The allowable stress for the single-groove welds is 0.40 x 55,000 psi = 22,000 psi. Therefore, the design has a margin of safety larger than six.

Item 3: Circular Weld

$d_o = 6.5$ $d_i = 6.0$

$$x' = \frac{d_o}{2} - \frac{2\left(d_o^3 - d_i^3\right)}{3\pi\left(d_o^2 - d_i^2\right)}$$

$$= \frac{6.5}{2} - \frac{2\left(6.5^3 - 6.0^3\right)}{3\pi\left(6.5^2 - 6.0^2\right)} = 1.26$$

$$I_o = \frac{.1098}{16}\left(d_o^4 - d_i^4\right) - \frac{.283 d_o^2 d_i^2 (d_o - d_i)}{16(d_o + d_i)}$$

$$= 3.36 - 1.08 = 2.28 \text{ in.}^4$$

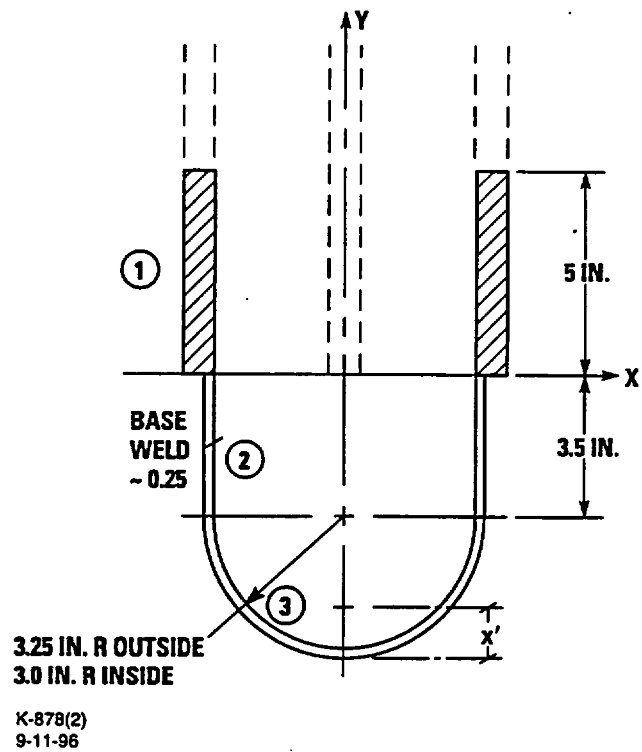

Item	y	A	Ay	Ay^2	I_{o-x}
1	2.5	(2)(.75)(5) = 7.5	18.75	46.88	$(2)(.75)(5)^3/12$ = 15.62
2	−1.75	(2)(.25)(3.5) = 1.75	−3.06	5.36	$(2)\frac{(.25)(3.5)^3}{12}$ = 1.79
3	−[3.5 + (3.25 −1.26)] = − 5.49	$\pi(3.25^2 - 3.0^2)/2$ = 2.45	−13.45	73.84	2.28
Total		11.7	2.24	126.08	19.69

$$\bar{y} = \frac{\sum Ay}{\sum A} = \frac{2.24}{11.7} = 0.19.$$

$$I_{x\text{-}x} = \sum I_{o\text{-}x} + \sum Ay^2 - \left(\sum A\right)\bar{y}^2,$$

$$= 19.69 + 126.08 - (11.7)(.19)^2 = 145.35 \text{ in.}^4$$

$$c_{max} = .19 + 3.5 + 3.25 = 6.94 \text{ in.}$$

Fig. 2.5-9. Properties of the outer ribs section of the redundant lift socket

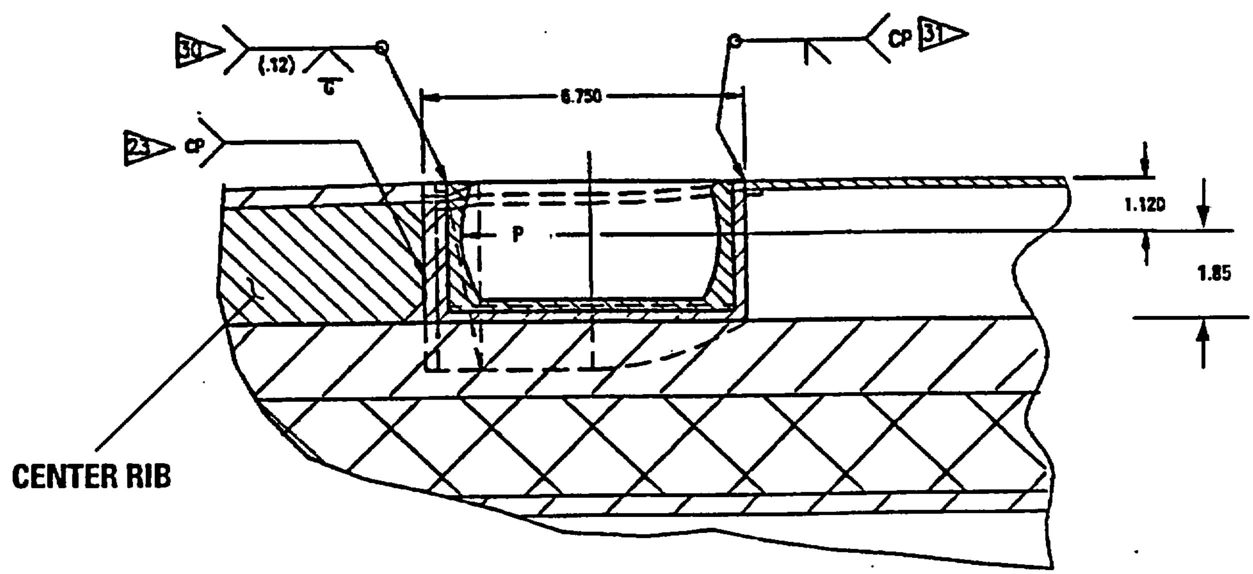

L-717(22)
6-17-96

Fig. 2.5-10. Redundant lift socket longitudinal cross section

THIS PAGE LEFT BLANK INTENTIONALLY

2.6 Normal Conditions of Transport

The GA-4 cask, when subjected to the conditions and tests specified in 10 CFR Part 71.71 (normal conditions of transport), meets the criteria specified in 10 CFR Part 71.43 and Part 71.51. Finite element analysis is used to demonstrate that the cask meets the criteria for increased and decreased external pressure, and for the free drops. The cask structure consists of corrosion-resistant metals and is consequently unaffected by water spray. Hand calculations are used to demonstrate that cask meets the criteria for all other normal conditions.

2.6.1 Heat

The thermal evaluation for the heat test is reported in Section 3.4. The input conditions are 100°F ambient temperature, maximum solar insolation, maximum decay heat, and maximum internal pressure.

2.6.1.1 Summary of Pressures and Temperatures. The maximum normal operating pressure (MNOP) for the 100°F heat test, is 74 psig (see Section 3.4.4). For the cask pressure and drop analyses 80 psig was conservatively used.

Table 2.6-1 shows the maximum temperatures and the cross section average temperatures resulting from the heat test.

2.6.1.2 Differential Thermal Growth. The GA-4 cask is designed to avoid interference between components caused by differential thermal expansion. Two aspects of differential thermal expansion were considered in its evaluation for the GA-4 cask, (1) the gaps important for safety were sized for the different temperature conditions and, (2) the stress resulting from the interaction of components caused by the differential thermal expansion. The differential thermal expansion stresses are used in combination with other stresses in the load case evaluations. The gaps important for safety include the following:

- Radial gap between the cavity liner and the DU (Gap A in Fig. 2.6-1),
- Radial gap between the DU and the cask wall or containment boundary (Gap B in Fig. 2.6-1),
- Radial gap between the B_4C pellets and the FSS (Gaps C and D in Fig. 2.6-1), and
- Axial gap between the DU, flange and bottom plate assemblies (Gap E in Fig. 2.6-2).

Stresses were calculated for interaction of the cavity liner and containment boundary during the hot environment condition and for any cases where the gaps described above closed. The interaction of the FSS and the cavity liner for the hot environment condition was evaluated using an ANSYS analysis in Section 2.10.9.3.5. Other components of the cask, including the flange and cask, the ILSS and the cask, the impact limiter and the ILSS, have similar thermal expansivities and temperatures. Therefore, interaction stresses between these components are negligible.

TABLE 2.6-1 SUMMARY OF TEMPERATURES FOR NORMAL CONDITIONS HEAT TEST, STEADY STATE (°F)			
COMPONENT	CROSS SECTION AVERAGE		AXIAL AVERAGE
	MIDLENGTH	BOTTOM END [a]	
FSS	271	202	251 [b]
Cavity liner	205	167	184
Gamma shield (DU)	200	164	180
Cask body	195	162	177
Neutron shield	191	160	172
Outer skin	188	158	175
Fuel cladding	313 max.		
Cavity gas	233 avg.		
Closure and gas sample port seals	135		
Drain seal	143	(a) 15 in. from cavity bottom.	
Closure (plug)	136	(b) At center.	
Impact limiters	135 max.	(c) Cask body temperature 30 in. from cavity bottom.	
Trunnions	178 [c]		

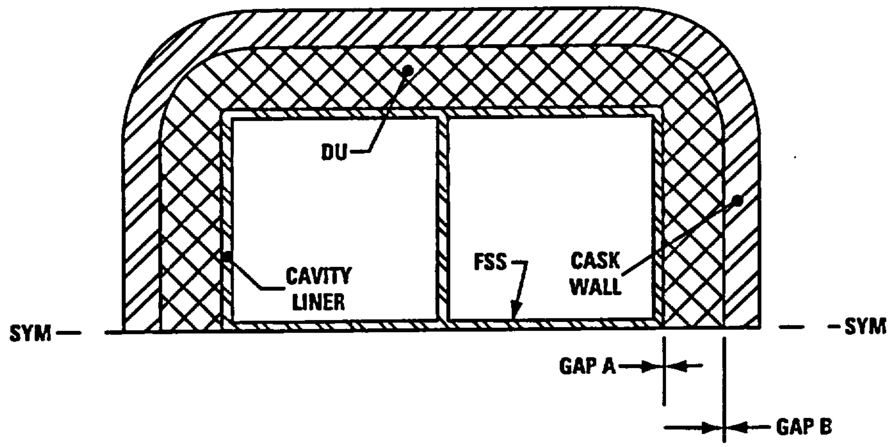

CASK CROSS SECTION

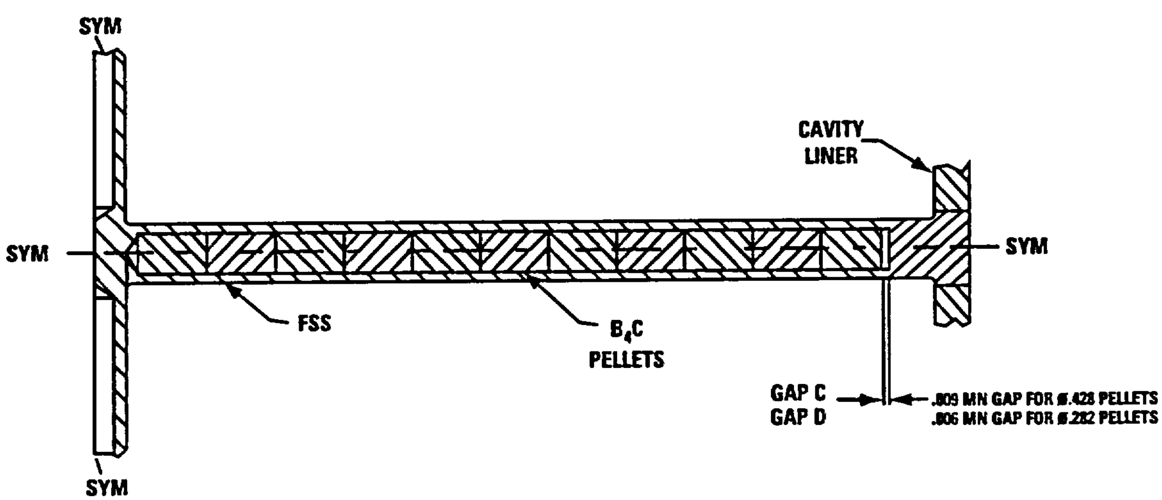

FSS CROSS SECTION

L-717(60)
7-26-96

Fig. 2.6-1. Radial gaps used for differential thermal expansion calculations

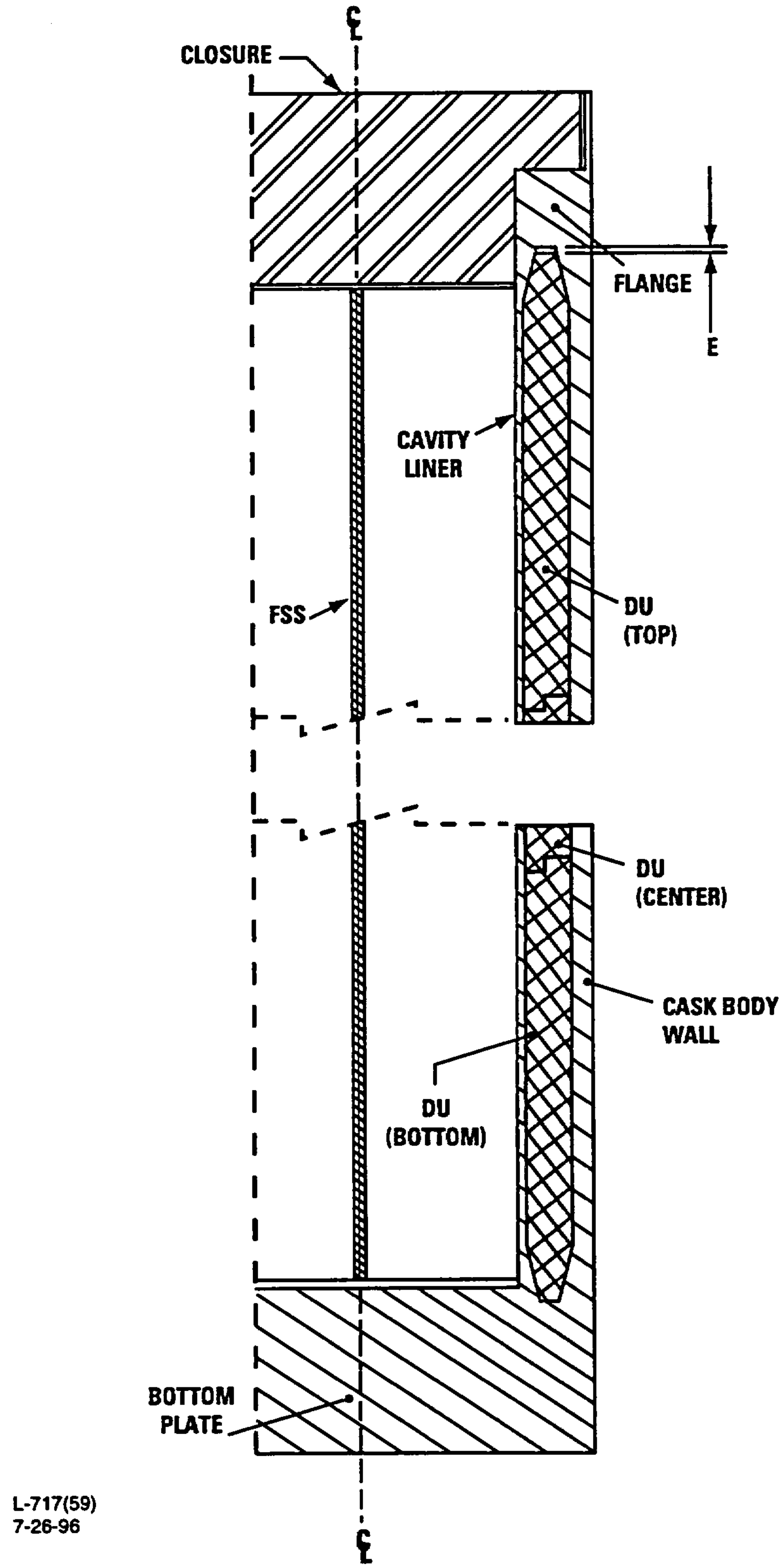

Fig. 2.6-2. Axial gaps used for differential thermal expansion calculations

How differential thermal growth affects the minimum gap sizes between the various components of the GA-4 cask was evaluated using hand calculations. The thermal conditions considered were for room temperature, normal operating conditions with an ambient temperature of 100°F (hot environment condition), and the cask and its internals at two different uniform temperature conditions: –20°F for the cold environment condition and –40°F minimum temperature condition. The following assumptions were used:

- The growth or contraction of each component is caused by the average temperature increase or decrease of the component.
- The FSS and cavity liner are assumed to grow radially as much as the FSS would freely expand. This assumption is conservative, because a smaller gap between the cavity liner and the DU results.
- Transient thermal effects are unimportant.
- Local hot spots have a negligible effect.
- The material properties are given in Section 2.3.
- The hot environment condition temperatures are those given in Table 2.6-1.
- The initial and ambient temperature conditions are 70°F.
- The ambient temperature gap tolerances are applied to the gaps calculated at other temperature conditions.
- The components are centered.

Using these assumptions, the temperatures and Drawing 031348 in Section 1.3.2, the following steps were used to evaluate the gaps caused by differential thermal expansion:

- The appropriate dimensions were taken from the drawings. These dimensions, tolerances and the references are summarized in Tables 2.6-2 and 2.6-3 for the transverse and the axial and circumferential dimensions, respectively.
- The temperatures for the different conditions were used to interpolate the values for the thermal expansivity and, where appropriate (if there was interaction with the component), the elastic modulus. The free thermal expansion of each component was calculated for the appropriate thermal conditions. These results are summarized in Tables 2.6-4 through 2.6-6 for the hot environment condition and in Tables 2.6-7 through 2.6-10 for the cold conditions.
- The nominal dimensions calculated for the different conditions were used to find the nominal gap sizes given in Table 2.6-11 for the hot and minimum temperature conditions. The nominal dimensions and the ambient temperature tolerances were then used to generate the minimum gaps presented in Table 2.6-12 for these thermal conditions.
- When interaction between the components was identified, as the result of contact between components which initially are separated, the interaction was considered and, if applicable, stresses in the affected components were calculated. These calculations are presented in Sections 2.6.1.3 and 2.6.2.

This evaluation showed, as summarized in Table 2.6-12, that all of the gaps are adequate to preclude interference for all of the thermal conditions, except for the axial gaps between the DU and the flange and bottom plate. For the two cold conditions there will be axial contact and interaction between the DU and the stainless steel components. The stress resulting from this interaction is calculated in Section 2.6.2.

TABLE 2.6-2 TRANSVERSE NOMINAL DIMENSIONS AT ROOM TEMPERATURE

LOCATION	L (in.)	SHEET NUMBER OF DRAWING 031348
B_4C PELLET ASSEMBLY		
0.428 Ø Pellets	8.010	9
FSS Wall	8.019	9
0.282 Ø Pellets	8.054	9
FSS Wall	8.060	9
FUEL SUPPORT STRUCTURE		
Flat: Outer	9.080	9
FUEL CAVITY LINER		
Flat: Inner	9.080	9
Outer	9.456	9
Corner: Inner	12.790	9
Outer	13.166	9
DEPLETED URANIUM		
Top/Bottom Rings		
Flat: Inner	9.507	4 & 10
Outer	12.142	4 & 10
Corner: Inner	13.255	10
Outer	15.322	10
Center Ring		
Flat: Inner	9.492	10
Outer	12.142	10
Corner: Inner	13.225	10
Outer	15.322	10
CASK WALL		
Flat: Inner	12.162	4
Outer	13.662	4
Corner: Inner	15.404	4
Outer	16.904	4

TABLE 2.6-3 AXIAL & CIRCUMFERENTIAL NOMINAL DIMENSIONS AT ROOM TEMPERATURE

LOCATION	L (in.)	SHEET NUMBER OF DRAWING 031348
AXIAL NEUTRON SHIELD SHELL TO CASK WALL		
Overall		
Shell	143.26	2
Cask Wall	143.26	2
AXIAL ILSS RIB TO SHELL & CASK WALL		
Overall		
Cask Wall	22.25	13
ILSS Rib -inner	22.25	13
ILSS Rib - outer	22.25	13
ILSS Shell	22.25	13
CIRCUMFERENTIAL ILSS SHELL & CASK WALL		
Overall		
Cask Wall	2.39	11 & 13
ILSS Shell	3.425	11 & 13
AXIAL DU TO CASK WALL & CAVITY LINER		
Overall		
Cavity Liner	170.79	2
DU	170.79	10
Cask Wall	170.79	2

TABLE 2.6-4 TRANSVERSE NOMINAL DIMENSIONS AT CASK MIDLENGTH FOR HOT CONDITIONS

LOCATION	MATERIAL	L (in.)	TEMP (°F)	α (in./in., °F)	ΔL (in.)	L' (in.)
B_4C Pellet Assembly						
0.428 ø pellets	B_4C	8.010	271.	2.70E-06	4.363E-03	8.014
FSS wall	XM-19	8.019	271.	8.60E-06	1.386E-02	8.033
Fuel Support Structure						
Flat: outer	XM-19	9.080	271.	8.60E-06	1.570E-02	9.096
Fuel Cavity Liner						
Flat: inner	XM-19	9.080	271.	8.60E-06	1.570E-02	9.096
outer	XM-19	9.456	271.	8.60E-06	1.635E-02	9.472
Corner: inner	XM-19	12.790	271.	8.60E-06	2.211E-02	12.812
outer	XM-19	13.166	271.	8.60E-06	2.276E-02	13.189
Depleted Uranium						
Center ring						
Flat: inner	DU	9.492	200.	8.48E-06	7.527E-03	9.500
outer	DU	12.142	200.	8.48E-06	9.629E-03	12.152
Corner: inner	DU	13.225	200.	8.48E-06	1.049E-02	13.235
outer	DU	15.322	200.	8.48E-06	1.215E-02	15.334
Cask Wall						
Flat: inner	XM-19	12.162	195.	8.47E-06	1.288E-02	12.175
outer	XM-19	13.662	195.	8.47E-06	1.446E-02	13.676
Corner: inner	XM-19	15.404	195.	8.47E-06	1.631E-02	15.420
outer	XM-19	16.904	195.	8.47E-06	1.790E-02	16.922

TABLE 2.6-5 TRANSVERSE NOMINAL DIMENSIONS AT CASK END FOR HOT CONDITIONS

LOCATION	MATERIAL	L (in.)	TEMP (°F)	α (in./in. °F)	ΔL (in.)	L' (in.)
B_4C Pellet Assembly						
0.428 ø pellets	B_4C	8.054	202	2.70E-06	2.85E-03	8.057
FSS wall	XM-19	8.060	202	8.48E-06	9.02E-03	8.069
Fuel Support Structure						
Flat: outer	XM-19	9.080	202	8.48E-06	1.02E-02	9.090
Fuel Cavity Liner						
Flat: inner	XM-19	9.080	167	8.42E-06	7.42E-03	9.087
outer	XM-19	9.456	167	8.42E-06	7.72E-03	9.464
Corner: inner	XM-19	12.790	167	8.42E-06	1.04E-02	12.800
outer	XM-19	13.166	167	8.42E-06	1.08E-02	13.177
Depleted Uranium						
Center ring						
Flat: inner	DU	9.507	164	5.83E-06	5.21E-03	9.512
outer	DU	12.142	164	5.83E-06	6.65E-03	12.149
Corner: inner	DU	13.255	164	5.83E-06	7.26E-03	13.262
outer	DU	15.322	164	5.83E-06	8.40E-03	15.330
Cask Wall						
Flat: inner	XM-19	12.162	162	8.41E-06	9.41E-03	12.171
outer	XM-19	13.662	162	8.41E-06	1.06E-02	13.673
Corner: inner	XM-19	15.404	162	8.41E-06	1.19E-02	15.416
outer	XM-19	16.904	162	8.41E-06	1.31E-02	16.917

TABLE 2.6-6 AXIAL & CIRCUMFERENTIAL NOMINAL DIMENSIONS FOR HOT ENVIRONMENT CONDITIONS

LOCATION	MATERIAL	L (in.)	TEMP (°F)	α (in./in. °F)	ΔL (in.)	L' (in.)
AXIAL NEUTRON SHIELD SHELL TO CASK WALL						
Overall						
Shell	XM-19	143.26	175.[a]	8.43E-06	1.268E-01	143.387
Cask Wall	XM-19	143.26	177.[a]	8.44E-06	1.294E-01	143.389
AXIAL ILSS RIB TO SHELL & CASK WALL						
Overall						
Cask Wall	XM-19	22.25	149.[b]	8.41E-06	1.47E-02	22.2647
ILSS Rib - R_i	XM-19	22.25	149.[b]	8.41E-06	1.47E-02	22.2647
ILSS Rib - R_o	XM-19	22.25	135.	8.36E-06	1.21E-02	22.2621
ILSS Shell	XM-19	22.25	135.	8.36E-06	1.21E-02	22.2621
CIRCUMFERENTIAL ILSS SHELL & CASK WALL						
Overall						
Cask Wall	XM-19	2.390	162	8.41E-06	1.8E-03	2.392
ILSS Shell	XM-19	3.425	135	8.36E-06	1.9E-03	3.427
AXIAL DU TO CASK WALL & CAVITY LINER						
Overall						
Cavity Liner	XM-19	170.79	184. [1]	8.45E-06	1.645E-01	170.954
DU	DU	170.79	180. [1]	5.92E-06	1.112E-01	170.901
Cask Wall	XM-19	170.79	177. [1]	8.44E-06	1.542E-01	170.944

(a) Axially averaged temperature used.
(b) Axially averaged temperature used. Based on closure temperature and cask wall temperature 15 in. from cavity end.

TABLE 2.6-7 TRANSVERSE NOMINAL DIMENSIONS FOR COLD ENVIRONMENT CONDITIONS						
LOCATION	MATERIAL	L (in.)	TEMP (°F)	α (in./in. °F)	ΔL (in.)	L' (in.)
B_4C Pellet Assembly						
0.428 ø pellets	B_4C	8.010	–20	2.70E-06	1.946E-03	8.008
FSS wall	XM-19	8.019	–20	8.16E-06	5.889E-03	8.013
0.282 ø pellets	B_4C	8.054	–20	2.70E-06	1.957E-03	8.052
FSS wall	XM-19	8.060	–20	8.16E-06	5.919E-03	8.054
Fuel Support Structure						
Flat: outer	XM-19	9.080	–20	8.16E-06	6.667E-03	9.073
Fuel Cavity Liner						
Flat: inner	XM-19	9.080	–20	8.16E-06	6.667E-03	9.073
outer	XM-19	9.456	–20	8.16E-06	6.944E-03	9.449
Corner: inner	XM-19	12.790	–20	8.16E-06	9.393E-03	12.781
outer	XM-19	13.166	–20	8.16E-06	9.669E-03	13.156
Depleted Uranium						
Top/bottom rings						
Flat: inner	DU	9.507	–20	4.80E-06	4.107E-03	9.503
outer	DU	12.142	–20	4.80E-06	5.245E-03	12.137
Corner: inner	DU	13.267	–20	4.80E-06	5.726E-03	13.249
outer	DU	15.322	–20	4.80E-06	6.619E-03	15.315
Center ring						
Flat: inner	DU	9.492	–20	4.80E-06	4.100E-03	9.488
outer	DU	12.142	–20	4.80E-06	5.245E-03	12.137
Corner: inner	DU	13.225	–20	4.80E-06	5.713E-03	13.219
outer	DU	15.322	–20	4.80E-06	6.619E-03	15.315
Cask Wall						
Flat: inner	XM-19	12.162	–20	8.16E-06	8.932E-03	12.153
outer	XM-19	13.662	–20	8.16E-06	1.003E-02	13.652
Corner: inner	XM-19	15.404	–20	8.16E-06	1.131E-02	15.393
outer	XM-19	16.904	–20	8.16E-06	1.241E-02	16.892

TABLE 2.6-8 TRANSVERSE NOMINAL DIMENSIONS FOR MINIMUM TEMPERATURE CONDITIONS						
LOCATION	MATERIAL	L (in.)	TEMP (°F)	α (in./in. °F)	ΔL (in.)	L' (in.)
B_4C Pellet Assembly						
0.428 ø pellets	B_4C	8.010	–40	2.70E-06	–2.38E-03	8.008
FSS wall	XM-19	8.019	–40	8.10E-06	–7.14E-03	8.012
0.282 ø pellets	B_4C	8.054	–40	2.70E-06	–2.39E-03	8.052
FSS wall	XM-19	8.060	–40	8.10E-06	–7.18E-03	8.053
Fuel Support Structure						
Flat: outer	XM-19	9.080	–40	8.10E-06	–8.09E-03	9.072
Fuel Cavity Liner						
Flat: inner	XM-19	9.080	–40	8.10E-06	–8.09E-03	9.072
outer	XM-19	9.456	–40	8.10E-06	–8.43E-03	9.448
Corner: inner	XM-19	12.790	–40	8.10E-06	–1.14E-02	12.779
outer	XM-19	13.166	–40	8.10E-06	–1.17E-02	13.154
Depleted Uranium						
Top/bottom rings						
Flat: inner	DU	9.507	–40	4.5E-06	–4.71E-03	9.502
outer	DU	12.142	–40	4.5E-06	–6.01E-03	12.136
Corner: inner	DU	13.255	–40	4.5E-06	–6.56E-03	13.248
outer	DU	15.322	–40	4.5E-06	–7.58E-03	15.314
Center ring						
Flat: inner	DU	9.492	–40	4.5E-06	–4.70E-03	9.487
outer	DU	12.142	–40	4.5E-06	–6.01E-03	12.136
Corner: inner	DU	13.225	–40	4.5E-06	–6.55E-03	13.219
outer	DU	15.322	–40	4.5E-06	–7.58E-03	15.314
Cask Wall						
Flat: inner	XM-19	12.162	–40	8.10E-06	–1.08E-02	12.151
outer	XM-19	13.662	–40	8.10E-06	–1.22E-02	13.650
Corner: inner	XM-19	15.404	–40	8.10E-06	–1.37E-02	15.390
outer	XM-19	16.904	–40	8.10E-06	–1.51E-02	16.889

TABLE 2.6-9 AXIAL & CIRCUMFERENTIAL NOMINAL DIMENSIONS FOR COLD ENVIRONMENT CONDITIONS

LOCATION	MATERIAL	L (in.)	TEMP (°F)	α (in./in. °F)	ΔL (in.)	L' (in.)
AXIAL NEUTRON SHIELD SHELL TO CASK WALL						
Overall						
Shell	XM-19	143.26	-20.	8.16E-06	-1.052E-01	143.155
Cask Wall	XM-19	143.25	-20.	8.16E-06	-1.052E-01	143.155
AXIAL ILSS RIB TO SHELL & CASK WALL						
Overall						
Cask Wall	XM-19	22.25	-20.	8.16E-06	-1.63E-02	22.234
ILSS Rib - R_i	XM-19	22.25	-20.	8.16E-06	-1.63E-02	22.234
ILSS Rib - R_o	XM-19	22.25	-20.	8.16E-06	-1.63E-02	22.234
ILSS Shell	XM-19	22.25	-20.	8.16E-06	-1.63E-02	22.234
CIRCUMFERENTIAL ILSS SHELL & CASK WALL						
Overall						
Cask Wall	XM-19	2.39	-20.	8.16E-06	-1.8E-03	2.388
ILSS Shell	XM-19	3.425	-20.	8.16E-06	-2.5E-03	3.422
AXIAL DU TO CASK WALL & CAVITY LINER						
Overall						
Cavity Liner	XM-19	170.79	-20.	8.16E-06	-1.25E-01	170.665
DU	DU	170.79	-20.	4.80E-06	-7.38E-02	170.716
Cask Wall	XM-19	170.79	-20.	8.16E-06	-1.25E-01	170.665

TABLE 2.6-10 AXIAL & CIRCUMFERENTIAL NOMINAL DIMENSIONS FOR MINIMUM TEMPERATURE CONDITIONS

LOCATION	MATERIAL	L (in.)	TEMP (°F)	α (in./in. °F)	ΔL (in.)	L' (in.)
AXIAL NEUTRON SHIELD SHELL TO CASK WALL						
Overall						
Shell	XM-19	143.26	-40.	8.10E-06	-1.276E-01	143.132
Cask Wall	XM-19	143.26	-40.	8.10E-06	-1.276E-01	143.132
AXIAL ILSS RIB TO SHELL & CASK WALL						
Overall						
Cask Wall	XM-19	22.25	-40.	8.10E-06	-1.98E-02	22.230
ILSS Rib - R_i	XM-19	22.25	-40.	8.10E-06	-1.98E-02	22.230
ILSS Rib - R_o	XM-19	22.25	-40.	8.10E-06	-1.98E-02	22.230
ILSS Shell	XM-19	22.25	-40.	8.10E-06	-1.98E-02	22.230
CIRCUMFERENTIAL ILSS SHELL & CASK WALL						
Overall						
Cask Wall	XM-19	2.39	-40.	8.10E-06	-2.1E-03	2.388
ILSS Shell	XM-19	3.425	-40.	8.10E-06	-3.1E-03	3.422
AXIAL DU TO CASK WALL & CAVITY LINER						
Overall						
Cavity Liner	XM-19	170.79	-40.	8.10E-06	-1.522E-01	170.638
DU	DU	170.79	-40.	4.50E-06	-8.45E-02	170.706
Cask Wall	XM-19	170.79	-40.	8.10E-06	-1.522E-01	170.638

TABLE 2.6-11 SUMMARY OF NOMINAL GAP SIZES RESULTING FROM DIFFERENTIAL THERMAL EXPANSION OF THE GA-4 COMPONENTS

GAP LOCATION	GAP[a] TYPE	NOMINAL GAP SIZE (in.)			
		ROOM TEMP (70°F)	HOT ENVIRONMENT CONDITIONS[e] AT MIDLENGTH	HOT ENVIRONMENT CONDITIONS[e] AT END	COLD TEMP (-40°F)
B_4C PELLET ASSEMBLY TO FSS WALL					
0.428 Ø Pellets (Midsection)	T	0.009[d]	0.018[d]	N/A	0.004[d]
0.282 Ø Pellets (End section)	T	0.006[d]	N/A	0.012[d]	0.001[d]
CAVITY LINER TO TOP OR BOTTOM DU					
Flat	T	0.051 ± 0.015[f]	N/A	0.046	0.055
Corner	T	0.089 ± 0.029[f]	N/A	0.086	0.094
CAVITY LINER TO CENTER DU					
Flat	T	0.036 ± 0.015[f]	0.027	N/A	0.040
Corner	T	0.059 ± 0.029[f]	0.047	N/A	0.064
DU TO CASK WALL					
Flat	T	0.020 ± 0.010[f]	0.023	0.023	0.015
Corner	T	0.083 ± 0.010[f]	0.086	0.085	0.076
DU TO CASK WALL & CAVITY LINER					
With No Gap	A	0.000	0.045[b]	N/A[b]	Contact[c]

NOTES:
(a) Gap types are the following: T is transverse and A is axial.
(b) Axially averaged temperature was used for the calculation.
(c) Differential expansion causes interaction of the components, the effect of which is considered in section 2.6.2.
(d) Minimum dimension. Given on sheet 9 of drawing 031348.
(e) Temperatures given in Table 2.6-1.
(f) Given on sheet 4 of drawing 031348.

TABLE 2.6-12 SUMMARY OF MINIMUM GAP SIZES RESULTING FROM DIFFERENTIAL THERMAL EXPANSION OF THE GA-4 COMPONENTS

GAP LOCATION	GAP[a] TYPE	MINIMUM GAP SIZE (in.) ROOM TEMP (70°F)	HOT ENVIRONMENT CONDITIONS[e] AT MIDLENGTH	HOT ENVIRONMENT CONDITIONS[e] AT END	COLD TEMP (-40°F)
B_4C PELLET ASSEMBLY TO FSS WALL					
0.428 Ø Pellets (Midsection)	T	0.009[d]	0.018	N/A	0.004
0.282 Ø Pellets (End section)	T	0.006[d]	N/A	0.012	0.001
CAVITY LINER TO TOP OR BOTTOM DU					
Flat	T	0.036	N/A	0.031	0.040
Corner	T	0.060	N/A	0.057	0.065
CAVITY LINER TO CENTER DU					
Flat	T	0.021	0.012	N/A	0.025
Corner	T	0.030	0.018	N/A	0.035
DU TO CASK WALL					
Flat	T	0.010	0.013	0.013	0.005
Corner	T	0.073	0.076	0.075	0.066
DU TO CASK WALL & CAVITY LINER					
With No Gap	A	0.000	0.045[b]	N/A[b]	Contact[c]

NOTES:
- (a) Gap types are the following: T is transverse and A is axial.
- (b) Axially averaged temperature was used for the calculation.
- (c) Differential expansion causes interaction of the components, the effect of which is considered in Section 2.6.2.
- (d) Given by Sheet 9 of Drawing 031348.
- (e) Temperatures given in Table 2.6-1.

Additionally, during the hot environment condition, there is interaction between the cavity liner and the cask containment boundary and the cask containment boundary and the outer shell. The stresses resulting from these interactions are given in Section 2.6.1.3.

2.6.1.3 Stress Calculations. This section presents the stresses produced by the heat test. The stresses due to other normal condition load cases are presented in Sections 2.6.2 through 2.6.5 and Section 2.6.7.

Stresses during the heat test are produced by pressure (80 psi), closure bolt preload (235 ft-lb torque), and temperature gradients. Figure 2.6-3 shows the most critical sections on the containment boundary. The containment boundary stress components and stress intensities due to pressure are presented in Tables 2.6-13 through 2.6-17. As shown by Tables 2.6-13 through 2.6-17, the pressure-induced stresses on the containment boundary are very small. The stresses are also small under the 10 CFR Part 71.85(b) specified 1.5 MNOP test and meet the stress requirements of NB-3226(a).

The stresses on the seal weld for the gas sample port passageway due to MNOP are negligible. The area of the 1/8-in. diameter passageway is equal to $A = \pi(1/16)^2 = 0.012$ in.^{2} The maximum stress in the weld is σ_{max} = (A x MNOP) / (π x diameter x thickness of weld) = (0.012 in.^{2} x 80 psi) / π (1/8 in.)(1/8 in.) = 20 psi. These stresses are very small, and therefore fatigue is also not a problem.

The pressure- and temperature-induced stresses for the cavity liner are described in Sections 2.10.9.5 and 2.10.9.6.

The fuel cavity liner is attached to the cask body at the flange and bottom plate. During the heat test, the cavity liner is hotter than the cask wall; therefore, thermally induced stresses are produced axially on the cask wall and the cavity liner. The difference in temperature creates a compressive stress on the cavity liner and a tensile stress on the cask wall.

Section 2.10.9.3.5 discusses the results of an ANSYS analysis of the thermally-induced stresses in the FSS. These thermal stresses are in the axial direction and are classified as secondary stresses. The maximum stresses are well below the allowable of 3.0 Sm.

The cask wall is hotter than the neutron shield outer shell. This difference in temperature between the outer shell and the cask wall causes differential thermal growth and interaction, resulting in thermal stress.

To calculate the stress in the outer shell for the hot environment condition, the average axial temperatures of the cask body and the outer shell were used. It was assumed that the shell experiences all of the stress because it is about one-tenth the thickness of the cask wall. Using the temperatures of Table 2.6-1, we have

$$
\begin{aligned}
\varepsilon &= \alpha_{cask}\,\Delta T_{cask} - \alpha_{shell}\,\Delta T_{shell}, \\
&= 8.44 \times 10^{-6}\,(177 - 70) - 8.43 \times 10^{-6}\,(175 - 70), \text{ and} \\
&= 1.793 \times 10^{-5}. \\
\therefore\ \sigma &= \varepsilon\, E_{shell}, \\
&= (1.793 \times 10^{-5})(27.6 \times 10^{6}), \\
&= 495 \text{ psi.}
\end{aligned}
$$

Therefore, during the hot environment condition, the outer shell of the GA-4 cask experiences a tensile axial stress of 495 psi.

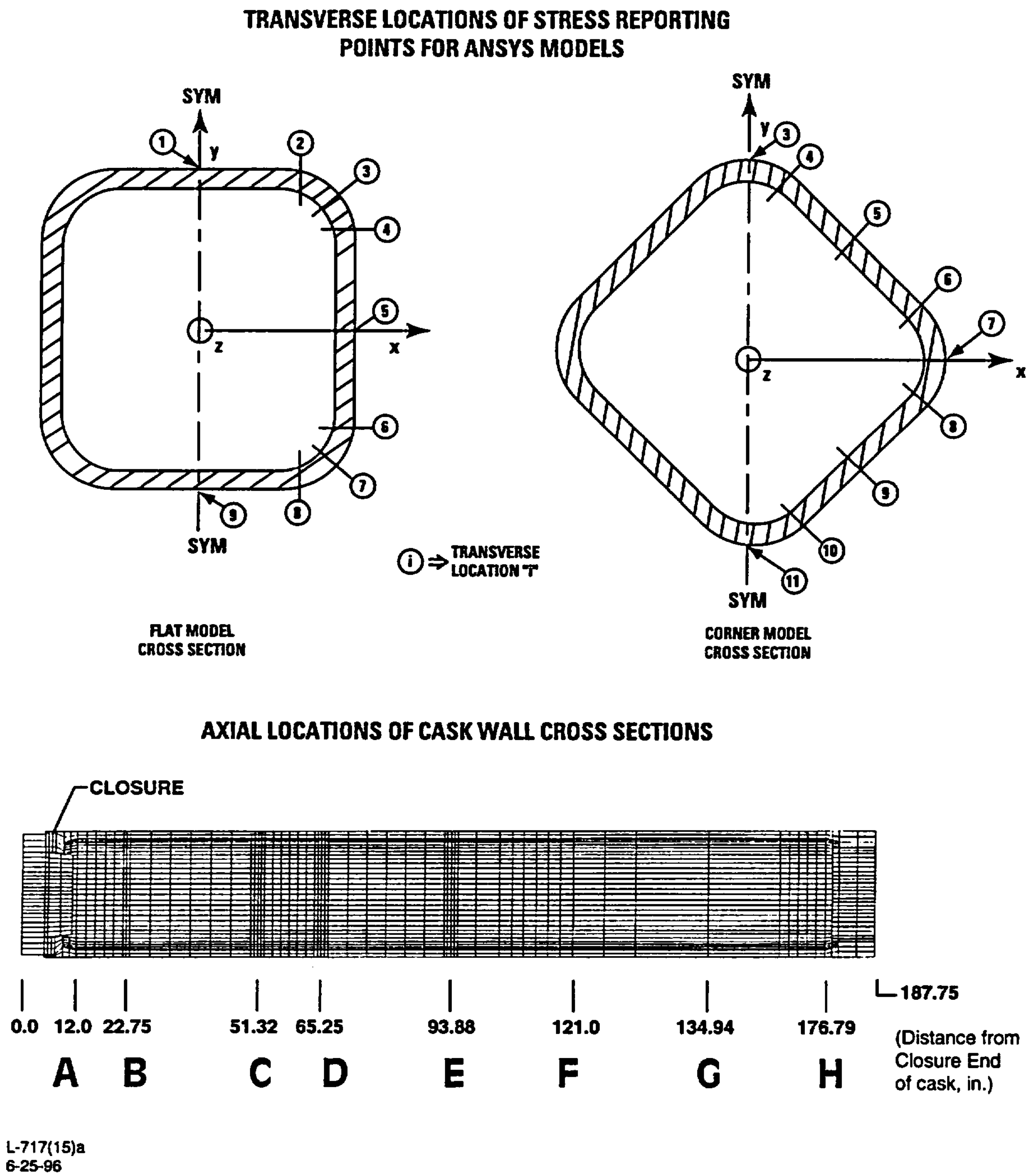

Fig. 2.6-3. Schematic of GA-4 cask wall showing symmetry planes and stress point reporting locations for ANSYS model of the GA-4 cask

TABLE 2.6-13 CONTAINMENT WALL STRESSES (ksi), FLAT MODEL, MNOP, 80 psig, (T=200°F), SECTION A

Stress Location		Node	Combined Stress Components						Principal Stresses			Stress	Stress	Stress	Design
			S_x	S_y	S_z	S_{xy}	S_{yz}	S_{xz}	S1	S2	S3	Int.	Type	Limit	Margin
1	Inside	1383	0.25	0.06	2.00	0.04	0.46	–0.04	2.11	0.26	–0.05	2.16	P_m+P_b	49.80	22.09
	Middle	1390	0.65	–0.01	0.64	0.04	0.26	0.03	0.75	0.64	–0.11	0.85	P_m	33.20	37.88
	Outside	1397	1.10	–0.04	–0.70	0.04	0.18	0.11	1.10	0.00	–0.75	1.85	P_m+P_b	49.80	25.88
2	Inside	1417	0.92	–0.00	0.91	–0.20	0.15	–0.54	1.50	0.37	–0.05	1.55	P_m+P_b	49.80	31.20
	Middle	1419	0.17	–0.03	0.20	–0.08	0.06	0.07	0.26	0.17	–0.08	0.34	P_m	33.20	97.73
	Outside	1421	–0.44	–0.00	–0.46	0.00	–0.04	0.69	0.24	–0.00	–1.13	1.37	P_m+P_b	49.80	35.24
3	Inside	1466	0.71	0.71	0.31	–0.75	–0.04	–0.04	1.45	0.32	–0.05	1.50	P_m+P_b	49.80	32.10
	Middle	1465	0.07	0.07	–0.07	–0.02	–0.06	–0.06	0.09	0.08	–0.11	0.21	P_m	33.20	159.91
	Outside	1464	–0.41	–0.41	–0.37	0.51	–0.06	–0.06	0.11	–0.39	–0.92	1.03	P_m+P_b	49.80	47.30
4	Inside	9981	–0.00	0.92	0.91	–0.20	–0.54	0.15	1.50	0.37	–0.05	1.55	P_m+P_b	49.80	31.20
	Middle	9983	–0.03	0.17	0.20	–0.08	0.07	0.06	0.26	0.17	–0.08	0.34	P_m	33.20	97.73
	Outside	9985	–0.00	–0.44	–0.46	0.00	0.69	–0.04	0.24	–0.00	–1.13	1.37	P_m+P_b	49.80	35.24
5	Inside	9947	0.06	0.25	2.00	0.00	0.00	0.46	2.11	0.25	–0.04	2.15	P_m+P_b	49.80	22.16
	Middle	9954	–0.01	0.65	0.64	0.00	0.00	0.26	0.73	0.65	–0.11	0.84	P_m	33.20	38.63
	Outside	9961	–0.04	1.10	–0.70	0.00	0.00	0.18	1.10	0.00	–0.74	1.84	P_m+P_b	49.80	26.08
6	Inside	27109	–0.00	0.92	0.91	0.20	0.54	0.15	1.50	0.37	–0.05	1.55	P_m+P_b	49.80	31.20
	Middle	27111	–0.03	0.17	0.20	0.08	–0.07	0.06	0.26	0.17	–0.08	0.34	P_m	33.20	97.73
	Outside	27113	–0.00	–0.44	–0.46	–0.00	–0.69	–0.04	0.24	–0.00	–1.13	1.37	P_m+P_b	49.80	35.24
7	Inside	18594	0.71	0.71	0.31	0.75	0.04	–0.04	1.45	0.32	–0.05	1.50	P_m+P_b	49.80	32.10
	Middle	18593	0.07	0.07	–0.07	0.02	0.06	–0.06	0.09	0.08	–0.11	0.21	P_m	33.20	159.91
	Outside	18592	–0.41	–0.41	–0.37	–0.51	0.06	–0.06	0.11	–0.39	–0.92	1.03	P_m+P_b	49.80	47.30
8	Inside	18545	0.92	–0.00	0.91	0.20	–0.15	–0.54	1.50	0.37	–0.05	1.55	P_m+P_b	49.80	31.20
	Middle	18547	0.17	–0.03	0.20	0.08	–0.06	0.07	0.26	0.17	–0.08	0.34	P_m	33.20	97.73
	Outside	18549	–0.44	–0.00	–0.46	–0.00	0.04	0.69	0.24	–0.00	–1.13	1.37	P_m+P_b	49.80	35.24
9	Inside	18511	0.25	0.06	2.00	–0.04	–0.46	–0.04	2.11	0.26	–0.05	2.16	P_m+P_b	49.80	22.09
	Middle	18518	0.65	–0.01	0.64	–0.04	–0.26	0.03	0.75	0.64	–0.11	0.85	P_m	33.20	37.88
	Outside	18525	1.10	–0.04	–0.70	–0.04	–0.18	0.11	1.10	0.00	–0.75	1.85	P_m+P_b	49.80	25.88

MNOP.TBL

TABLE 2.6-14 CONTAINMENT WALL STRESSES (ksi), FLAT MODEL, MNOP, 80 psig, (T=200°F), SECTION B

Stress Location		Node	Combined Stress Components						Principal Stresses			Stress Int.	Stress Type	Stress Limit	Design Margin
			S_x	S_y	S_z	S_{xy}	S_{yz}	S_{xz}	S1	S2	S3				
1	Inside	2748	–3.05	–0.07	–1.36	–0.02	0.02	–0.03	–0.07	–1.36	–3.05	2.98	P_m+P_b	49.80	15.69
	Middle	2755	0.66	–0.00	0.38	–0.03	0.03	0.00	0.66	0.38	–0.01	0.67	P_m	33.20	48.29
	Outside	2762	4.35	0.06	2.11	–0.07	0.00	0.05	4.36	2.11	0.06	4.30	P_m+P_b	49.80	10.58
2	Inside	2965	2.52	0.00	0.70	–0.51	–0.03	–0.33	2.68	0.66	–0.10	2.78	P_m+P_b	49.80	16.92
	Middle	2967	0.55	–0.11	0.23	–0.36	–0.06	0.06	0.72	0.21	–0.27	0.99	P_m	33.20	32.47
	Outside	2969	–0.92	–0.20	–0.08	–0.16	0.03	0.40	0.08	–0.17	–1.11	1.20	P_m+P_b	49.80	40.64
3	Inside	3053	2.78	2.78	1.69	–2.85	–0.04	–0.04	5.63	1.69	–0.07	5.70	P_m+P_b	49.80	7.74
	Middle	3052	0.28	0.28	0.18	–0.24	–0.03	–0.03	0.52	0.19	0.03	0.49	P_m	33.20	66.58
	Outside	3051	–1.52	–1.52	–0.92	1.64	–0.03	–0.03	0.12	–0.92	–3.16	3.28	P_m+P_b	49.80	14.19
4	Inside	11529	0.00	2.52	0.70	–0.51	–0.33	–0.03	2.68	0.66	–0.10	2.78	P_m+P_b	49.80	16.92
	Middle	11531	–0.11	0.55	0.23	–0.36	0.06	–0.06	0.72	0.21	–0.27	0.99	P_m	33.20	32.47
	Outside	11533	–0.20	–0.92	–0.08	–0.16	0.40	0.03	0.08	–0.17	–1.11	1.20	P_m+P_b	49.80	40.64
5	Inside	11312	–0.07	–3.05	–1.36	0.00	0.00	0.02	–0.07	–1.36	–3.05	2.98	P_m+P_b	49.80	15.70
	Middle	11319	–0.00	0.66	0.38	0.00	0.00	0.03	0.66	0.38	–0.01	0.67	P_m	33.20	48.47
	Outside	11326	0.06	4.35	2.11	0.00	0.00	0.00	4.35	2.11	0.06	4.30	P_m+P_b	49.80	10.59
6	Inside	28657	0.00	2.52	0.70	0.51	0.33	–0.03	2.68	0.66	–0.10	2.78	P_m+P_b	49.80	16.92
	Middle	28659	–0.11	0.55	0.23	0.36	–0.06	–0.06	0.72	0.21	–0.27	0.99	P_m	33.20	32.47
	Outside	28661	–0.20	–0.92	–0.08	0.16	–0.40	0.03	0.08	–0.17	–1.11	1.20	P_m+P_b	49.80	40.64
7	Inside	20181	2.78	2.78	1.69	2.85	0.04	–0.04	5.63	1.69	–0.07	5.70	P_m+P_b	49.80	7.74
	Middle	20180	0.28	0.28	0.18	0.24	0.03	–0.03	0.52	0.19	0.03	0.49	P_m	33.20	66.58
	Outside	20179	–1.52	–1.52	–0.92	–1.64	0.03	–0.03	0.12	–0.92	–3.16	3.28	P_m+P_b	49.80	14.19
8	Inside	20093	2.52	0.00	0.70	0.51	0.03	–0.33	2.68	0.66	–0.10	2.78	P_m+P_b	49.80	16.92
	Middle	20095	0.55	–0.11	0.23	0.36	0.06	0.06	0.72	0.21	–0.27	0.99	P_m	33.20	32.47
	Outside	20097	–0.92	–0.20	–0.08	0.16	–0.03	0.40	0.08	–0.17	–1.11	1.20	P_m+P_b	49.80	40.64
9	Inside	19876	–3.05	–0.07	–1.36	0.02	–0.02	–0.03	–0.07	–1.36	–3.05	2.98	P_m+P_b	49.80	15.69
	Middle	19883	0.66	–0.00	0.38	0.03	–0.03	0.00	0.66	0.38	–0.01	0.67	P_m	33.20	48.29
	Outside	19890	4.35	0.06	2.11	0.07	–0.00	0.05	4.36	2.11	0.06	4.30	P_m+P_b	49.80	10.58

MNOP.TBL

TABLE 2.6-15 CONTAINMENT WALL STRESSES (ksi), FLAT MODEL, MNOP, 80 psig, (T=200°F), SECTION C

Stress Location		Node	Combined Stress Components						Principal Stresses			Stress Int.	Stress Type	Stress Limit	Design Margin
			S_x	S_y	S_z	S_{xy}	S_{yz}	S_{xz}	S1	S2	S3				
1	Inside	2937	–3.47	–0.05	–0.96	–0.03	–0.00	0.00	–0.05	–0.96	–3.47	3.42	P_m+P_b	49.80	13.55
	Middle	2944	0.76	–0.04	0.31	–0.03	–0.00	0.00	0.76	0.31	–0.04	0.80	P_m	33.20	40.48
	Outside	2951	4.99	–0.03	1.58	–0.03	–0.00	0.00	4.99	1.58	–0.03	5.02	P_m+P_b	49.80	8.92
2	Inside	3019	3.10	0.04	1.03	–0.60	–0.00	0.01	3.21	1.03	–0.07	3.28	P_m+P_b	49.80	14.17
	Middle	3021	0.60	0.04	0.28	–0.40	–0.00	0.00	0.81	0.28	–0.17	0.97	P_m	33.20	33.12
	Outside	3023	–1.32	0.06	–0.28	–0.25	–0.00	–0.00	0.11	–0.28	–1.36	1.47	P_m+P_b	49.80	32.86
3	Inside	3188	3.16	3.16	1.97	–3.25	0.00	0.00	6.41	1.97	–0.10	6.51	P_m+P_b	49.80	6.65
	Middle	3187	0.23	0.23	0.24	–0.22	0.00	0.00	0.46	0.24	0.01	0.45	P_m	33.20	73.60
	Outside	3186	–1.82	–1.82	–0.98	1.92	0.00	0.00	0.10	–0.98	–3.75	3.85	P_m+P_b	49.80	11.94
4	Inside	11583	0.04	3.10	1.03	–0.60	0.01	–0.00	3.21	1.03	–0.07	3.28	P_m+P_b	49.80	14.17
	Middle	11585	0.04	0.60	0.28	–0.40	0.00	–0.00	0.81	0.28	–0.17	0.97	P_m	33.20	33.12
	Outside	11587	0.06	–1.32	–0.28	–0.25	–0.00	–0.00	0.11	–0.28	–1.36	1.47	P_m+P_b	49.80	32.86
5	Inside	11501	–0.05	–3.47	–0.96	0.00	0.00	–0.00	–0.05	–0.96	–3.47	3.42	P_m+P_b	49.80	13.55
	Middle	11508	–0.04	0.76	0.31	0.00	0.00	–0.00	0.76	0.31	–0.04	0.80	P_m	33.20	40.60
	Outside	11515	–0.03	4.99	1.58	0.00	0.00	–0.00	4.99	1.58	–0.03	5.02	P_m+P_b	49.80	8.92
6	Inside	28711	0.04	3.10	1.03	0.60	–0.01	–0.00	3.21	1.03	–0.07	3.28	P_m+P_b	49.80	14.17
	Middle	28713	0.04	0.60	0.28	0.40	–0.00	–0.00	0.81	0.28	–0.17	0.97	P_m	33.20	33.12
	Outside	28715	0.06	–1.32	–0.28	0.25	0.00	–0.00	0.11	–0.28	–1.36	1.47	P_m+P_b	49.80	32.86
7	Inside	20316	3.16	3.16	1.97	3.25	–0.00	0.00	6.41	1.97	–0.10	6.51	P_m+P_b	49.80	6.65
	Middle	20315	0.23	0.23	0.24	0.22	–0.00	0.00	0.46	0.24	0.01	0.45	P_m	33.20	73.60
	Outside	20314	–1.82	–1.82	–0.98	–1.92	–0.00	0.00	0.10	–0.98	–3.75	3.85	P_m+P_b	49.80	11.94
8	Inside	20147	3.10	0.04	1.03	0.60	0.00	0.01	3.21	1.03	–0.07	3.28	P_m+P_b	49.80	14.17
	Middle	20149	0.60	0.04	0.28	0.40	0.00	0.00	0.81	0.28	–0.17	0.97	P_m	33.20	33.12
	Outside	20151	–1.32	0.06	–0.28	0.25	0.00	–0.00	0.11	–0.28	–1.36	1.47	P_m+P_b	49.80	32.86
9	Inside	20065	–3.47	–0.05	–0.96	0.03	0.00	0.00	–0.05	–0.96	–3.47	3.42	P_m+P_b	49.80	13.55
	Middle	20072	0.76	–0.04	0.31	0.03	0.00	0.00	0.76	0.31	–0.04	0.80	P_m	33.20	40.48
	Outside	20079	4.99	–0.03	1.58	0.03	0.00	0.00	4.99	1.58	–0.03	5.02	P_m+P_b	49.80	8.92

MNOP.TBL

TABLE 2.6-16 CONTAINMENT WALL STRESSES (ksi), FLAT MODEL, MNOP, 80 psig, (T=200°F), SECTION D

Stress Location		Node	Combined Stress Components						Principal Stresses			Stress Int.	Stress Type	Stress Limit	Design Margin
			S_x	S_y	S_z	S_{xy}	S_{yz}	S_{xz}	S1	S2	S3				
1	Inside	3399	–3.47	–0.05	–0.96	–0.03	0.00	–0.00	–0.05	–0.96	–3.47	3.42	P_m+P_b	49.80	13.56
	Middle	3406	0.76	–0.04	0.31	–0.03	0.00	–0.00	0.76	0.31	–0.04	0.80	P_m	33.20	40.48
	Outside	3413	4.99	–0.03	1.58	–0.03	0.00	–0.00	4.99	1.58	–0.03	5.02	P_m+P_b	49.80	8.93
2	Inside	3481	3.10	0.04	1.03	–0.60	0.00	–0.00	3.21	1.03	–0.07	3.28	P_m+P_b	49.80	14.18
	Middle	3483	0.60	0.04	0.28	–0.40	0.00	–0.00	0.81	0.28	–0.17	0.97	P_m	33.20	33.13
	Outside	3485	–1.32	0.06	–0.28	–0.25	0.00	0.00	0.11	–0.28	–1.36	1.47	P_m+P_b	49.80	32.89
3	Inside	3650	3.15	3.15	1.97	–3.25	–0.00	–0.00	6.41	1.97	–0.10	6.50	P_m+P_b	49.80	6.66
	Middle	3649	0.23	0.23	0.24	–0.22	–0.00	–0.00	0.46	0.24	0.01	0.44	P_m	33.20	73.73
	Outside	3648	–1.82	–1.82	–0.98	1.92	–0.00	–0.00	0.10	–0.98	–3.74	3.85	P_m+P_b	49.80	11.95
4	Inside	12045	0.04	3.10	1.03	–0.60	–0.00	0.00	3.21	1.03	–0.07	3.28	P_m+P_b	49.80	14.18
	Middle	12047	0.04	0.60	0.28	–0.40	–0.00	0.00	0.81	0.28	–0.17	0.97	P_m	33.20	33.13
	Outside	12049	0.06	–1.32	–0.28	–0.25	0.00	0.00	0.11	–0.28	–1.36	1.47	P_m+P_b	49.80	32.89
5	Inside	11963	–0.05	–3.47	–0.96	0.00	0.00	0.00	–0.05	–0.96	–3.47	3.42	P_m+P_b	49.80	13.56
	Middle	11970	–0.04	0.76	0.31	0.00	0.00	0.00	0.76	0.31	–0.04	0.80	P_m	33.20	40.60
	Outside	11977	–0.03	4.99	1.58	0.00	0.00	0.00	4.99	1.58	–0.03	5.02	P_m+P_b	49.80	8.93
6	Inside	29173	0.04	3.10	1.03	0.60	0.00	0.00	3.21	1.03	–0.07	3.28	P_m+P_b	49.80	14.18
	Middle	29175	0.04	0.60	0.28	0.40	0.00	0.00	0.81	0.28	–0.17	0.97	P_m	33.20	33.13
	Outside	29177	0.06	–1.32	–0.28	0.25	–0.00	0.00	0.11	–0.28	–1.36	1.47	P_m+P_b	49.80	32.89
7	Inside	20778	3.15	3.15	1.97	3.25	0.00	–0.00	6.41	1.97	–0.10	6.50	P_m+P_b	49.80	6.66
	Middle	20777	0.23	0.23	0.24	0.22	0.00	–0.00	0.46	0.24	0.01	0.44	P_m	33.20	73.73
	Outside	20776	–1.82	–1.82	–0.98	–1.92	0.00	–0.00	0.10	–0.98	–3.74	3.85	P_m+P_b	49.80	11.95
8	Inside	20609	3.10	0.04	1.03	0.60	–0.00	–0.00	3.21	1.03	–0.07	3.28	P_m+P_b	49.80	14.18
	Middle	20611	0.60	0.04	0.28	0.40	–0.00	–0.00	0.81	0.28	–0.17	0.97	P_m	33.20	33.13
	Outside	20613	–1.32	0.06	–0.28	0.25	–0.00	0.00	0.11	–0.28	–1.36	1.47	P_m+P_b	49.80	32.89
9	Inside	20527	–3.47	–0.05	–0.96	0.03	–0.00	–0.00	–0.05	–0.96	–3.47	3.42	P_m+P_b	49.80	13.56
	Middle	20534	0.76	–0.04	0.31	0.03	–0.00	–0.00	0.76	0.31	–0.04	0.80	P_m	33.20	40.48
	Outside	20541	4.99	–0.03	1.58	0.03	–0.00	–0.00	4.99	1.58	–0.03	5.02	P_m+P_b	49.80	8.93

MNOP.TBL

TABLE 2.6-17 CONTAINMENT WALL STRESSES (ksi),
FLAT MODEL, MNOP, 80 psig, (T=200°F), SECTION E

Stress Location		Node	Combined Stress Components						Principal Stresses			Stress Int.	Stress Type	Stress Limit	Design Margin
			S_x	S_y	S_z	S_{xy}	S_{yz}	S_{xz}	S1	S2	S3				
1	Inside	3861	–3.48	–0.05	–0.97	–0.03	0.00	–0.00	–0.05	–0.97	–3.49	3.44	P_m+P_b	49.80	13.50
	Middle	3868	0.75	–0.04	0.31	–0.03	0.00	–0.00	0.75	0.31	–0.04	0.79	P_m	33.20	40.94
	Outside	3875	4.98	–0.03	1.58	–0.03	0.00	–0.00	4.98	1.58	–0.03	5.01	P_m+P_b	49.80	8.93
2	Inside	3943	3.09	0.04	1.02	–0.60	0.00	–0.00	3.21	1.02	–0.07	3.28	P_m+P_b	49.80	14.20
	Middle	3945	0.59	0.04	0.28	–0.40	0.00	–0.00	0.80	0.28	–0.17	0.97	P_m	33.20	33.19
	Outside	3947	–1.32	0.06	–0.28	–0.25	0.00	–0.00	0.11	–0.28	–1.36	1.47	P_m+P_b	49.80	32.87
3	Inside	4112	3.14	3.14	1.94	–3.27	0.00	0.00	6.41	1.94	–0.13	6.54	P_m+P_b	49.80	6.62
	Middle	4111	0.23	0.23	0.25	–0.23	0.00	0.00	0.46	0.25	–0.00	0.46	P_m	33.20	71.05
	Outside	4110	–1.83	–1.83	–0.95	1.92	0.00	0.00	0.10	–0.95	–3.75	3.85	P_m+P_b	49.80	11.95
4	Inside	12507	0.04	3.09	1.02	–0.60	–0.00	0.00	3.21	1.02	–0.07	3.28	P_m+P_b	49.80	14.20
	Middle	12509	0.04	0.59	0.28	–0.40	–0.00	0.00	0.80	0.28	–0.17	0.97	P_m	33.20	33.19
	Outside	12511	0.06	–1.32	–0.28	–0.25	–0.00	0.00	0.11	–0.28	–1.36	1.47	P_m+P_b	49.80	32.87
5	Inside	12425	–0.05	–3.48	–0.97	0.00	0.00	0.00	–0.05	–0.97	–3.48	3.43	P_m+P_b	49.80	13.50
	Middle	12432	–0.04	0.75	0.31	0.00	0.00	0.00	0.75	0.31	–0.04	0.79	P_m	33.20	41.07
	Outside	12439	–0.03	4.98	1.58	0.00	0.00	0.00	4.98	1.58	–0.03	5.01	P_m+P_b	49.80	8.93
6	Inside	29635	0.04	3.09	1.02	0.60	0.00	0.00	3.21	1.02	–0.07	3.28	P_m+P_b	49.80	14.20
	Middle	29637	0.04	0.59	0.28	0.40	0.00	0.00	0.80	0.28	–0.17	0.97	P_m	33.20	33.19
	Outside	29639	0.06	–1.32	–0.28	0.25	0.00	0.00	0.11	–0.28	–1.36	1.47	P_m+P_b	49.80	32.87
7	Inside	21240	3.14	3.14	1.94	3.27	–0.00	0.00	6.41	1.94	–0.13	6.54	P_m+P_b	49.80	6.62
	Middle	21239	0.23	0.23	0.25	0.23	–0.00	0.00	0.46	0.25	–0.00	0.46	P_m	33.20	71.05
	Outside	21238	–1.83	–1.83	–0.95	–1.92	–0.00	0.00	0.10	–0.95	–3.75	3.85	P_m+P_b	49.80	11.95
8	Inside	21071	3.09	0.04	1.02	0.60	–0.00	–0.00	3.21	1.02	–0.07	3.28	P_m+P_b	49.80	14.20
	Middle	21073	0.59	0.04	0.28	0.40	–0.00	–0.00	0.80	0.28	–0.17	0.97	P_m	33.20	33.19
	Outside	21075	–1.32	0.06	–0.28	0.25	–0.00	–0.00	0.11	–0.28	–1.36	1.47	P_m+P_b	49.80	32.87
9	Inside	20989	–3.48	–0.05	–0.97	0.03	0.00	–0.00	–0.05	–0.97	–3.49	3.44	P_m+P_b	49.80	13.50
	Middle	20996	0.75	–0.04	0.31	0.03	0.00	–0.00	0.75	0.31	–0.04	0.79	P_m	33.20	40.94
	Outside	21003	4.98	–0.03	1.58	0.03	0.00	–0.00	4.98	1.58	–0.03	5.01	P_m+P_b	49.80	8.93

MNOP.TBL

The stresses caused by the interaction of the cavity liner and the cask containment boundary were evaluated in Table 2.6-18. It was assumed that the two components were connected at the ends by a rigid bar and that only the stiffness of the cavity liner and cask containment boundary contributed to the interaction of these parts. The effect of the FSS on the interaction was neglected. The stresses for the hot environment condition are 1.4 ksi axial compression for the cavity liner and 300 psi axial tension for the cask containment boundary. These stresses were treated as primary stresses in the evaluation of the hot environment condition load cases.

2.6.2 Cold

A steady-state temperature of –40°F (design cold condition) will have no detrimental effect upon the GA-4 cask. The austenitic stainless steel cask and the nonferrous nickel-base alloy steel used for bolts do not undergo a ductile to brittle transition; therefore, brittle fracture is precluded for this condition.

With no decay heat, the steady-state cold conditions do not have thermal gradients through the cask wall. There are two cold conditions: the cold environment condition, which is a uniform –20°F, and the minimum temperature condition, which is a uniform –40°F. For both of these conditions, interaction between components is the result of the different thermal expansivities. Tables 2.6-7 through 2.6-10 show that the only components which interact are the DU, cavity liner and cask wall in the axial direction. As shown by Tables 2.6-19 and 2.6-20, the difference in the shrinkage of the DU and the XM-19 of the cavity liner and the cask wall, causes axial tensile stresses in the XM-19 components and axial compression in the DU. For the –20°F cold environment condition, the DU experiences 3.8 ksi compression, while the XM-19 components experience a tensile stress of 5.0 ksi. For the –40°F temperature, the values are 5.0 ksi compression and 6.6 ksi tension, respectively.

2.6.3 Reduced External Pressure

The reduced external pressure condition requires that the cask be evaluated at 3.5 psia external pressure, at maximum internal pressure, and at ambient temperature between 100°F and –20°F. Reducing the external pressure from 14.7 to 3.5 psia raises the cask internal pressure by 11.2 psi. Since the MNOP is 74 psig, the resulting maximum internal pressure differential is 85.2 psi. The cask was analyzed for an external pressure of 85.4 psi, which is conservative. The resulting stresses for the GA-4 cask containment boundary are presented in Tables 2.6-21 through 2.6-25. The design margin values are very high due to the relatively low stresses.

In addition to the cask containment boundary, the neutron shield outer shell was evaluated for the reduced external pressure load case. As described in Section 2.10.11.4, the shield's outer shell was analyzed as a thin-walled cylinder with internal pressure. The hoop and axial stresses were 6.63 ksi and 3.32 ksi, respectively. The lowest design margin was 4.01, using the membrane allowable of 33.2 ksi. Therefore, the neutron shield's shell design is acceptable for the reduced external pressure load case.

TABLE 2.6-18 INTERACTION OF CAVITY LINER AND CASK WALL AT HOT ENVIRONMENT CONDITIONS

MATERIAL PROPERTY OR GEOMETRIC CHARACTERISTIC	COMPONENT		
	CAVITY LINER	DEPLETED URANIUM	CASK WALL
L - Length (in.)	170.79	170.79	170.79
A - Area (in.)	27.67	224.	141.85
T - Temperature (°F)	184.	180.	177.
E - Elastic Modulus (psi)	27.5E06	30.0E06	27.7E06
α - Thermal Expansivity (in./in. °F)	8.45E-06	5.92E-06	8.44E-06
δ_{free} - Unrestrained growth (in.)	0.16452	0.11122	0.15425
L'_{free} - Unrestrained length (in.)	170.9545	170.9012	170.9442
EA - (lb)	7.61E08	—	3.92E09
$EA\delta_{free}$ - (in.-lb)	1.25E08	—	6.05E08
$\delta_{combined}$ (in.)[a]	0.1559	—	0.1559
$\delta_{constrained}$ (in.)[b]	-0.00861	—	0.00167
E/L - (lb/in.)	1.61E05	—	1.62E05
σ - Stress from interaction (psi)[c]	-1390.	—	270.

NOTES:

(a) $\delta_{combined} = (\Sigma EA\delta_{free})/(\Sigma EA)$

(b) $\delta_{constrained} = \delta_{combined} - \delta_{free}$

(c) $\sigma = (E/L) * \delta_{constrained}$

TABLE 2.6-19 INTERACTION OF CAVITY LINER, DU, AND CASK WALL AT COLD ENVIRONMENT CONDITIONS

MATERIAL PROPERTY OR GEOMETRIC CHARACTERISTIC	COMPONENT		
	CAVITY LINER	DEPLETED URANIUM	CASK WALL
L - Length (in.)	170.79	170.79	170.79
A - Area (in.)	27.67	224.	141.85
T - Temperature (°F)	-20.	-20.	-20.
E - Elastic Modulus (psi)	28.7E06	30.0E06	28.7E06
α - Thermal Expansivity (in./in. °F)	8.16E-06	4.80E-06	8.16E-06
δ_{free} - Unrestrained growth (in.)	-0.1254	-0.0738	-0.1254
L'_{free} - Unrestrained length (in.)	170.6646	170.7162	170.6646
EA - (lb)	7.94E08	6.72E09	4.07E09
$EA\delta_{free}$ - (in.-lb)	-9.96E07	-4.96E08	-5.11E08
$\delta_{combined}$ (in.) [(a)]	-0.09547	-0.09547	-0.09547
$\delta_{constrained}$ (in.) [(b)]	0.02996	-0.02169	0.02996
E/L - (lb/in.)	1.68E05	1.76E05	1.68E05
σ - Stress from interaction (psi) [(c)]	5,034.	-3,810.	5,034.

NOTES:

(a) $\delta_{combined}=(\Sigma EA\delta_{free})/(\Sigma EA)$

(b) $\delta_{constrained} = \delta_{combined} - \delta_{free}$

(c) $\sigma = (E/L) * \delta_{constrained}$

TABLE 2.6-20 INTERACTION OF CAVITY LINER, DU, AND CASK WALL AT MINIMUM TEMPERATURE CONDITIONS

MATERIAL PROPERTY OR GEOMETRIC CHARACTERISTIC	COMPONENT		
	CAVITY LINER	DEPLETED URANIUM	CASK WALL
L - Length (in.)	170.79	170.79	170.79
A - Area (in.)	27.67	224.	141.85
T - Temperature (°F)	-40.	-40.	-40.
E - Elastic Modulus (psi)	28.8E06	30.0E06	28.8E06
α - Thermal Expansivity (in./in. °F)	8.10E-06	4.50E-06	8.10E-06
δ_{free} - Unrestrained growth (in.)	-0.15217	-0.08454	-0.15217
L'_{free} - Unrestrained length (in.)	170.6378	170.7055	170.6378
EA - (lb)	7.97E08	6.72E09	4.09E09
$EA\delta_{free}$ - (in.-lb)	-1.21E08	-5.68E08	-6.22E08
$\delta_{combined}$ (in.) [(a)]	-0.1130	-0.1130	-0.1130
$\delta_{constrained}$ (in.) [(b)]	0.03917	-0.02846	0.03917
E/L - (lb/in.)	1.69E05	1.76E05	1.69E05
σ - Stress from interaction (psi) [(c)]	6,605.	-4,999.	6,605.

NOTES:

(a) $\delta_{combined} = (\Sigma EA\delta_{free})/(\Sigma EA)$

(b) $\delta_{constrained} = \delta_{combined} - \delta_{free}$

(c) $\sigma = (E/L) * \delta_{constrained}$

TABLE 2.6-21 CONTAINMENT WALL STRESSES (ksi),
MNOP WITH REDUCED EXTERNAL PRESSURE (P_{int} = 85.4 psig, T=200°F), SECTION A

Stress Location		Node	Combined Stress Components						Principal Stresses			Stress Int.	Stress Type	Stress Limit	Design Margin
			S_x	S_y	S_z	S_{xy}	S_{yz}	S_{xz}	S1	S2	S3				
1	Inside	1383	0.27	0.07	2.14	0.04	0.50	–0.04	2.25	0.28	–0.05	2.30	P_m+P_b	49.80	20.63
	Middle	1390	0.69	–0.01	0.68	0.04	0.28	0.03	0.80	0.68	–0.12	0.91	P_m	33.20	35.42
	Outside	1397	1.17	–0.04	–0.74	0.04	0.20	0.11	1.18	0.00	–0.80	1.98	P_m+P_b	49.80	24.18
2	Inside	1417	0.98	–0.00	0.97	–0.21	0.16	–0.58	1.60	0.40	–0.05	1.65	P_m+P_b	49.80	29.16
	Middle	1419	0.19	–0.04	0.22	–0.08	0.06	0.07	0.27	0.18	–0.09	0.36	P_m	33.20	91.48
	Outside	1421	–0.47	–0.00	–0.49	0.00	–0.04	0.73	0.26	–0.01	–1.21	1.47	P_m+P_b	49.80	32.94
3	Inside	1466	0.75	0.75	0.33	–0.80	–0.04	–0.04	1.55	0.34	–0.05	1.61	P_m+P_b	49.80	30.01
	Middle	1465	0.07	0.07	–0.08	–0.02	–0.06	–0.06	0.10	0.09	–0.12	0.22	P_m	33.20	149.74
	Outside	1464	–0.44	–0.44	–0.40	0.54	–0.06	–0.06	0.11	–0.41	–0.99	1.10	P_m+P_b	49.80	44.25
4	Inside	9981	–0.00	0.98	0.97	–0.21	–0.58	0.16	1.60	0.40	–0.05	1.65	P_m+P_b	49.80	29.16
	Middle	9983	–0.04	0.19	0.22	–0.08	0.07	0.06	0.27	0.18	–0.09	0.36	P_m	33.20	91.48
	Outside	9985	–0.00	–0.47	–0.49	0.00	0.73	–0.04	0.26	–0.01	–1.21	1.47	P_m+P_b	49.80	32.94
5	Inside	9947	0.07	0.27	2.14	0.00	0.00	0.50	2.25	0.27	–0.05	2.29	P_m+P_b	49.80	20.70
	Middle	9954	–0.01	0.69	0.68	0.00	0.00	0.28	0.78	0.69	–0.12	0.89	P_m	33.20	36.12
	Outside	9961	–0.04	1.17	–0.74	0.00	0.00	0.20	1.17	0.00	–0.79	1.96	P_m+P_b	49.80	24.37
6	Inside	27109	–0.00	0.98	0.97	0.21	0.58	0.16	1.60	0.40	–0.05	1.65	P_m+P_b	49.80	29.16
	Middle	27111	–0.04	0.19	0.22	0.08	–0.07	0.06	0.27	0.18	–0.09	0.36	P_m	33.20	91.48
	Outside	27113	–0.00	–0.47	–0.49	–0.00	–0.73	–0.04	0.26	–0.01	–1.21	1.47	P_m+P_b	49.80	32.94
7	Inside	18594	0.75	0.75	0.33	0.80	0.04	–0.04	1.55	0.34	–0.05	1.61	P_m+P_b	49.80	30.01
	Middle	18593	0.07	0.07	–0.08	0.02	0.06	–0.06	0.10	0.09	–0.12	0.22	P_m	33.20	149.74
	Outside	18592	–0.44	–0.44	–0.40	–0.54	0.06	–0.06	0.11	–0.41	–0.99	1.10	P_m+P_b	49.80	44.25
8	Inside	18545	0.98	–0.00	0.97	0.21	–0.16	–0.58	1.60	0.40	–0.05	1.65	P_m+P_b	49.80	29.16
	Middle	18547	0.19	–0.04	0.22	0.08	–0.06	0.07	0.27	0.18	–0.09	0.36	P_m	33.20	91.48
	Outside	18549	–0.47	–0.00	–0.49	–0.00	0.04	0.73	0.26	–0.01	–1.21	1.47	P_m+P_b	49.80	32.94
9	Inside	18511	0.27	0.07	2.14	–0.04	–0.50	–0.04	2.25	0.28	–0.05	2.30	P_m+P_b	49.80	20.63
	Middle	18518	0.69	–0.01	0.68	–0.04	–0.28	0.03	0.80	0.68	–0.12	0.91	P_m	33.20	35.42
	Outside	18525	1.17	–0.04	–0.74	–0.04	–0.20	0.11	1.18	0.00	–0.80	1.98	P_m+P_b	49.80	24.18

MNOP_REDext.TBL

TABLE 2.6-22 CONTAINMENT WALL STRESSES (ksi), MNOP WITH REDUCED EXTERNAL PRESSURE (P_{int} = 85.4 psig, T=200°F), SECTION B

Stress Location		Node	Combined Stress Components						Principal Stresses			Stress Int.	Stress Type	Stress Limit	Design Margin
			S_x	S_y	S_z	S_{xy}	S_{yz}	S_{xz}	S1	S2	S3				
1	Inside	2748	–3.26	–0.07	–1.46	–0.02	0.02	–0.04	–0.07	–1.46	–3.26	3.19	P_m+P_b	49.80	14.64
	Middle	2755	0.70	–0.00	0.40	–0.03	0.03	0.00	0.71	0.40	–0.01	0.72	P_m	33.20	45.18
	Outside	2762	4.65	0.06	2.25	–0.07	0.00	0.06	4.65	2.25	0.06	4.59	P_m+P_b	49.80	9.85
2	Inside	2965	2.69	0.00	0.75	–0.54	–0.04	–0.36	2.86	0.71	–0.11	2.97	P_m+P_b	49.80	15.79
	Middle	2967	0.59	–0.12	0.24	–0.38	–0.07	0.07	0.77	0.23	–0.29	1.06	P_m	33.20	30.36
	Outside	2969	–0.98	–0.21	–0.09	–0.17	0.04	0.43	0.09	–0.18	–1.19	1.28	P_m+P_b	49.80	38.01
3	Inside	3053	2.97	2.97	1.80	–3.04	–0.04	–0.04	6.01	1.81	–0.08	6.08	P_m+P_b	49.80	7.19
	Middle	3052	0.30	0.30	0.19	–0.26	–0.03	–0.03	0.55	0.20	0.03	0.52	P_m	33.20	62.31
	Outside	3051	–1.62	–1.62	–0.98	1.75	–0.03	–0.03	0.13	–0.98	–3.37	3.50	P_m+P_b	49.80	13.22
4	Inside	11529	0.00	2.69	0.75	–0.54	–0.36	–0.04	2.86	0.71	–0.11	2.97	P_m+P_b	49.80	15.79
	Middle	11531	–0.12	0.59	0.24	–0.38	0.07	–0.07	0.77	0.23	–0.29	1.06	P_m	33.20	30.36
	Outside	11533	–0.21	–0.98	–0.09	–0.17	0.43	0.04	0.09	–0.18	–1.19	1.28	P_m+P_b	49.80	38.01
5	Inside	11312	–0.07	–3.26	–1.46	0.00	0.00	0.02	–0.07	–1.46	–3.26	3.18	P_m+P_b	49.80	14.64
	Middle	11319	–0.00	0.70	0.40	0.00	0.00	0.03	0.70	0.40	–0.01	0.72	P_m	33.20	45.35
	Outside	11326	0.06	4.65	2.25	0.00	0.00	0.00	4.65	2.25	0.06	4.59	P_m+P_b	49.80	9.86
6	Inside	28657	0.00	2.69	0.75	0.54	0.36	–0.04	2.86	0.71	–0.11	2.97	P_m+P_b	49.80	15.79
	Middle	28659	–0.12	0.59	0.24	0.38	–0.07	–0.07	0.77	0.23	–0.29	1.06	P_m	33.20	30.36
	Outside	28661	–0.21	–0.98	–0.09	0.17	–0.43	0.04	0.09	–0.18	–1.19	1.28	P_m+P_b	49.80	38.01
7	Inside	20181	2.97	2.97	1.80	3.04	0.04	–0.04	6.01	1.81	–0.08	6.08	P_m+P_b	49.80	7.19
	Middle	20180	0.30	0.30	0.19	0.26	0.03	–0.03	0.55	0.20	0.03	0.52	P_m	33.20	62.31
	Outside	20179	–1.62	–1.62	–0.98	–1.75	0.03	–0.03	0.13	–0.98	–3.37	3.50	P_m+P_b	49.80	13.22
8	Inside	20093	2.69	0.00	0.75	0.54	0.04	–0.36	2.86	0.71	–0.11	2.97	P_m+P_b	49.80	15.79
	Middle	20095	0.59	–0.12	0.24	0.38	0.07	0.07	0.77	0.23	–0.29	1.06	P_m	33.20	30.36
	Outside	20097	–0.98	–0.21	–0.09	0.17	–0.04	0.43	0.09	–0.18	–1.19	1.28	P_m+P_b	49.80	38.01
9	Inside	19876	–3.26	–0.07	–1.46	0.02	–0.02	–0.04	–0.07	–1.46	–3.26	3.19	P_m+P_b	49.80	14.64
	Middle	19883	0.70	–0.00	0.40	0.03	–0.03	0.00	0.71	0.40	–0.01	0.72	P_m	33.20	45.18
	Outside	19890	4.65	0.06	2.25	0.07	–0.00	0.06	4.65	2.25	0.06	4.59	P_m+P_b	49.80	9.85

MNOP_REDext.TBL

TABLE 2.6-23 CONTAINMENT WALL STRESSES (ksi), MNOP WITH REDUCED EXTERNAL PRESSURE (P_{int} = 85.4 psig, T=200°F), SECTION C

Stress Location		Node	Combined Stress Components						Principal Stresses			Stress Int.	Stress Type	Stress Limit	Design Margin
			S_x	S_y	S_z	S_{xy}	S_{yz}	S_{xz}	S1	S2	S3				
1	Inside	2937	–3.71	–0.05	–1.03	–0.03	–0.00	0.00	–0.05	–1.03	–3.71	3.65	P_m+P_b	49.80	12.63
	Middle	2944	0.81	–0.04	0.33	–0.03	–0.00	0.00	0.81	0.33	–0.04	0.85	P_m	33.20	37.85
	Outside	2951	5.33	–0.03	1.68	–0.03	–0.00	0.00	5.33	1.68	–0.03	5.36	P_m+P_b	49.80	8.29
2	Inside	3019	3.31	0.05	1.10	–0.64	–0.00	0.01	3.43	1.10	–0.07	3.50	P_m+P_b	49.80	13.21
	Middle	3021	0.64	0.05	0.30	–0.43	–0.00	0.00	0.86	0.30	–0.18	1.04	P_m	33.20	30.96
	Outside	3023	–1.41	0.07	–0.30	–0.26	–0.00	–0.00	0.11	–0.30	–1.46	1.57	P_m+P_b	49.80	30.72
3	Inside	3188	3.37	3.37	2.10	–3.47	0.00	0.00	6.84	2.10	–0.11	6.95	P_m+P_b	49.80	6.17
	Middle	3187	0.25	0.25	0.26	–0.24	0.00	0.00	0.49	0.26	0.01	0.48	P_m	33.20	68.88
	Outside	3186	–1.94	–1.94	–1.04	2.05	0.00	0.00	0.11	–1.04	–4.00	4.11	P_m+P_b	49.80	11.12
4	Inside	11583	0.05	3.31	1.10	–0.64	0.01	–0.00	3.43	1.10	–0.07	3.50	P_m+P_b	49.80	13.21
	Middle	11585	0.05	0.64	0.30	–0.43	0.00	–0.00	0.86	0.30	–0.18	1.04	P_m	33.20	30.96
	Outside	11587	0.07	–1.41	–0.30	–0.26	–0.00	–0.00	0.11	–0.30	–1.46	1.57	P_m+P_b	49.80	30.72
5	Inside	11501	–0.05	–3.71	–1.03	0.00	0.00	–0.00	–0.05	–1.03	–3.71	3.65	P_m+P_b	49.80	12.63
	Middle	11508	–0.04	0.81	0.33	0.00	0.00	–0.00	0.81	0.33	–0.04	0.85	P_m	33.20	37.97
	Outside	11515	–0.03	5.33	1.68	0.00	0.00	–0.00	5.33	1.68	–0.03	5.36	P_m+P_b	49.80	8.29
6	Inside	28711	0.05	3.31	1.10	0.64	–0.01	–0.00	3.43	1.10	–0.07	3.50	P_m+P_b	49.80	13.21
	Middle	28713	0.05	0.64	0.30	0.43	–0.00	–0.00	0.86	0.30	–0.18	1.04	P_m	33.20	30.96
	Outside	28715	0.07	–1.41	–0.30	0.26	0.00	–0.00	0.11	–0.30	–1.46	1.57	P_m+P_b	49.80	30.72
7	Inside	20316	3.37	3.37	2.10	3.47	–0.00	0.00	6.84	2.10	–0.11	6.95	P_m+P_b	49.80	6.17
	Middle	20315	0.25	0.25	0.26	0.24	–0.00	0.00	0.49	0.26	0.01	0.48	P_m	33.20	68.88
	Outside	20314	–1.94	–1.94	–1.04	–2.05	–0.00	0.00	0.11	–1.04	–4.00	4.11	P_m+P_b	49.80	11.12
8	Inside	20147	3.31	0.05	1.10	0.64	0.00	0.01	3.43	1.10	–0.07	3.50	P_m+P_b	49.80	13.21
	Middle	20149	0.64	0.05	0.30	0.43	0.00	0.00	0.86	0.30	–0.18	1.04	P_m	33.20	30.96
	Outside	20151	–1.41	0.07	–0.30	0.26	0.00	–0.00	0.11	–0.30	–1.46	1.57	P_m+P_b	49.80	30.72
9	Inside	20065	–3.71	–0.05	–1.03	0.03	0.00	0.00	–0.05	–1.03	–3.71	3.65	P_m+P_b	49.80	12.63
	Middle	20072	0.81	–0.04	0.33	0.03	0.00	0.00	0.81	0.33	–0.04	0.85	P_m	33.20	37.85
	Outside	20079	5.33	–0.03	1.68	0.03	0.00	0.00	5.33	1.68	–0.03	5.36	P_m+P_b	49.80	8.29

MNOP_REDext.TBL

TABLE 2.6-24 CONTAINMENT WALL STRESSES (ksi),
MNOP WITH REDUCED EXTERNAL PRESSURE (P_{int} = 85.4 psig, T=200°F), SECTION D

Stress Location		Node	Combined Stress Components						Principal Stresses			Stress Int.	Stress Type	Stress Limit	Design Margin
			S_x	S_y	S_z	S_{xy}	S_{yz}	S_{xz}	S1	S2	S3				
1	Inside	3399	–3.70	–0.05	–1.03	–0.03	0.00	–0.00	–0.05	–1.03	–3.71	3.65	P_m+P_b	49.80	12.64
	Middle	3406	0.81	–0.04	0.33	–0.03	0.00	–0.00	0.81	0.33	–0.04	0.85	P_m	33.20	37.85
	Outside	3413	5.32	–0.03	1.68	–0.03	0.00	–0.00	5.32	1.68	–0.03	5.36	P_m+P_b	49.80	8.30
2	Inside	3481	3.31	0.05	1.10	–0.64	0.00	–0.00	3.43	1.10	–0.08	3.50	P_m+P_b	49.80	13.22
	Middle	3483	0.64	0.05	0.30	–0.43	0.00	–0.00	0.86	0.30	–0.18	1.04	P_m	33.20	30.97
	Outside	3485	–1.41	0.07	–0.30	–0.26	0.00	0.00	0.11	–0.30	–1.45	1.57	P_m+P_b	49.80	30.75
3	Inside	3650	3.37	3.37	2.10	–3.47	–0.00	–0.00	6.84	2.10	–0.10	6.94	P_m+P_b	49.80	6.17
	Middle	3649	0.25	0.25	0.26	–0.24	–0.00	–0.00	0.49	0.26	0.01	0.47	P_m	33.20	69.01
	Outside	3648	–1.94	–1.94	–1.04	2.05	–0.00	–0.00	0.11	–1.04	–4.00	4.11	P_m+P_b	49.80	11.13
4	Inside	12045	0.05	3.31	1.10	–0.64	–0.00	0.00	3.43	1.10	–0.08	3.50	P_m+P_b	49.80	13.22
	Middle	12047	0.05	0.64	0.30	–0.43	–0.00	0.00	0.86	0.30	–0.18	1.04	P_m	33.20	30.97
	Outside	12049	0.07	–1.41	–0.30	–0.26	0.00	0.00	0.11	–0.30	–1.45	1.57	P_m+P_b	49.80	30.75
5	Inside	11963	–0.05	–3.70	–1.03	0.00	0.00	0.00	–0.05	–1.03	–3.70	3.65	P_m+P_b	49.80	12.64
	Middle	11970	–0.04	0.81	0.33	0.00	0.00	0.00	0.81	0.33	–0.04	0.85	P_m	33.20	37.97
	Outside	11977	–0.03	5.32	1.68	0.00	0.00	0.00	5.32	1.68	–0.03	5.36	P_m+P_b	49.80	8.30
6	Inside	29173	0.05	3.31	1.10	0.64	0.00	0.00	3.43	1.10	–0.08	3.50	P_m+P_b	49.80	13.22
	Middle	29175	0.05	0.64	0.30	0.43	0.00	0.00	0.86	0.30	–0.18	1.04	P_m	33.20	30.97
	Outside	29177	0.07	–1.41	–0.30	0.26	–0.00	0.00	0.11	–0.30	–1.45	1.57	P_m+P_b	49.80	30.75
7	Inside	20778	3.37	3.37	2.10	3.47	0.00	–0.00	6.84	2.10	–0.10	6.94	P_m+P_b	49.80	6.17
	Middle	20777	0.25	0.25	0.26	0.24	0.00	–0.00	0.49	0.26	0.01	0.47	P_m	33.20	69.01
	Outside	20776	–1.94	–1.94	–1.04	–2.05	0.00	–0.00	0.11	–1.04	–4.00	4.11	P_m+P_b	49.80	11.13
8	Inside	20609	3.31	0.05	1.10	0.64	–0.00	–0.00	3.43	1.10	–0.08	3.50	P_m+P_b	49.80	13.22
	Middle	20611	0.64	0.05	0.30	0.43	–0.00	–0.00	0.86	0.30	–0.18	1.04	P_m	33.20	30.97
	Outside	20613	–1.41	0.07	–0.30	0.26	–0.00	0.00	0.11	–0.30	–1.45	1.57	P_m+P_b	49.80	30.75
9	Inside	20527	–3.70	–0.05	–1.03	0.03	–0.00	–0.00	–0.05	–1.03	–3.71	3.65	P_m+P_b	49.80	12.64
	Middle	20534	0.81	–0.04	0.33	0.03	–0.00	–0.00	0.81	0.33	–0.04	0.85	P_m	33.20	37.85
	Outside	20541	5.32	–0.03	1.68	0.03	–0.00	–0.00	5.32	1.68	–0.03	5.36	P_m+P_b	49.80	8.30

MNOP_REDext.TBL

TABLE 2.6-25 CONTAINMENT WALL STRESSES (ksi),
MNOP WITH REDUCED EXTERNAL PRESSURE (P_{int} = 85.4 psig, T=200°F), SECTION E

Stress Location		Node	Combined Stress Components						Principal Stresses			Stress Int.	Stress Type	Stress Limit	Design Margin
			S_x	S_y	S_z	S_{xy}	S_{yz}	S_{xz}	S1	S2	S3				
1	Inside	3861	–3.72	–0.05	–1.03	–0.03	0.00	–0.00	–0.05	–1.03	–3.72	3.67	P_m+P_b	49.80	12.58
	Middle	3868	0.80	–0.04	0.33	–0.03	0.00	–0.00	0.80	0.33	–0.04	0.85	P_m	33.20	38.29
	Outside	3875	5.32	–0.03	1.69	–0.03	0.00	–0.00	5.32	1.69	–0.03	5.35	P_m+P_b	49.80	8.30
2	Inside	3943	3.30	0.05	1.09	–0.64	0.00	–0.00	3.42	1.09	–0.08	3.50	P_m+P_b	49.80	13.24
	Middle	3945	0.63	0.05	0.30	–0.43	0.00	–0.00	0.86	0.30	–0.18	1.04	P_m	33.20	31.02
	Outside	3947	–1.41	0.07	–0.30	–0.26	0.00	–0.00	0.11	–0.30	–1.46	1.57	P_m+P_b	49.80	30.73
3	Inside	4112	3.35	3.35	2.07	–3.49	0.00	0.00	6.84	2.07	–0.13	6.98	P_m+P_b	49.80	6.14
	Middle	4111	0.24	0.24	0.26	–0.25	0.00	0.00	0.49	0.26	–0.00	0.49	P_m	33.20	66.49
	Outside	4110	–1.95	–1.95	–1.02	2.05	0.00	0.00	0.10	–1.02	–4.00	4.11	P_m+P_b	49.80	11.13
4	Inside	12507	0.05	3.30	1.09	–0.64	–0.00	0.00	3.42	1.09	–0.08	3.50	P_m+P_b	49.80	13.24
	Middle	12509	0.05	0.63	0.30	–0.43	–0.00	0.00	0.86	0.30	–0.18	1.04	P_m	33.20	31.02
	Outside	12511	0.07	–1.41	–0.30	–0.26	–0.00	0.00	0.11	–0.30	–1.46	1.57	P_m+P_b	49.80	30.73
5	Inside	12425	–0.05	–3.72	–1.03	0.00	0.00	0.00	–0.05	–1.03	–3.72	3.67	P_m+P_b	49.80	12.58
	Middle	12432	–0.04	0.80	0.33	0.00	0.00	0.00	0.80	0.33	–0.04	0.84	P_m	33.20	38.41
	Outside	12439	–0.03	5.32	1.69	0.00	0.00	0.00	5.32	1.69	–0.03	5.35	P_m+P_b	49.80	8.31
6	Inside	29635	0.05	3.30	1.09	0.64	0.00	0.00	3.42	1.09	–0.08	3.50	P_m+P_b	49.80	13.24
	Middle	29637	0.05	0.63	0.30	0.43	0.00	0.00	0.86	0.30	–0.18	1.04	P_m	33.20	31.02
	Outside	29639	0.07	–1.41	–0.30	0.26	0.00	0.00	0.11	–0.30	–1.46	1.57	P_m+P_b	49.80	30.73
7	Inside	21240	3.35	3.35	2.07	3.49	–0.00	0.00	6.84	2.07	–0.13	6.98	P_m+P_b	49.80	6.14
	Middle	21239	0.24	0.24	0.26	0.25	–0.00	0.00	0.49	0.26	–0.00	0.49	P_m	33.20	66.49
	Outside	21238	–1.95	–1.95	–1.02	–2.05	–0.00	0.00	0.10	–1.02	–4.00	4.11	P_m+P_b	49.80	11.13
8	Inside	21071	3.30	0.05	1.09	0.64	–0.00	–0.00	3.42	1.09	–0.08	3.50	P_m+P_b	49.80	13.24
	Middle	21073	0.63	0.05	0.30	0.43	–0.00	–0.00	0.86	0.30	–0.18	1.04	P_m	33.20	31.02
	Outside	21075	–1.41	0.07	–0.30	0.26	–0.00	–0.00	0.11	–0.30	–1.46	1.57	P_m+P_b	49.80	30.73
9	Inside	20989	–3.72	–0.05	–1.03	0.03	0.00	–0.00	–0.05	–1.03	–3.72	3.67	P_m+P_b	49.80	12.58
	Middle	20996	0.80	–0.04	0.33	0.03	0.00	–0.00	0.80	0.33	–0.04	0.85	P_m	33.20	38.29
	Outside	21003	5.32	–0.03	1.69	0.03	0.00	–0.00	5.32	1.69	–0.03	5.35	P_m+P_b	49.80	8.30

MNOP_REDext.TBL

2.6.4 Increased External Pressure

The increased external pressure condition requires that the cask be evaluated at an external pressure of 20.3 psia per 10 CFR Part 71.71c(4). To be conservative, we analyzed the cask for the expected pool maximum pressure of 20 psig (34.7 psia). The resulting cask containment boundary stresses for this loading case are presented in Tables 2.6-26 through 2.6-30. As seen, the low stresses produce high design margins.

In addition to the cask containment boundary, the neutron shield outer shell was evaluated for the increased external pressure load case. As described in Section 2.10.11.4, two sections of the neutron shield were evaluated for buckling. The sections chosen for evaluation were the lower cylindrical region and the stiffening ring region. The design margins were 0.49 and 0.89, respectively. The weld attaching the main outer shell to the stiffening ring has a design margin of 7.7 for the stress in the weld. Therefore, the neutron shield shell's design is acceptable for the increased external pressure load case.

2.6.5 Vibration/Fatigue

The vibration loads listed below present the peak and design vibration accelerations that are applied to the cask. The design vibration values are 75 percent of the peak vibration accelerations. These values are conservative based on the test results given in Ref. 2.6-1.

	Peak Vibration (g)	Design Vibration (g)
Vertical	1.2	0.9
Longitudinal	0.4	0.3
Transverse	0.4	0.3

The critical components for vibration are (1) the trunnions and (2) the cask body under or near each trunnion.

In addition to the vibration loading due to transportation, the cask was evaluated for lifting and dead load cycles and shown to be free from fatigue failure when cycled between extreme pressure conditions.

For the fatigue evaluation, the cask is assumed to be used for 50 one-way trips each year for a conservative design life of 50 years. Therefore, the number of design cycles is 2500. In each trip the cask is assumed to encounter the two worst loading combinations, which produce the highest range of primary plus secondary stress intensity.

The closure bolts are evaluated for fatigue. The maximum cyclic stress in the closure bolts is due to the applying and removal of the preload.

2.6.5.1 Trunnion Location. The stresses on the trunnion and the cask wall at the trunnion location due to vibration loads of 0.3g longitudinal, 0.3g lateral, and 0.9g vertical were obtained by using the tiedown load from the ANSYS model presented in Section 2.5.2.

TABLE 2.6-26 CONTAINMENT WALL STRESSES (ksi), INCREASED EXTERNAL PRESSURE OF 20 psig, (T=200°F), SECTION A

Stress Location		Node	Combined Stress Components						Principal Stresses			Stress Int.	Stress Type	Stress Limit	Design Margin
			S_x	S_y	S_z	S_{xy}	S_{yz}	S_{xz}	S1	S2	S3				
1	Inside	1383	–0.06	–0.04	–0.46	–0.00	–0.11	0.02	–0.01	–0.06	–0.48	0.47	P_m+P_b	49.80	104.84
	Middle	1390	–0.13	–0.03	–0.13	–0.00	–0.06	–0.00	0.00	–0.13	–0.16	0.16	P_m	33.20	209.24
	Outside	1397	–0.22	–0.02	0.17	–0.00	–0.04	–0.02	0.18	–0.03	–0.22	0.40	P_m+P_b	49.80	123.84
2	Inside	1417	–0.20	–0.02	–0.14	0.04	–0.02	0.18	0.02	–0.02	–0.36	0.37	P_m+P_b	49.80	133.58
	Middle	1419	–0.09	–0.02	–0.04	0.02	–0.00	–0.01	–0.01	–0.04	–0.09	0.08	P_m	33.20	406.04
	Outside	1421	0.00	–0.02	0.04	0.00	0.01	–0.20	0.22	–0.02	–0.17	0.39	P_m+P_b	49.80	125.61
3	Inside	1466	–0.18	–0.18	–0.10	0.18	0.02	0.02	–0.00	–0.11	–0.36	0.36	P_m+P_b	49.80	138.74
	Middle	1465	–0.04	–0.04	–0.06	0.01	0.02	0.02	–0.01	–0.06	–0.07	0.06	P_m	33.20	596.63
	Outside	1464	0.06	0.06	–0.03	–0.10	0.02	0.02	0.17	–0.01	–0.06	0.23	P_m+P_b	49.80	219.60
4	Inside	9981	–0.02	–0.20	–0.14	0.04	0.18	–0.02	0.02	–0.02	–0.36	0.37	P_m+P_b	49.80	133.58
	Middle	9983	–0.02	–0.09	–0.04	0.02	–0.01	–0.00	–0.01	–0.04	–0.09	0.08	P_m	33.20	406.04
	Outside	9985	–0.02	0.00	0.04	0.00	–0.20	0.01	0.22	–0.02	–0.17	0.39	P_m+P_b	49.80	125.61
5	Inside	9947	–0.04	–0.06	–0.46	0.00	0.00	–0.11	–0.01	–0.06	–0.48	0.47	P_m+P_b	49.80	105.28
	Middle	9954	–0.03	–0.13	–0.13	0.00	0.00	–0.06	0.00	–0.13	–0.16	0.16	P_m	33.20	210.09
	Outside	9961	–0.02	–0.22	0.17	0.00	0.00	–0.04	0.18	–0.03	–0.22	0.40	P_m+P_b	49.80	124.54
6	Inside	27109	–0.02	–0.20	–0.14	–0.04	–0.18	–0.02	0.02	–0.02	–0.36	0.37	P_m+P_b	49.80	133.58
	Middle	27111	–0.02	–0.09	–0.04	–0.02	0.01	–0.00	–0.01	–0.04	–0.09	0.08	P_m	33.20	406.04
	Outside	27113	–0.02	0.00	0.04	–0.00	0.20	0.01	0.22	–0.02	–0.17	0.39	P_m+P_b	49.80	125.61
7	Inside	18594	–0.18	–0.18	–0.10	–0.18	–0.02	0.02	–0.00	–0.11	–0.36	0.36	P_m+P_b	49.80	138.74
	Middle	18593	–0.04	–0.04	–0.06	–0.01	–0.02	0.02	–0.01	–0.06	–0.07	0.06	P_m	33.20	596.63
	Outside	18592	0.06	0.06	–0.03	0.10	–0.02	0.02	0.17	–0.01	–0.06	0.23	P_m+P_b	49.80	219.60
8	Inside	18545	–0.20	–0.02	–0.14	–0.04	0.02	0.18	0.02	–0.02	–0.36	0.37	P_m+P_b	49.80	133.58
	Middle	18547	–0.09	–0.02	–0.04	–0.02	0.00	–0.01	–0.01	–0.04	–0.09	0.08	P_m	33.20	406.04
	Outside	18549	0.00	–0.02	0.04	–0.00	–0.01	–0.20	0.22	–0.02	–0.17	0.39	P_m+P_b	49.80	125.61
9	Inside	18511	–0.06	–0.04	–0.46	0.00	0.11	0.02	–0.01	–0.06	–0.48	0.47	P_m+P_b	49.80	104.84
	Middle	18518	–0.13	–0.03	–0.13	0.00	0.06	–0.00	0.00	–0.13	–0.16	0.16	P_m	33.20	209.24
	Outside	18525	–0.22	–0.02	0.17	0.00	0.04	–0.02	0.18	–0.03	–0.22	0.40	P_m+P_b	49.80	123.84

PEXT_20.TBL

TABLE 2.6-27 CONTAINMENT WALL STRESSES (ksi), INCREASED EXTERNAL PRESSURE OF 20 psig, (T=200°F), SECTION B

Stress Location		Node	Combined Stress Components						Principal Stresses			Stress Int.	Stress Type	Stress Limit	Design Margin
			S_x	S_y	S_z	S_{xy}	S_{yz}	S_{xz}	S1	S2	S3				
1	Inside	2748	0.77	–0.00	0.35	0.00	–0.00	0.01	0.77	0.35	–0.00	0.77	P_m+P_b	49.80	63.55
	Middle	2755	–0.17	–0.02	–0.10	0.00	–0.00	–0.00	–0.02	–0.10	–0.17	0.16	P_m	33.20	212.96
	Outside	2762	–1.11	–0.03	–0.55	0.02	–0.00	–0.01	–0.03	–0.55	–1.11	1.07	P_m+P_b	49.80	45.38
2	Inside	2965	–0.61	–0.02	–0.19	0.13	0.00	0.10	0.00	–0.17	–0.66	0.67	P_m+P_b	49.80	73.87
	Middle	2967	–0.14	0.00	–0.08	0.09	0.01	–0.01	0.05	–0.07	–0.18	0.23	P_m	33.20	141.04
	Outside	2969	0.21	0.03	–0.00	0.04	–0.00	–0.10	0.26	0.02	–0.05	0.31	P_m+P_b	49.80	161.85
3	Inside	3053	–0.78	–0.78	–0.50	0.71	0.00	0.00	–0.07	–0.50	–1.50	1.42	P_m+P_b	49.80	33.99
	Middle	3052	–0.10	–0.10	–0.08	0.03	0.00	0.00	–0.06	–0.08	–0.13	0.06	P_m	33.20	518.09
	Outside	3051	0.39	0.39	0.23	–0.46	0.00	0.00	0.85	0.23	–0.07	0.92	P_m+P_b	49.80	53.19
4	Inside	11529	–0.02	–0.61	–0.19	0.13	0.10	0.00	0.00	–0.17	–0.66	0.67	P_m+P_b	49.80	73.87
	Middle	11531	0.00	–0.14	–0.08	0.09	–0.01	0.01	0.05	–0.07	–0.18	0.23	P_m	33.20	141.04
	Outside	11533	0.03	0.21	–0.00	0.04	–0.10	–0.00	0.26	0.02	–0.05	0.31	P_m+P_b	49.80	161.85
5	Inside	11312	–0.00	0.77	0.35	0.00	0.00	–0.00	0.77	0.35	–0.00	0.77	P_m+P_b	49.80	63.58
	Middle	11319	–0.02	–0.17	–0.10	0.00	0.00	–0.00	–0.02	–0.10	–0.17	0.15	P_m	33.20	213.84
	Outside	11326	–0.03	–1.11	–0.55	0.00	0.00	–0.00	–0.03	–0.55	–1.11	1.07	P_m+P_b	49.80	45.42
6	Inside	28657	–0.02	–0.61	–0.19	–0.13	–0.10	0.00	0.00	–0.17	–0.66	0.67	P_m+P_b	49.80	73.87
	Middle	28659	0.00	–0.14	–0.08	–0.09	0.01	0.01	0.05	–0.07	–0.18	0.23	P_m	33.20	141.04
	Outside	28661	0.03	0.21	–0.00	–0.04	0.10	–0.00	0.26	0.02	–0.05	0.31	P_m+P_b	49.80	161.85
7	Inside	20181	–0.78	–0.78	–0.50	–0.71	–0.00	0.00	–0.07	–0.50	–1.50	1.42	P_m+P_b	49.80	33.99
	Middle	20180	–0.10	–0.10	–0.08	–0.03	–0.00	0.00	–0.06	–0.08	–0.13	0.06	P_m	33.20	518.09
	Outside	20179	0.39	0.39	0.23	0.46	–0.00	0.00	0.85	0.23	–0.07	0.92	P_m+P_b	49.80	53.19
8	Inside	20093	–0.61	–0.02	–0.19	–0.13	–0.00	0.10	0.00	–0.17	–0.66	0.67	P_m+P_b	49.80	73.87
	Middle	20095	–0.14	0.00	–0.08	–0.09	–0.01	–0.01	0.05	–0.07	–0.18	0.23	P_m	33.20	141.04
	Outside	20097	0.21	0.03	–0.00	–0.04	0.00	–0.10	0.26	0.02	–0.05	0.31	P_m+P_b	49.80	161.85
9	Inside	19876	0.77	–0.00	0.35	–0.00	0.00	0.01	0.77	0.35	–0.00	0.77	P_m+P_b	49.80	63.55
	Middle	19883	–0.17	–0.02	–0.10	–0.00	0.00	–0.00	–0.02	–0.10	–0.17	0.16	P_m	33.20	212.96
	Outside	19890	–1.11	–0.03	–0.55	–0.02	0.00	–0.01	–0.03	–0.55	–1.11	1.07	P_m+P_b	49.80	45.38

PEXT_20.TBL

TABLE 2.6-28 CONTAINMENT WALL STRESSES (ksi),
INCREASED EXTERNAL PRESSURE OF 20 psig, (T=200°F), SECTION C

Stress Location		Node	Combined Stress Components						Principal Stresses			Stress Int.	Stress Type	Stress Limit	Design Margin
			S_x	S_y	S_z	S_{xy}	S_{yz}	S_{xz}	S1	S2	S3				
1	Inside	2937	0.90	–0.00	0.23	0.00	0.00	–0.00	0.90	0.23	–0.00	0.90	P_m+P_b	49.80	54.13
	Middle	2944	–0.18	–0.01	–0.09	0.00	0.00	–0.00	–0.00	–0.09	–0.18	0.17	P_m	33.20	191.11
	Outside	2951	–1.26	–0.01	–0.41	0.00	0.00	0.00	–0.01	–0.41	–1.26	1.25	P_m+P_b	49.80	38.92
2	Inside	3019	–0.75	–0.03	–0.27	0.15	–0.00	–0.00	–0.00	–0.27	–0.78	0.78	P_m+P_b	49.80	63.17
	Middle	3021	–0.14	–0.03	–0.08	0.10	–0.00	–0.00	0.03	–0.08	–0.20	0.23	P_m	33.20	143.98
	Outside	3023	0.32	–0.04	0.05	0.06	–0.00	0.00	0.33	0.05	–0.05	0.38	P_m+P_b	49.80	131.10
3	Inside	3188	–0.91	–0.91	–0.58	0.82	–0.00	–0.00	–0.09	–0.58	–1.72	1.63	P_m+P_b	49.80	29.54
	Middle	3187	–0.09	–0.09	–0.09	0.01	–0.00	–0.00	–0.08	–0.09	–0.11	0.03	P_m	33.20	+HIGH
	Outside	3186	0.48	0.48	0.26	–0.55	–0.00	–0.00	1.03	0.26	–0.07	1.10	P_m+P_b	49.80	44.33
4	Inside	11583	–0.03	–0.75	–0.27	0.15	–0.00	–0.00	–0.00	–0.27	–0.78	0.78	P_m+P_b	49.80	63.17
	Middle	11585	–0.03	–0.14	–0.08	0.10	–0.00	–0.00	0.03	–0.08	–0.20	0.23	P_m	33.20	143.98
	Outside	11587	–0.04	0.32	0.05	0.06	0.00	–0.00	0.33	0.05	–0.05	0.38	P_m+P_b	49.80	131.10
5	Inside	11501	–0.00	0.90	0.23	0.00	0.00	0.00	0.90	0.23	–0.00	0.90	P_m+P_b	49.80	54.14
	Middle	11508	–0.01	–0.18	–0.09	0.00	0.00	0.00	–0.00	–0.09	–0.18	0.17	P_m	33.20	191.86
	Outside	11515	–0.01	–1.26	–0.41	0.00	0.00	0.00	–0.01	–0.41	–1.26	1.25	P_m+P_b	49.80	38.92
6	Inside	28711	–0.03	–0.75	–0.27	–0.15	0.00	–0.00	–0.00	–0.27	–0.78	0.78	P_m+P_b	49.80	63.17
	Middle	28713	–0.03	–0.14	–0.08	–0.10	0.00	–0.00	0.03	–0.08	–0.20	0.23	P_m	33.20	143.98
	Outside	28715	–0.04	0.32	0.05	–0.06	–0.00	–0.00	0.33	0.05	–0.05	0.38	P_m+P_b	49.80	131.10
7	Inside	20316	–0.91	–0.91	–0.58	–0.82	0.00	–0.00	–0.09	–0.58	–1.72	1.63	P_m+P_b	49.80	29.54
	Middle	20315	–0.09	–0.09	–0.09	–0.01	0.00	–0.00	–0.08	–0.09	–0.11	0.03	P_m	33.20	+HIGH
	Outside	20314	0.48	0.48	0.26	0.55	0.00	–0.00	1.03	0.26	–0.07	1.10	P_m+P_b	49.80	44.33
8	Inside	20147	–0.75	–0.03	–0.27	–0.15	0.00	–0.00	–0.00	–0.27	–0.78	0.78	P_m+P_b	49.80	63.17
	Middle	20149	–0.14	–0.03	–0.08	–0.10	0.00	–0.00	0.03	–0.08	–0.20	0.23	P_m	33.20	143.98
	Outside	20151	0.32	–0.04	0.05	–0.06	0.00	0.00	0.33	0.05	–0.05	0.38	P_m+P_b	49.80	131.10
9	Inside	20065	0.90	–0.00	0.23	–0.00	–0.00	–0.00	0.90	0.23	–0.00	0.90	P_m+P_b	49.80	54.13
	Middle	20072	–0.18	–0.01	–0.09	–0.00	–0.00	–0.00	–0.00	–0.09	–0.18	0.17	P_m	33.20	191.11
	Outside	20079	–1.26	–0.01	–0.41	–0.00	–0.00	0.00	–0.01	–0.41	–1.26	1.25	P_m+P_b	49.80	38.92

PEXT_20.TBL

TABLE 2.6-29 CONTAINMENT WALL STRESSES (ksi),
INCREASED EXTERNAL PRESSURE OF 20 psig, (T=200°F), SECTION D

Stress Location		Node	Combined Stress Components						Principal Stresses			Stress Int.	Stress Type	Stress Limit	Design Margin
			S_x	S_y	S_z	S_{xy}	S_{yz}	S_{xz}	S1	S2	S3				
1	Inside	3399	0.90	–0.00	0.23	0.00	0.00	0.00	0.90	0.23	–0.00	0.90	P_m+P_b	49.80	54.16
	Middle	3406	–0.18	–0.01	–0.09	0.00	0.00	0.00	–0.00	–0.09	–0.18	0.17	P_m	33.20	191.11
	Outside	3413	–1.26	–0.01	–0.41	0.00	0.00	0.00	–0.01	–0.41	–1.26	1.25	P_m+P_b	49.80	38.93
2	Inside	3481	–0.75	–0.03	–0.27	0.15	0.00	–0.00	–0.00	–0.27	–0.78	0.78	P_m+P_b	49.80	63.21
	Middle	3483	–0.14	–0.03	–0.08	0.10	0.00	–0.00	0.03	–0.08	–0.20	0.23	P_m	33.20	144.00
	Outside	3485	0.32	–0.04	0.05	0.06	0.00	0.00	0.33	0.05	–0.05	0.38	P_m+P_b	49.80	131.22
3	Inside	3650	–0.91	–0.91	–0.58	0.81	0.00	0.00	–0.09	–0.58	–1.72	1.63	P_m+P_b	49.80	29.56
	Middle	3649	–0.09	–0.09	–0.09	0.01	0.00	0.00	–0.08	–0.09	–0.11	0.03	P_m	33.20	+HIGH
	Outside	3648	0.48	0.48	0.26	–0.55	0.00	0.00	1.03	0.26	–0.07	1.10	P_m+P_b	49.80	44.35
4	Inside	12045	–0.03	–0.75	–0.27	0.15	–0.00	0.00	–0.00	–0.27	–0.78	0.78	P_m+P_b	49.80	63.21
	Middle	12047	–0.03	–0.14	–0.08	0.10	–0.00	0.00	0.03	–0.08	–0.20	0.23	P_m	33.20	144.00
	Outside	12049	–0.04	0.32	0.05	0.06	0.00	0.00	0.33	0.05	–0.05	0.38	P_m+P_b	49.80	131.22
5	Inside	11963	–0.00	0.90	0.23	0.00	0.00	0.00	0.90	0.23	–0.00	0.90	P_m+P_b	49.80	54.17
	Middle	11970	–0.01	–0.18	–0.09	0.00	0.00	0.00	–0.01	–0.09	–0.18	0.17	P_m	33.20	191.86
	Outside	11977	–0.01	–1.26	–0.41	0.00	0.00	0.00	–0.01	–0.41	–1.26	1.25	P_m+P_b	49.80	38.94
6	Inside	29173	–0.03	–0.75	–0.27	–0.15	0.00	0.00	–0.00	–0.27	–0.78	0.78	P_m+P_b	49.80	63.21
	Middle	29175	–0.03	–0.14	–0.08	–0.10	0.00	0.00	0.03	–0.08	–0.20	0.23	P_m	33.20	144.00
	Outside	29177	–0.04	0.32	0.05	–0.06	–0.00	0.00	0.33	0.05	–0.05	0.38	P_m+P_b	49.80	131.22
7	Inside	20778	–0.91	–0.91	–0.58	–0.81	0.00	0.00	–0.09	–0.58	–1.72	1.63	P_m+P_b	49.80	29.56
	Middle	20777	–0.09	–0.09	–0.09	–0.01	0.00	0.00	–0.08	–0.09	–0.11	0.03	P_m	33.20	+HIGH
	Outside	20776	0.48	0.48	0.26	0.55	0.00	0.00	1.03	0.26	–0.07	1.10	P_m+P_b	49.80	44.35
8	Inside	20609	–0.75	–0.03	–0.27	–0.15	0.00	–0.00	–0.00	–0.27	–0.78	0.78	P_m+P_b	49.80	63.21
	Middle	20611	–0.14	–0.03	–0.08	–0.10	0.00	–0.00	0.03	–0.08	–0.20	0.23	P_m	33.20	144.00
	Outside	20613	0.32	–0.04	0.05	–0.06	0.00	0.00	0.33	0.05	–0.05	0.38	P_m+P_b	49.80	131.22
9	Inside	20527	0.90	–0.00	0.23	–0.00	0.00	0.00	0.90	0.23	–0.00	0.90	P_m+P_b	49.80	54.16
	Middle	20534	–0.18	–0.01	–0.09	–0.00	0.00	0.00	–0.00	–0.09	–0.18	0.17	P_m	33.20	191.11
	Outside	20541	–1.26	–0.01	–0.41	–0.00	0.00	0.00	–0.01	–0.41	–1.26	1.25	P_m+P_b	49.80	38.93

PEXT_20.TBL

TABLE 2.6-30 CONTAINMENT WALL STRESSES (ksi), INCREASED EXTERNAL PRESSURE OF 20 psig, (T=200°F), SECTION E

Stress Location		Node	Combined Stress Components						Principal Stresses			Stress	Stress	Stress	Design
			S_x	S_y	S_z	S_{xy}	S_{yz}	S_{xz}	S1	S2	S3	Int.	Type	Limit	Margin
1	Inside	3861	0.90	–0.00	0.23	0.00	0.00	0.00	0.90	0.23	–0.00	0.90	P_m+P_b	49.80	54.16
	Middle	3868	–0.18	–0.01	–0.09	0.00	0.00	0.00	–0.00	–0.09	–0.18	0.17	P_m	33.20	191.09
	Outside	3875	–1.26	–0.01	–0.41	0.00	0.00	0.00	–0.01	–0.41	–1.26	1.25	P_m+P_b	49.80	38.93
2	Inside	3943	–0.75	–0.03	–0.27	0.15	0.00	0.00	–0.00	–0.27	–0.78	0.78	P_m+P_b	49.80	63.21
	Middle	3945	–0.14	–0.03	–0.08	0.10	0.00	0.00	0.03	–0.08	–0.20	0.23	P_m	33.20	144.00
	Outside	3947	0.32	–0.04	0.05	0.06	0.00	0.00	0.33	0.05	–0.05	0.38	P_m+P_b	49.80	131.22
3	Inside	4112	–0.91	–0.91	–0.58	0.81	0.00	0.00	–0.09	–0.58	–1.72	1.63	P_m+P_b	49.80	29.56
	Middle	4111	–0.09	–0.09	–0.09	0.01	0.00	0.00	–0.08	–0.09	–0.11	0.03	P_m	33.20	+HIGH
	Outside	4110	0.48	0.48	0.26	–0.55	0.00	0.00	1.03	0.26	–0.07	1.10	P_m+P_b	49.80	44.36
4	Inside	12507	–0.03	–0.75	–0.27	0.15	0.00	0.00	–0.00	–0.27	–0.78	0.78	P_m+P_b	49.80	63.21
	Middle	12509	–0.03	–0.14	–0.08	0.10	0.00	0.00	0.03	–0.08	–0.20	0.23	P_m	33.20	144.00
	Outside	12511	–0.04	0.32	0.05	0.06	0.00	0.00	0.33	0.05	–0.05	0.38	P_m+P_b	49.80	131.22
5	Inside	12425	–0.00	0.90	0.23	0.00	0.00	0.00	0.90	0.23	–0.00	0.90	P_m+P_b	49.80	54.17
	Middle	12432	–0.01	–0.18	–0.09	0.00	0.00	0.00	–0.01	–0.09	–0.18	0.17	P_m	33.20	191.85
	Outside	12439	–0.01	–1.26	–0.41	0.00	0.00	0.00	–0.01	–0.41	–1.26	1.25	P_m+P_b	49.80	38.94
6	Inside	29635	–0.03	–0.75	–0.27	–0.15	0.00	0.00	–0.00	–0.27	–0.78	0.78	P_m+P_b	49.80	63.21
	Middle	29637	–0.03	–0.14	–0.08	–0.10	0.00	0.00	0.03	–0.08	–0.20	0.23	P_m	33.20	144.00
	Outside	29639	–0.04	0.32	0.05	–0.06	0.00	0.00	0.33	0.05	–0.05	0.38	P_m+P_b	49.80	131.22
7	Inside	21240	–0.91	–0.91	–0.58	–0.81	0.00	0.00	–0.09	–0.58	–1.72	1.63	P_m+P_b	49.80	29.56
	Middle	21239	–0.09	–0.09	–0.09	–0.01	0.00	0.00	–0.08	–0.09	–0.11	0.03	P_m	33.20	+HIGH
	Outside	21238	0.48	0.48	0.26	0.55	0.00	0.00	1.03	0.26	–0.07	1.10	P_m+P_b	49.80	44.36
8	Inside	21071	–0.75	–0.03	–0.27	–0.15	0.00	0.00	–0.00	–0.27	–0.78	0.78	P_m+P_b	49.80	63.21
	Middle	21073	–0.14	–0.03	–0.08	–0.10	0.00	0.00	0.03	–0.08	–0.20	0.23	P_m	33.20	144.00
	Outside	21075	0.32	–0.04	0.05	–0.06	0.00	0.00	0.33	0.05	–0.05	0.38	P_m+P_b	49.80	131.22
9	Inside	20989	0.90	–0.00	0.23	–0.00	0.00	0.00	0.90	0.23	–0.00	0.90	P_m+P_b	49.80	54.16
	Middle	20996	–0.18	–0.01	–0.09	–0.00	0.00	0.00	–0.00	–0.09	–0.18	0.17	P_m	33.20	191.09
	Outside	21003	–1.26	–0.01	–0.41	–0.00	0.00	0.00	–0.01	–0.41	–1.26	1.25	P_m+P_b	49.80	38.93

PEXT_20.TBL

The vibration loads of 0.3g, 0.3g, and 0.9g are calculated as follows (assuming a nominal position of the cask on the trailer supports):

$$\Sigma F_{vertical} = 0.0,$$
$$0.0 = 4 F_{trun,vert} - F_{wt} \times 0.9g,$$
$$F_{trun,vert} = (0.9)(55{,}000)/4,$$
$$= 12{,}375 \text{ lb},$$

$$\Sigma F_{lateral} = 0.0,$$
$$0.0 = 2 F_{trun,lat} - F_{wt} \times 0.3g,$$
$$F_{trun,lat} = (0.3)(55{,}000)/2,$$
$$= 8{,}250 \text{ lb},$$

$$\Sigma F_{long} = 0.0,$$
$$0.0 = 2 F_{trun,long} - F_{wt} \times 0.3g,$$
$$F_{trun,long} = (0.3)(55{,}000)/2,$$
$$= 8{,}250 \text{ lb}.$$

The resultant in the vertical/longitudinal plane is

$$F_{shear} = \sqrt{(12{,}375)^2 + (8{,}250)^2} = 14{,}873 \text{ lb}$$

Therefore the loads on the trunnion are

$$F_{shear} = 14{,}873 \text{ lb, and}$$
$$F_{lateral} = 8{,}250 \text{ lb.}$$

The trunnion tiedown analyses used a 10g/5g/2g tiedown load, which translated into these results (see Section 2.5.2.1):

$$F_{shear} = 278{,}000 \text{ lb}$$
$$F_{lateral} = 138{,}800 \text{ lb}$$

The vibration stresses were conservatively computed by scaling the ANSYS results for tiedown loads by the ratio of the vibration forces to the tiedown forces. These ratios are 0.05 for shear and 0.06 for lateral forces. The larger factor, 0.06, was used to envelop both ratios.

As shown in Section 2.5.2.2.1, the maximum stresses caused by tiedown loads occur at the intersection of the gusset and the trunnion (Point 2 in Table 2.5-1). The stresses in the rest of the trunnion and cask are lower.

At this point the principal stresses are

$$\sigma_1 = 39{,}600 \text{ psi},$$
$$\sigma_2 = 3{,}730 \text{ psi, and}$$
$$\sigma_3 = 860 \text{ psi},$$

as taken from Table 2.10.5-1.

Applying the 0.06 factor, the stress state caused by vibration loads is

σ_1 = 2,376 psi,
σ_2 = 224 psi, and
σ_3 = 52 psi.

Using ASME Code Section III, Div. 1, NB-3216, the corresponding stress differences, assuming a complete stress reversal, are

$$S'_{12} = (\sigma_{1i} - \sigma_{1j}) - (\sigma_{2i} - \sigma_{2j}),$$
$$S'_{23} = (\sigma_{2i} - \sigma_{2j}) - (\sigma_{3i} - \sigma_{3j}),$$
$$S'_{31} = (\sigma_{3i} - \sigma_{3j}) - (\sigma_{1i} - \sigma_{1j}),$$
$$S'_{12} = [(2)(2{,}376) - (2)(224)] = 4304 \text{ psi},$$
$$S'_{23} = [(2)(224) - (2)(52)] = 344 \text{ psi, and}$$
$$S'_{31} = [(2)(52) - (2)(2{,}376)] = -4{,}648 \text{ psi}.$$

The maximum alternating stress is

$$S_a = 1/2 \max | S'_{12}, S'_{23}, S'_{31} |.$$

Therefore, S_a = 1/2 (4,648) = 2,324 psi and $N > 10^{11}$ cycles (from ASME Code, Fig. I-9.2.2 curve C, shown in Fig. 2.1-2).

2.6.5.2 Cask. Conservatively assuming a 50 year design life for the cask, the maximum number of normal operating cycles will be 50 years x 50 trips a year = 2500 cycles. In each trip the cask is assumed to encounter the two worst loading combinations, which produce the highest range of primary plus secondary stress intensity. This loading condition can be conservatively approximated by assuming that any normal operating stress can reverse direction, thus developing a maximum stress range condition. It is assumed that the magnitude of this stress range is equal to the allowable range of primary plus secondary stress of 3 S_m (Table 2.1-3). The resulting stress amplitude for this condition would be 1.5 S_m or 49.8 ksi at 200°F. Using Table I-9.1 and Fig. I-9.2.1 from ASME Code Section III, Div. 1 Appendices (shown in Table 2.1-8 and Fig. 2.1-1), the number of allowable cycles for an alternating stress of 1.5 S_m is

$$S_a = 49.8 \times 28.3/27.6 = 51 \text{ ksi},$$

$$N = 20000 \left[\frac{50000}{20000}\right]^{(\log 55.5/51)/(\log 55.5/46.3)}$$

$$N = 30{,}668 \text{ cycles}.$$

The allowable used to develop this stress amplitude is based on the maximum primary plus secondary stress range under normal conditions, not including the effects of local stress concentrations. It can therefore be concluded that there is not a fatigue concern for areas of the cask with no stress concentrations. This involves essentially all regions of the cask except the closure area at the plug transition and those areas next to the flange/taper region. These regions have geometry discontinuities that have the potential for a stress concentration effect, and the ANSYS results include these effects. Even in these areas the ANSYS results have relatively low stresses and meet this conservative approach.

2.6.5.3 Closure Bolts. The maximum cyclic stress in the closure bolts is caused by the application and removal of the bolt preload and the heating and cooling of the cask. The force due to the preload is calculated as follows:

$P = T/cD,$

where

P = force, lb,

T = torque = 235 ±15 ft-lb, using the maximum value of 250 ft-lb,

c = friction coefficient = 0.162 (Never-Seez Pure Nickel Special),

D = bolt diameter, 0.878 in.

The bolt stress due to preload, S_p, is calculated as follows:

For coarse threads, 1.00 - 8 threads/in., stress area A = 0.606 in.^{2},

$$S_p = T/cDA = (250 \text{ ft-lb} \times 12 \text{ in./ft}) / [(0.162)(0.878 \text{ in.})(0.606 \text{ in.}^2)]$$
$$= 34{,}805 \text{ psi.}$$

The stress in the closure bolts caused by differential thermal expansion is:

$$S_{de} = E_B \times (\alpha_C - \alpha_B) \times \Delta T$$
$$= 2{,}842 \text{ psi}$$

where

E_B = 28.65 x 10^6 psi at 150°F,

ΔT = (150° - 70°) = 80°F,

α_B = 7.15 x 10^{-6} in./in./°F (Closure bolts), and

α_C = 8.39 x 10^{-6} in./in./°F (Closure).

The total static load bolt stress is the sum of the preload and differential thermal expansion stresses. The MNOP load is not added since it is less than the preload:

$$S_{bolt} = S_p + S_{de},$$
$$= 34{,}805 \text{ psi} + 2{,}842 \text{ psi, and}$$
$$= 37{,}647 \text{ psi.}$$

The primary membrane bolt stress is limited to 2.0 S_m (= 96,000 psi at 200°F for SB-637, Alloy N07718). Therefore, the design margin is:

$$S_{bolt} = S_p + S_{de},$$
$$= 37{,}647 \text{ psi.}$$

$$\text{D.M.} = \frac{96{,}000}{37{,}647} - 1 = 1.55.$$

From ASME Code Section III, NB-3232.3(c), the fatigue strength reduction factor on the threads is taken to be 4.0. Therefore, the stress range is given by

S_{bolt} (range) = 37,647 x 4 = 150,588 psi,

adjusting for the change of modulus of elasticity at 150°F,

S_{bolt} (range) = 150,588 x 30./28.6 = 157,959 psi.

Since the alternating stress is one-half of the stress range,

S_{bolt} (alt) = 78,980 psi .

Using the ASME Code Section III, Fig. I-9.4 and Table I-9.1 (shown in Fig. 2.1-3 and Table 2.1-8), the allowable number of operating cycles is

N ~ 1600 cycles.

At a maximum of 50 load and unload cycles per year, the bolts would have an expected fatigue life of 30 years. This is a longer period than the 20-year replacement schedule given in Chapter 8.2.

2.6.5.4 Impact Limiter Bolts. The maximum cyclic stress in the impact limiter bolts is also due to the application and removal of the preload. Using the same formulas as above, the stresses due to the preload can be calculated thus:

P = force, lb,

T = torque = 230 ±15 ft-lb, using the maximum value of 245 ft-lb,

c = friction coefficient = 0.162, (Never-Seez Pure Nickel Special),

D = bolt diameter, 0.838 in.,

A = stress area = 0.551 in.^{2},

S_{bolt} = T/cDA,

S_{bolt} = (245 ft-lb x 12 in./ft)/[(0.162)(0.838 in.)(0.551 in.^{2})] = 39,304 psi .

The primary membrane bolt stress is limited to 2.0 S_m (= 96,000 psi at 200°F for SB-637, Alloy N07718). Therefore, 245 ft-lb represents approximately 41 percent of the maximum torque that is acceptable for this condition.

From ASME Code Section III, NB-3232.3(c), the fatigue strength reduction factor on the threads is taken to be 4.0. Therefore, the stress range is given by

S_{bolt} (range) = 39,304 x 4 = 157,216 psi.

Adjusting for the change of modulus of elasticity at 200°F,

S_{bolt} (range) = 157,216 x 30./28.3 = 166,660 psi.

The alternating stress is one-half of the stress range,

S_{bolt} (alt) = 83,330 psi.

Using the ASME Code Section III, Fig. I-9.4 and Table I-9.1 (shown in Fig. 2.1-3 and Table 2.1-8), the allowable number of operating cycles is

$$N = 1000 \left[\frac{2000}{1000}\right]^{(\log 100/83.33)/(\log 100/71)},$$

$$N = 1,446 \text{ cycles.}$$

At a maximum of 50 load and unload cycles per year, the bolts would have an expected fatigue life of more than 28 years. This is a longer period than the 20-year replacement schedule given in Chapter 8.2.

2.6.5.5 Cavity Liner. Section 2.10.9.7 discusses the normal condition fatigue evaluation of the cavity liner for the maximum primary loading condition (MNOP and thermal stress). The maximum alternating stress is 47.5 ksi, which gives 30,000 allowable operating cycles.

Since the cavity liner is assumed to be pressurized 25 times each year for an assumed 50 years, the number of design cycles is 1250. The allowable cycles indicate that there is not a fatigue concern for the cavity liner.

2.6.5.6 Neutron Shield Structure. The neutron shield was evaluated for repeated pressurization loads that may contribute to mechanical fatigue of the neutron shield structure. The stresses caused by transportation vibration are small and were therefore neglected in the calculations presented in Section 2.10.11.5. The highest stress range in the neutron shield outer shell occurs at its connection to the ILSS during pressurization cycles. Although this discontinuity stress at the ILSS connection is a secondary stress, it must be evaluated for fatigue failure. As given in Section 2.10.11.5, the allowable number of cycles for this critical area is greater than 10^6. Since the normal operating cycles are 25 shipments per year for an assumed 50 years and conservatively assuming wet loading and unloading (2500 total numbers of cycles), the design is adequate.

2.6.6 Water Spray

The cask structure consists of metallic materials whose strength is unaffected by water spray. These stainless steel and Inconel materials are corrosion-resistant and not subject to any corroding effects from water spray.

2.6.7 1-ft Free Drop

The GA-4 shipping cask is a Type B package that maintains containment when subjected to the sequential normal conditions of 10 CFR Part 71.73. Analyses, using the approach outlined in Fig. 2.6-4, verify the adequacy of the cask design for the normal condition involving a 1-ft free drop. Normal load conditions are subject to a number of initial environmental conditions, as detailed in Table 2.1-1, which can be classified as either an initially hot or cold environment.

The cask components considered in the analyses include the cask containment boundary, closure bolts, FSS/cavity liner, and neutron shield. The ILSS and ILSS bolts were not considered because the hypothetical accident conditions analyses in Sections 2.7.1.3.5 and 2.7.1.3.6 envelop the normal condition results. All of the components considered were shown to have acceptable design margins or stresses for the normal conditions. The lowest design margins for each of the components are summarized in Table 2.6-31. As shown by the table, the component with the lowest design margin is the FSS/cavity liner.

Section 2.6.7.1 explains the GACAP analyses and results which were used as input to the detailed ANSYS models and hand-calculations. The various ANSYS models used for the evaluation of the cask components are described in Section 2.6.7.2. The evaluations used the GACAP and ANSYS computer results and hand-calculations as described in Section 2.6.7.3. Section 2.6.7.4 shows that the containment boundary, cavity liner and neutron shield will not buckle using conservative loading assumptions.

The free drop accident conditions involve different orientations of the cask cross section and axis relative to the impacted surface. For most of the analyses, only the flat and corner orientations are considered because they envelop the range of possible results. The orientations used for the analyses are described in the applicable subsection for a particular component.

TABLE 2.6-31 LOWEST DESIGN MARGINS FOR THE GA-4 CASK DURING NORMAL CONDITIONS

COMPONENT	CONDITION	DESIGN MARGIN
Cask wall	MNOP with 1-ft side drop and cold environment	0.51
FSS/cavity liner	MNOP with 1-ft side drop and cold environment	0.09
Closure bolts	MNOP with 1-ft end drop	3.68
Neutron shield	1-ft side drop	0.85

2.6.7.1 <u>GACAP Analyses</u>. The GACAP program was used to analyze the impact load conditions. The code uses a 2-D, lumped mass, single-axis beam model of the cask body to analyze impacts from different drop heights and angles. The results provided by the code include: time-history information on accelerations, velocities, and displacements. GACAP provides the impact limiter depth of crush, maximum impact force, maximum effective linear and angular accelerations of the CG, energy dissipation information, and a summary of the maximum values and times at which they occur.

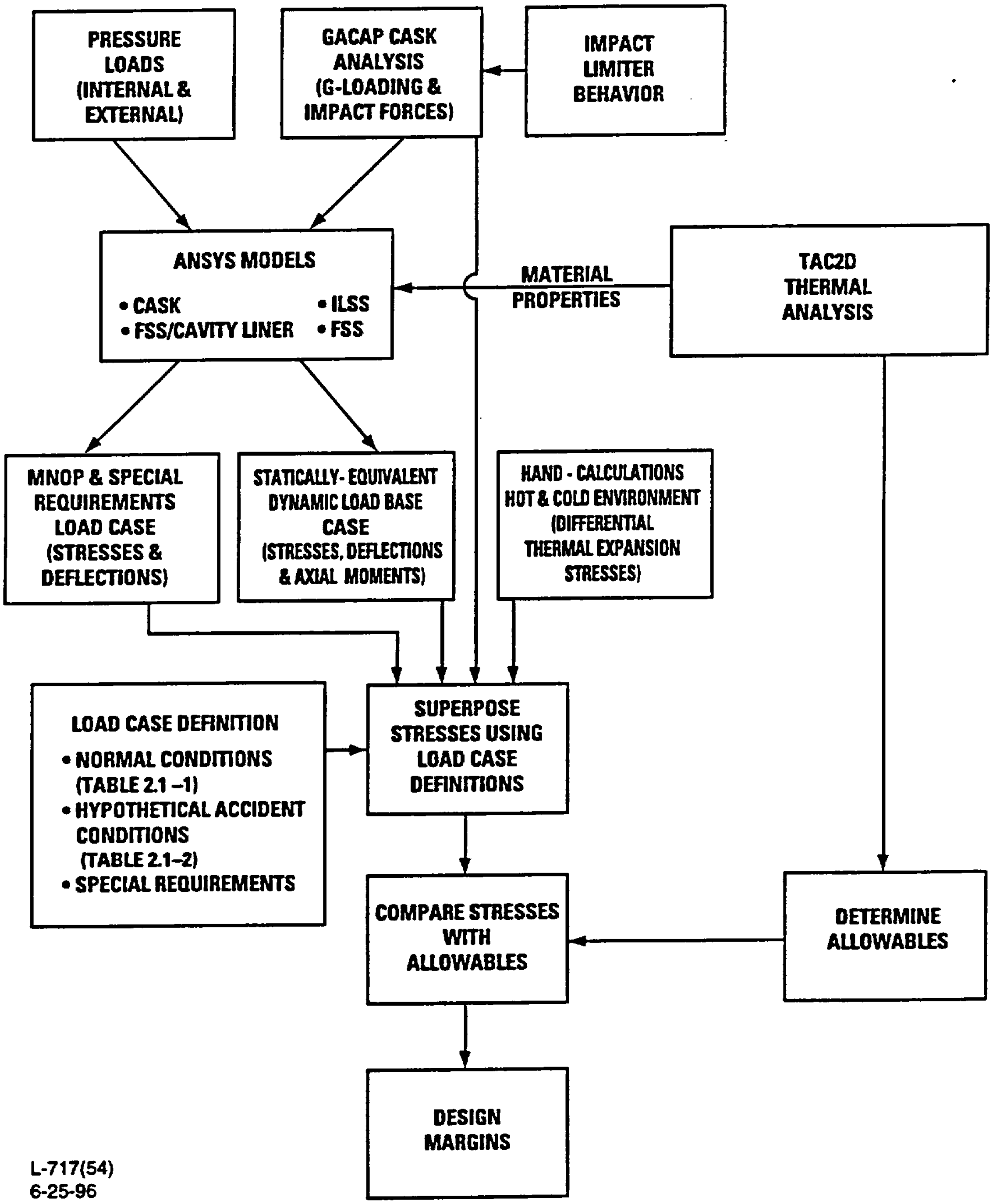

Fig. 2.6-4. Analysis procedure flow chart for the drop events

The GA-4 cask was modeled as a linear elastic solid without structural damping. The impact limiters were simulated with nonlinear force-deflection tables. Section 2.10.4 provides the details of the GACAP analyses. GACAP was used to evaluate the GA-4 cask for 30-ft free drops at 0° (side drop), 15°, 30°, 45°, 60°, 75°, 78° (CG over corner), and 90° (end drop). The 30-ft free drop results were scaled to provide the necessary results for the 1-ft drops. Section 2.7.1.2.1 provides additional information.

The GACAP analyses evaluated a range of impact limiter material properties and considered maximum and minimum content's weights, to find the worst case conditions for each of the components. These conditions are given in Tables 2.6-32 and 2.6-33. The results of the GACAP analyses were used as input to the ANSYS analyses of the cask wall and FSS/cavity liner. The impact limiter crush depth was evaluated in Section 2.10.4. The low crush strength impact limiter produced the greatest depth of honeycomb crush. The margins against the impact limiter bottoming out and the trunnion being impacted are greater than those presented in Table 2.7-4 for the 30-ft hypothetical accident condition drops and are tabulated for different types of honeycomb in Tables 2.10.4-8 through 2.10.4-10.

2.6.7.2 ANSYS Analyses.

2.6.7.2.1 Cask. Two ANSYS finite element models were used to evaluate the stresses in the cask wall for normal and hypothetical accident conditions. These models are referred to as either the "corner" or "flat" model. The label identifies the location of the cask cross section relative to the impacted surface for the horizontal drops. For the corner model, a longitudinal edge of the cask impacts the surface. For the flat model, a flat side of the cask impacts the surface. The corner model uses a plane of symmetry which passes through the cask wall corners and the flat model is symmetric about the center of the flat wall of the cask, as shown in Fig. 2.6-3. These two cross sections envelop the results for any other clocking positions of the cask relative to the impact surface. The stresses resulting from the loads acting on the cask are either independent of the cross section clocking position or maximum for the flat or corner model. The loads acting on the cask and how they are affected by the cross section clocking position are described below:

1. Internal and external pressure load stresses are not affected by the clocking position of the cask about its axis.
2. Stresses resulting from axial bending induced during the side drop or slapdown events are maximum for the corner drop. The maximum moment acting on the cask and its location are the same for the flat and corner models. Since the moment of inertia of the cross section is constant irrespective of the clocking position of the cask's neutral axis, the maximum axial bending stresses are caused by the clocking position which has the largest extreme fiber distance. For the cask this is the corner drop model.
3. Differential thermal expansion stresses are independent of the cask clocking position.
4. The local loads imparted to the cask from the ILSS are shown in Section 2.10.3.6.5 to vary with the impact clocking position, but are bounded by results for the flat and corner model. The local effects of these loads are included in the model, but are not design limiting for the containment boundary.

TABLE 2.6-32 GACAP ACCELERATIONS AND IMPACT FORCES FOR ANALYSIS OF THE CASK CONTAINMENT BOUNDARY, CLOSURE BOLTS, FSS, CAVITY LINER AND ILSS FOR 1-FT DROPS			
IMPACT ANGLE	CG ACCELERATIONS (g)		IMPACT FORCE (lb)
	TRANSVERSE	AXIAL	
0°	15.6	0.	8.57 E+05
15°	7.4	2.0	4.22 E+05
30°	4.7	2.7	2.98 E+05
45°	3.7	3.7	2.90 E+05
60°	6.5	11.2	7.14 E+05
75°	2.6	9.9	5.61 E+05
90°	0.	14.9	8.17 E+05

TABLE 2.6-33 GACAP ACCELERATIONS AND IMPACT FORCES FOR ANALYSIS OF THE NEUTRON SHIELD STRUCTURE FOR 1-FT DROPS			
IMPACT ANGLE	CG ACCELERATIONS (g)		IMPACT FORCE (lb)
	TRANSVERSE	AXIAL	
0°	16.6	0.	8.01E+05
15°	8.2	2.2	4.11E+05
30°	5.4	3.1	2.99E+05
45°	4.1	4.1	2.79E+05
60°	6.9	11.9	6.66E+05
75°	2.7	10.1	5.06E+05
78°	2.2[a]	11.4[a]	5.67E+05[a]
90°	0	16.8	8.11E+05
[a]Interpolated between the 75° and 90° drops.			

Figure 2.6-3 also shows the locations used to report stress results. Internal and external pressure cases were considered, as well as statically equivalent, dynamic load cases. The dynamic load cases simulated a side drop with both impact limiters reacting the drop load and an end and oblique drop with a single impact limiter. The results for the end and oblique drops are normalized to 10 g.

To adequately and efficiently evaluate the normal conditions, a summary of worst case loads for a range of impact angles and drop heights was developed for the dynamic load cases; using the GACAP computer program. The results are summarized in Table 2.6-32 for the cask and its internals and in Table 2.6-33 for the neutron shield structure. As shown in the tables, the results are given in terms of the acceleration in the transverse and axial directions for different angle drops. To find the stresses in the cask wall resulting from these different dynamic load cases, the stresses for the base case end drop and the base case oblique drop were scaled by the appropriate axial and transverse g-levels given in Table 2.6-32. After superposing the transverse and axial dynamic stress distributions, the results were combined with the appropriate pressure case results to obtain the complete stress distribution for the load case. The resulting stresses are combined to find the stress intensity, SI, and to determine the design margin for different sections along the cask wall.

In Section 2.10.2, the two ANSYS models are described, the loading conditions defined and the analysis procedure is explained. Section 2.10.6 presents the detailed results of the analyses for the normal and the hypothetical accident conditions and 290 psi external water pressure load.

2.6.7.2.2 FSS/Cavity Liner. There were two different types of ANSYS models used for the analysis of the FSS/cavity liner. The first was a frame model of an axial section of the complete FSS/cavity liner cross section and the second was a plate model of one of the legs of the FSS. The frame model assumed a uniform loading of the fuel assemblies on the FSS during either a side drop or slapdown event. The plate model simulated a section of the FSS and considered the effects of fuel assembly support grid and end-plate loading.

The frame model used two coordinate axis orientations. The model geometries are shown in Figs. 2.6-5 and 2.6-6 for the flat and corner model, respectively. These two model geometries envelop the results for any other clocking positions of the cask relative to the impacting surface. The stresses resulting from the loads acting on the cask are either independent of the cross section clocking or maximum for the flat or corner model. The loads acting on the cask and how they are affected by the cross section clocking are described below:

1. Internal and external pressure load stresses are not affected by the clocking position of the cask about its axis.
2. Stresses resulting from axial bending induced during the side drop or slapdown events are maximum for the corner drop. The maximum moment acting on the cask and its location are the same for the flat and corner models. Since the moment of inertia of the cross section is constant irrespective of the clocking position of the cask's neutral axis, the maximum axial bending stresses are caused by the clocking position which has the largest extreme fiber distance. For the cask this is the corner drop model.
3. Differential thermal expansion stresses are independent of the cask clocking position.

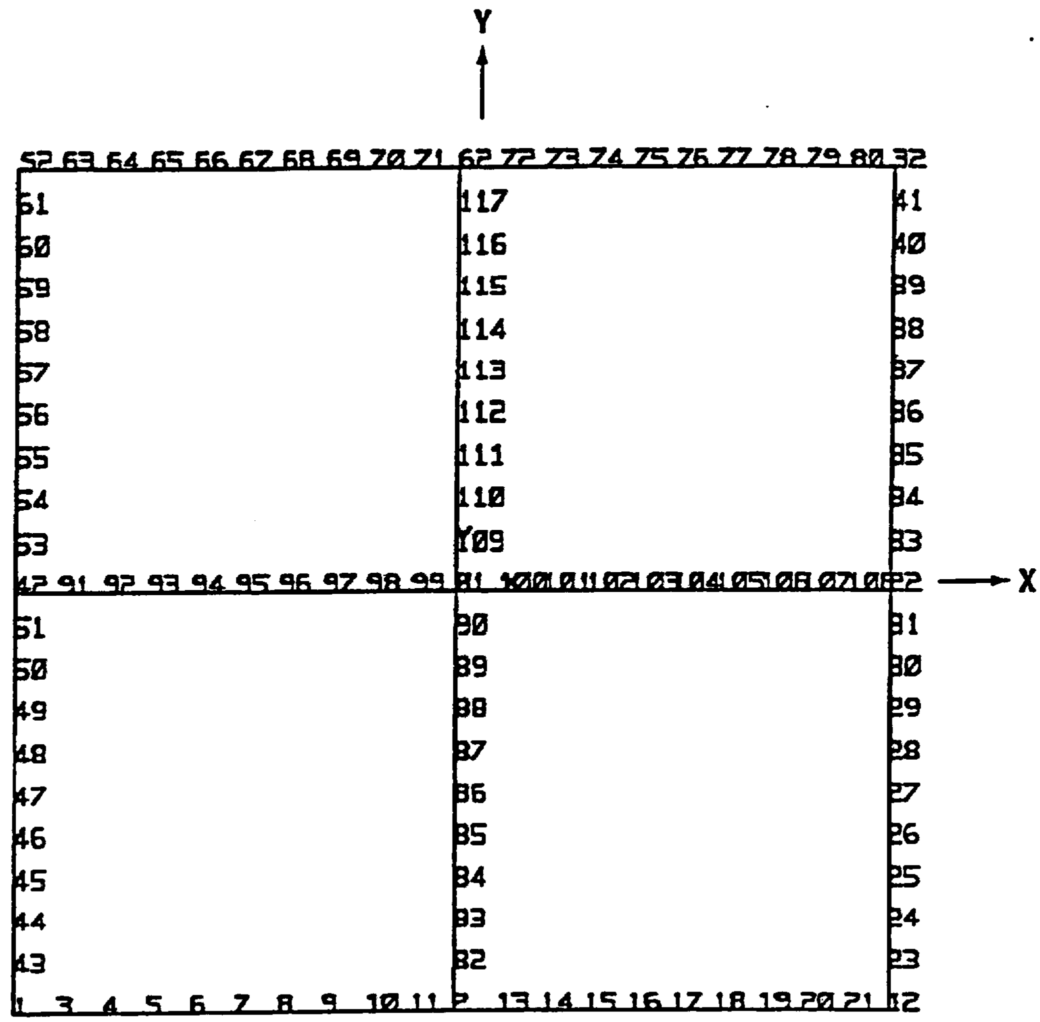

L-764(6)
8-19-96

Fig. 2.6-5. Flat model node locations for ANSYS FSS/cavity liner frame analysis

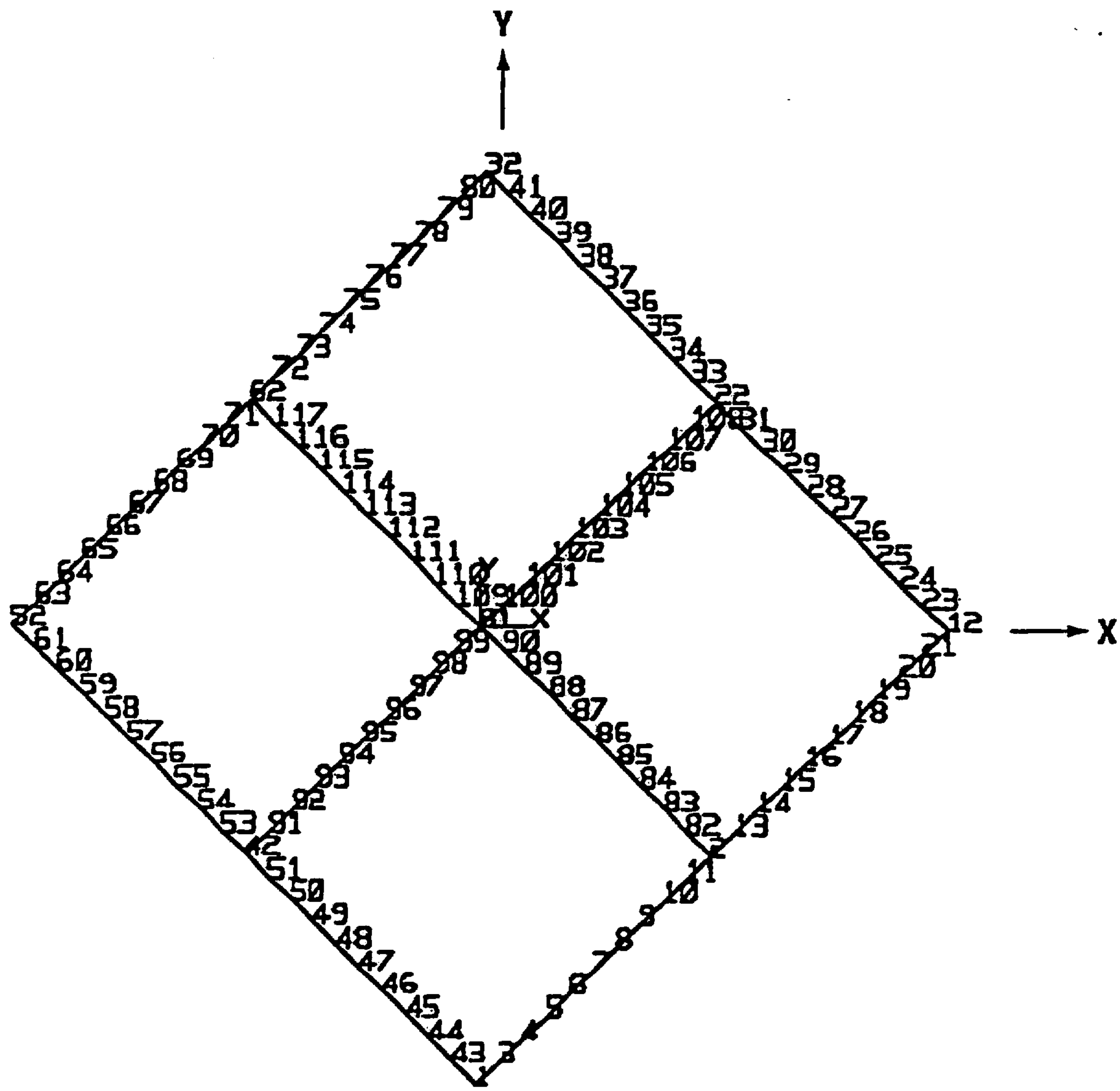

L-764(5)
8-19-96

Fig. 2.6-6. Corner model node locations for ANSYS FSS/cavity liner frame analysis

4. The stresses from the fuel element and postulated DU inertial loadings on the FSS/cavity liner are maximum for the flat model. The applied loading is resolved into its components as the angle varies from the flat model to the corner model.
5. The deflection profiles used to simulate the effect of cask wall ovalization on the FSS/cavity liner were assumed the same as those derived for the flat and corner models of the cask. For other clocking positions, the deflection profile would be obtained from the appropriate combination of results from the flat and corner models. As given in Section 2.10.9.5, the deflections for the other clocking positions would be smaller and, therefore, the stresses would be lower than those for the flat or corner model.

The stress reporting points shown in Fig. 2.6-7 are the same for both of the models. The basic model is a frame structure composed of two-dimensional BEAM3 elements which simulate a one-inch length axial section of the FSS/cavity liner. The model used 120 beam elements and 117 nodes. The FSS portion of the model used actual section properties and material modulus values in the B_4C pellet hole region. The boundary conditions applied to the model include fixed displacements for the edge of the model which hit the impacted surface and pressure loads which simulated the effects of the various load cases. Fixed displacements are used to characterize the ovalization information obtained from the cask containment boundary ANSYS analysis. The inertial loads of the DU, fuel and non-fuel assembly hardware (NFAH) are simulated using equivalent pressure loads on the FSS and the upper portion of the cavity liner. Both full and partial fuel assembly loadings (three or four fuel elements) are considered. The MNOP load case applies a uniform 80 psig pressure to the internal walls of the cavity liner. The ANSYS models and the loadings used are described in detail in Section 2.10.9 for a uniformly loaded FSS.

The ANSYS frame analyses were used to find the stresses for the different load cases. In Section 2.10.9 the inertial loading results were combined with the MNOP and thermal stresses and the out-of-plane bending stresses derived from the moment developed from the cask containment boundary analyses.

The plate model of the FSS was used to detail the inertial effects of a nonuniform fuel and NFAH loading on the FSS. A three-dimensional plate model was used with the loads applied at either the middle or the end of the model. The loadings represented either a midcavity or cavity end loading condition on the FSS. The model used the SHELL63 element from ANSYS. The model is a section of the FSS 31.5 in. long and 8.77 in. wide. Orthotropic properties are used to simulate the effects of the B_4C pellet holes. Both sides of the model (one side represents the center of the FSS and the other its attachment to the cavity liner) are clamped. The two loading conditions simulated by the model geometry are sketched in Fig. 2.6-8. In the simulation of the bottom edge of the FSS, 2.25 in. of the edge simulating the cavity liner attachment to the FSS was also free, as shown in Fig. 2.6-9. The details of the model and loadings are described in further detail in Section 2.10.10. The local effects evaluated by this model were superposed upon the results of the frame model to incorporate the ovality effects of the containment wall.

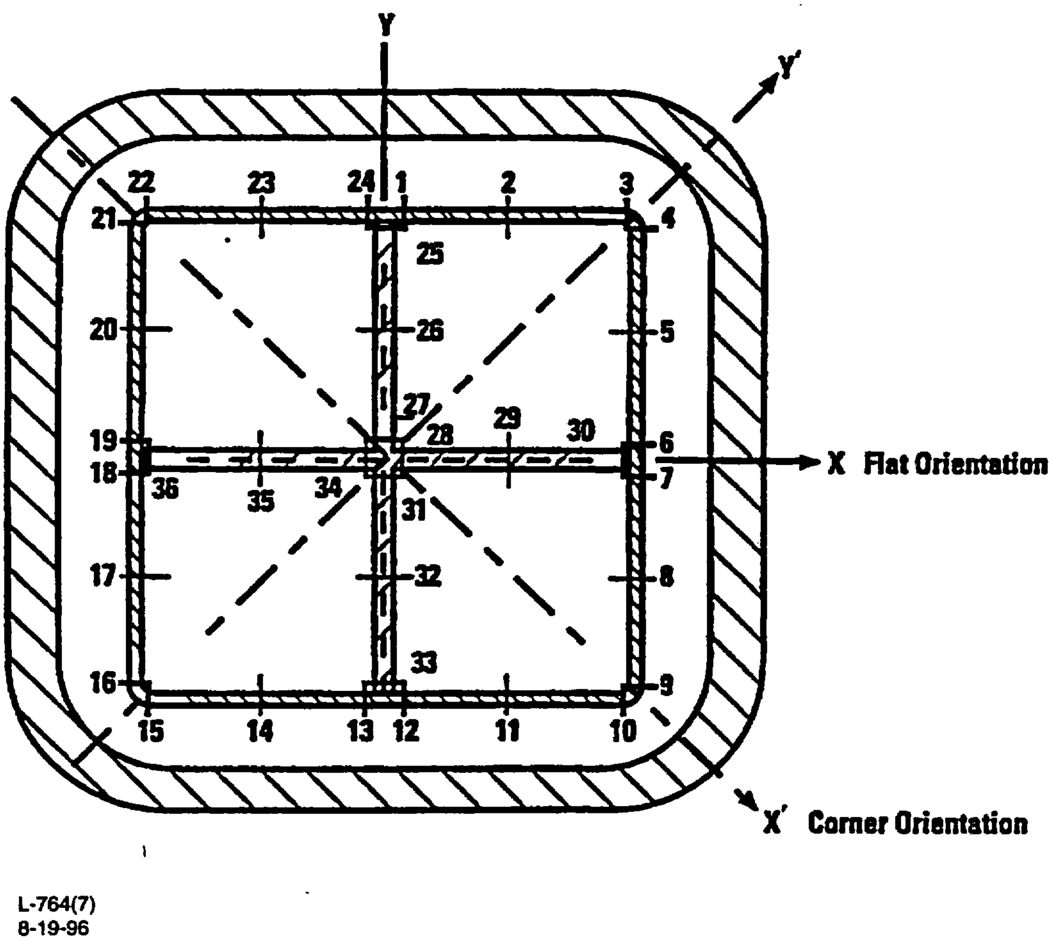

Fig. 2.6-7. Location of stress reporting points for the ANSYS models of the FSS/cavity liner

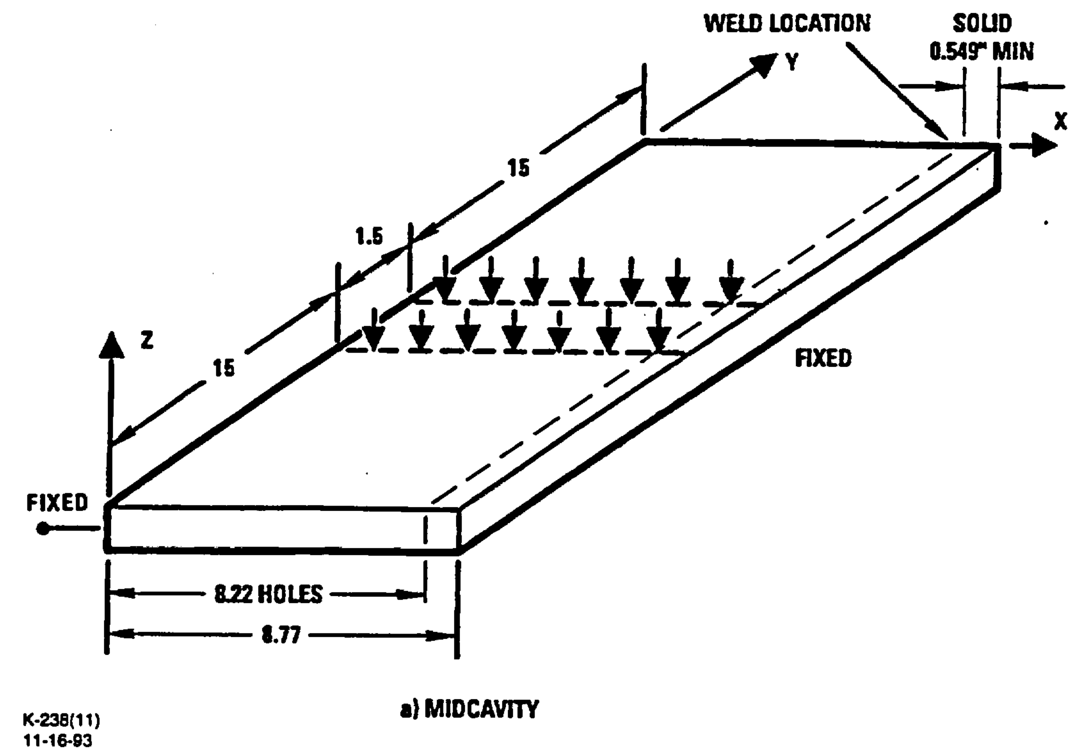

a) MIDCAVITY

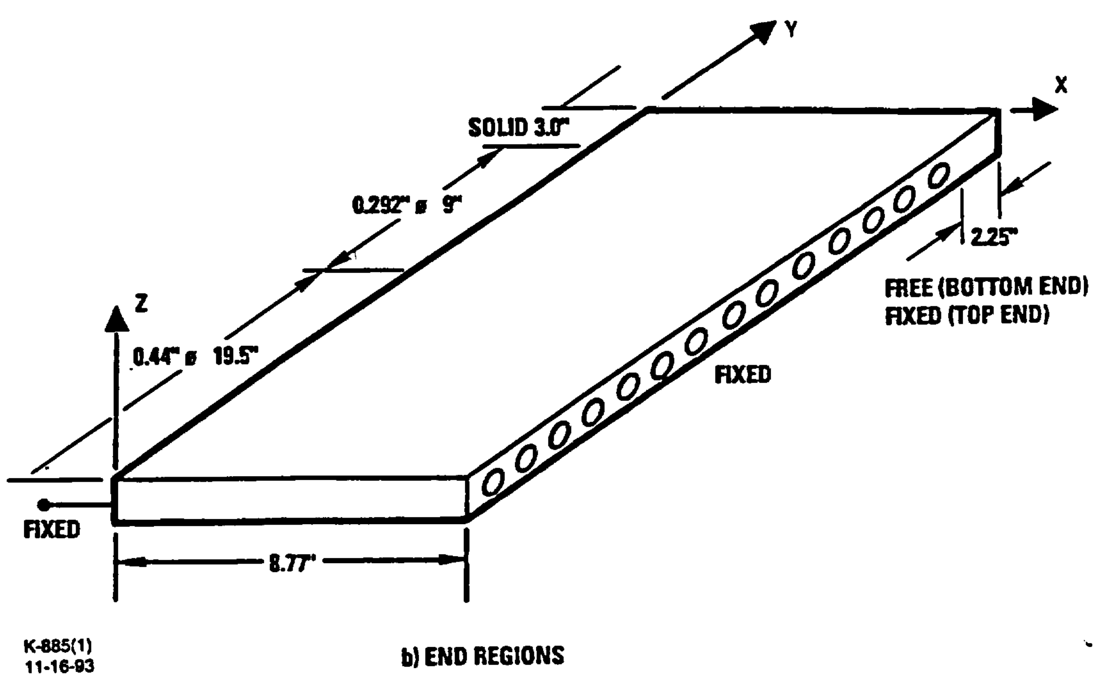

b) END REGIONS

Fig. 2.6-8. ANSYS FSS plate models for the concentrated load cases

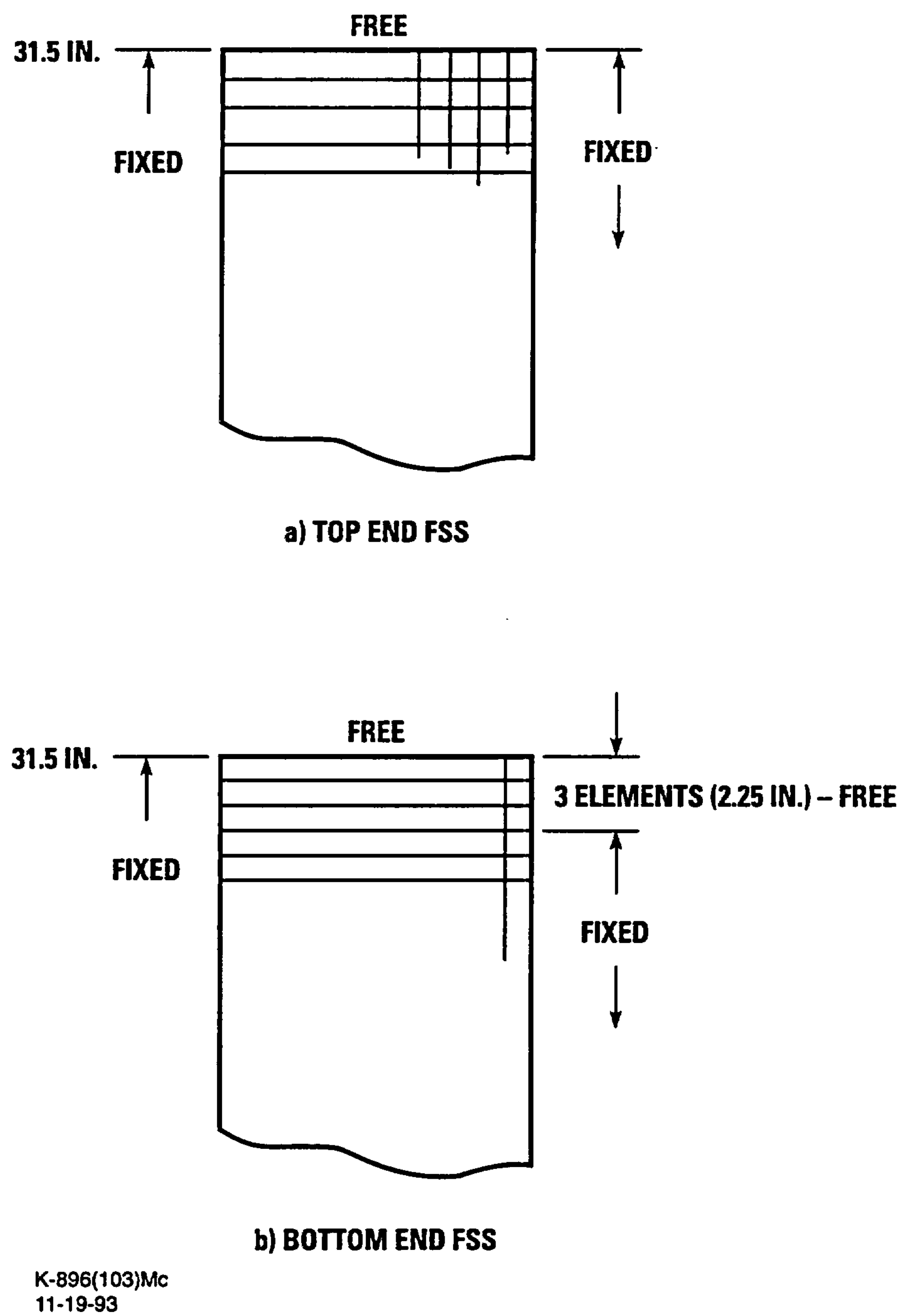

Fig. 2.6-9. Boundary conditions for the ANSYS model of the cavity end FSS

2.6.7.3 Load Case Evaluations.

2.6.7.3.1 Cask Containment Boundary. As mentioned in Section 2.6.7.2.1, after each of the ANSYS analyses was performed, a stress summary table with the directionally-dependent stress components was developed for each of the base cases. These results are presented in Tables 2.10.6-13 through 2.10.6-62 for the two models, flat and corner. To evaluate the cask containment boundary for the different normal conditions, the results for the applicable base cases were superposed at the stress component level and the principal stresses, stress intensities and design margins were calculated. For the initial evaluation, thermal stresses were not considered. After the results for the normal conditions load cases described in Section 2.10.2.3.3 were considered, six of the load cases were chosen to include the cold environment differential thermal expansion stresses. The hot environment differential thermal expansion stresses were not considered, because they were low (≈ 300 psi) in comparison with the stresses induced by the different drop loads.

The results for the load cases without thermal effects are summarized in Table 2.6-34 and 2.6-35 for the flat and corner cask models, respectively. The case with the lowest design margin is MNOP with 1-ft side drop for the corner model with a design margin of 1.01. The results for the selected load cases which include the cold environment stresses are summarized in Table 2.6-36. The load cases presented in Table 2.6-36 were selected because they represent the end and side drops, and the worst case slapdown. The lowest design margin for these cases was 0.51 for MNOP with 1-ft side drop for the corner model. As shown by comparison of the tables, the design margins for the end drop increased, while they decreased for the side drop and slapdown. These results are reasonable, because the cold environment induces a tensile differential thermal expansion stress in the axial direction for the cask wall. When this stress is combined with the dynamic load case stresses, it decreases the axial compressive stress for the end drop and increases the tensile axial stresses for the side drop and slapdown conditions. These act in turn to reduce the stress intensity for the end drop and increase it for the side drop and slapdown.

2.6.7.3.2 Closure Bolt Stresses. The twelve SB-637, Alloy N07718 closure bolts are preloaded after the cask is loaded and the closure is installed to ensure that a seal is maintained. The bolts are torqued to 235 ft-lb ±15, which is greater than the sum of the load needed to compress the seals and the MNOP. For normal conditions, the maximum load on the bolts occurs during the 1-ft drop when the closure end impact limiter strikes an unyielding surface. The bolt stresses are calculated for all drop angles, for both the flat and corner angular orientations.

Analysis Methodology. The methodology is the same for normal conditions and hypothetical accident conditions. All loads are considered, (1) bolt preload, (2) differential thermal expansion, (3) MNOP pressure loading and (4) closure/contents impact loading. The hot condition is the most critical loading because differential thermal expansion introduces tension in the bolts and the allowable stresses are a minimum. The maximum normal condition temperature of the closure and bolts is 136°F (avg.). Bolt allowables and closure and bolt properties are taken at 150°F to be conservative.

TABLE 2.6-34 SUMMARY OF NORMAL CONDITION LOAD CASE RESULTS FOR FLAT MODEL WITHOUT DIFFERENTIAL THERMAL EXPANSION EFFECTS

LOAD CASE		STRESS POINT LOCATION				
No.	Description	Axial[a] Section	Transverse Position[a]	Position in Wall	Stress Type	Design Margin
1	MNOP with 1-ft end drop	E	3 7	inside inside	$P_m + P_b$ $P_m + P_b$	6.62 6.62
2	MNOP with 1-ft side drop	E	9	inside	$P_m + P_b$	1.13
3	MNOP with 1-ft drop at 15°	C	9	outside	$P_m + P_b$	1.63
4	MNOP with 1-ft drop at 30°	C	9	outside	$P_m + P_b$	2.60
5	MNOP with 1-ft drop at 45°	C	9	outside	$P_m + P_b$	3.16
6	MNOP with 1-ft drop at 60°	C	9	outside	$P_m + P_b$	1.89
7	MNOP with 1-ft drop at 75°	C	9	outside	$P_m + P_b$	4.03
8	MNOP with 1-ft drop at 78°	C	9	outside	$P_m + P_b$	4.03
9	1-ft end drop	A	1 9	inside inside	$P_m + P_b$ $P_m + P_b$	15.23 15.23
10	1-ft side drop	E	9	inside	$P_m + P_b$	1.39
11	1-ft drop at 15°	C	9	outside	$P_m + P_b$	2.58
12	1-ft drop at 30°	C	9	inside	$P_m + P_b$	4.86
13	1-ft drop at 45°	C	9	outside	$P_m + P_b$	6.17
14	1-ft drop at 60°	C	9	outside	$P_m + P_b$	3.08
15	1-ft drop at 75°	C	9	outside	$P_m + P_b$	9.20
16	1-ft drop at 78°	C	9	outside	$P_m + P_b$	9.20

[a]Locations shown schematically in Fig. 2.6-3.

TABLE 2.6-35 SUMMARY OF NORMAL CONDITION LOAD CASE RESULTS FOR CORNER MODEL WITHOUT DIFFERENTIAL THERMAL EXPANSION EFFECTS

LOAD CASE		STRESS POINT LOCATION				
No.	Description	Axial[a] Section	Transverse Position[a]	Position in Wall	Stress Type	Design Margin
1	MNOP with 1-ft end drop	E	3 11	inside inside	$P_m + P_b$ $P_m + P_b$	6.45 6.45
2	MNOP with 1-ft side drop	E	11	middle	P_m	1.01
3	MNOP with 1-ft drop at 15°	D	11	middle	P_m	2.70
4	MNOP with 1-ft drop at 30°	C	7	inside	$P_m + P_b$	4.08
5	MNOP with 1-ft drop at 45°	C	7	inside	$P_m + P_b$	4.47
6	MNOP with 1-ft drop at 60°	D	7	inside	$P_m + P_b$	3.51
7	MNOP with 1-ft drop at 75°	C D	7 7	inside inside	$P_m + P_b$ $P_m + P_b$	4.98 4.98
8	MNOP with 1-ft drop at 78°	C D	7 7	inside inside	$P_m + P_b$ $P_m + P_b$	4.98 4.98
9	1-ft end drop	A	5 9	inside inside	$P_m + P_b$ $P_m + P_b$	15.47 15.47
10	1-ft side drop	E	11	middle	P_m	1.04
11	1-ft drop at 15°	D	11	middle	P_m	2.80
12	1-ft drop at 30°	D	11	middle	P_m	5.10
13	1-ft drop at 45°	D	11	middle	P_m	6.97
14	1-ft drop at 60°	D	11	middle	P_m	3.77
15	1-ft drop at 75°	D	3	middle	P_m	9.86
16	1-ft drop at 78°	D	3	middle	P_m	9.86

[a]Locations shown schematically in Fig. 2.6-3.

TABLE 2.6-36 SUMMARY OF SELECTED LOAD CASE RESULTS FOR NORMAL CONDITIONS WITH COLD ENVIRONMENT DIFFERENTIAL THERMAL EXPANSION EFFECTS

LOAD CASE		STRESS POINT LOCATION				
No.	Description	Axial[a] Section	Transverse Position[a]	Position in Wall	Stress Type	Design Margin
Flat Model Results						
1	MNOP with 1-ft end drop	A	1 5 9	middle middle middle	P_m P_m P_m	3.73 3.73 3.73
2	MNOP with 1-ft side drop	D E	9 8	inside middle	$P_m + P_b$ P_m	0.83 0.83
9	1-ft end drop	A	2 4 6 8	middle middle middle middle	P_m P_m P_m P_m	4.09 4.09 4.09 4.09
10	1-ft side drop	E	8	middle	P_m	0.87
Corner Model Results						
1	MNOP with 1-ft end drop	A	5 9	middle middle	P_m P_m	3.71 3.71
2	MNOP with 1-ft side drop	E	11	middle	P_m	0.51
9	1-ft end drop	A	4 6 8 10	middle middle middle middle	P_m P_m P_m P_m	4.09 4.09 4.09 4.09
10	1-ft side drop	E	11	middle	P_m	0.54

[a]Locations shown schematically in Fig. 2.6-3.

Closure Bolt Dimensions. For 1-in. - 8UNC reduced shank bolt,

A_{stress} = 0.606 in.^{2}

Use same area for the reduced shank, therefore:

D = 4x A_{stress}/π = 4 x 0.606/π = 0.878 in.

Bolt Material Allowable at 150°F, Table 2.1-4.

SB-637 Alloy N07718

Primary Membrane

2 x S_m = 97,500 psi, normal conditions

Static Loading.

The static loads on the bolts include the preload, differential thermal expansion and MNOP.

The stress on the closure bolts caused by MNOP is:

$$S_{MNOP} = \frac{MNOPxD_c^2}{N_BxA_B},$$

$$= 4{,}226 \text{ psi},$$

where

MNOP = 80 psig,

D_c = distance to inside of primary seal = 19.86 - 0.25 = 19.6 in.,

NB = 12, and

A_B = 0.606 in.^{2}

The stress due to differential thermal expansion was calculated in Section 2.6.5.3 and is 2842 psi.

The stress due to preload was calculated in Section 2.6.5.3 and is: S_p = 34,805 psi.

The total static load bolt stress is the sum of the preload and differential thermal expansion stresses. The MNOP load is not added since it is less than the preload:

S_s = $S_p + S_{de}$,

= 34,805 psi + 2,842 psi,

= 37,647 psi < primary membrane allowable = 97.5 ksi, and the design margin is:

DM = (97.5/37.65) – 1 = 1.6.

1-ft Free Drop Loading.

The closure bolts are loaded during a 1-ft free drop on the closure end impact limiter. If the impact and MNOP forces do not cause the bolt stresses to exceed the preload, then the maximum stress in the bolt is the preload stress. This section calculates the impact and MNOP loads on the bolts to show that the preload is not exceeded.

The forces on the closure bolts are calculated by assuming that the inertial loading of the contents and the closure cause the closure to pivot around its outer edge. The resistance of the portion of the impact limiter that backs the inertial loading is conservatively ignored. This assumption is especially conservative for the end drop, where the impact limiter crush force directly resists the inertial loading. The results of the 78° CG-over-corner drop test of the half-scale model, reported in Section 2.10.13, indicated that the contents impact on the closure before the time of maximum g loading. Therefore, no dynamic amplification is applied to the inertial loading of the contents.

Following is an example of the calculation for one drop angle. Tables 2.6-37 through 2.6-39 summarize the results for all drop angles for both the flat and corner drop orientations. As shown in the tables, the worst orientation is when the cask impacts on the longitudinal corner of the cask.

The maximum axial impact force on the closure is calculated as follows for a normal condition 1-ft 60° drop:

$$F_{axial} = W \times g,$$
$$= 8{,}160 \times 11.2,$$
$$= 91{,}392 \text{ lb},$$

where

W = closure weight + fuel weight = 1512 + 6648 = 8160 lb, and

g = 11.2 axial for 60° drop (Table 2.6-32).

The maximum axial load on the bolts can be calculated by using Fig. 2.6-10 for impacts on the flat side of the cask and Fig. 2.6-11 for impacts on the longitudinal corner of the cask as follows:

M_P = moment about P,

$M_P = F_{axial} \times 13.06$ in. (cask flat side),

$= F_{axial} \times 16.30$ in. (cask corner),

$M_P = 91{,}392$ lb $\times$ 13.06 in. (cask flat side),

$= 91{,}392 \times 16.30$ in. (cask corner),

= 1,193,580 in.-lb (cask flat side),

= 1,489,690 in.-lb (cask corner),

$$M_P = 3f\left(24.81 + \frac{1.31^2}{24.81}\right) + 2f\left(\frac{19.93^2 + 13.06^2 + 6.18^2}{24.81}\right), \text{ (cask flat side)},$$

TABLE 2.6-37 1-ft DROP BOLT STRESSES - AXIAL STRESS - FLAT ANGULAR ORIENTATION					
Drop Angle (Deg)	Normal Condition Axial g	Moment Mp (in.-lb)	Impact Bolt Stress (psi)	MNOP Bolt Stress (psi)	Max Stress (Impact + MNOP) (psi)
side (0)	0.0	0	0	4,226	4,226
15	2.0	213,139	2,848	4,226	7,074
30	2.7	287,738	3,845	4,226	8,071
45	3.7	394,308	5,269	4,226	9,495
60	11.2	1,193,580	15,949	4,226	20,176
75	9.9	1,055,039	14,098	4,226	18,324
90	14.9	--	16,719	4,226	20,946

TABLE 2.6-38 1-ft DROP BOLT STRESS - SHEAR STRESS FLAT AND CORNER ANGULAR ORIENTATION		
Drop Angle (Deg)	Normal Condition Transverse g	Shear Stress (psi)
side (0)	15.6	3,244
15	7.4	1,539
30	4.7	977
45	3.7	769
60	6.5	1,351
75	2.6	541
90	0	NA

TABLE 2.6-39 1-ft DROP BOLT STRESSES - AXIAL STRESS - CORNER ANGULAR ORIENTATION					
Drop Angle (Deg)	Normal Condition Axial g	Moment Mp (in.-lb)	Impact Bolt Stress (psi)	MNOP Bolt Stress (psi)	Max Stress (Impact + MNOP) (psi)
side (0)	0.0	0	0	4,226	4,226
15	2.0	266,016	3,075	4,226	7,301
30	2.7	359,122	4,152	4,226	8,378
45	3.7	492,130	5,689	4,226	9,916
60	11.2	1,489,690	17,222	4,226	21,448
75	9.9	1,316,779	15,223	4,226	19,449
90	14.9	--	16,719	4,226	20,946

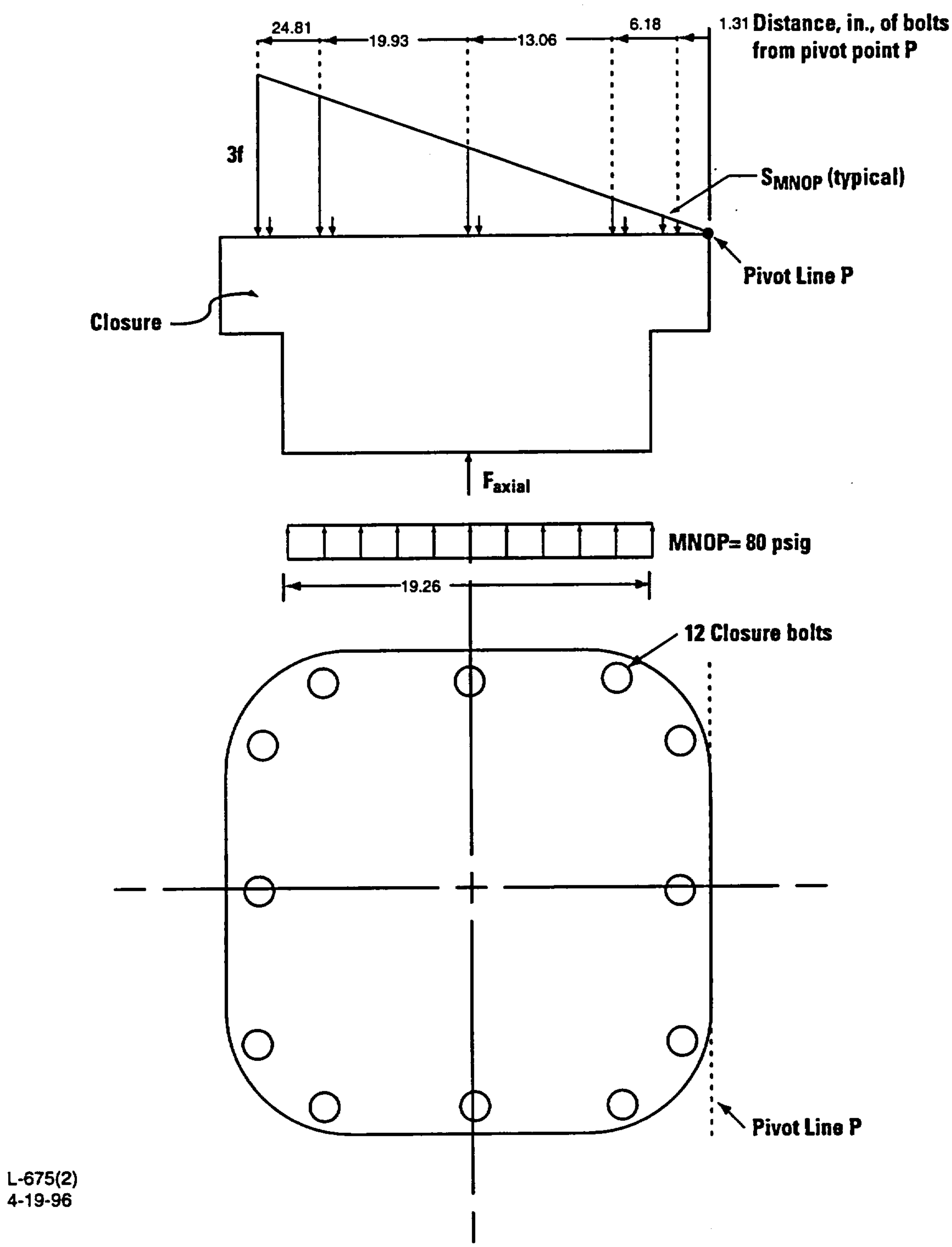

Fig. 2.6-10. Closure bolt reaction load for flat drop orientation

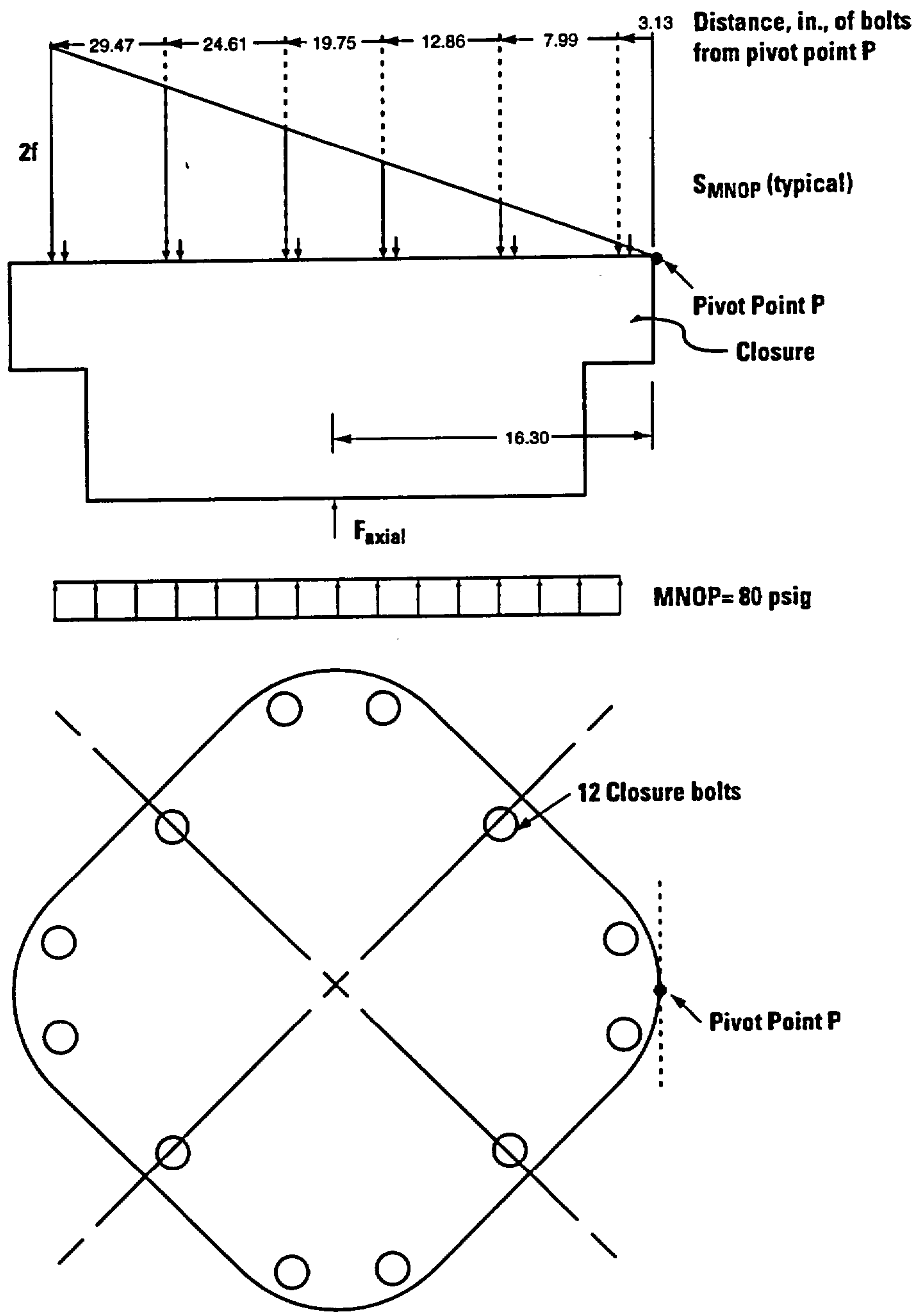

L-675(1)
7-26-96

Fig. 2.6-11. Closure bolt reaction load for corner drop orientation

$$= 2f\left(29.47+\frac{24.61^2+19.75^2+12.86^2+7.99^2+3.13^2}{29.47}\right) \text{ (cask corner)},$$

f = $M_p/123.49$ = 9,665 lb per bolt (cask flat side),

= $M_p/142.74$ = 10,436 lb (cask corner).

Maximum stress on the bolt = S_i = 9,665/.606 = 15,949 psi (cask flat side),

= 10,436/.606 = 17,222 psi (cask corner).

Stress on the bolts caused by the MNOP = S_{MNOP} = 4,226 psi.

Total membrane stress on the bolt is the sum of the impact load and the MNOP load. As shown in Tables 2.6-37 and 2.6-39, the preload is not exceeded by the impact and MNOP load:

S_t = $S_i + S_{MNOP}$

= 15,949 + 4,226 (cask flat side),

= 17,222 + 4,226 (cask corner),

= 20,175 psi (cask flat side), and

= 21,448 psi (cask corner).

Therefore, the maximum axial stress in the bolts is the preload plus thermal.

The transverse impact force on the closure is calculated as follows for a normal condition 60° drop:

F_{trans} = W x g,

= 1,512 x 6.5,

= 9,828 lb,

where

W = closure weight = 1,512 lb, and

g = 6.5 transverse for 60° drop (Table 2.6-32).

The impact force shear stress in the bolts is:

S_{shear} = F_{trans}/(0.606 x 12),

= 1,351 psi.

A summary of the design margins for both the 1-ft drop flat and corner orientations is presented in Tables 2.6-40 and 2.6-41.

2.6.7.3.3 FSS/Cavity Liner. The evaluation of the FSS and cavity liner for normal conditions combine the stresses calculated by the ANSYS frame analysis with the hand-calculated stresses induced by the out-of-plane moment from the cask ANSYS model and the thermal stresses induced in the FSS and cavity liner by either the cold or hot environment.

TABLE 2.6-40 CLOSURE BOLT DESIGN MARGIN SUMMARY FOR NORMAL CONDITION - FLAT ANGULAR ORIENTATION						
Drop Angle (Deg)	S_x (axial) (ksi)	S_{xy} (shear) (ksi)	S1 (ksi)	S2 (ksi)	SI (ksi)	D.M.
side (0)	4.23	3.24	5.98	-1.75	7.74	11.60
15	7.07	1.54	7.39	-0.32	7.71	11.64
30	8.07	0.98	8.19	-0.12	8.31	10.73
45	9.50	0.77	9.56	-0.06	9.62	9.14
60	20.18	1.35	20.27	-0.09	20.36	3.79
75	18.32	0.54	18.34	-0.02	18.35	4.31
90	20.95	NA	20.95	0.00	20.95	3.65

TABLE 2.6-41 CLOSURE BOLT DESIGN MARGIN SUMMARY FOR NORMAL CONDITION - CORNER ANGULAR ORIENTATION						
Drop Angle (Deg)	S_x (axial) (ksi)	S_{xy} (shear) (ksi)	S1 (ksi)	S2 (ksi)	SI (ksi)	D.M.
side (0)	4.23	3.24	5.98	-1.76	7.74	11.59
15	7.30	1.54	7.61	-0.31	7.92	11.31
30	8.38	0.98	8.49	-0.11	8.60	10.33
45	9.91	0.77	9.98	-0.06	10.04	8.72
60	21.44	1.35	21.53	-0.08	21.62	3.51
75	19.44	0.54	19.46	-0.02	19.48	4.01
90	20.95	NA	20.95	0.00	20.95	3.66

The stresses generated by the ANSYS frame model described in Section 2.6.7.2.2 included the effects of the cask internals and the deflection profile of the cask containment boundary ovalization during the side drop or slapdown events. The results of the ANSYS plate model were also combined with the results of the frame model and hand-calculations for some of the critical load cases which were identified for the uniform fuel and NFAH inertial loads. After combination of the directional stress components, the principal stresses, stress intensities and the design margins were calculated. The load cases considered and the results obtained are detailed in Sections 2.10.9 and 2.10.10. Using the results of these sections, the lowest design margin for each of the load cases is given in Tables 2.6-42 through 2.6-44. As shown by the tables, the lowest design margin is 0.09, which occurs for load cases 2 and 4 with the cold environment.

2.6.7.3.4 Neutron Shield Structure. Hand calculations were used to evaluate the adequacy of the neutron shield structure during normal conditions. The effects of inertial loads, impact forces and [Prop. Info.] were all considered. The inertial loads and impact forces were taken from Table 2.10.4-7. [Proprietary Information] The results of the assessment detailed in Section 2.10.11 are summarized in Table 2.6-45. As shown by the table, the design margins for all of the stresses resulting from the normal conditions are acceptable. The lowest design margin is 0.85 and is obtained during the 1-ft side drop.

2.6.7.4 Buckling Evaluation. The buckling resistance of the cask body, cavity liner, fuel support structure and neutron shield shell have been shown in Section 2.10.7 to meet the criteria described in Section 2.1.2.6 for all normal conditions. Following is a summary of the results of these analyses.

Cask Body Buckling. The cask body was analyzed for buckling for combined axial compression and bending. The minimum design margin occurs for the side 1-ft drop where the bending in the cask is a maximum. The minimum design margin is 1.12 as shown in Table 2.10.7-1.

Cavity Liner and Fuel Support Structure (FSS) Buckling. The cavity liner and FSS were analyzed for buckling for combined axial compression and bending. The minimum design margin occurs for the side 1-ft drop where the bending in the cavity liner and FSS is a maximum. The minimum design margin is .99 for the corner angular orientation as shown in Tables 2.10.7-2 and 2.10.7-3.

Neutron Shield Shell. Overall, buckling of the neutron shield shell is precluded by the stiffness and buckling strength of the cask body. The shell was shown to not buckle due to the maximum external pressure that occurs when the cask is loaded into a fuel pool with a design margin of 0.49 as shown in Section 2.10.11.4.

TABLE 2.6-42 DESIGN MARGIN SUMMARY OF NORMAL CONDITION RESULTS FOR UNIFORM LOAD CASES APPLIED TO THE FSS/CAVITY LINER HOT ENVIRONMENT

LOAD CASE			STRESS POINT LOCATION				SUMMARY	
No.	Description 1-ft	Config.[a]	Component	Axial[b] Section	Trans Pos.[b]	Position in Wall	Stress Type	Design Margin
1	Side Drop	Flat /4	cavity liner	E	1/24	outside	P_m+P_b	1.58
			FSS		33	middle	P_m	1.31
2	Side Drop + MNOP	Flat/4	cavity liner	E	9/16	outside	P_m+P_b	0.27
			FSS		25	middle	P_m	1.06
3	Side Drop	Flat/3	cavity liner	E	22	outside	P_m+P_b	1.57
			FSS		33	middle	P_m	1.29
4	Side Drop + MNOP	Flat /3	cavity liner	E	16	outside	P_m+P_b	0.26
			FSS		33	middle	P_m	1.46
5	Side Drop	Corner/4	cavity liner	E	3/4	outside	P_m+P_b	0.89
			FSS		36	outside	P_m+P_b	1.00
6	Side Drop + MNOP	Corner/4	cavity liner	E	1/6	inside	P_m+P_b	0.41
			FSS		30	outside	P_m+P_b	0.86
7	Side Drop	Corner/3	cavity liner	E	3/4	outside	P_m+P_b	0.92
			FSS		36	outside	P_m+P_b	1.03
8	Side Drop + MNOP	Corner/3	cavity liner	E	1/6	inside	P_m+P_b	0.45
			FSS		30	outside	P_m+P_b	0.94
9	15° Impact, Drop	Flat/4	cavity liner	B	1/24	outside	P_m+P_b	1.74
			FSS		33	middle	P_m	5.06
10	15° Impact + MNOP	Flat/4	cavity liner	B	6/19	inside	P_m+P_b	0.72
			FSS		30	outside	P_m+P_b	6.06
11	15° Impact, Drop	Flat/3	cavity liner	B	24	outside	P_m+P_b	1.72
			FSS		33	middle	P_m	5.67
12	15° Impact + MNOP	Flat/3	cavity liner	B	19	inside	P_m+P_b	0.70
			FSS		36	middle	P_m	5.69
13	15° Impact, Drop	Corner/4	cavity liner	D	3/4	outside	P_m+P_b	1.94
			FSS		30	outside	P_m+P_b	3.43
14	15° Impact + MNOP	Corner/4	cavity liner	D	1/6	inside	P_m+P_b	0.66
			FSS		25	inside	P_m+P_b	1.95
15	15° Impact, Drop	Corner/3	cavity liner	D	3/4	outside	P_m+P_b	2.00
			FSS		36	outside	P_m+P_b	3.94
16	15° Impact + MNOP	Corner/3	cavity liner	D	1/6	inside	P_m+P_b	0.70
			FSS		30	outside	P_m+P_b	2.08

(a) Flat or corner orientation with 3 or 4 fuel element assemblies
(b) Locations shown schematically in Fig. 2.6-7

TABLE 2.6-43 DESIGN MARGIN SUMMARY OF NORMAL CONDITION RESULTS FOR UNIFORM LOAD CASES APPLIED TO THE FSS/CAVITY LINER COLD ENVIRONMENT

LOAD CASE			STRESS POINT LOCATION				SUMMARY	
No.	Description 1-ft	Config.[a]	Component	Axial[b] Section	Trans Pos.[b]	Position in Wall	Stress Type	Design Margin
1	Side Drop	Flat /4	cavity liner	E	9/16	outside	P_m+P_b	0.95
			FSS		33	middle	P_m	1.44
2	Side Drop + MNOP	Flat/4	cavity liner	E	9/16	outside	P_m+P_b	0.09
			FSS		25	middle	P_m	1.18
4	Side Drop + MNOP	Flat/3	cavity liner	E	16	outside	P_m+P_b	0.09
			FSS		25	middle	P_m	1.18
5	Side Drop	Corner /4	cavity liner	E	15/16	middle	P_m	0.49
			FSS		36	outside	P_m+P_b	1.12
6	Side Drop + MNOP	Corner/4	cavity liner	E	15/16	middle	P_m	0.35
			FSS		30	outside	P_m+P_b	0.96
7	Side Drop	Corner/3	cavity liner	E	14/17	middle	P_m	0.53
			FSS		36	outside	P_m+P_b	1.15
8	Side Drop + MNOP	Corner/3	cavity liner	E	15/16	middle	P_m	0.35
			FSS		30	outside	P_m+P_b	1.06

(a) Flat or corner orientation with 3 or 4 fuel element assemblies
(b) Locations shown schematically in Fig. 2.6-7

TABLE 2.6-44 DESIGN MARGIN SUMMARY OF NORMAL CONDITION RESULTS FOR CONCENTRATED LOAD CASES APPLIED TO THE FSS

LOAD CASE		STRESS LOCATION		TYPE	D.M.
Description	Config.				
Side Drop	Flat[a]	Center of FSS	Section E[b]	P_m+P_b	1.72
Side Drop	Flat	0.549 in. from cavity liner wall	Section E	P_m+P_b	0.59
Side Drop	Corner	0.549 in. from cavity liner wall Below neutal axis	Section E	P_m+P_b	2.22
Side Drop	Corner	Center of FSS Above neural axis	Section E	P_m+P_b	2.87
Side Drop	Corner	0.549 in. from cavity liner wall Above neural axis	Section E	P_m+P_b	0.67
15° Impact	Flat	Center of FSS	Section H	P_m+P_b	3.01
15° Impact	Flat	0.549 in. from cavity liner wall	Section H	P_m+P_b	1.69

(a) Flat or corner orientation
(b) Axial location on cask, shown in Fig. 2.6-7

TABLE 2.6-45 DESIGN MARGIN SUMMARY OF NORMAL CONDITIONS RESULTS FOR THE NEUTRON SHIELD STRUCTURE

Component	1-ft Drop Loading	Type	Design Margin
Outer Shell	End Drop	P_m	1.33
Outer Shell	Side Drop	P_m	0.85
ILSS, End Plate	End Drop	P_m+P_b	3.05

2.6.8 Penetration

This condition is defined in 10 CFR Part 71.71(c)(10) as a 40-in. drop of a 13-lb, 1.25-in.-diameter penetration cylinder with a hemispherical end onto any exposed surface of the cask. This event should not adversely affect the ability of the cask to maintain containment of the contents or to survive a hypothetical accident.

The components that would be most vulnerable to the penetration event are the outer skin (on neutron shield support structure) and the impact limiter.

In order to determine if the outer skin or the impact limiter skin would be perforated by the penetration cylinder, we used the Ballistic Research Laboratory (BRL) formula that was developed to determine the minimum thickness required to prevent perforation of a steel target by a missile (Ref. 2.6-4). This formula is applicable because it was developed to determine the penetrability of such steel elements as pipes and mechanical equipment vessels.

$$T = \frac{\left(\frac{mV_s^2}{2}\right)^{2/3}}{672\ d},$$

where

t = steel plate thickness to just perforate (in.),

m = mass of penetration cylinder = 13 lb/32.2 ft/sec^2 = 0.404 lb sec^2/ft,

V_s^2 = striking velocity of the cylinder, squared,

= 2 x 32.2 ft/sec^2 x (40 in./12 in./ft) = 214.67 ft^2/sec^2, and

d = diameter of cylinder = 1.25 in.

The equation above shows that a plate of 0.015 in. thickness will prevent perforation by the penetration cylinder. The neutron shield outer skin is 0.188 in. thick, and the impact limiter skin is 0.04 in. Therefore, in both components there may be a dent at the point of impact, but the cylinder will not perforate the skins. The margins of safety against perforation are 12.5 and 1.6 for the outer skin and the impact limiter skin, respectively.

2.7 Hypothetical Accident Conditions

The GA-4 shipping cask is a Type B package that maintains containment when subjected to the sequential hypothetical accident conditions of 10 CFR Part 71.73. Analyses and in some cases model tests verify the adequacy of the cask design under accident conditions involving a free drop, puncture, thermal environment, and water immersion. These accident conditions are subject to a number of initial conditions, as detailed in Table 2.1-2, which can be classified as either an initially hot or cold environment. Each of the hypothetical accident conditions is discussed in one of the following subsections.

The cask components considered in the analyses include the cask containment boundary, closure bolts, FSS/cavity liner, neutron shield, ILSS and ILSS bolts. All of the components were shown to have acceptable design margins or stresses for the hypothetical accident conditions. The lowest design margin and its location for each of the components is summarized in Table 2.7-1. As shown by the table, the component with the lowest design margin is the ILSS outer shell.

2.7.1 30-ft Free Drop

The GA-4 cask is required by 10 CFR Part 71.73 to demonstrate structural adequacy for a free drop through a distance of 30 ft (9 m) onto a flat, unyielding horizontal surface. The cask should strike the surface in a position which is expected to inflict the maximum damage. To satisfy these requirements, the approach outlined in Fig. 2.7-1 was used. The first step in the evaluation was to develop load-deflection curves for the impact limiter at different orientations. ILMOD (Section 2.10.1.4), was used to find the load-deflection curves for the impact limiter as a function of the drop angle. As described in Section 2.10.3, the impact limiter analysis was verified by 1/4-scale testing. The impact limiter load-deflection curves were used as input to the GACAP computer code (Section 2.10.1.1). The GACAP computer code was used to obtain accelerations and impact limiter crush forces and distances for the drop orientations that bound all possible drops. The GACAP analyses are described in Sections 2.7.1.1 and 2.10.4. GACAP results were used for the ANSYS analyses of the ILSS, the cask containment boundary and the FSS/cavity liner.

The four basic ANSYS models developed for the stress analysis are described in Section 2.7.1.2. The four ANSYS models include models of the ILSS, the cask containment boundary, the FSS/cavity liner and the FSS. Because the cask is not rotationally symmetric, each of the ANSYS models, except for the FSS plate model, had two variations, either a flat or a corner configuration. The ILSS model also had two additional variations, 15° and 30° from the flat orientation. The ANSYS model of the ILSS used the GACAP-derived impact forces to find the load distributions for the ILSS ribs. These results were combined with the GACAP accelerations to provide the input loading for the cask containment boundary model. The cask containment boundary model had two objectives, (1) to calculate the base case stresses for the cask wall and (2) to use the cask wall deformations as ovality input for the FSS/cavity liner detailed ANSYS model. The base case stresses for the cask wall were combined to evaluate the load cases identified in Table 2.1-2. The detailed load case evaluations for the cask components are given in Section 2.7.1.3 for each of the major components. All of the cask components are shown to have positive design margins. In addition, the load case with the

TABLE 2.7-1 LOWEST DESIGN MARGINS FOR THE GA-4 CASK DURING HYPOTHETICAL ACCIDENT CONDITIONS		
COMPONENT	CONDITION	LOWEST DESIGN MARGIN
Cask wall	MNOP with 30-ft side drop and cold environment	0.27
Closure bolts	MNOP with 30-ft CG over corner drop	0.40
ILSS outer shell	30-ft side drop - corner orientation	0.01
ILSS ribs	30-ft 75° drop - flat orientation	1.06
FSS/cavity liner	MNOP with 30-ft side drop and cold environment	0.16
Neutron shield	30-ft side drop	0.39
Impact limiter bolts	30-ft oblique drop	0.32

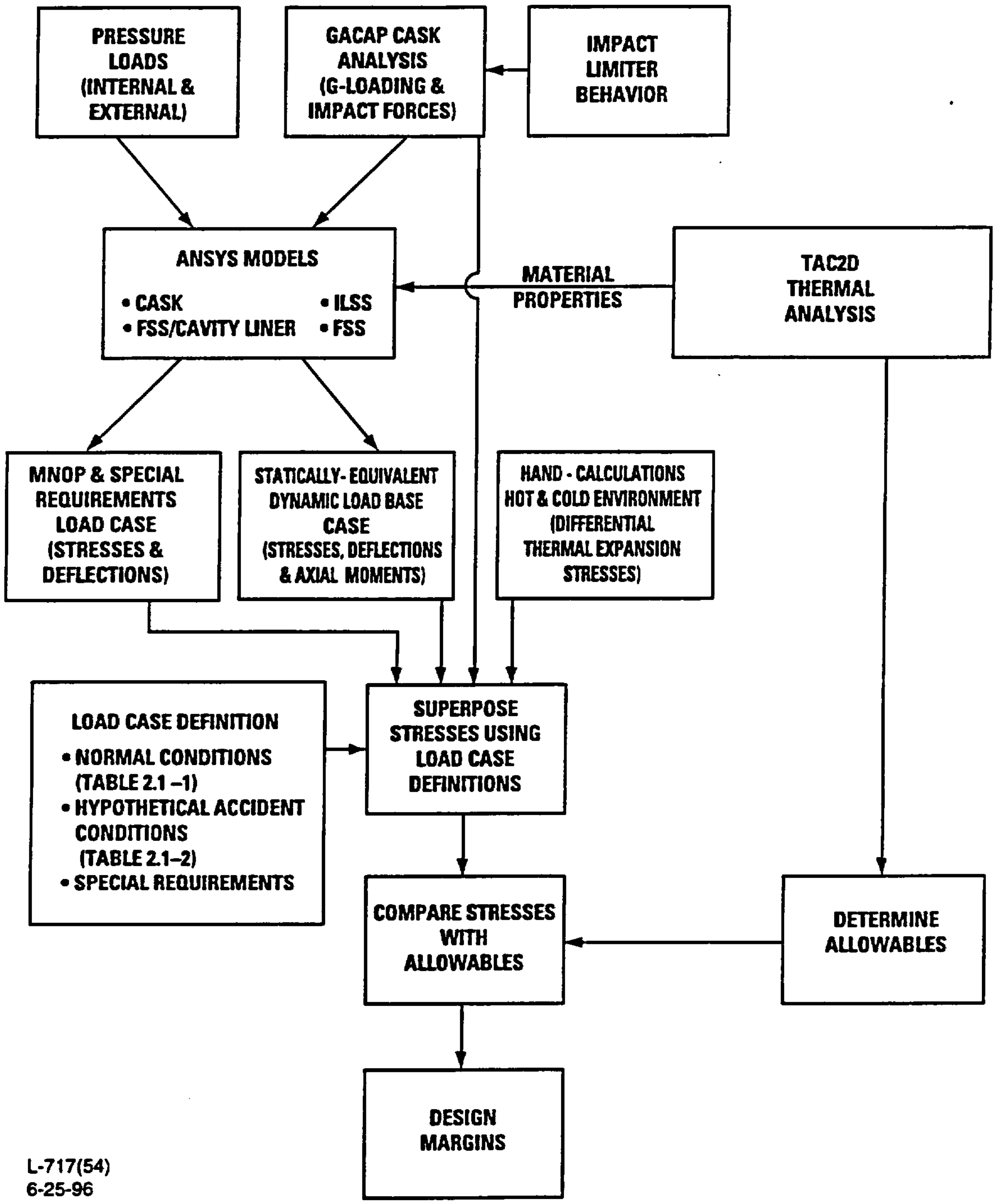

Fig. 2.7-1. Analysis procedure flow chart for drop events

highest compressive stress was shown acceptable against buckling in Section 2.7.1.4. The comparison of test results with analytical results in Section 2.7.1.5 further confirms both the analytical technique and the design adequacy of the GA-4 cask.

2.7.1.1 GACAP Analyses. The GACAP program was used to analyze the impact load conditions. The code uses a 2-D, lumped mass, single-axis beam model of the cask body to analyze impacts from different drop heights and angles. The results provided by the code include time-history information on accelerations, velocities, and displacements. GACAP provides the impact limiter depth of crush, maximum impact force, maximum effective linear and angular accelerations of the CG, energy dissipation information, and a summary of the maximum values and times at which they occur.

The GA-4 cask was modeled as a linear elastic solid without structural damping. The impact limiters were simulated with nonlinear force-deflection tables. Section 2.10.4 provides the details of the GACAP analyses. GACAP was used to evaluate the GA-4 cask for 30-ft free drops at 0° (side drop), 15°, 30°, 45°, 60°, 75°, 78° (CG-over-corner), and 90° (end drop). The side drop hits both impact limiters simultaneously and the end drop hits flat on either end of the cask. All of the impact energy is absorbed during the primary impact for these cases and for the CG-over-corner case. The other drops are called oblique drops and involve a primary and secondary impact, i.e. the cask hits first one end (primary) and then the other end slaps down (secondary). The GACAP analyses assumed the following:

1. The DU is nonstructural, (i.e., adds mass but not strength), except that it transfers compressive loads.
2. The cask acts as a rigid body.
3. The cask/cavity liner behaves as a structural unit.
4. The ILSS and neutron shield structure strengths and stiffnesses are ignored.
5. The cask is symmetric with respect to impacts on the top or bottom ends.
6. Only one impact occurs on the primary impact side. The energy remaining after the primary impact is absorbed during the secondary impact.
7. No energy is dissipated through friction.

The GACAP analyses evaluated a range of impact limiter material properties and considered maximum and minimum content's weights, to find the worst case conditions for each of the components. These conditions are given in Tables 2.7-2 and 2.7-3. The results of the GACAP analyses were either used as input to the ANSYS analyses of the cask wall and FSS/cavity liner or used directly in the structural evaluation of the ILSS. The impact limiter crushed depth was evaluated in Section 2.10.4. The low crush strength impact limiter produced the greatest depth of honeycomb core crush. The margins against the impact limiter bottoming out and the trunnion being impacted are presented in Table 2.7-4. As given in the table, the minimum margin is 2.7 in. against bottoming out.

TABLE 2.7-2
GACAP ACCELERATIONS AND IMPACT FORCES FOR ANALYSIS OF THE CASK CONTAINMENT BOUNDARY, CLOSURE BOLTS, FSS, CAVITY LINER AND ILSS

	CG ACCELERATIONS (g)		
IMPACT ANGLE (deg.)	TRANSVERSE	AXIAL	IMPACT FORCE (lb)
0	47.7	0.0	$2.62x10^6$
15	21.5	5.8	$1.23x10^6$
30	21.4	12.3	$1.36x10^6$
45	23.1	23.1	$1.79x10^6$
60	21.8	37.8	$2.40x10^6$
75	14.9	55.4	$3.16x10^6$
78	11.9[a]	56.5[a]	$3.20x10^6$[a]
90	0.0	61.0	$3.36x10^6$
Secondary Impact (0°)	26.3	0.0	$1.45x10^6$

[a]Interpolated between the 75° and 90° drops.

TABLE 2.7-3
GACAP ACCELERATIONS AND IMPACT FORCES FOR ANALYSIS OF THE NEUTRON SHIELD STRUCTURE

	CG ACCELERATIONS (g)		
IMPACT ANGLE (deg.)	TRANSVERSE	AXIAL	IMPACT FORCE (lb)
0	53.0	0.0	$2.56x10^6$
15	23.6	6.3	$1.18x10^6$
30	23.2	13.4	$1.30x10^6$
45	24.4	24.4	$1.67x10^6$
60	23.0	39.8	$2.22x10^6$
75	16.4	61.3	$3.07x10^6$
78	13.1[a]	62.9[a]	$3.13x10^6$[a]
90	0.0	69.4	$3.36x10^6$
Secondary Impact (0°)	28.2	0.0	$1.36x10^6$

[a]Interpolated between the 75° and 90° drops.

TABLE 2.7-4
LOWEST MARGINS AGAINST IMPACT LIMITER BOTTOMING OUT OR HITTING TRUNNION DURING IMPACT LIMITER CRUSHING FOR GA-4 30-FT DROP CONDITIONS

Drop Angle (Degrees)	Margin[a] (in.) Against Bottoming Out			
	Primary Impact		Secondary Impact[b]	
	Impact Limiter Bottoming Out	Hitting Trunnion	Impact Limiter Bottoming Out	Hitting Trunnion
0	5.8	10.1	—	—
15	7.7	N/A	2.8	7.1
30	5.7	N/A	3.1	7.4
45	4.9	N/A	4.3	8.8
60	2.7	N/A	7.2	11.5
75	3.4	N/A	—	—
78	4.6	N/A	—	—
90	5.5	N/A	—	—

[a]Where the margin implies remaining crush height (in inches) before bottoming out and the lowest margins are for the case with the low impact limiter strength.
[b]Secondary impact cask angle with respect to the impact surface is small.

2.7.1.2 ANSYS Analyses.

2.7.1.2.1 Cask. Two ANSYS finite element models were used to evaluate the stresses in the cask wall for normal and hypothetical accident conditions. These models are referred to as either the corner or flat model. The label identifies the location of the cask cross section relative to the impacted surface for the horizontal drops. For the corner model, the longitudinal edge, or corner, of the cask impacts the surface. For the flat model, the flat side of the cask is parallel to the impact surface. The corner model uses a plane of symmetry which passes through the cask wall corners and the flat model is symmetric about the center of the flat wall of the cask, as shown in Fig. 2.7.1-2. These two cross sections envelop the results for any other clocking positions of the cask relative to its impacting surface. The stresses resulting from the loads acting on the cask are either independent of the cross section geometry or maximum for the flat or corner model. The loads acting on the cask and how they are affected by the cross section geometry are described below:

1. Internal and external pressure load stresses are not affected by the clocking position of the cask about its axis.
2. Stresses resulting from bending induced during the side drop or slapdown events are maximum for the corner drop. The maximum moment acting on the cask and its location are the same for the flat and corner models. Since the moment of inertia of the cross section is constant irrespective of the clocking position of the cask neutral-axis, the maximum bending stresses are caused by the clocking position which has the largest extreme fiber distance. For the cask this is the corner drop model.
3. Differential thermal expansion stresses are independent of the cask clocking position.
4. The local loads imparted to the cask from the ILSS are shown in Section 2.10.3.6 to be bracketed by results for the flat and corner model. The local effects of these loads are not design limiting for the cask containment boundary.

Fig. 2.7.1-2 also shows the locations used to report stress results. The ANSYS models were used to evaluate statically applied loads only. Internal and external pressure cases were considered, as well as statically equivalent, dynamic load cases. The dynamic load cases simulated a 30-ft end drop and side drops with either both or a single impact limiter (oblique drop case) reacting the drop load.

To adequately and efficiently evaluate the hypothetical accident conditions, a summary of worst case loads for a range of impact angles and drop heights was developed for the dynamic load cases, using the GACAP computer program. The results are summarized in Table 2.7-2 for the cask and its internals and in Table 2.7-3 for the neutron shield structure. As shown in the tables, the results are given in terms of the acceleration in the lateral and axial cask directions for different angle drops. To find the stresses in the cask wall resulting from these different dynamic load cases, the stresses for the base case end drop and the base case oblique drop were scaled by the appropriate axial and transverse g levels given in Table 2.7-3.

After superposing the lateral and axial dynamic stress distributions, the results were combined with the appropriate pressure and temperature case results to obtain the complete stress distribution for the load case. The resulting stresses are combined to find the stress intensity, SI, and to determine the design margin for different sections along the cask wall.

In Section 2.10.2 the two ANSYS models are described, the loading conditions are defined and the analysis procedure is explained. Section 2.10.6 presents the results of the analyses for the normal and hypothetical accident conditions and the 290 psi external water pressure loading.

Model Descriptions. The GA-4 shipping cask has a non-axisymmetric cross section, which must be simulated using three-dimensional models. Since there is cross-sectional symmetry about the lines shown in Fig. 2.7-2; it was not necessary to model the entire cask. Using the two lines of cross-sectional symmetry, two ANSYS models were developed, a flat model and a corner model. The flat model used symmetry about the cross sectional line which passes through the center of the flat section of the cask wall. The corner model used cross-sectional symmetry about the line which passes through the corners of the cask. The resulting models represent half sections of the total geometry and include the closure, FSS, cavity liner and the cask body with the bottom head. The ILSS, the DU, and neutron shield shell are not explicitly included in the models. The ILSS adds stiffness in the closure/flange and bottom head regions, therefore making the model stress results conservative (i.e., higher stresses) in those regions. The effects of the DU and the neutron shield are simulated as mass added to the cask wall, to give the proper weight distribution. Ignoring the stiffness of the DU and neutron shield shell makes the model's stress results conservative for the cask wall.

Although the models have different impact orientations, the finite element discretization was essentially the same. The ANSYS input for the geometric model, material properties, boundary conditions, and loadings was generated using a FORTRAN program. Section 2.10.2 provides the details about the element types, model geometries, material and section properties and boundary conditions. The loadings for the base case analyses included the internal and external pressure loads, the 10 g end and oblique drops, and a 30-ft side drop. ANSYS analyses were conducted for each of the models, for each of the cases described above. The individual runs considered are classified as either normal condition, hypothetical accident condition, or special requirement condition (290 psi external pressure). These runs are described in subsections 2.10.2.3.1 through 2.10.2.3.3.

After each of the ANSYS analyses was performed, a stress summary table was developed for the important cross sections of the cask wall. These cross sections are shown in Fig. 2.7-2. The cross sections' axial positions were the same for the flat and corner models. The specific points used for the stress summaries are detailed in Tables 2.10.2-6 through 2.10.2-10 for the flat model and in Tables 2.10.2-11 through 2.10.2-15 for the corner model. The directionally dependent stress components were tabulated for the base cases.

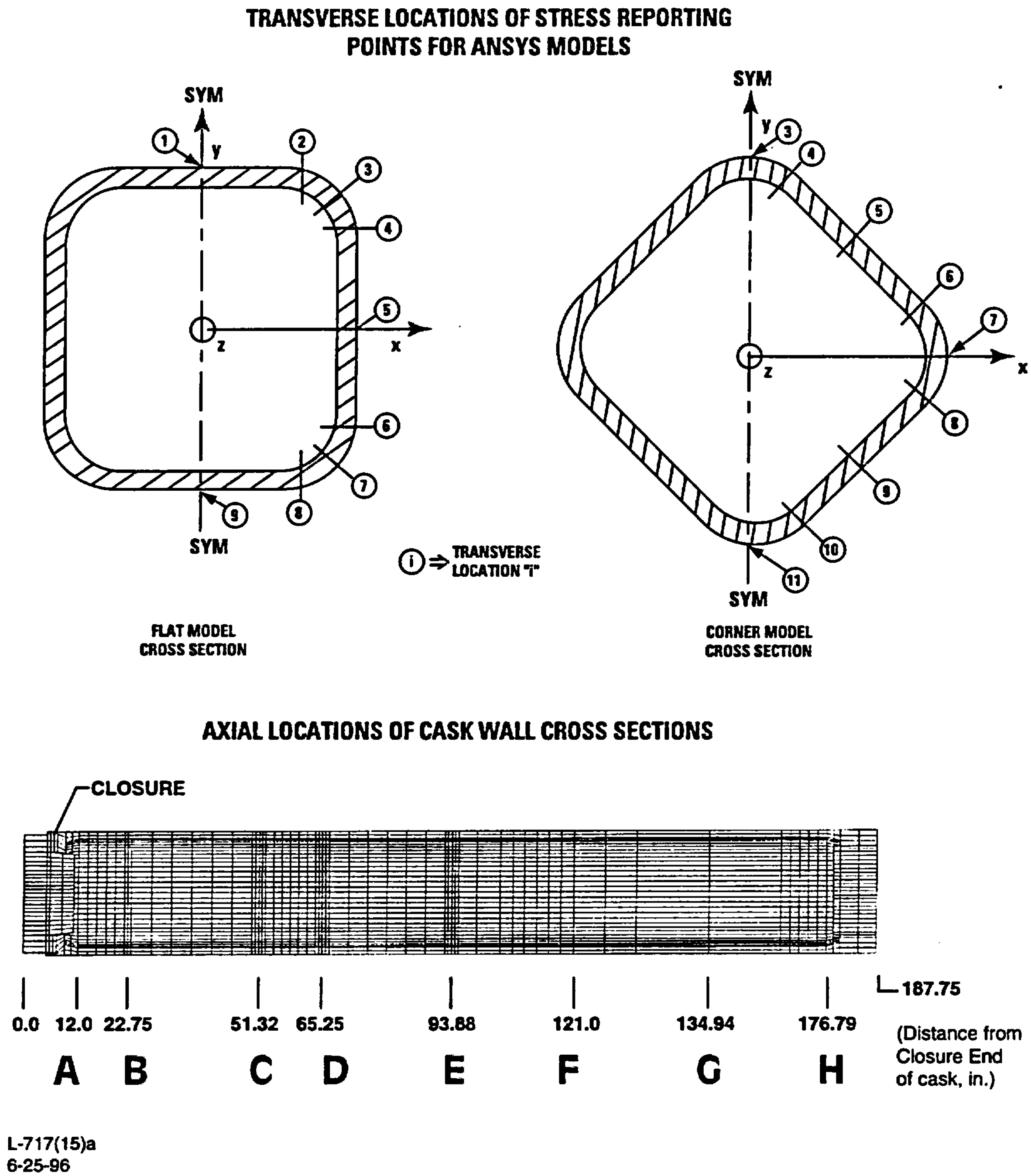

Fig. 2.7-2. Schematic of GA-4 cask wall showing symmetry planes and stress point reporting locations for ANSYS model

2.7.1.2.2 FSS/Cavity Liner. There are two different types of ANSYS models used for the analysis of the FSS/cavity liner. The first was a frame model of an axial section of the complete FSS/cavity liner cross section and the second was a plate model of one of the legs of the FSS. The frame model assumed a uniform loading of the fuel assembly on the FSS structure during either a side drop or slapdown event. The plate model simulated a section of the FSS and considered the effects of fuel assembly support grid and/or end-plate loading.

The frame model used two coordinate axes orientations. The model geometries are shown in Figs. 2.7-3 and 2.7-4 for the flat and corner model, respectively. These two model geometries envelop the results for any other clocking positions of the cask relative to its impacting surface. The stresses resulting from the loads acting on the cask are either independent of the cross section geometry or maximum for the flat or corner model. The loads acting on the cask and how they are affected by the cross section geometry are described below.

1. Internal and external pressure load stresses are not affected by the clocking position of the cask about its axis.
2. Stresses resulting from bending induced during the side drop or slapdown events are maximum for the corner drop. The maximum moment acting on the cask and its location are the same for the flat and corner models. Since the moment of inertia of the cross section is constant irrespective of the clocking position of the cask's neutral-axis, the maximum bending stresses are caused by the clocking position which has the largest extreme fiber distance. For the cask this is the corner drop model.
3. Differential thermal expansion stresses are independent of the cask clocking position.
4. The stresses from the fuel element and postulated DU inertial loadings on the FSS/cavity liner are maximum for the flat model. The applied loading is resolved into its components as the angle varies from the flat model to the corner model.
5. The deflection profiles used to simulate the effect of cask wall ovalization on the FSS/cavity liner were assumed the same as those derived for the flat and corner models of the cask. For other clocking positions, the deflection profile would be obtained from the appropriate combination of results from the flat and corner models. As given in Section 2.10.9, the deflections for the other clocking positions would be smaller and, therefore, the stresses would be lower than those for the flat or corner model.

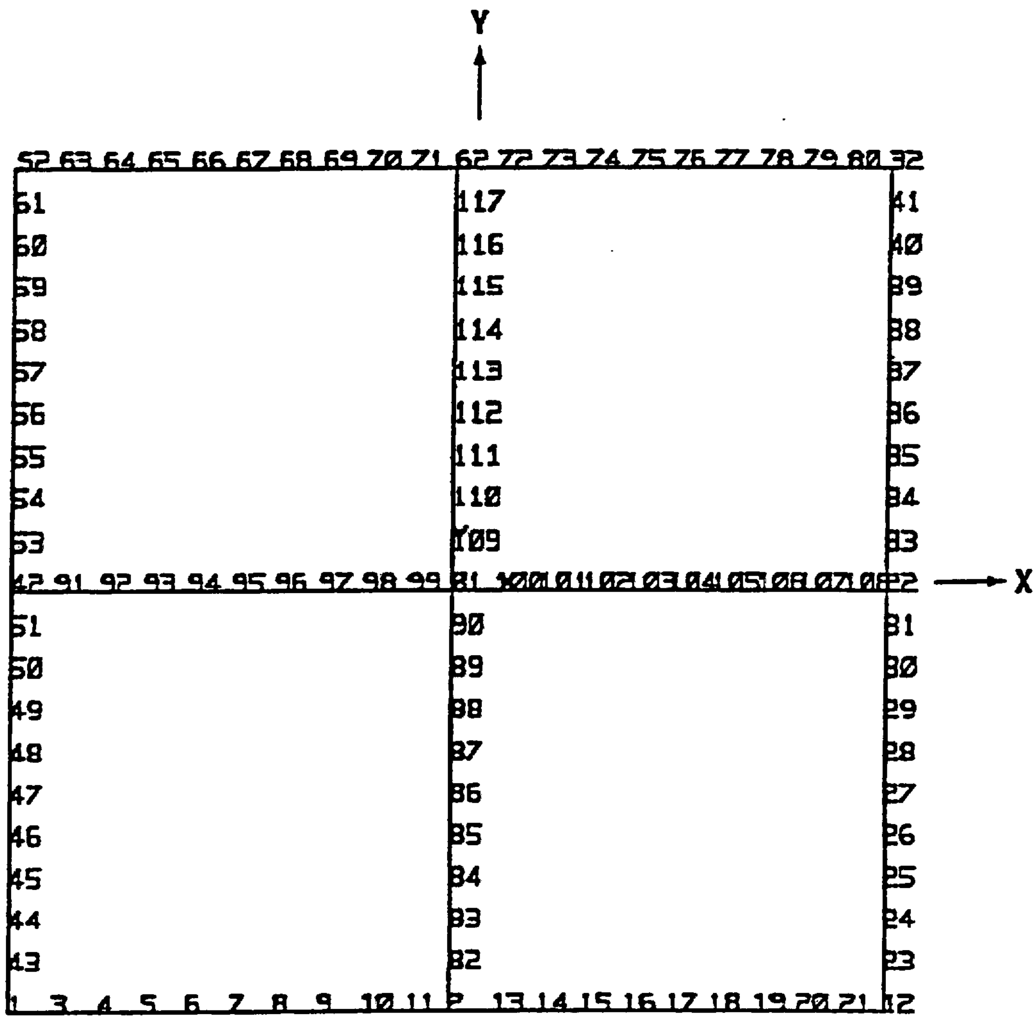

L-764(6)
8-19-96

Fig. 2.7-3. Flat model node locations for ANSYS FSS/cavity liner frame analysis

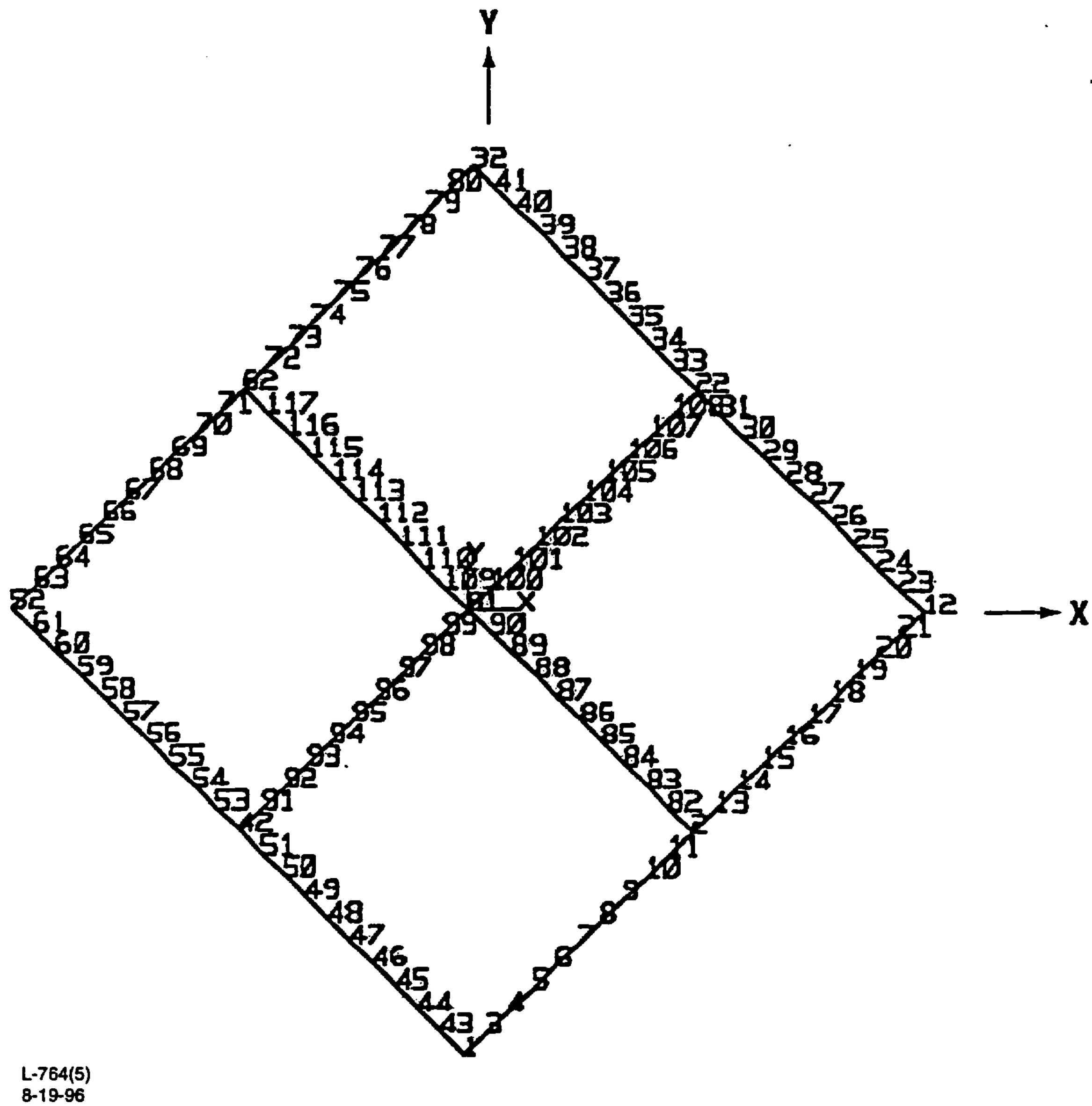

Fig. 2.7-4. Corner model node locations for ANSYS FSS/cavity liner frame analysis

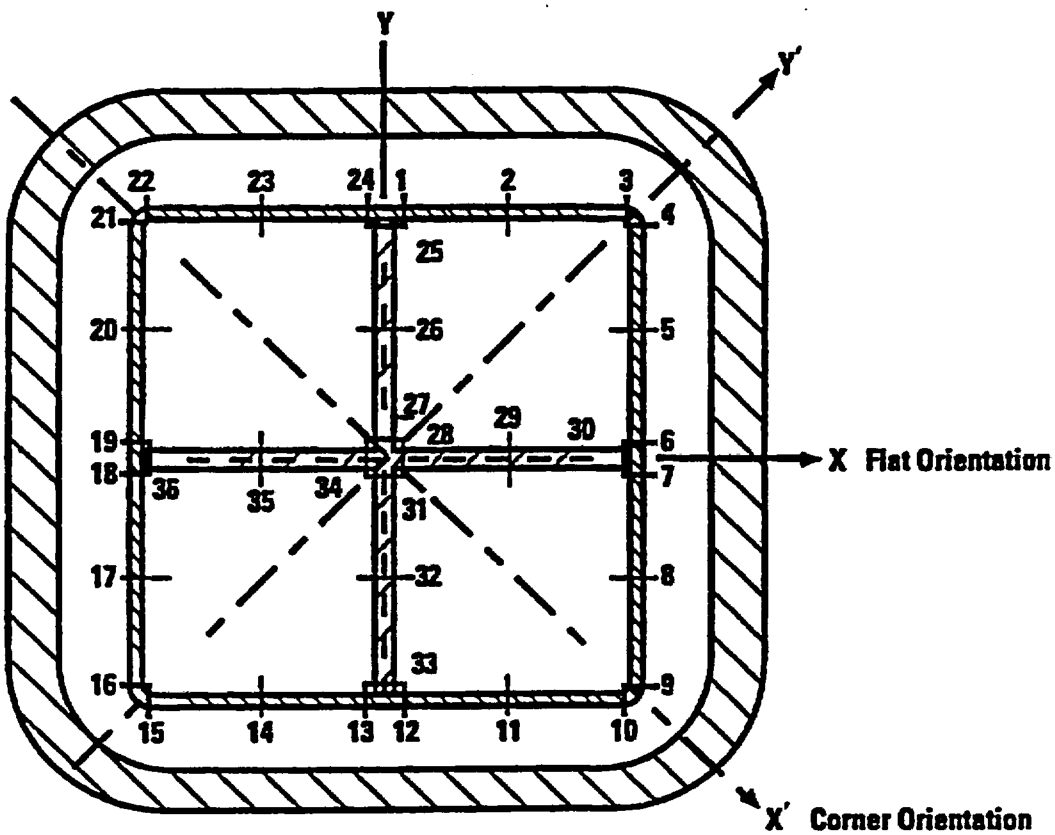

L-764(7)
8-19-96

Fig. 2.7-5. Location of stress reporting points for the ANSYS models of the FSS/cavity liner

The stress reporting points shown in Fig. 2.7-5 are the same for both of the models. The basic model is a frame structure composed of two-dimensional BEAM3 elements which simulated a one inch length axial section of the FSS/cavity liner. The model used 120 beam elements and 117 nodes. The FSS portion of the model used actual section properties and material modulus values in the B_4C pellet hole region. The boundary conditions applied to the model included fixed displacements for the edge of the model which hit the impacted surface and pressure loads which simulated the effects of the various load cases. Fixed displacements were used to characterize the ovalization information obtained from the cask containment boundary ANSYS analysis. The inertial loads of the DU, fuel and non-fuel assembly hardware (NFAH) were simulated using equivalent pressure loads on the FSS and the upper portion of the cavity liner. Both full and partial fuel assembly loadings (three or four fuel elements) were considered. The MNOP load case applied a uniform 80 psig pressure to the internal walls of the cavity liner. The ANSYS models and the loadings used are described in detail in Section 2.10.9 for a uniformly loaded FSS.

The ANSYS frame analyses were used to find the stresses for the different load cases. In Section 2.10.9, the inertial loading results were combined with the MNOP and thermal stress results and the out-of-plane bending stresses derived from the moment developed from the cask containment boundary analyses in order to evaluate the design of the FSS and cavity liner.

The plate model of the FSS was used to detail the inertial effects of a nonuniform fuel and NFAH loading on the FSS. A three-dimensional plate model was used with the loads applied at either the middle or the end of the model. The loadings represented either a midcavity or cavity end loading condition on the FSS. The model used the SHELL63 element from ANSYS. The model is a section of the FSS 31.5 in. long and 8.77 in. wide. Orthotropic properties are used to simulate the effects of the differently sized B_4C pellet holes. Both sides of the model (one side represents the center of the FSS and the other its attachment to the cavity liner) are clamped. The two loading conditions simulated by the model geometry are sketched in Fig. 2.7-6. In the simulation of the bottom edge of the FSS, 2.25 in. of the edge simulating the cavity liner attachment to the FSS was also free, as shown in Fig. 2.7-7. The details of the model and loadings are described in further detail in Section 2.10.10. The local effects evaluated by this model were superposed upon the results of the frame model to incorporate the ovality effects of the containment wall.

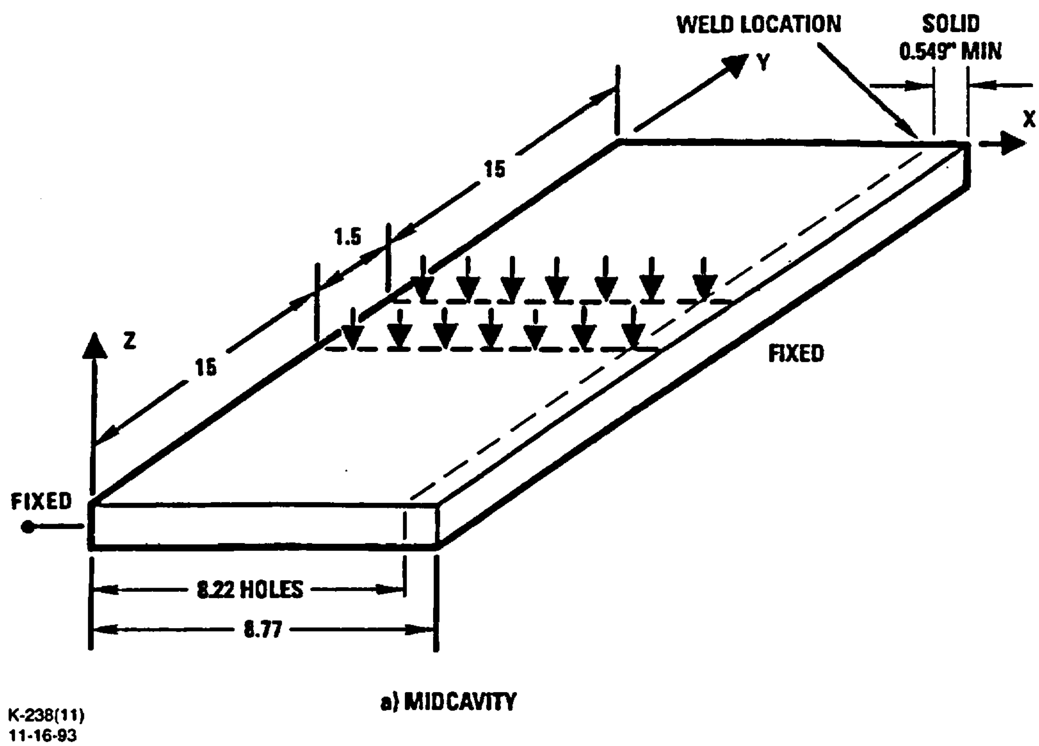

a) MIDCAVITY

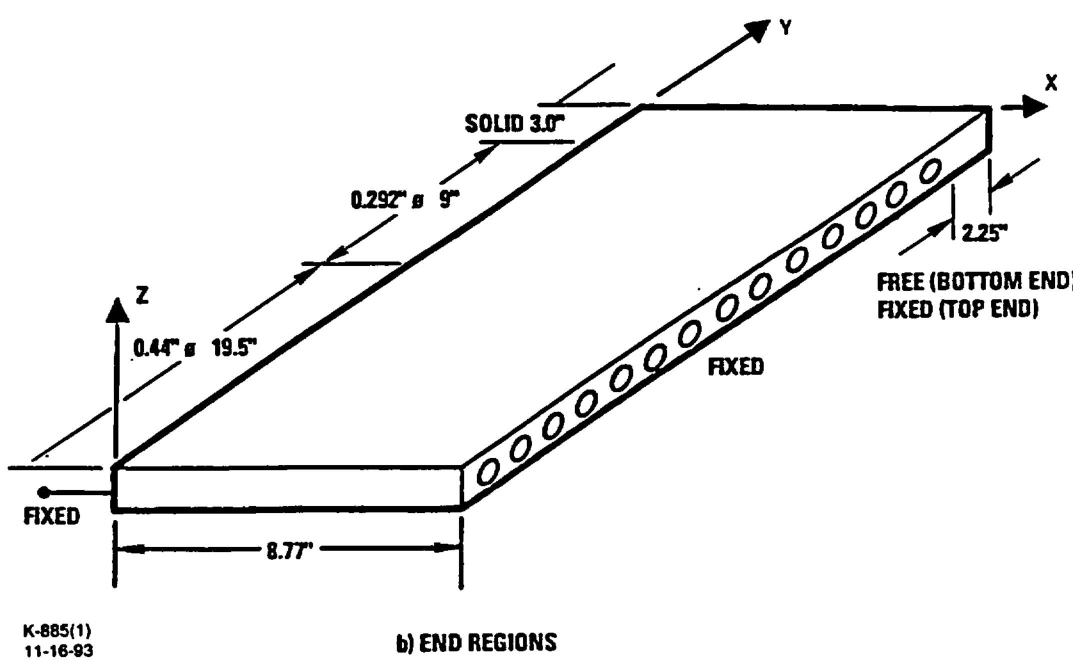

b) END REGIONS

Fig. 2.7-6. ANSYS FSS plate model's loading conditions for the concentrated load cases

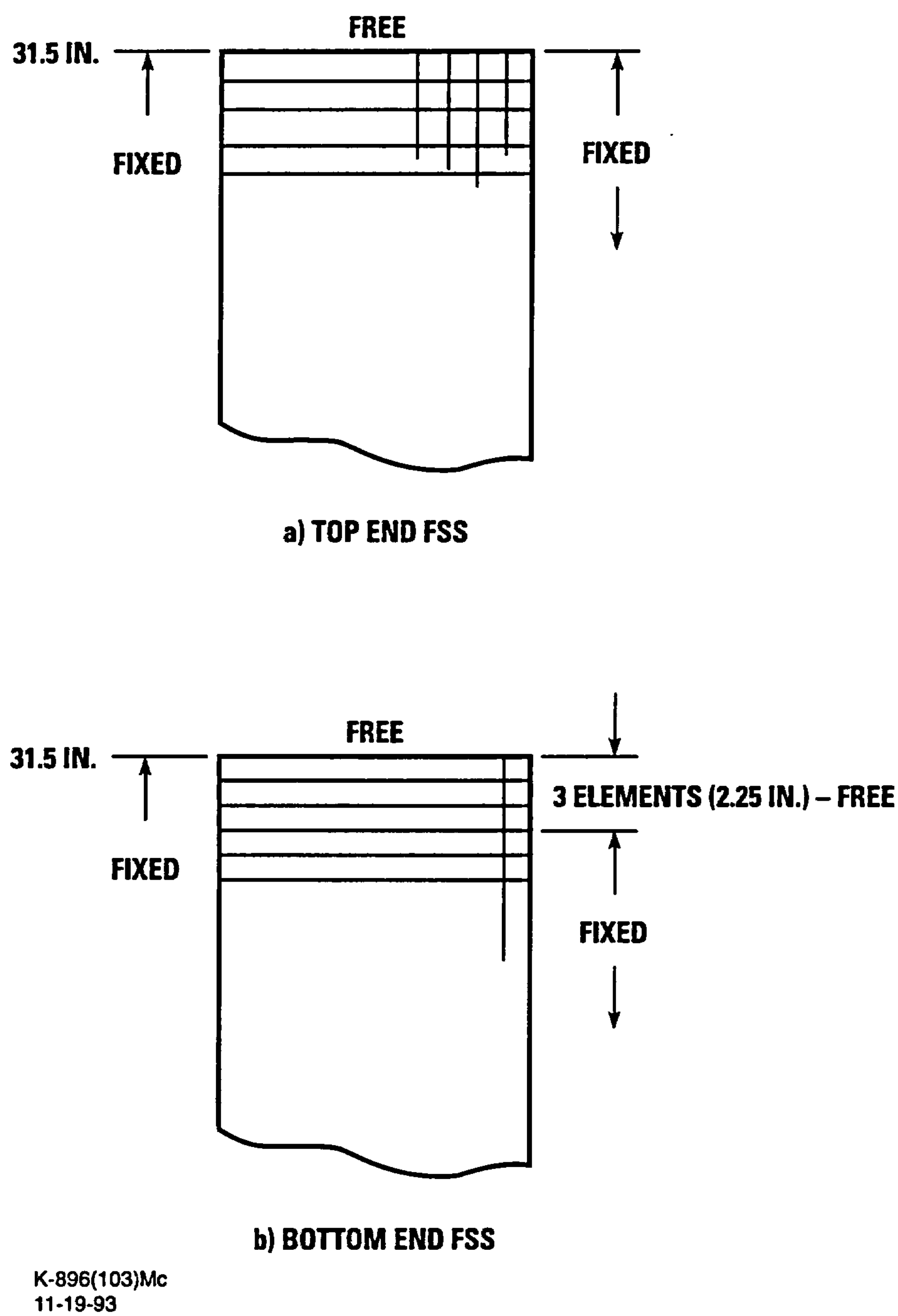

Fig. 2.7-7. Boundary conditions for the ANSYS model of the cavity end FSS

2.7.1.2.3 ILSS. A two-dimensional model was developed using BEAM3 elements to represent a 1-in. axial section of the ILSS. Only the rib and outer shell structures of the ILSS were modeled. No details of the cask or the impact limiter were included in this model. The cask body at the attachment of the ILSS was assumed to be rigid, therefore, the ends of each rib were assumed to be clamped, i.e., no rotation or displacement. The ribs were simulated using reduced section properties to account for the lightening holes drilled into the ribs. Both the cross-sectional area and moment of inertia were given effective values to account for the reduction in properties. The model used 196 nodes and 232 elements. The model and its element numbers are shown in Fig. 2.10.3-30, along with the rib labels used in post-processing the results of the ANSYS analysis. Figure 2.10.3-32 shows the four loadings used to evaluate the ILSS performance. The model node numbers are shown in Fig. 2.10.3-31. The loadings simulated various clocking positions of the cask cross section relative to the impact surface. A uniform pressure on the ILSS projected area was simulated by applying a sinusoidally distributed pressure load to one-half of the outer ring elements. The different clocking positions were achieved by rotating the pressure distribution about the cask axis. As shown in the figure, elements 1 through 40 were used for the flat model (clocking angle of 0°); elements 5 through 44 were used for the loading at 15°; elements 8 through 47 were used for the 30° load case, and the corner model (clocking angle of 45°) used elements 11 through 50. The modeling details are discussed in Section 2.10.3.6.1c.

These analyses were used to find the loads needed to evaluate the maximum rib stress intensity, the maximum stress at the plug-welded connection of the outer plate structure and the ribs, the maximum stress in the fillet welds connecting the rib to the cask wall, and the maximum plate stress for the side and oblique drops. The resultant loads at the fixed nodes were used to provide the ILSS load distribution which was input to the ANSYS cask model during side and oblique drop simulations.

2.7.1.3 Load Case Evaluations.

2.7.1.3.1 Cask Containment Boundary. As mentioned in Section 2.7.1.2.1, after each of the ANSYS analyses was performed, a stress summary table with the directionally-dependent stress components was developed for each of the base cases. These results are presented in Tables 2.10.6-13 through 2.10.6-37 for the flat model and in Tables 2.10.6-38 through 2.10.6-62 for the corner model. To evaluate the cask containment boundary for the different hypothetical accident conditions, the results for the applicable base cases were superposed at the stress component level and the principal stresses, stress intensities and design margins were calculated. For the initial evaluation, thermal stresses were not considered. After the results for the thirty-six load cases described in Sections 2.10.2.3.3 and 2.10.2.3.4 were considered, six of the load cases were chosen to include the cold environment differential thermal expansion stress. The hot environment differential thermal expansion stresses were not considered, because they were low (≈ 300 psi) in comparison with the stresses induced by the different drop loads.

The results for the load cases without thermal effects are summarized in Tables 2.7-5 and 2.7-6 for the flat and corner models, respectively. The case with the lowest design margin is the MNOP with 30-ft side drop for the corner model with a design margin of 0.40. The results for the selected load cases which include the cold environment stresses are summarized in Table 2.7-7. The load cases presented in Table 2.7-7 were selected because they represent the end and side drops, and the worst case slapdown. The lowest design margin for these cases is 0.27 for MNOP with a 30-ft side drop for the corner model. As shown by comparison of the tables, the design margins for the end drop increase, while they decrease for the side drop and slapdown. These results are reasonable, because the cold environment induces a tensile differential thermal expansion stress in the axial direction for the cask wall. When this stress is combined with the dynamic load case stresses, it decreases the axial compressive stress for the end drop and increases the tensile axial stresses for the side drop and slapdown conditions. These act, in turn, to reduce the stress intensity for the end drop and increase it for the side drop and slapdown. The lowest design margin for the cask during the hypothetical accident conditions is 0.27 for the cold environment conditions.

TABLE 2.7-5
SUMMARY OF HYPOTHETICAL ACCIDENT CONDITION LOAD CASE RESULTS
FOR FLAT MODEL WITHOUT DIFFERENTIAL THERMAL EXPANSION EFFECTS

Load Case		Stress Point Location				
No.	Description	Axial[a] Section	Transverse Position[a]	Position in Wall	Stress Type	Design Margin
17	MNOP with 30-ft end drop	A	1 9	inside inside	P_m+P_b P_m+P_b	6.62 6.62
18	MNOP with 30-ft side drop	E	9	inside	P_m+P_b	0.52
19	MNOP with 30-ft drop at 15°	C	9	outside	P_m+P_b	1.19
20	MNOP with 30-ft drop at 30°	C	9	outside	P_m+P_b	1.20
21	MNOP with 30-ft drop at 45°	C	9	outside	P_m+P_b	1.06
22	MNOP with 30-ft drop at 60°	C	9	outside	P_m+P_b	1.16
23	MNOP with 30-ft drop at 75°	C	9	outside	P_m+P_b	2.01
24	MNOP with 30-ft drop at 78°	C	9	outside	P_m+P_b	2.59
25	MNOP with 30-ft slapdown (15°)	C	9	outside	P_m+P_b	0.83
26	30-ft end drop	A	9	inside	P_m+P_b	6.92
27	30-ft side drop	E	9	outside	P_m+P_b	0.58
28	30-ft drop at 15°	C	9	outside	P_m+P_b	1.46
29	30-ft drop at 30°	C	9	outside	P_m+P_b	1.48
30	30-ft drop at 45°	C	9	outside	P_m+P_b	1.29
31	30-ft drop at 60°	C	9	outside	P_m+P_b	1.43
32	30-ft drop at 75°	C	9	outside	P_m+P_b	2.55
33	30-ft drop at 78°	C	9	outside	P_m+P_b	3.38
34	30-ft slapdown (15°)	C	9	outside	P_m+P_b	1.01

[a]Locations shown schematically in Figure 2.7-2.

TABLE 2.7-6
SUMMARY OF HYPOTHETICAL ACCIDENT CONDITION LOAD CASE RESULTS
FOR CORNER MODEL WITHOUT DIFFERENTIAL THERMAL EXPANSION EFFECTS

Load Case		Stress Point Location			Stress Type	Design Margin
No.	Description	Axial[a] Section	Transverse Position[a]	Position in Wall		
17	MNOP with 30-ft end drop	A	5 9	inside inside	$P_m + P_b$ $P_m + P_b$	5.85 5.85
18	MNOP with 30-ft side drop	E	11	middle	P_m	0.40
19	MNOP with 30-ft drop at 15°	D	11	middle	P_m	1.72
20	MNOP with 30-ft drop at 30°	D	11	middle	P_m	1.78
21	MNOP with 30-ft drop at 45°	D	11	inside	$P_m + P_b$	1.65
22	MNOP with 30-ft drop at 60°	D	11	middle	P_m	1.95
23	MNOP with 30-ft drop at 75°	D	3	middle	P_m	2.95
24	MNOP with 30-ft drop at 78°	D	3	middle	P_m	3.57
25	MNOP with 30-ft slapdown (15°)	D	11	middle	P_m	1.19
26	30-ft end drop	A	5 9	inside inside	$P_m + P_b$ $P_m + P_b$	7.04 7.04
27	30-ft side drop	E	11	middle	P_m	0.41
28	30-ft drop at 15°	D	11	middle	P_m	1.74
29	30-ft drop at 30°	D	11	middle	P_m	1.81
30	30-ft drop at 45°	D	11	middle	P_m	1.68
31	30-ft drop at 60°	D	11	middle	P_m	1.98
32	30-ft drop at 75°	D	3	middle	P_m	3.00
33	30-ft drop at 78°	D	3	middle	P_m	3.64
34	30 ft slapdown (15°)	D	11	middle	P_m	1.21

[a]Locations shown schematically in Figure 2.7-2.

TABLE 2.7-7
SUMMARY OF SELECTED LOAD CASE RESULTS FOR
HYPOTHETICAL ACCIDENT CONDITIONS WITH
COLD ENVIRONMENT DIFFERENTIAL THERMAL EXPANSION EFFECTS

LOAD CASE		STRESS POINT LOCATION				
No.	Description	Axial[a] Section	Transverse Position[a]	Position in Wall	Stress Type	Design Margin
FLAT MODEL RESULTS						
17	MNOP with 30-ft End Drop	A	1 9	inside inside	$P_m + P_b$ $P_m + P_b$	4.06 4.06
18	MNOP with 30-ft Side Drop	E	9	inside	$P_m + P_b$	0.41
25	MNOP with 30-ft Slapdown (15°)	C	9	inside	$P_m + P_b$	0.76
26	30-ft End Drop	A	1 9	inside inside	$P_m + P_b$ $P_m + P_b$	4.67 4.67
27	30-ft Side Drop	E	9	inside	$P_m + P_b$	0.46
34	30-ft Slapdown (15°)	C	9	inside	$P_m + P_b$	0.85
CORNER MODEL RESULTS						
17	MNOP with 30-ft End Drop	A	5 9	inside inside	$P_m + P_b$ $P_m + P_b$	4.09 4.09
18	MNOP with 30-ft Side Drop	E	11	middle	P_m	0.27
25	MNOP with 30-ft Slapdown (15°)	D	11	middle	P_m	0.88
26	30-ft End Drop	A	5 9	inside inside	$P_m + P_b$ $P_m + P_b$	4.74 4.74
27	30-ft Side Drop	E	11	middle	P_m	0.28
34	30-ft Slapdown (15°)	D	11	middle	P_m	0.89

[a]Locations shown schematically in Figure 2.7-2.

2.7.1.3.2 Closure Bolts. The maximum load on the bolts occurs during the 30-ft drop when the closure end impact limiter strikes an unyielding surface. The bolt stresses are calculated for all drop angles for the flat and corner angular orientations.

Analysis Methodology. The methodology for calculating the bolt stresses for the free drop is the same as used for normal conditions shown in Section 2.6.7.3.2. All loads are considered, including (1) bolt preload, (2) differential thermal expansion, (3) MNOP pressure loading and (4) closure/contents loading. The hot environment condition is the most critical loading because differential thermal expansion introduces tension in the bolts and the allowable stresses are a minimum. For hypothetical accident conditions, the hot environment temperature of the closure and bolts is 136°F (avg.). Bolt allowables and closure and bolt properties are taken at 150°F to be conservative. The bolt stress during the hypothetical accident condition thermal event is calculated in Section 2.10.12 and summarized in Section 2.7.3.

Bolt Material Allowable at 150°F interpolated from Table 2.3-1.

For SB-637 Alloy N07718,

S_u = 179,500 psi.

By definition the primary membrane allowable for accident conditions is

Lesser of S_y or 0.7 x S_u = 125,600 psi.

The forces on the closure bolts are calculated by assuming that the inertial loading of the contents and the closure cause the closure to pivot around its outer edge. The resistance of the portion of the impact limiter that backs the inertial loading is conservatively ignored. This assumption is especially conservative for the end drop where the impact limiter crush force directly resists the inertial loading. The results of the 78° CG-over-corner drop test of the half-scale model, reported in Section 2.10.13, indicate that the contents impact on the closure before the time of maximum g loading. Therefore, no dynamic amplification is applied to the inertial loading of the contents. Following is an example of the calculation for one drop angle. Tables 2.7-8 through 2.7-10 summarize the results for all drop angles, both the flat and corner angular orientation, around the axis of the cask. As shown below the worst angular orientation is when the cask impacts on the longitudinal corner of the cask.

TABLE 2.7-8 30-FT DROP BOLT STRESSES, AXIAL STRESS, FLAT ANGULAR ORIENTATION					
Drop Angle (Deg.)	Accident Condition Axial g	Moment M_p (in.-lb)	Impact Bolt Stress (psi)	MNOP Bolt Stress (psi)	Max Stress (Impact + MNOP) (psi)
side (0)	0	0	0	4,226	4,226
15	5.8	618,104	8,260	4,226	12,486
30	12.3	1,310,806	17,516	4,226	21,742
45	23.1	2,461,758	32,896	4,226	37,122
60	37.8	4,028,331	53,830	4,226	58,056
75	55.4	5,903,956	78,893	4,226	83,119
78	56.5	6,021,182	80,460	4,226	84,686
90	61	—	68,449	4,226	72,675

TABLE 2.7-9 30-FT DROP BOLT STRESSES, SHEAR STRESS, FLAT AND CORNER ANGULAR ORIENTATIONS		
Drop Angle (Deg.)	Accident Condition Transverse g	Shear Stress (psi)
side (0)	47.7	9,918
15	21.5	4,470
30	21.4	4,450
45	23.1	4,803
60	21.8	4,533
75	14.9	3,098
78	11.9	2,474
90	0	NA

TABLE 2.7-10
30-ft DROP BOLT STRESSES - AXIAL STRESS
CORNER ANGULAR ORIENTATION

Drop Angle (Deg)	Accident Condition Axial g	Moment M_p (in.-lb)	Impact Bolt Stress (psi)	MNOP Bolt Stress (psi)	Max Stress (Impact + MNOP) (psi)
side (0)	0	0	0	4,226	4,226
15	5.8	771,446	8,918	4,226	13,145
30	12.3	1,635,998	18,913	4,226	23,139
45	23.1	3,072,485	35,520	4,226	39,746
60	37.8	5,027,702	58,123	4,226	62,350
75	55.4	7,368,643	85,186	4,226	89,412
78	56.5	7,514,952	86,878	4,226	91,104
90	61	--	68,449	4,226	72,675

The maximum axial impact force on the closure is calculated as follows for a hypothetical accident condition 30-ft 78° drop (CG-over-corner):

$$F_{axial} = W \times g,$$
$$= 8{,}160 \times 56.5,$$
$$= 461{,}040 \text{ lb},$$

where

W = closure weight + fuel weight = 1512 + 6648 = 8160 lb, and

g = 56.5 axial for 78° drop (Table 2.10.4-6).

The maximum membrane load on the bolts (f) can be calculated by using Fig. 2.7-8 for impacts on the flat side of the cask and Fig. 2.7-9 for impacts on the longitudinal corner of the cask as follows:

M_p = moment about P,

M_p = F_{axial} x 13.06 in. (cask flat side),

= F_{axial} x 16.30 in. (cask corner),

M_p = 461,040 lb x 13.06 in. (cask flat side),

= 6,021,182 in.-lb (cask flat side),

= 461,040 x 16.30 in. (cask corner),

= 7,514,952 in.-lb (cask corner).

$$M_p = 3f\left(24.81+\frac{1.31^2}{24.81}\right)+2f\left(\frac{19.93^2+13.06^2+6.18^2}{24.81}\right) \text{ (cask flat side), and}$$

$$= 2f\left(29.47+\frac{24.61^2+19.75^2+12.86^2+7.99^2+3.13^2}{29.47}\right) \text{ (cask corner), gives}$$

f = M_p/123.49 = 48,759 lb per bolt (cask flat side), and

= M_p/142.74 = 52,649 lb per bolt (cask corner).

Maximum stress on the bolt = S_i = 48,759/.606 = 80,460 psi (cask flat side),

= 52,649/.606 = 86,878 psi (cask corner).

Stress on the bolts caused by the MNOP = S_{MNOP} = 4,226 psi (from Section 2.6.7.3.2).

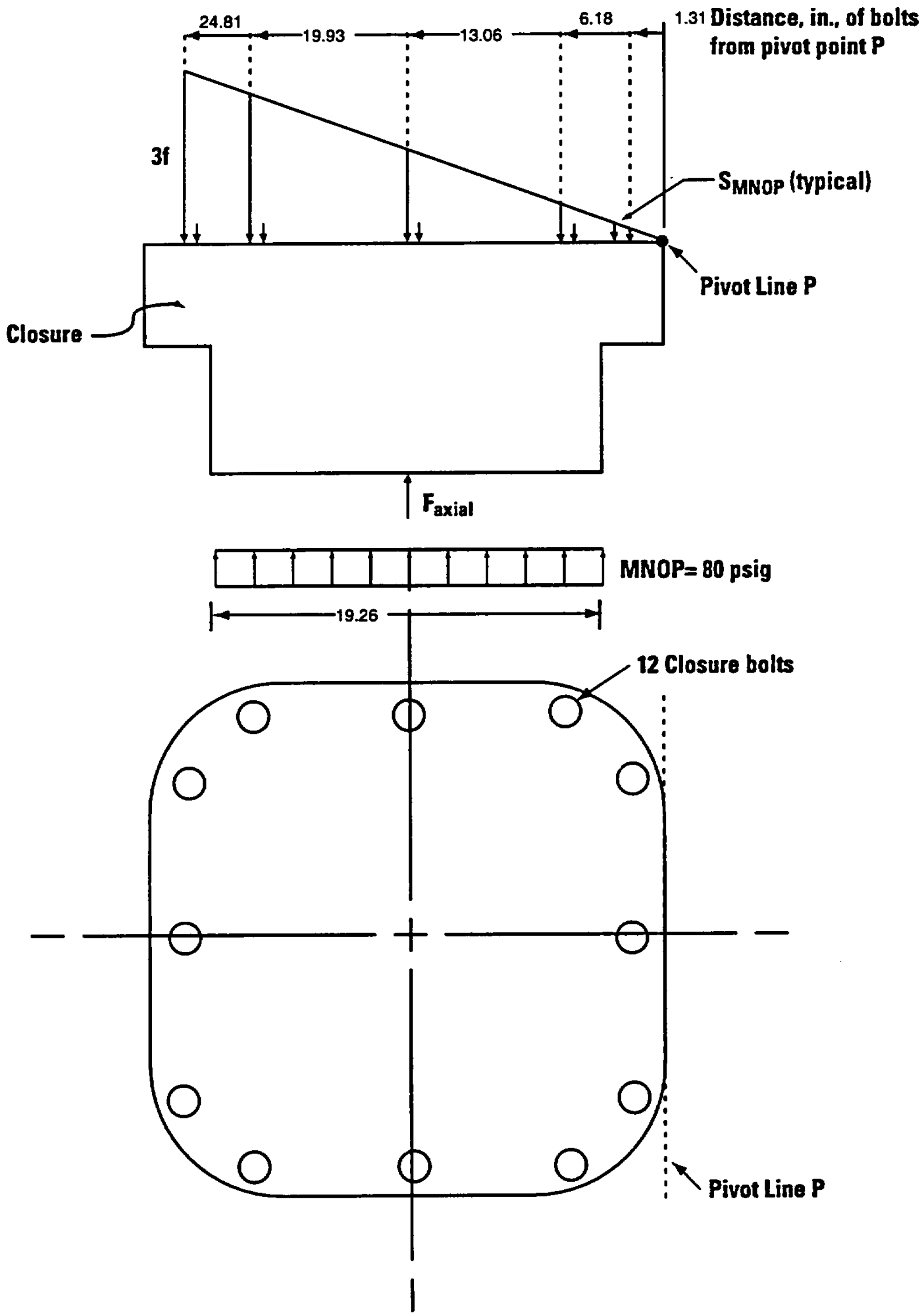

L-675(2)
4-19-96

Fig. 2.7-8. Closure bolt reaction load for flat drop orientation

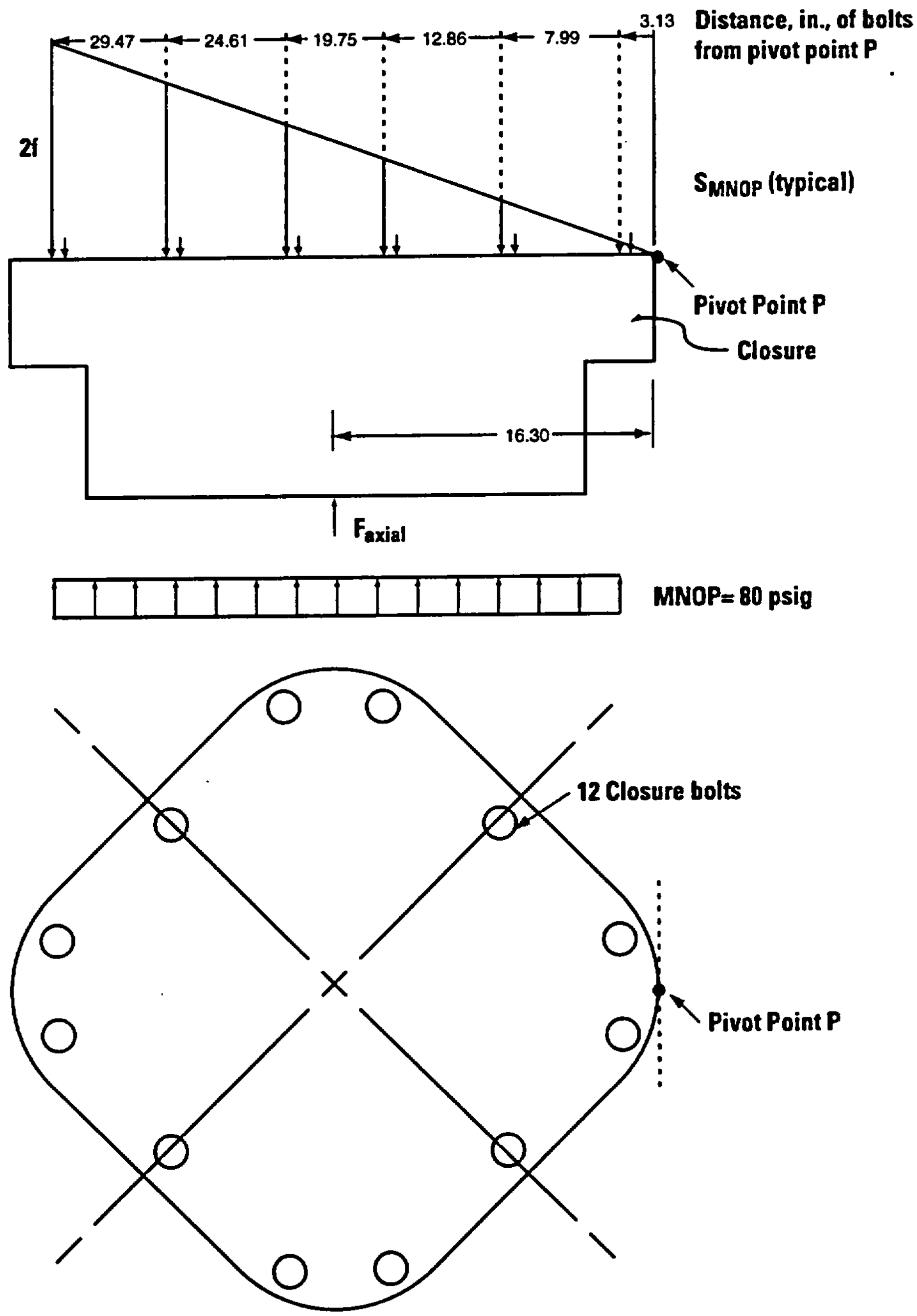

L-675(1)
7-26-96

Fig. 2.7-9. Closure bolt reaction load for corner drop orientation

Total membrane stress on the bolt is the sum of the impact load and the MNOP load. The preload and differential thermal expansion load are not added since they are exceeded by the impact and MNOP load:

$$
\begin{aligned}
S_t &= S_i + S_{MNOP} \\
&= 80{,}460 + 4{,}226 \text{ (cask flat side),} \\
&= 86{,}878 + 4{,}226 \text{ (cask corner),} \\
&= 84{,}686 \text{ psi (cask flat side), and} \\
&= 91{,}104 \text{ psi (cask corner).}
\end{aligned}
$$

Therefore, the corner angular orientation has the lower design margin.

The transverse impact force on the closure is calculated as follows for a hypothetical accident condition 78° drop (CG-over-corner):

$$
\begin{aligned}
F_{trans} &= W \times g, \\
&= 1{,}512 \times 11.9, \\
&= 17{,}993 \text{ lb,}
\end{aligned}
$$

where

W = closure weight = 1,512 lb, and

g = 11.9 transverse for 78° drop (Table 2.10.4-6).

The impact force shear stress in the bolts is:

$$
\begin{aligned}
S_{shear} &= F_{trans}/0.606 \times 12, \\
&= 2{,}474 \text{ psi.}
\end{aligned}
$$

A summary of the design margins for both the 30-ft drop flat and corner orientations is presented in Tables 2.7-11 and 2.7-12.

2.7.1.3.3 FSS/Cavity Liner. The evaluation of the FSS and cavity liner for hypothetical accident conditions combined the stresses calculated by the ANSYS frame analysis with the hand-calculated stresses induced by the out-of-plane moment from the cask ANSYS model and the thermal stresses induced in the FSS and cavity liner by either the cold or hot environment. The stresses generated by the ANSYS frame model described in Section 2.7.1.2.2 included the effects of the cask internals and the deflection profile of the cask containment boundary ovalization during the side drop or slapdown events. The results of the ANSYS plate model were also combined with the results of the frame model and hand-calculations for some of the critical load cases which were identified for the uniform fuel and NFAH inertial loads. After combination of the directional stress components, the principal stresses, the stress intensities and the design margins were calculated. The load cases considered and the results obtained are detailed in Sections 2.10.9 and 2.10.10. Using the results of these sections, the lowest design margin for each of the load cases is given in Tables 2.7-13 through 2.7-15. As shown by the tables, the lowest design margin is 0.16, which is obtained during load cases 18 and 20 under the cold environment.

TABLE 2.7-11 30-FT DROP BOLT DESIGN MARGIN SUMMARY FLAT ANGULAR ORIENTATION						
Drop Angle (Deg)	S_x (axial) (ksi)	S_{xy} (shear) (ksi)	S_1 (ksi)	S_2 (ksi)	SI (ksi)	D.M.
side (0)	4.23	9.92	12.26	-8.03	20.29	5.19
15	12.49	4.47	13.93	-1.43	15.36	9.16
30	21.74	4.45	22.62	-0.88	23.49	4.35
45	37.12	4.80	37.73	-0.61	38.34	2.28
60	58.06	4.53	58.41	-0.35	58.76	1.14
75	83.12	3.10	83.24	-0.12	83.35	0.51
78	84.69	2.47	84.76	-0.07	84.83	0.48
90	72.68	NA	72.68	0.00	72.68	0.73

TABLE 2.7-12 30-FT DROP BOLT DESIGN MARGIN SUMMARY CORNER ANGULAR ORIENTATION						
Drop Angle (Deg)	S_x (axial) (ksi)	S_{xy} (shear) (ksi)	S_1 (ksi)	S_2 (ksi)	SI (ksi)	D.M.
side (0)	4.23	9.92	12.26	-8.03	20.29	5.19
15	13.15	4.47	14.53	-1.38	15.90	6.9
30	23.14	4.45	23.97	-0.83	24.79	4.07
45	39.75	4.80	40.32	-0.57	40.89	2.07
60	62.35	4.53	62.68	-0.33	63.01	0.99
75	89.41	3.10	89.52	-0.11	89.63	0.4
78	91.1	2.47	91.17	-0.07	91.23	0.38
90	72.68	NA	72.68	0.00	72.68	0.73

TABLE 2.7-13
DESIGN MARGIN SUMMARY OF HYPOTHETICAL ACCIDENT LOAD CASE RESULTS
APPLIED TO THE FSS/CAVITY LINER HOT ENVIRONMENT

LOAD CASE			STRESS POINT LOCATION				SUMMARY	
No.	Description 30-ft	Config.[a]	Component	Axial[b] Section	Trans Pos.[b]	Position in Wall	Stress Type	Design Margin
17	Side Drop	Flat /4	cavity liner	E	9/16	outside	P_m+P_b	0.68
			FSS		33	middle	P_m	0.51
18	Side Drop + MNOP	Flat/4	cavity liner	E	9/16	outside	P_m+P_b	0.24
			FSS		33	middle	P_m	0.66
19	Side Drop	Flat/3	cavity liner	E	16	outside	P_m+P_b	0.66
			FSS		33	middle	P_m	0.57
20	Side Drop + MNOP	Flat /3	cavity liner	E	16	outside	P_m+P_b	0.24
			FSS		33	middle	P_m	0.69
21	Side Drop	Corner/4	cavity liner	E	3/4	outside	P_m+P_b	0.26
			FSS		36	outside	P_m+P_b	0.33
22	Side Drop + MNOP	Corner/4	cavity liner	E	14/17	middle	P_m	0.35
			FSS		30	outside	P_m+P_b	0.43
23	Side Drop	Corner/3	cavity liner	E	3/4	outside	P_m+P_b	0.28
			FSS		36	outside	P_m+P_b	0.35
24	Side Drop + MNOP	Corner/3	cavity liner	E	14/17	middle	P_m	0.35
			FSS		30	outside	P_m+P_b	0.51
25	15° Impact, Drop	Flat/4	cavity liner	B	3/22	outside	P_m+P_b	1.20
			FSS		33	middle	P_m	1.32
26	15° Impact + MNOP	Flat/4	cavity liner	B	9/16	outside	P_m+P_b	0.56
			FSS		30/36	outside	P_m+P_b	1.26
27	15° Impact, Drop	Flat/3	cavity liner	B	24	outside	P_m+P_b	0.80
			FSS		33	middle	P_m	3.16
28	15° Impact + MNOP	Flat/3	cavity liner	B	19	outside	P_m+P_b	1.31
			FSS		36	outside	P_m+P_b	5.69
29	15° Impact, Drop	Corner/4	cavity liner	D	3/4	outside	P_m+P_b	0.75
			FSS		30	outside	P_m+P_b	1.50
30	15° Impact + MNOP	Corner/4	cavity liner	D	13/18	middle	P_m+P_b	1.24
			FSS		30	outside	P_m+P_b	1.17
31	15° Impact, Drop	Corner/3	cavity liner	D	3/4	outside	P_m+P_b	0.79
			FSS		30	outside	P_m+P_b	1.75
32	15° Impact + MNOP	Corner/3	cavity liner	D	13/18	middle	P_m	1.29
			FSS		30	outside	P_m+P_b	1.36

(a) Flat or corner orientation with 3 or 4 fuel element assemblies
(b) Locations shown schematically in Fig. 2.7-5

TABLE 2.7-14
DESIGN MARGIN SUMMARY OF HYPOTHETICAL ACCIDENT LOAD CASE RESULTS
APPLIED TO THE FSS/CAVITY LINER COLD ENVIRONMENT

LOAD CASE			STRESS POINT LOCATION				SUMMARY	
No.	Description 30-ft	Config.[a]	Component	Axial[b] Section	Trans Pos.[b]	Position in Wall	Stress Type	Design Margin
17	Side Drop	Flat /4	cavity liner	E	9/16	outside	P_m+P_b	0.52
			FSS		33	middle	P_m	0.60
18	Side Drop + MNOP	Flat/4	cavity liner	E	9/16	outside	P_m+P_b	0.16
			FSS		33	middle	P_m	0.76
20	Side Drop + MNOP	Flat/3	cavity liner	E	16	outside	P_m+P_b	0.16
			FSS		25/33	middle	P_m	0.78
21	Side Drop	Corner /4	cavity liner	E	14/17	middle	P_m	0.20
			FSS		36	outside	P_m+P_b	0.40
22	Side Drop + MNOP	Corner/4	cavity liner	E	14/17	middle	P_m	0.20
			FSS		30	outside	P_m+P_b	0.51
23	Side Drop + MNOP	Corner/3	cavity liner	E	14	middle	P_m	0.20
			FSS		36	outside	P_m+P_b	0.42

(a) Flat or corner orientation with 3 or 4 fuel element assemblies
(b) Locations shown schematically in Fig. 2.7-5

TABLE 2.7-15
DESIGN MARGIN SUMMARY OF HYPOTHETICAL ACCIDENT RESULTS
FOR CONCENTRATED LOAD CASES APPLIED TO THE FSS

LOAD CASE		STRESS LOCATION		TYPE	D.M.
Description	Config.				
Side Drop	Flat[a]	Center of FSS	Section E[b]	P_m+P_b	0.95
Side Drop	Flat	0.549 in. from cavity liner wall	Section E	P_m+P_b	0.33
Side Drop	Corner	0.549 in. from cavity liner wall Below neutral axis	Section E	P_m+P_b	1.02
Side Drop	Corner	Center of FSS Above neutral axis	Section E	P_m+P_b	1.97
Side Drop	Corner	0.549 in. from cavity liner wall Above neutral axis	Section E	P_m+P_b	0.39
15° Impact	Flat	Center of FSS	Section H	P_m+P_b	1.69
15° Impact	Flat	0.549 in. from cavity liner wall	Section H	P_m+P_b	0.72

(a) Flat or corner orientation
(b) Axial location on cask, shown in Fig. 2.7-2

2.7.1.3.4 Neutron Shield Structure. Hand calculations were used to evaluate the adequacy of the neutron shield during hypothetical accident conditions. The effects of inertial loads, impact forces and [Prop. Info.] were all considered. The inertial loads and impact forces were taken from Table 2.10.4-7. Pressure variations caused by the [Prop. Info.] neutron shield are discussed in Section 2.10.11.4. The results of the assessment detailed in Section 2.10.11 are summarized in Table 2.7-16. As shown by the table, the design margins for all of the stresses resulting from the accident conditions are acceptable. The lowest design margin is 0.39 and is obtained during the 30-ft side drop condition. This demonstrates that the neutron shield structure will remain attached for the accident condition, and act as a thermal shield for the fire event.

2.7.1.3.5 ILSS. The evaluation of the ILSS considered only the effects of the various hypothetical accident condition drops. Internal pressure and thermal effects were negligible for this component. The drops considered included the side, oblique and end drops and the secondary impact (or slapdown) condition. Where appropriate to get the most conservative results, different clocking angles about the cask axis were used to evaluate the impact forces. Using the GACAP results, hand-calculations, and ANSYS ILSS models, the adequacy of the ILSS to transfer loads from the impact limiter to the cask body was confirmed.

As detailed in Section 2.10.3.6, hand calculations were used to evaluate the two side drop and slapdown conditions: one caused the maximum shear load from the impact limiter to the ILSS, and the other transferred the highest compressive loads from the impact limiter to the cask body. The free body diagram of the ILSS loading condition which produces the maximum shear load is shown in Fig. 2.10.3-29. Assuming none of the load was transferred by the ribs, hand calculations were performed which showed that the shear plates had a design margin of 2.8 for the 0.5 in. end plate and 3.8 for the 0.38 in. plate. The cask body extension was checked using the shear and moment from the side drop and the effects of the neutron shield [Prop. Info.]. Its design margin was 0.6.

The maximum compressive loads from the impact limiter to the cask body were evaluated using an ANSYS model with different loading conditions to simulate the different clocking positions of the impact surface. The load applied to the model was derived using the assumptions that none of the load is transferred by the shear plates and that the load is uniform along the ILSS length. The different loadings on the ANSYS model were used to find the load distribution for each rib and the outer shell. The output information included the axial and shear forces and the moments at each end of the beam elements. The loads were used to calculate stresses in the ribs and shell. The locations chosen for evaluation included the ribs, the shell, and the welds, both the plug welds at the rib-shell connection and the fillet welds which connect the ILSS ribs to the cask wall. Hand calculations were used to evaluate the stresses for the end drop condition. The loads from the GACAP analysis were used as shown in Fig. 2.10.3-33.

The results for the side and end drop analyses were combined for evaluation of the oblique drops by resolving the stresses into the appropriate components for each drop angle. Table 2.7-17 summarizes the lowest design margins for each component and identifies the drop angle. The lowest design margin is 0.01 for the outer shell.

TABLE 2.7-16
DESIGN MARGIN SUMMARY OF HYPOTHETICAL ACCIDENT RESULTS FOR THE NEUTRON SHIELD STRUCTURE

COMPONENT	30-FT DROP LOADING	TYPE	DESIGN MARGIN
Outer Shell	End Drop	P_m	0.60
Outer Shell	Side Drop	P_m	0.39
ILSS, End Plate	End Drop	P_m+P_b	1.65

TABLE 2.7-17
DESIGN MARGIN SUMMARY OF HYPOTHETICAL ACCIDENT CONDITION RESULTS FOR SIDE DROP LOAD CASES APPLIED TO THE ILSS

COMPONENT OR STRESS LOCATION	LOAD CASE	STRESS INTENSITY (ksi)	STRESS TYPE	STRESS ALLOWABLE (ksi)	DESIGN MARGIN
Outer Shell	30-ft corner side (0°) drop	98.3	P_m+P_b	99.5	0.01
Ribs	30-ft flat side (75°) drop	48.4	P_m+P_b	99.5	1.06
Cask Body Extension	30-ft flat side (0°) drop	62.9	P_m+P_b	99.5	0.60
Shell-to-Rib Plug Welds	30-ft flat side (0°) drop	12.7	Shear[(a)] (PT/MT)	18.8	0.48
Rib-to-Cask Body Fillet Welds	30-ft flat side (0°) drop	13.8	Shear[(b)]	16.7	0.21
Bearing on Ribs	30-ft end (90°) drop	37.0	Bearing	99.5	1.69

[(a)]The inspection techniques affect the shear allowables for welds. PT/MT means magnetic particle inspection.
[(b)]Welds with visual inspection requirement.

2.7.1.3.6 Impact Limiter Bolts. Section 2.10.3.7 calculates the maximum stresses in the impact limiter bolts resulting from the 30-ft drop event. The half-scale model tests described in Section 2.10.13 confirmed that the impact limiter bolts did not fail and the impact limiters remained on the cask for three 30-ft drop orientations; side drop, 30° slapdown and CG-over-closure corner. These orientations give the maximum loading on the impact limiter bolts as shown in Section 2.10.3.7.1.

For most orientations and crush depths, the impact limiter crush force is transmitted to the cask body directly; hence, the forces seen by the impact limiter bolts are relatively small. This is not true at the start of an oblique crush, when the crush area is not backed by the cask. Therefore, the impact limiter bolts are designed conservatively to take the moment produced by the crush of the total unbacked area on the side of the cask during both a nearly vertical and a nearly horizontal oblique drop. The moment produced by crushing during the nearly vertical oblique drop is 4,165,322 in.-lb, while the nearly horizontal oblique drop produces a 4,430,000 in.-lb moment.

The moments produced by oblique drops which have load components perpendicular to the cask axis and parallel to the cask axis, will be less for the closure bolts than the two bounding cases given above, because the moments produced by each load component oppose each other, reducing the total moment.

The bolts' reaction due to the maximum moment was conservatively analyzed by assuming that the edge of the impact limiter has a pinned boundary condition. Assuming that the impact limiter remains rigid, the force per bolt of 38,010 lb causes a stress of 69.0 ksi, which is less than the P_m allowable of 146.3 ksi at T = 150°F for non-containment bolts (SB-637, Alloy N07718). The design margin is (146.3/69) -1 = +1.12.

The cask impact limiter attachment method was designed so that there is no interference and minimum shear stress imposed on the impact limiter bolts during the drop events. The diametral clearance between the impact limiter housing and the impact limiter support structure is 40.00 – 39.75 = 0.25 in. This clearance is smaller than the clearance between the bolt and the edge of the hole in the plate of the impact limiter support structure. During a side impact, as the impact limiter moves laterally relative to the cask, the impact limiter canister will contact the impact limiter support structure before the bolts contact the edge of the hole in the plate. This will be true even if the impact limiter is installed completely against one side of the cask and then subjected to a side drop on the opposite side. The maximum impact limiter movement is 0.25 in. After moving 0.25 in., the impact limiter attachment bolts will not contact the side of the impact limiter support plate. Therefore, the only loads on the impact limiter bolts will be the tension loads from the moment produced by the crush of the unbacked portion of the impact limiter and the bending produced by the 0.25-in. side movement. The stress on the bolts due to this movement is 67.1 ksi, as shown in Section 2.10.3.7.1. Combining these stresses, the total stress on the bolt during impact and side movement is 136.1 ksi, which is less than the $P_m + P_b$ allowable of 179.5 ksi (T = 150°F) for non-containment bolts. The design margin is (179.5/136) – 1 = +0.32.

2.7.1.4 Buckling Evaluation. The buckling resistance of the cask body, cavity liner, fuel support structure, neutron shield shell and ILSS ribs have been shown in Section 2.10.7 to meet the criteria described in Section 2.1.2.6 for all hypothetical accident conditions. Following is a summary of the results of these analyses.

Cask Body Buckling. The cask body was analyzed for buckling for combined axial compression and bending. The minimum design margin occurs for the side 30-ft drop where the bending in the cask is a maximum. The minimum design margin is 0.52 as shown in Table 2.10.7-1.

Cavity Liner and Fuel Support Structure (FSS) Buckling. The cavity liner and FSS were analyzed for buckling for combined axial compression and bending. The minimum design margin occurs for the side 30-ft drop where the bending in the cavity liner and FSS is a maximum. The minimum design margin is 0.18 for the corner angular orientation as shown in Tables 2.10.7-2 and 2.10.7-3.

Neutron Shield Shell. Overall buckling of the neutron shield shell is precluded by the stiffness and buckling strength of the cask body under the drop conditions.

Impact Limiter Support Structure (ILSS) Rib Buckling. The ILSS rib was analyzed for buckling for combined axial compression and bending and is shown in Section 2.10.3.6.1c. The minimum design margin occurs for the side 30-ft drop where the bending in the cavity liner and FSS is a maximum. The minimum design margin is 0.12 for the corner angular orientation as shown in Table 2.10.3-15.

2.7.1.5 30-ft Drop Test Results. A half-scale model of the GA-4 cask was tested to verify the structural design. A scale of one-half was chosen because it allows direct scaling of all critical cask components. All significant features that might affect the structural performance during the regulatory drop events were modeled. The FSS in the model is not welded to the cavity liner, but instead is supported by a keyway in the cavity liner (as shown in Section 2.10.13, Fig. 2.10.13-3). This is conservative because, in general, the stresses in the keyway design are greater than in the welded design.

The FSS in the model is not welded to the cavity liner, but instead is supported by a keyway in the cavity liner, as shown in Section 2.10.13, Fig. 2.10.13-3. This is conservative because, in general, the stresses in the keyway design are greater than in the welded design.

The test program verified the design structural analyses of the 30-ft (9-meter) drop event requirements set forth in 10 CFR Part 71.73. This section summarizes the results of the three 30-ft drop tests and gives a comparison of the results with the analyses discussed above. A complete discussion of the test results and evaluation is given in Section 2.10.13.

The model was tested with contents that were 11% heavier than would ever be needed for a full-scale spent fuel shipment. Some of this extra weight accounted for the B_4C pellets that were omitted from the FSS in the model. The total test weight for the model was 6889 lb, including 15 lb of rigging and instrumentation mounting hardware. Eight times this weight scales to 55,112 lb full scale. The maximum design weight for the GA-4 cask used in the SARP for structural analysis is 55,000 lb. Therefore, the model was tested at slightly above the cask's design weight.

2.7.1.5.1 Test Program Description. The three 30-ft drop tests were performed at ambient temperature, and the initial internal pressure in the model's cavity was 80 psig.

1. Side Drop - 30-ft drop with the model oriented horizontally and a longitudinal edge of the model facing the impact surface.

2. Slapdown - 30-ft drop with the model axis tilted 30° from the horizontal position, the closure end striking first, and the flat side of the model facing the impact surface.

3. CG-over-corner - 30-ft CG-over-corner drop (corner is the closure corner) with the model axis tilted 12° from the vertical position and a longitudinal edge of the model facing the impact surface.

2.7.1.5.2 Instrumentation and Data Acquisition. The model was fitted with multiple strain gages and accelerometers to measure its response during the drop events. Strain gages were located midlength on the outer shell where the maximum deflection was expected. Accelerometers were mounted at each end of the outer shell and at midlength. Two high speed 16-mm movie cameras (1000 to 2000 fps), one intermediate speed 16-mm movie camera (400 fps), and several video camcorders were employed to record the drop events.

2.7.1.5.3 Testing. Testing was conducted in San Diego, CA, at a facility operated by the S-Cubed Division of Maxwell Laboratories. GA constructed a concrete and steel drop pad which meets IAEA guidelines for an unyielding surface. Impact limiters, impact limiter bolts, and closure seals were replaced after each test. For each drop, the model was rigged in the proper orientation, lifted to a height of 30 ft by a crane, and released by simultaneously firing multiple explosive cable cutters.

The closure O-ring seals and the gas sample port seals were leak tested before and after each test sequence. The impact limiters were inspected after each test to determine the crush caused by the test. Dimensional checks and helium leakage tests of the containment boundary and cavity liner were performed on the model cask after all testing was completed.

2.7.1.5.4 Test Results and Conclusions. The half-scale model drop tests showed that the GA-4 cask design is robust. Measurements showed that there was no permanent deformation of the cask body, internals, closure or impact limiter bolts for any of the 30-ft drop tests. In particular, the FSS remained in its keyway, all closure bolts remained torqued with no measurable deformation and the impact limiters remained attached; crushing and producing expected deceleration rates. Helium leakage tests of the closure seals and gas sample port seals showed that leaktight conditions were maintained before and after each test sequence. After completion of the final test, the closure seals were satisfactorily leak-tested. Additionally, two helium leakage tests showed that the liner and cask containment body were leaktight. For more details about the test results, see Section 2.10.13.

2.7.1.5.5 Comparison with Analyses. Axial and transverse deceleration levels predicted by GACAP (Section 2.10.4) were compared to the results obtained from the half-scale model tests and presented below in Table 2.7-18. Agreement was very good for maximum decelerations in the directions of most interest, e.g. axial deceleration during the end drop, and transverse deceleration during the side drop and slapdown.

TABLE 2.7-18
COMPARISON BETWEEN HALF-SCALE MODEL
TEST RESULTS AND ANALYSIS

	Analysis		Test[b],[c]
	High Str.[a]	Low Str.[a]	
30-ft Sidedrop - corner orientation			
g-level at CG	47.7	39.6	40-44
Crush (in.)	11.9	14.2	12
Strain, Z-direction (με)	1854	—	1400
Calculated stress, σ, (ksi)	52.89		38.77
30-ft Slapdown - flat orientation			
g-level at CG			
Axial - primary impact	12.3	10.7	7
secondary impact	0	0	16
Transverse - primary impact	21.4	18.6	16
secondary impact	25.9	23.7	24-30
g-level - closure end			
Transverse - primary impact	58	—	30
secondary impact	–28	—	–15
g-level - bottom end			
Transverse - primary impact	–16	—	–10
secondary impact	69	—	51.5
Crush (in.)			
- primary impact	14.7	16.3	15
- secondary impact	14.5	16.9	15.8
Strain, Z-dir., secondary impact (με)	756	—	530
30-ft CG-over-corner			
g-level, axial	56.5	39.3	46-51.5
Crush (in.)	14.2	16.4	12.6
Strain, Z-direction (με)	–475		–290

[a]High strength and low strength honeycomb used in the analysis.
[b]Deceleration values represent the full cask value (test value x 1/2).
[c]Crush heights represent the full cask value (test value x 2).

In Section 2.10.4 the GACAP computer code was used to predict decelerations at points along the length of the body under possible drop orientations. The drop orientations included the three 30-ft drop orientations (side, end, and slapdown) tested with the GA-4 half-scale model. The model used different impact limiter load-deflection curves that bounded the honeycomb crush strength characteristics. Three different impact limiter load-deflection curves for each drop orientation were used as input for GACAP. The maximum and minimum strength curves considered manufacturing crush strength tolerances and temperature effects including a factor for strain rate effects on the crush strength. The three curves represent:

1. Maximum strength impact limiters,
2. Minimum strength impact limiters, and
3. Actual quarter-scale impact limiters used in the development tests.

The results are shown in Section 2.10.13, in Figs. 2.10.13-66 through 2.10.13-69, along with maximum deceleration values taken from the half-scale tests. A detailed comparison is contained in Section 2.10.13.

2.7.2 Puncture Drop

10 CFR Part 71.73 requires a 40-in. (1-m) drop of the cask onto a vertical mild steel punch with a diameter of 6 in. (0.15 m). The punch must be mounted on an essentially unyielding horizontal surface. Its top must be horizontal, with the edge rounded to a radius of no more than 0.25 in. (0.006 m). The length of the punch must be sufficient to cause maximum damage to the package, but no less than 8 in. (0.2 m). During the drop, the cask is to be oriented in a position for which maximum damage is expected.

To satisfy these requirements, analytical evaluations were performed to show that the cask is of sufficient thickness to prevent punching shear failure. The cask was also evaluated to ensure that the punch would not produce bending moments across the cask's cross section and closure that would result in stresses that exceeded allowables. In addition, the shear stresses caused by puncture on the side of the closure were evaluated.

The gas sample port and drain valve are protected under an impact limiter and recessed into the closure and bottom head, respectively, so that they will not be impacted by the puncture pin. The half-scale model test reported in Sections 2.7.2.3 and 2.10.13 contained a gas sample port which was directly attacked in one of the 40-in. puncture tests. The gas sample port was not damaged. Two other puncture tests were performed when the cask was dropped in a horizontal orientation, one which attacked the cask at the midlength and one which attacked the cask near midlength at one of the DU joints. The containment boundary was only dented locally.

2.7.2.1 Local Behavior. The austenitic stainless steel closure, bottom plate, and cask body side wall are of sufficient thickness to preclude punching shear failure. Material properties were conservatively used at a temperature of 221°F rather than the maximum cask body temperature of 198°F.

Two methods were used to demonstrate the puncture resistance of the cask:

1. Nelms' equation, and
2. Lower bound of experimental data compiled by Larder and Arthur,

using the following parameters,

h = drop height = 40 in.,
r = punch edge radius = 0.25 in.,
d = punch diameter = 6 in.,
W = weight of cask = 55,000 lb,
S_u = cask ultimate tensile strength at 221°F = 98.4 ksi,
S_y = cask yield strength at 221°F = 46.2 ksi,
t = thickness of steel in cask = 1.5 in. (side wall),
= 9.5 in. (bottom plate).

2.7.2.1.1 Nelms' Equation. (Ref. 2.7-3, p. 17, Eq. 2.1) Nelms' equation was developed for flat-sided and cylindrical lead-backed cask walls. It is conservative to use lead-backed equations because R. A. Larder and D. F. Arthur demonstrated in Ref. 2.7-4, Vol. 2, p. 33, that uranium-backed plates are significantly less penetrable than lead-backed plates. In the tests they conducted, the uranium-backed plates failed at 1.8 to 4.9 times the punch force required to fail the equivalent lead-backed plates.

Reference 2.7-3 suggests using 1.3 times the weight for casks with diameters less than 30 in. This factor will be used for conservatism.

$$t_{req} = (W/S_u)^{0.71},$$
$$= (55 \times 1.3/98.4)^{0.71},$$
$$= 0.80 \text{ in.},$$

for side wall:

Margin of Safety = (1.5/0.80) – 1 = + 0.88

for bottom plate:

Margin of Safety = (9.5/0.80) –1 = + 10.9

The closure is thicker than the bottom plate and will have a larger margin of safety.

2.7.2.1.2 Experimental Data. Larder and Arthur summarized experimental data from puncture tests on DU-backed and lead-backed austenitic stainless steel plates. The lead-backed data is shown in Fig. 11, Ref. 2.7-4, Vol. 1. For conservatism in this analysis, the lower bound in this figure is used. This lower bound neglects energy absorbed in structural deformation such as membrane stretching or bending around the periphery of the punch. All of the available kinetic energy is assumed to be directed toward shearing through the containment boundary around the pin contact area. Using the lower-bound curve, the minimum normalized energy $\bar{E}$ to initiate puncture can be computed as

$$\bar{E}_{MIN} = 0.7\, e^{2t/d} (d/t)^{1.8}.$$

The total normalized energy available for puncture is

$$\bar{E} = W\, h/S_u\, t^3,$$

for side wall:

$$t = 1.5 \text{ in.}$$

$$\bar{E} = \frac{55{,}000 \times 40 \text{ in.}}{98{,}400 \times (1.5 \text{ in.})^3} = 6.62,$$

$$\bar{E}_{MIN} = 0.7e^{2(1.5)/6} (6/1.5)^{1.8} = 13.99, \text{ and}$$

$$\text{Margin of Safety} = \frac{13.99}{6.62} - 1 = +1.11.$$

The minimum margin of safety for the closure or bottom plates (using the minimum thickness in any design of 9.5 in.) is calculated from

$$\bar{E} = 0.026, \text{ and}$$

$$\bar{E}_{MIN} = 7.26,$$

$$\text{Margin of Safety} = \frac{7.26}{0.026} - 1 = +278.$$

Both methods show significant margins of safety against local punch shear failure.

2.7.2.2 Overall Cask Behavior.

2.7.2.2.1 Cask Body. To determine the overall effect on the cask, we considered the puncture impact occurring at the midlength of the package, on its side. This orientation will cause the highest stresses due to bending of the cask.

For a unit acceleration of 1g and conservatively using only the outer steel shell for strength, the membrane stress in the containment boundary induced by the bending moment can be calculated as follows:

$$M = \frac{W_1(\ell_1)^2}{8} + \frac{W_2(\ell_2)}{2}$$

See Fig. 2.7-10.

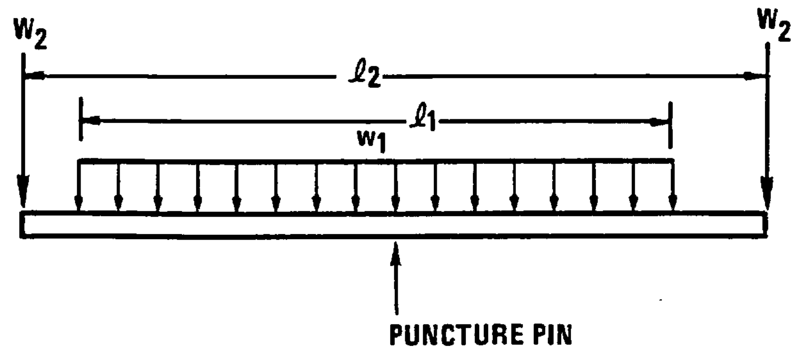

K-238(31)
10-8-91

Fig. 2.7-10. Puncture impact model

The maximum acceleration of the cask at impact is a function of the area of the punch (A) and the dynamic flow stress (σ_f) in the punch. Assuming the dynamic flow stress is the mean of the yield and ultimate stresses for ASTM-36 structural steel, the dynamic flow stress in the punch is

$$\sigma_f = (\sigma_y + \sigma_u)/2 = 47{,}000 \text{ psi},$$

where

σ_y = 36,000 psi, and

σ_u = 58,000 psi.

The acceleration of the cask is

$$a = \sigma_f A/W = 24.18 \text{ g},$$

where

$A = \pi R^2 = 28.3 \text{ in.}^2$,

R = 6.0/2 = 3.0 in.,

W = 55,000 lb, and

using

W_1 = 265.2 lb/in. (see Section 2.2) weight per inch of cask,

ℓ_1 = 167.25 in., and

ℓ_2 = 188.25 in. (conservative value).

Conservatively using the design cask weight of 55,000 lb,

W_2 = weight at ends of cask,

W_2 = [55,000 – (265.2 (167.25))/2] = 5,322.7 lb,

$$M = W_1 \frac{(\ell_1)^2}{8} + W_2 \frac{(\ell_2)}{2},$$

$$M = \frac{265.2(167.25)^2}{8} + \frac{5322.7(188.25)}{2},$$

M = 1,428,290 in.-lb,

I = cask wall moment of inertia = 14,793 in.^{4},

c = 16.15 in.,

Primary membrane stress,

$$\frac{a\,Mc}{I} = \frac{24.18(1,428,290)(16.15)}{14,793} = 37,704 \text{ psi},$$

Maximum shear,

τ = a(W/2)/A = 24.18 (55,000/2)/141.85 = 4,688 psi,

where

A = 141.85 in.^{2} cask cross-sectional area.

2.7.2.2.2 Closure and Bottom Plates. The minimum thickness of the bottom plate is 9.5 in. The maximum primary membrane-plus-bending stress in the bottom plate occurs when the punch strikes the center of the plate. The maximum stresses are computed as follows (Ref. 2.7-5, Table 26, case 1b):

$$\text{Max } \sigma = \frac{3W}{2\pi t^2}\left[(1+\mu)\ln\frac{2b}{\pi r_o} + \beta\right]$$

(conservatively assuming all edges are simply supported), where

W = 55,000 lb for 1g,

t = 9.5 in.,

μ = 0.3,

b = a = 25.93 in. (conservative value),

r_o' = 3 in. < 0.5 t = 4.75 in.,

r_o = $\sqrt{1.6(3)^2 + 9.5^2} - 0.675(9.5) = 3.817$ in., and

β = 0.435.

For 1 g

Max σ = 680.5 psi, and

for 24.18 g,

Max σ = 16,454 psi.

The closure thickness is larger than that used above; therefore, the stresses are negligible.

Maximum closure deflection for the above case can be calculated as follows (conservatively using 9.5 in. for thickness of the closure — the closure thickness is 11 in.):

$$y = \frac{\alpha W b^2}{E t^3},$$

using

$$\alpha = 0.1267,$$

$$\text{Max } y = -\frac{0.1267(55{,}000)25.93^2}{28 \times 10^6 (9.5)^3} = -0.0002 \text{ in. for 1 g.}$$

For 24.18 g,

$$\text{Max } y = -0.005 \text{ in.}$$

This deflection is negligible. Therefore, the cask will remain leaktight. The seals can accommodate the movement caused by a puncture drop on the closure.

2.7.2.2.3 Puncture Impact on Side of Closure. The analysis uses flow stress on punch as the total load on the closure. This is extremely conservative because the impact limiter surrounds the closure and would absorb some of the punch energy.

Total load = 47 ksi (28.3 in.^{2}) = 1330 kips.

The force transferred across closure flange interface (F_T) is equal to

F_T = total load – (weight of top head x g-level),

weight of top head = closure + impact limiter weight = 3.5 kips (conservative),

F_T = 1330 kips – (3.5 kips x 24.18 g) = 1245 kips.

This load would be transmitted by the closure directly into the cask body flange. The smallest interface area occurs during a puncture in the flat orientation. During this event, the punch load is transferred through an area 1.125-in. by 18.276-in.

The maximum bearing stress in this area is

$$\sigma = \frac{1{,}245 \text{ kips}}{1.125 \text{ in.} \times 18.276 \text{ in.}}$$

$$= 60.6 \text{ ksi} < 98.4 \text{ ksi bearing allowable (conservative value).}$$

The design margin is calculated thus:

$$\text{D.M.} = \frac{98.4}{60.6} - 1 = 0.62.$$

2.7.2.2.4 Conclusion. The containment boundary of the GA-4 cask is of sufficient thickness to preclude punching shear failure. The primary stresses across the cask cross section and the closure and bottom plates due to a puncture drop event are always less than 39 ksi, which is less than the stresses developed during a 30-ft side-drop event. The closure/flange bearing area transfers the load caused by a side puncture on the closure.

2.7.2.3 Puncture Test. This section describes the results and evaluation of the four puncture tests that were performed using the GA-4 half-scale model. A complete description of the GA-4 half-scale model test program is found in section 2.10.13.

2.7.2.3.1 Test Description. The four puncture tests performed were

1. ILSS - Forty-inch puncture drop with the model oriented horizontally and the punch striking the model's impact limiter support structure adjacent to the corner of the closure,

2. Cask wall - Forty-inch puncture drop with the model oriented horizontally, the flat side facing the impact surface, and the punch striking the center of the model body,

3. Closure - Forty-inch puncture drop with the model oriented 7° from the vertical and the punch striking the closure in the vicinity of the gas sample port and closure bolts.

4. DU Joint - Forty-inch puncture drop with the model oriented horizontally with the punch striking a longitudinal edge of the model body near midlength at the location of a joint between two depleted uranium (DU) rings .

The cask model was fitted with multiple strain gages and accelerometers to measure its response during the puncture tests. Strain gages were located midlength on the outer shell where the maximum deflection was expected. Accelerometers were mounted at each end of the outer shell and at midlength.

A 3-in. diameter mild steel puncture pin was bolted to the steel plate covering the reinforced concrete pad and was fitted with strain gages in order to measure axial deflection of the spike and calculate the total load.

The pin material was tested and found to have a yield strength of 43 ksi and an ultimate tensile strength of 64.5 ksi.

Two high speed 16-mm movie cameras (1000 to 2000 fps), one intermediate speed 16-mm movie camera (400 fps), and several video camcorders were employed to record the drop events.

All tests were performed at ambient temperature. The initial pressure in the model's fuel cavity was 80 psig (0.55 mpa). For each puncture drop, the model was rigged in the proper orientation, lifted to a height of 40 in. by a crane, and released by simultaneously firing multiple explosive cable cutters.

2.7.2.3.2 Test Results and Conclusions. The tests demonstrated that the half-scale model of the GA-4 cask containment boundary is highly resistant to puncture tests. During the ILSS test the punch penetrated the previously damaged closure end impact limiter, but did not punch through the 0.125-in. thick stainless steel impact limiter housing. For the cask wall test, the cask wall experienced local deformation with a 0.15 in. deep dent, while examination of the interior revealed a small local 0.07 in. deformation of the cavity liner and the edge of one FSS plate. During the closure test, the impact limiter end skin pried off, as a result of the cask's rotation, after the initial end drop impact. Although there was damage to the gas sample port cover, the quick-connect nipple was undamaged. Pressure check tests confirmed that the cask containment boundary was not breached. The DU joint test showed only local minor indentation of the rounded corner of the containment wall.

After the DU joint test, the closure seals were shown to be sealing properly. In two additional helium leakage tests, the liner and cask body were shown to be leaktight.

2.7.2.3.3 Comparison with Analyses. In Section 2.7.2.2 we showed that the punch would not produce bending moments across the cask's cross section that would result in stresses that exceeded allowables. The maximum strain in the cask body during the puncture test at the cask body flat side was higher than predicted by analysis, but was still within allowables.

2.7.3 Thermal: Fire Accident

The calculations of thermally induced displacements and stresses reported here use the ANSYS model described in Section 2.10.12. We obtain temperatures and pressures from the analytical methods described in Section 3.5.

2.7.3.1 Summary of Pressures and Temperatures. From Table 3.1-1, the maximum internal pressure during the hypothetical accident is 90.2 psig, and the maximum containment boundary temperature is 780°F. To calculate thermal stresses and displacements, we use the temperature distribution of the ANSYS model at 0.5 hr into the thermal accident considering both hot and cold initial conditions. The temperature of the closure bolt at this time is 187°F for hot initial conditions and 47°F for cold initial conditions.

2.7.3.2 Differential Thermal Expansion. Thermal gradients during the hypothetical accident cause the interface between the closure and flange to open and produce a maximum temporary gap (i.e., a reduction in seal compression) of 0.024 in. at the location of the primary closure seal. This gap occurs along a section through the flat side of the cask. The maximum gap of 0.024 in. occurs for the cold initial condition; the gap is 0.022 in. for the hot initial condition.

In Section 4.5 it is shown that these gaps are acceptable and will not cause a loss of containment integrity. The calculations of these gap sizes use the ANSYS model and temperature distribution described in Section 2.10.12.

The gaps between components which are important for safety are evaluated using the method described in Section 2.6.1.2. This evaluation, as summarized in Tables 2.7-18 and 2.7-19, shows that all of the gaps are acceptable.

TABLE 2.7-19
SUMMARY OF NOMINAL GAP SIZES RESULTING FROM
DIFFERENTIAL THERMAL EXPANSION OF THE GA-4 COMPONENTS

GAP LOCATION	GAP[a] TYPE	NOMINAL GAP SIZE (inches) FOR: ROOM TEMP (70°F)	FIRE TEST CONDITIONS[c] MAXIMUM TRANSIENT	FIRE TEST CONDITIONS[c] STEADY STATE
B_4C PELLET ASSEMBLY TO FSS WALL				
0.428 Ø Pellets (Midsection)	T	0.009[b]	0.026[b]	0.026[b]
0.282 Ø Pellets (End section)	T	0.006[b]	0.024[b]	0.023[b]
CAVITY LINER TO TOP OR BOTTOM DU				
Flat	T	0.051 ± 0.015[d]	0.047	0.046
Corner	T	0.089 ± 0.029[d]	0.083	0.082
CAVITY LINER TO CENTER DU				
Flat	T	0.036 ± 0.015[d]	0.032	0.031
Corner	T	0.059 ± 0.029[d]	0.053	0.052
DU TO CASK WALL				
Flat	T	0.020 ± 0.010[d]	0.046	0.025
Corner	T	0.083 ± 0.010[d]	0.115	0.089
DU TO CASK WALL & CAVITY LINER				
With No Gap	A	0.000	0.313	0.079

NOTES:
(a) Gap types are the following: T is transverse and A is axial.
(b) Minimum dimension. Given on Sheet 9 of Drawing 031348.
(c) Temperatures given in Table 3.1-1.
(d) Given on Sheet 4 of Drawing 031348.

TABLE 2.7-20
SUMMARY OF MINIMUM GAP SIZES RESULTING FROM
DIFFERENTIAL THERMAL EXPANSION OF THE GA-4 COMPONENTS

GAP LOCATION	GAP[a] TYPE	NOMINAL GAP SIZE (inches) FOR: ROOM TEMP (70°F)	FIRE TEST CONDITIONS[c] MAXIMUM TRANSIENT	STEADY STATE
B_4C PELLET ASSEMBLY TO FSS WALL				
0.428 Ø Pellets (Midsection)	T	0.009[b]	0.026[b]	0.026[b]
0.282 Ø Pellets (End section)	T	0.006[b]	0.024[b]	0.023[b]
CAVITY LINER TO TOP OR BOTTOM DU				
Flat	T	0.036	0.032	0.031
Corner	T	0.060	0.054	0.053
CAVITY LINER TO CENTER DU				
Flat	T	0.021	0.017	0.016
Corner	T	0.030	0.024	0.023
DU TO CASK WALL				
Flat	T	0.010	0.036	0.015
Corner	T	0.073	0.105	0.079
DU TO CASK WALL & CAVITY LINER				
With No Gap	A	0.000	0.313	0.079

NOTES:
(a) Gap types are the following: T is transverse and A is axial.
(b) Minimum dimension. Given on Sheet 9 of Drawing 031348.
(c) Temperatures given in Table 3.1-1.
(d) Given on Sheet 4 of Drawing 031348.

2.7.3.3 Stress Calculations. Table 2.7-20 summarizes calculated thermal stresses for the bolts and the containment boundary. The relative motion between the closure and flange produces axial and bending stresses in the closure bolts. The bolt stresses reported in the table assume the maximum bolt torque of 250 ft-lb and include MNOP.

Although the maximum internal pressure during the thermal accident is 90.2 psig, this pressure occurs much later than 0.5 hr., the time corresponding to the imposed temperature load. At 0.5 hr, the internal pressure is essentially still the MNOP, conservatively taken as 80 psig (see Fig. 3.5-5 for the average cavity temperature). Therefore, MNOP is used when calculating total bolt stress. Note that using MNOP for the cold case is conservative.

2.7.3.4 Comparison with Allowable Stresses. All stresses are well within allowables, as shown in Table 2.7-20. The allowables are determined from the criteria of Section 2.1.2.

2.7.4 Immersion: Fission Materials

The criticality evaluation presented in Section 6.0 considers the effect of water inleakage. Thus, the requirement of 10 CFR Part 71.73(c)(4) is not applicable.

2.7.5 Immersion: All Packages

The effect of a 21.7-psig external pressure due to immersion in 50 ft of water, as required by 10 CFR Part 71.73(c)(5), is of negligible consequence for the GA-4 cask because that effect is less than the 200-m immersion test presented in Section 2.4.6.

TABLE 2.7-21
THERMAL STRESS RESULTS VS. ALLOWABLES PER SEC. 2.1.2

	Hot Conditions				Cold Conditions			
Component	Temp. (°F)	Maximum Calculated Stress (ksi)	Allowable Stress (ksi)	Design Margin	Temp. (°F)	Maximum Calculated Stress (ksi)	Allowable Stress (ksi)	Design Margin
Closure bolt	187				47			
Membrane		84.5	123.8	+0.47		86.7	129.5	+0.49
Membrane + bending		110	144.8	+0.32		112	150.0	+0.34
Seal surface	187[a]				47[b]			
Bearing stress		29	47.8	+0.65		33	55	+0.67
Containment boundary	777				703			
10-cycle fatigue		73.3[c]	1400	high		82.4[c]	1400	high

[a]Gap opening = 0.022 in.
[b]Gap opening = 0.024 in.
[c]Max stress intensity anywhere on the containment boundary.

2.7.6 Summary of Damage

The analyses presented in Sections 2.7.1 through 2.7.5 show that the hypothetical accident condition test sequence will not result in any significant structural damage to the GA-4 cask.

Minor amounts of damage can occur to the cask containment boundary as follows:

For a 30-ft drop, the greatest damage occurs at cask midlength.

Maximum stress = 57.4 ksi (Table 2.10.6-191)

Residual stress after drop (elastic) = 57.4 - 47 (S_y at 200°F) = 10.4 ksi

For a 40-in. drop on a 6-in. diameter mild steel punch with the impact occurring on the side of the cask at midlength, localized damage can occur at the impact point. The containment boundary will, however, not be perforated.

During the thermal fire accident, a slight bow of the closure or the cask wall can occur, but all bolt and seal area stresses remain below yield

For these reasons, the integrity of the cask is not compromised by the hypothetical accident condition test sequence.

THIS PAGE LEFT BLANK INTENTIONALLY

2.8 Special Form

This section is not applicable to the GA-4 cask because the spent fuel to be transported in the cask is not a special-form radioactive material.

THIS PAGE LEFT BLANK INTENTIONALLY

2.9 Fuel Rod

In Chapter 4 the GA-4 cask is considered leaktight. Therefore, no credit is taken for the fuel rod cladding providing containment of radioactive materials under normal conditions of transport or hypothetical accident condition tests.

THIS PAGE LEFT BLANK INTENTIONALLY